85

CRANFIELD INSTITUTE OF TECHNOLOGY

SCHOOL OF INDUSTRIAL SCIENCE

PhD THESIS

JILONG MA

METAL TRANSFER IN MIG WELDING

Supervisor: Professor R.L. Apps

OCTOBER 1982

LIST OF CONTENTS

LIST OF CONTENTS PAGE

ABSTRACT

The metal transfer process in MIG welding has been investigated. The heat balance of the melting process, forces acting on the wire tip and droplets, and droplet movement were examined quantitatively both under steady current and pulsed current conditions. A novel transistorised power source was employed for precision current adjustment which with the use of high speed cinephotography and careful metallographic techniques has allowed a re-assessment of current theories to be made.

A new metal transfer mode designated as 'Drop Spray' has been discovered. This transfer mode is located between the well known globular and spray transfer modes and only occurs in a very narrow current range of 20A, but it has several important features.

The relationship between metal transfer mode and the welding variables has been established quantitatively for the first time. It was found that the extension resistance and heat content of droplets are determined by current and hence metal transfer modes. The amount of spatter and fume was also found to be determined by transfer mode.

Metal transfer under pulsed current was also investigated. It was found that the metal transfer modes under pulsed current are the same as that of steady current. It was also found that the first drop of every pulse is of drop spray mode and the subsequent droplets will be stream spray. Careful observations and measurements have been made at various stages of the current pulse to enable greater understanding of the influence of the pulse parameters.

Based on the results mentioned above, a concept of controlled MIG welding was proposed, based on the control of metal transfer mode. By this concept any predetermined feature of conventional MIG welding can be achieved consistently and repeatedly.

As an application of the proposed concept, drop spray transfer was reproduced over a wide current range by means of metal transfer control. A new controlled MIG process designated as 'controlled drop spray MIG' has been developed which features high efficiency, all positional ability, freedom from spatter, low fume generation and good bead appearance. The preliminary bead on plate trial shows that all the expected results have been achieved although many more trials are necessary to fully prove the process.

ACKNOWLEDGEMENTS

The writer wishes to acknowledge the valuable help and advice given by many members of the Welding and Joining Technology Centre of the School of Industrial Science in particular his Supervisor Professor R.L. Apps. Thanks must also be given to Professor W.I. Pumphrey, Mr. C.J. Allum, Mr. K.A. Nelson, Mr. J. Bassett, Mr. G. Hills and Mr. J. Holmes, Mr. P. Cook and Mr. R.E. Fry (Photographic).

He also wishes to express his gratitude to Mrs. P. Craig and Mrs. P. Stuart for their patience and tolerance in typing the thesis.

Finally, thanks are due to the People's Republic of China and the School of Industrial Science for supporting the writer during his stay at Cranfield.

LIST OF FIGURES

LIST OF FIGURES

22. The region of solid and liquid. Partially melted region of electrode extension (83)

23. Model of globular transfer mechanism (83)

24. Model of spray transfer mechanism (83)

25. Discussion about drop detachment mechanism

26. Characteristic curves for droplet movement, l, with pulsed current

27. Research programme

28. Transistor power source AWP M500

29. The test rig and the lens

30. The layout of instrumentation rig, connection diagram

31. Globular transfer in MIG welding. 1.2mm dia. mild steel wire, Ar + 5% CO_2, 200A

32. The wire tips of globular transfer. 1.2mm dia. wire, AR + 5% CO_2

33. Detachment frequency, f, of MIG welding, 1.2mm mild steel wire, Ar + 5% CO_2

34. UVO traces of arc voltages, globular transfer mode

35. The fume generated from the boiling surface of liquid drop suspended under the wire tip, 1.2mm wire, AR + 5% CO_2

36. Arc shape in drop spray transfer, 1.2mm dia. mild steel wire, Ar + 5% CO_2

37. Drop formation and transfer, drop spray transfer mode. Arc shape is formed by metal vapour of drop surface

38. Drop transfer mode: the arc root covers the drop surface just beneath the neck but not the conic tip surface

39. UVO traces of arc voltage, drop spray transfer mode

40. Drop displacement with time. 1.2mm wire, Ar + 5% CO_2

41. Microstructure of a drop spray transfer wire tip

42. Copper coating on wire electrodes

43. Arc shape of stream spray transfer mode, 1.2mm mild steel wire, Ar + 5% CO_2

44. Features of stream spray transfer mode

45. UVO trace of arc voltage, stream spray transfer mode at 290A, compared with drop spray transfer mode of 260A

46. Droplet displacement in stream spray transfer mode

47. UVO traces of transition points

48. Relationship between the wire melting rate and welding current, 1.2mm mild steel wire, Ar + 5% CO_2

49. Variation of wire melting rate with current

50. Temperature distribution along electrode extension, 1.2mm wire, 10mm electrode extension, Ar + 5% CO_2

51. Resistivity of mild steel wire

52. Variation of electrical resistance of electrode extension with welding current, 1.2mm dia. wire

53. Drop formation, growth and detachment processes of drop spray transfer mode, 1.2mm mild steel wire, Ar + 5% CO_2, 261A, 7000 frames per second

54. Metal transfer process of stream spray mode, 1.2mm mild steel wire, Ar + 5% CO_2, 290A, 7000 frames per second

55. Schematic diagram of drop detachment mechanisms

56. Schematic representation of current pulse indicating stages examined for drop development and detachment

57. Metal transfer process during which a high current is being imposed, 1.2mm dia. wire, 50A, 380A

58. Macrostructure of molten tip

59. Drop displacement with time and instant velocity during application of current pulse (Reference Figure 57)

60. Metal transfer during the current pulse

61. Drop displacement and instant velocity with time during the current pulse (Reference Figure 60)

62. Metal transfer process when the current reduction from peak (380A) to base (100A) occurred during drop formation in drop spray transfer

63. Drop displacement and instant velocity with time in drop spray transfer during current reduction (Reference Figure 62)

64. Metal transfer process when the current reduction from peak (380A) to base (50A) occurred before drop detachment in stream spray transfer, 1.2mm mild steel wire

65. Drop displacement and instant velocity with time in stream spray transfer during current reduction (Reference Figure 64)

66. Contour and macrostructure of wire tip at different stages of pulse current (UVO traces show the moments when the current was switched off) 375A and 50A, 1.2mm wire

67. UVO traces of controlled drop spray MIG welding, 1.2mm mild steel wire, Ar + 5% CO_2

68. Controlled drop spray transfer process, mean current 302A, wire feed rate 6.1 m/min., 1.2mm mild steel wire, Ar + 5% CO_2

69. Comparison of fume formation rate of different MIG processes

70. Fume formation comparison of different MIG processes

71. Bead on plate deposit in horizontal-vertical position welding, controlled drop spray MIG, 1.2mm mild steel wire, welding speed 200mm/min, Ar + 5% CO^2

72. Bead on plate deposit in overhead position welding, controlled drop spray MIG, 1.2mm mild steel wire, welding speed 200mm/min, Ar + 5% CO^2

73. Fume formation rate (FFR) versus welding current, 1.2mm mild steel electrode (106)

74. Surface tension, σ, of molten metal as function of temperature, T. (23)

75. Equilibrium diagram for Fe-C

76. Calculated mean drop temperature as a function of welding current

77. Comparison of calculated drop temperatures reported by various investigators

78. Variation of wire melting efficiency, α, with welding current.

79. Model of globular transfer mechanism

80. Model of drop spray transfer mechanism

81. Model of stream spray transfer mechanism

82. Rotating transfer mode (10)

83. Surface of the conic tip of a heated wire

84. The initial stage of the necking process

85. The major forces influencing metal transfer as a function of time (using data from Figure 53)

86. Relationship between the detachment time, t_d, and the trigger current of the necking process

87. Diameter of interface between solid and liquid parts of the conic tip with time, in same condition as Figure 66

88. Spatter mechanism of globular transfer

89. Spatter mechanism of stream spray transfer. Time lapse between frames is 0.43ms, 290A, 1.2mm dia. wire

90. Detachment mechanism of stream spray transfer

91. Globular transfer, 1.2mm dia. wire, 91A and 147A

92. Drop spray transfer with 1.2mm dia. wire, 253A

93. Relationship between detachment time and current

94. Variation of drop frequency with wire melting rate, 1.2mm dia. wire, Ar + 5% CO_2

LIST OF TABLES

LIST OF TABLES

NOMENCLATURE

NOMENCLATURE

A	wire cross section area (m^2)
C_p	specific heat ($J\ Kg^{-1}K^{-1}$)
C_{pl}	specific heat of liquid steel between melting and boiling points ($J\ Kg^{-1}K^{-1}$)
C_{pm}	specific heat of steel between ambient and melting points ($J\ Kg^{-1}K^{-1}$)
d_b	diameter of liquid bar (m)
D	diameter of interface between solid wire and liquid drop (m)
e	electron charge
d_w	wire diameter (m)
F_g	gravity force ($Kg\ m\ s^{-2}$)
F_{gf}	drag force by gas flow ($Kg\ m\ s^{-2}$)
F_m	electromagnetic force ($Kg\ m\ s^{-2}$)
F_p	pinch force ($Kg\ m\ s^{-2}$)
F_s	surface tension force ($Kg\ m\ s^{-2}$)
F_r	reaction force of vaporisation ($Kg\ m\ s^{-2}$)
g	gravitational acceleration ($m\ s^{-2}$)
H	heat energy (J)
H_{dm}	heat content of liquid drop at melting point (J)
H_e	heat energy consumed on vaporisation (J)
H_l	latent heat (J)
H_{lv}	latent heat of vaporisation (J)
H_m	heat needed to bring unit mass of metal from ambient temperature to liquid state (J)
H_a	anode heating (J)
H_r	Joule heating (J)

H_w	heat consumed on wire melting (J)
I	current (A)
I_m	mean current of pulsed current (A)
j	current density ($I\ M^{-2}$)
k	Boltzman's constant
l	wire extension (m)
m	mass of droplet (Kg)
M_e	mass of vaporised metal ($Kg\ s^{-1}$)
M_{dr}	volume of droplet (m^3)
M_m	melting rate by mass ($Kg\ s^{-1}$)
Q	heat energy (J)
R	resistance (Ω)
R'	effective conductive cross section (m)
S	distance (m)
T	temperature (K)
t_d	drop detachment time (s)
T_{dr}	mean temperature of molten droplet (K)
T_m	melting point of steel (K)
T_b	boiling point of steel (K)
T_o	ambient temperature (K)
v	velocity ($m\ s^{-1}$)
v_{dr}	velocity of droplet ($m\ s^{-1}$)
v_{bar}	velocity of liquid string beneath wire tip ($m\ s^{-1}$)
v_m	mean velocity of droplet ($m\ s^{-1}$)
v_v	velocity of vapour ($m\ s^{-1}$)
v_w	velocity of wire ($m\ s^{-1}$)

V	voltage (V)
V_a	anode fall (v)
V_l	fall voltage on extension (v)
W_m	wire melting rate by length ($m\ s^{-1}$)
ρ	resistivity ($R\ m^{-1}$)
γ	density of steel ($Kg\ m^{-3}$)
σ	coefficient of surface tension ($N\ m^{-1}$)
Φ_o	work function

NOTE: In the interest of clarity, all equations and other expressions have used the above symbols even when the original work quoted has adopted a different nomenclature.

Where a relatively obscure symbol is used only once it is defined in the text.

CHAPTER 1 - INTRODUCTION

CHAPTER 1. INTRODUCTION

Since 1945 the MIG welding process has been introduced into industry. At that time it was mainly used for aluminium and them adopted for steel and other non-ferrous alloys. In the early years the constant current, or drooping characteristic, power source was employed but the arc voltage control needed rapid response and so it was not satisfactory. Subsequently, the constant potential power source was introduced and the self adjustment effect has been of great use in practice. Since the sixties, the application of MIG welding has increased considerably, partly at the expense of manual metal arc welding and partly with new applications resulting from improvements in welding equipment and procedures. The fundamental research work of MIG welding was carried out mainly in the fifties: the general study of arcs, metal transfer and heat flow is well developed, but it is only recently that significant progress has been made in the detailed study of those physical phenomena which are associated with metal transfer and mass flows in welding arcs.

So far, it has been generally accepted that the metal transfer modes have been established as globular, spray and dip transfer. IIW have issued a relative classification which represents the work carried out in recent years. High speed films were used as a basic approach in the research work of welding arcs but compared with the development of application, the fundamental research into MIG welding is still unsatisfied.

One of the important developments of MIG was the introduction of the pulsed MIG process. It was claimed that the artificial spray transfer could be obtained by current pulsing techniques on the basis of 'one drop per pulse'. However, the detailed investigation of metal transfer in pulsed MIG welding has not been carried out yet. As for the application side, the pulsed MIG has many advantages but there are some difficulties in practical use such as the problem of reproducibility and difficulaties in adjusting the pulse parameters in practice.

All the work in the field of metal transfer done before has been limited by the power sources which can only provide an increment larger than 50A so that some details of the processes were not revealed. For

example, it is known that the burn-off curve of Al has discontinuities but it is generally believed that mild steel has not. As a matter of fact, this belief is not true.

In order to improve MIG welding, which was often considered as less good than TIG or even MMAW due to problems of fume generation, spatter, porosity and lack of fusion, much work has been carried out already. Some dealt with materials, some concentrated on parameter adjustment and others resulted in very complicated machines, but the results were limited because of lack of sufficient understanding of the fundamental aspects of the process.

Development of transistorised power sources allow the production of reliable, consistant, reproducible welding current and it is also possible to change the V-I curve at will, set current independent of voltage and reproduce welding conditions repeatedly. Having these improved experimental conditions created by the new power sources, and since MIG welding applications have increased significantly in recent years, it was considered worthwhile to reevaluate the process in terms of metal transfer and other physical phenomena occurring at the wire tip during welding.

Invention of synergic MIG welding has also increased the potential range of application of MIG with its proposal of a valuable idea of simplification of parameter adjustment. However, synergic MIG had yet been investigated from the metal transfer aspects and additionally, its basic principles appeared to be based on an over-simplified view so that further investigation was worthwhile.

The objective of the present work was to examine the existing theory of MIG welding by means of an experimental approach based on a new transistorised power source. The examination was done by a combination of high speed cinematography, electrical recording and metallurgical examination of arc phenomena using small current increments with both continuous current and pulsed current MIG. Based on these results and a theoretical examination of them, an explanation of metal transfer has been developed. The logical examination of the wide range of arc phenomena together with the theoretical analysis sub-

sequently developed, has enabled a new improved controlled MIG process to be developed. It mainly features high efficiency, low fume, freedom from spatter and good positional characteristics. This new method is self consistent with the proposed theory and might be a new start of MIG development.

CHAPTER 2 - LITERATURE SURVEY

CHAPTER 2. LITERATURE SURVEY

2.1. General Review (Refs. 1, 2, 3)

2.1.1. Development of Arc Welding

For centuries, the only method man had for metallurgically joining metals was forge welding. Then, within the span of a few years prior to 1900, three new processes came into existence. Arc welding and resistance welding were developed in the late 1980's and put to work in industry a few years later. Oxyacetylene welding was developed during the same period and was first used industrially in the early 1900's.

The electric arc was of scientific interest only until 1881. The first attempt to use the intense heat of the carbon arc for welding was made in 1881 by Auguste de Meritens. In 1885, Nikolas de Benardos and Stanislar Olszewski experimented with this process and obtained a British patent for a welding process employing carbon electrodes. Benardos also filed for a patent in his homeland of Russia. Subsequently this welding process was used to make tanks, casks, pipes, locomotive maintenance etc. Two years after Benardos' patent was granted, another Russian, N.G. Slavianoff, announced a process in which the carbon electrode was replaced by a metal rod which was melted gradually and so added fused metal to the weld.

In the early work with metal arc welding, it was apparent that the limiting factor was the electrode. The weld was embrittled by reaction with the air. Oscar Kjellborg, of Sweden, developed a covered electrode in 1907. His thin electrode covering was mainly used for stabilisation of the arc. In 1912 Strohmenger obtained a U.S. patent for a heavily covered electrode which gave good weld metal properties but the initial cost was high.

Arc welding techniques developed very quickly during World War I. The sudden need for large numbers of transport ships was a dominant factor. In 1920 the British launched their first all welded ship, the Fulagar. At the same time, the first application of arc welding to aircraft also occurred. Anthony Fokker, the Dutch aeroplane manufacturer, used the process to produce some German fighter planes. However, further development of arc welding was relatively slow, although applications of arc welding gradually expanded in shipbuilding, steel frameworks and similar areas of steel fabrication.

In the 1930's many developments occurred. In manual metal arc welding new electrode coatings and improved AC welding transformers gave improved arc stability and weld quality. Numerous attempts were also made to introduce mechanized arc welding, of which submerged arc welding has proved the most successful, offering high deposition rates with acceptable weld quality. However, none of these predominantly slag shielded arc welding processes provided enough shielding to adequately protect the more reactive metals such as aluminium and magnesium from atmospheric contamination. To overcome this difficulty, welding engineers began to use bottled inert gases as shielding agents in the early 1930's. At the end of the decade, successful gas shielded processes began to emerge in the aircraft industry to weld magnesium.

The first gas-shielded process employed a tungsten electrode and helium shielding gas, and became known as the Heliarc process. Subsequently, argon shielding gas has proved more popular, at least in Europe, and the process has been termed the tungsten arc inert gas (TIG) welding process. DC electrode negative welding was proved satisfactory for stainless steel, but was not suitable for magnesium or aluminium due to oxide removal problems. However, AC with a high frequency high voltage to stabilize the arc was used successfully on Al and Mg. In 1953, a nozzle was used to constrict the arc and the resulting method became known as the plasma arc process.

The TIG process proved unsatisfactory for welding thick sections of highly conductive materials because the workpieces tended to act as heat sinks. To overcome this difficulty, a consumable metal electrode was substituted for the tungsten electrode. The resulting process, announced in 1948, became known as gas metal arc or metal arc inert gas or (MIG) welding. It proved successful for welding aluminium, and was subsequently adapted for other non-ferrous and ferrous metals and alloys. Most of the early work with MIG welding used argon gas shielding although studies showed that gas mixtures gave improved arc stability.

Early in the 1950's it was found that the shielding gases based on argon or helium were too costly and Lincoln Electric in the U.S.A. applied for a patent for the use of carbon dioxide as a shielding gas. This process was developed for welding steel and adopted by automatove shops and other metal working plants for applications were the quality of the weld was not particularly critical. However, for high quality welding of steel argon-

oxygen or argon-carbon dioxide gas mixtures were found to be preferable since they gave better weld profile, fusion and properties.

MIG welding applications with ferrous alloys have gradually increased since 1955, with several developments contributing to overall quality. Perhaps the most important aspect has been the improved understanding of process fundamentals but the use of pulsed current MIG welding and Synergic MIG welding has shown that independent control of metal transfer and heat input is possible and recent developments have looked at the potential of this route.

2.2. Characteristics of the MIG Welding Process (Refs. 4, 5)

The metal inert gas (MIG) process, or gas metal arc welding (GMAW) is a particular welding process which uses a continuous wire to serve as a source of weld metal and as a terminal (electrode) for the electric arc. It uses gas to shield the arc and weld metal. If inert gases such as argon or helium are used, the process is referred to as MIG. If an active gas (0_2 or CO_2) or a gas mixture which contains a certain amount of active constituents such as oxygen or carbon dioxide is added to argon or helium, the process is termed as MAG (Metal Active Gas) welding.

The gas metal arc welding process can also be designated by mode of metal transfer from electrode to work as follows; spray transfer, buried arc, pulsed arc (GMAW-P) and short circuiting arc (GMAQ-S). Alternatively, reference may be made to free flight transfer which includes globular, spray and pulse or to dip (short circuit) transfer (Ref.4).

2.2.1. Metal transfer in the MIG process.

Metal transfer mode.

To the present, classification of MIG metal transfer has been generally placed in two categories: free flight transfer and dip transfer (Ref.4)

There are three types of free flight transfer that have been reported;

a) Spray transfer; typical spray transfer is described as 'a spray of very small molten metal droplets which are propelled in a straight line towards the workpiece by electrical forces within the welding arc'. This mode of transfer is particularly suited to welding in the flat position when used with steel, but it may be used in the vertical or overhead position when used with aluminium and its alloys. Spray transfer is usually

carried out with Ar/CO_2 based gases and does not occur with steel when CO_2 is used.

b) Globular transfer; at currents below the level required for spray transfer, globular transfer occurs. It features large size droplets which are detached by gravity force. Other features of globular transfer are high spatter levels and a restriction to welding in the flat position.

c) Pulsed transfer; this is a kind of artificial spray transfer using a peak current and a base current alternatively. Then spray-like transfer can be obtained during the peak current pulses but at mean current well below the transition current. The advantage of pulsed transfer is that spray transfer can be used under lower heat input.

d) Short circuiting or dip transfer (Refs. 1; 4, 5, 6) occurs when the wire is fed at a rate which is just greater than the rate at which it can be melted by the welding arc. As a result the wire touches the weld pool causing a short circuit. The current supplied by the power source rises rapidly, the filler wire then acts as a fuse and when it melts a free burning arc is recreated, and the current falls to its previous value. This phenomenon is repeated regularly up to 200 times every second. The overall effect is continuous melting with a low heat input and small weld pool. The low heat input is useful on thin gauge material whilst the small weld pool allows welding to be carried out in any welding position. However, defects such as lack of fusion can occur in thicker materials which have restricted application of dip transfer welding in medium and heavy fabrication.

Transition current (Refs. 7, 4, 5).

There are transition currents between different metal transfer; transition current depends on wire diameter electrode extension and, so some extent, shielding gas composition. For 1.2mm mild steel using argon rich gas mixtures, Fig.1, the transition current at which the globular transfer changes to spray transfer has been reported to be 220 $\pm$ 10A. (Ref.4)

Another transition current, often referred to as the upper limit of welding current is defined by the initiation of a spatter forming rotation of the arc and globular on the electrode tip (Ref.4). This arc form has been termed 'jet rotation'. As with the development of the axial spray arc at a lower current, the current at which the axial spray disappears is proportional to the electrode diameter and varies inversely with stick-out.

Figures 2 and 3 show the variation of transition current with electrode extension and of melting rate with electrode extension. It should be noted that this data was reported in 1958 (Ref.8) and it will be demonstrated later that the results are not completely satisfactory.

Electrode polarity.

The gas metal arc welding process was developed largely as a technique to be used with electrode positive polarity since the arc becomes very unstable and gives excessive spatter when electrode negative is used. The drop size with electrode negative (cathode electrode) is very large and, due to arc forces, the drops are propelled away from the workpiece as spatter. A number of methods have been developed to improve the thermionic properties of an electrode. Oxygen additions to argon were helpful for ferrous metals by forming 'thermionic' iron oxides on the wire surface but had no effect for Al. Wash coatings on steel wires of oxide mixtures containing calcium and titanius have been used and with these coatings, the metal transfer and stability become equivalent to those that had been associated only with reverse polarity (electrode positive).

2.2.2 Burnoff characteristic

Burnoff characteristic means the relationship between the rate at which wire is fed into the arc and the current required to burn it off to maintain an equilibrium arc length. This is also referred to as the burn-off relationship and is a characteristic property of each filler wire composition and diameter. This characteristic is of significance because a constant arc length is an essential requirement of sound welding operation. Additionally, mechanisation of the MIG process must be based on burn-off characteristics in order to realize the optimum wire feed rate. For steel, the traditional conception of burn-off rate is nearly linear (Fig.1). However, it is necessary to consider Joule heating and early in 1958 it was found that the curve for steel is of the form shown in Figure 4, (Ref.8). For aluminium, the burn-off curve is as shown in Figure 5, (Ref.9). Even in 1979 it was still asserted (Ref.10) that there was no discontinuity in the burn-off - current relationship for steel which was conceived as a smooth curve at all current levels, unlike the case of MIG arcs with aluminium. Unfortunately, this generally accepted conclusion is a presumption and there is a lack of experimental evidence, but to the present all the text books and welding reference books, such as the AWS welding hand-book still use this conception for the description of the basic features of the MIG process.

2.2.3 The power source and self adjustment (Refs. 4, 11, 12, 13)

Conventional welding power sources can be divided into 'flat' voltage-ampere characteristics (constant potential) and drooping characteristics (constant current). The generally accepted fact (Refs.14, 1) is that when a constant potential power source is used, the control of current merely involves selecting a wire feed speed from the burn-off characteristic; the current will rise automatically to the required value at a voltage not greatly below that selected for the open circuit. An important property of the constant potential power source is its ability to produce a self adjusting arc. When a constant potential power source is used a small voltage change caused by arc length fluctuation will induce a large current change. For example, if the arc length is shortened, there will be an increase in current resulting in a faster burn-off rate and the arc length will be restored. A longer arc length would increase the arc voltage resulting in less current and slower burn-off rate so that the arc length will shorten.

The constant current source is designed to provide a virtually uniform constant current whatever the arc length. Since deposition rate and penetration are predominantly controlled by arc current, a drooping characteristic constant current power source provides a fixed burn-off and penetration whatever the arc length and hence arc voltage. Constant current power sources are ideal for manual welding, where strict control of arc length is not possible, and for mechanized systems, where variation of arc length is relatively slow and can be controlled by monitoring the arc voltage. Constant current power sources have rarely been used in MIG welding systems because arc length control mechanisms are too slow to adjust quickly enough to present burn back or electrode stubbing. However, there is still a degree of self-adjustment, even if the power source is of the constant current type. This occurs because Joule heating contributes to the wire melting rate, amounting to some 30-60% depending on the electrode stick-out. Modern transistorised power sources offer sufficient stability to remove the need for self adjustment so that a return to constant current power sources is possible.

2.2.4 Shielding gas (Refs. 4, 1, 14)

The primary purpose of the shielding gas in metal arc welding is to protect the molten weld from contamination and damage by the surrounding atmosphere.

However, several other factors affect the choice of a shielding gas. Some of these are:

a) Arc and metal transfer characteristics during welding;

b) Penetration, width of fusion and shape of reinforcement;

c) Speed of welding;

d) Tendency to undercutting.

All of these factors influence the finished weld and the overall result; cost also must be considered.

Although the inert gases Ar and He protect the weld metal from reaction with arc atmosphere, they are not suitable for all welding applications. By mixing controlled quantities of reactive gases with them, a stable arc and substantially spatter-free metal transfer are obtained. Tables 1 and 2 give the possible gas mixtures for MIG welding from different authors.

2.2.5 Brief summary

The MIG wedling process has been widely used in industry since 1955. From the foregoing paragraphs it can be seen that the most important features of MIG processes are; metal transfer mode, the burn-off characteristics and their relationship with the other welding parameters. However, in spite of the wide application for many years, some explanations of these features still remain at the same rather elementary stage that was offered initially. These explanations cover wire melting curves, transition currents and burn-off rate. Some curves or data obtained more than twenty years ago are still repeated in the most up to date books and papers and are even used as the basic starting point for research work and equipment design. Compared with the progress of scientific and industrial development in welding and associated fields, this situation is very unsatisfactory. This situation will be seen again in the next section on fundamental research in MIG welding even though this has been developed rapidly in recent years.

2.3. Innovations in the MIG Welding Process

The wider application of MIG welding combined with developments in alloy steels, and more sophisticated structural designs, have led to an increased requirement on the operational characteristics of MIG welding and the quality of its deposits. The shortcomings of the original MIG process became more evident, such as, for example, the fact that the metal transfer modes were determined by particular current ranges. Therefore the desirable metal transfer characteristics obtained at a particular power source setting could only be used for a particular thickness of workpiece and a limited welding position. The control of a stable arc and the adjustment of welding parameters were not particularly convenient, the training cost of welders was high and the fume generation and spatter were continuously troublesome, so that efforts were made to improve the MIG process and its techniques. Many improvements and innovations both on the process and equipment have been carried out but two aspects of these improvements are particularly important. They are the improvement of the control of metal transfer and more exact and positive control of the welding parameters and associated adjustments during operation.

In this section improvements in the MIG process are covered dealing with consumable development, the physical and electrical process of metal transfer, parameter control and overall adjustment of the process during operation. No attempt has been made to be comprehensive but an attempt is made to demonstrate the wide range of developments that have occurred, many of them completely unrelated to the fundamental aspects of MIG welding.

2.3.1. Flux Cored Wire Arc Welding (Ref. 15-25)

The use of tubular electrodes for hard facing has been known for many years but, filled with flux or powdered metals they have attractions in MIG welding. Principally they allow very high deposition rates in the flat or horizontal vertical (fillet) welding positions, but thinner wires have been developed for positional welding and to give good weld metal properties. Many tubular wires have been developed for use with supplementary gas shielding, generally, CO_2 or Ar-CO_2 mixtures, but others are self-shielded and require no additional shielding, thus allowing simpler, lighter welding guns to be used, leading to higher deposition rates.

With the externally shielded electrodes the core is used solely to increase deposition rates or improve deposit properties but with self-shielded electrodes a protective shield also has to be generated. This is generally done by generating a metal vapour shield (such as lithium) or a gas shield (such as CO_2). All flux cored electrodes contain additions to improve arc ionisation, promote stable metal transfer and produce heavy quick freezing slags to aid positional welding.

Despite the work that has gone into the constitution of the flux metal powder core very little has been done on the characteristics of the process. Power sources and equipment have been based on MIG welding sets and it has been assumed that the same principles apply. This approach has worked well in that FCAW has been used increasingly over the last 10-15 years but technical understanding lags well behind practice.

2.3.2. Alternative current MIG welding (Refs. 26,27)

Despite the extensive use of alternating current (AC) for the manual metal arc (MMA), submerged arc, and TIG welding processes, MIG welding with solid wire is restricted to direct current (DC) and almost exclusively to electrode positive polarity. The main problem of using AC in MIG welding is the re-ignition of the arc every half-cycle. Lucas (Ref. 28) employed a re-ignition system which injects a high voltage and short duration surge within 30 msec of the instant of current zero, and re-ignition was obtained successfully. It was claimed that more stable arc and metal transfer at high current levels, more tolerance to magnetic fields, elimination of porosity associated with the finger, etc. have been achieved. However, this work still remains of academic significance only.

2.3.3. Modulated Wire Feed (Refs. 29,30)

This technique was introduced in an attempt to improve the stability and consistency of dip transfer welding. The principle of modulated wire feed is that the wire feed rate is changed regularly at fixed frequency. For CO_2 MIG welding Rider (Ref. 30) used 280A and a frequency of 1Hz to

stop the wire feed repeatedly. The arc extinguished and then re-initiated by short circuit. By this method a 3 mm thick plate was welded on to a plate of 13 mm, the technique has also been used for surfacing.

Paton et al, (Ref. 29) used a pulse frequency of 15 to 100 Hz with wire feed rate of 1.5 - 2 m/sec. In fact this is a kind of forced metal transfer. The essentials of the welding process being described here consists of the use of an additional force which, when applied to a droplet, alters the manner in which metal transfers in a very similar manner to the electrodynamic force pulse impulsed arc welding. In the case in point, this force is inertia developing during accelerated movement in the electrode-droplet system. The results reported showed that the range of working currents of MIG can be greatly extended by a programme with which there is constrained transfer of molten metal into the weld pool. The transition current can be reduced by 50-67% compared to that of steady wire feed speed and current conditions.

2.3.4. Mesospray MIG (Ref. 31)

This method has been proposed for the welding of aluminium. The mesospray MIG process involves a new control to improve arc stabilisation and simplicity of operation between the region of spray-type metal transfer and short circuiting arc.

Using a constant current power source, in the case of a long arc, the wire melting rate only depends on the current. However, when the arc length is reduced to a certain value, the wire melting rate will increase with the reduction of arc length but no details have been given as to how this is achieved. This particular arc has been termed the 'mesospray arc'. One of the important features of mesospray arc is the self-controlling effect. A constant current or a constant voltage power source is used, the arc length change can be compensated by this self-controlling effect. In other words, the system has the ability to maintain a stable arc. The advantages include: irrespective of the condition of the base metal surface an optimum arc length is maintained and results in an even weld. Wire feed speed can be obtained automatically merely by setting the welding current. So the selection of optimum welding conditions is simplified.

2.3.5. Pulsed Current MIG (Refs. 9,32,33,34,35,36,37,38,39,40,41)

Application of pulse techniques is the most significant progress in MIG welding. The pulsed arc welding process was first introduced in 1962 by Needham of The Welding Institute (9). The technique was initially developed for the welding of thinner section aluminium but was subsequently extended to other metals including steels. The basic principle is that the metal transfer in MIG welding is controlled by the repeated regular application of a current pulse. In this way, spray transfer can be obtained at a mean current lower than that at which spray transfer occurs naturally. This is achieved by modulating the welding current such that it alternates between two levels, the high level giving axial free flight (spray) metal transfer and the lower level doing little more than provide a pilot arc and some background heating.

The main problems encountered in the application of MIG welding to ferritic steels before the introduction of pulsed arc were concerned with the optimisation of conditions for certain thicknesses of plate and also the control of quality when welding relatively thick plate out of position. At that stage the dip transfer technique was the unique MIG welding technique applied to positional welding, but the welding current was limited below 200A, with the result that only thin workpieces could be welded satisfactorily by dip transfer. The major problem was lack of fusion defects arising from the low heat generation, which was unavoidable because of the strict requirement of the welding parameter control. Pulsed arc MIG welding eliminates some of the major factors which contribute to lack of fusion defects in dip transfer welding, conbining a low deposition rate with a reasonable heat input. As a result, the pulsed arc process became an attractive tool for positional welding of heavy plate, but the adjustment and control of the parameters was very complicated and the optimum parameter combinations required improvement. As a result pulsed MIG welding never achieved the potential that was initially indicated.

Some work has been done on power sources (Ref. 45) for pulsed MIG, but no explanation on metal transfer has been given.

2.3.6. One Knob MIG Sets (Refs. 46,47)

The quality of the welded joint and the cost are determined significantly by the ability of the welder to set up a good welding condition as well as the ability of the welding system to reproduce this condition consistently. The 'one knob' control machines were designed to give the optimum combination of current, voltage and inductance (for dip transfer), but selection of that optimum combination was predetermined so that a single control could be used by the welding operator. More than one welding condition may be chosen by the selector knob and each of the positions give a parameter combination for certain thickness. For example, the BOC 'Autolynx 100' can be used for 0.6 to 3 mm plates. However it must be mentioned that the 'one knob' technique is nothing but a simplification of the adjustment controls for the welding machines. (Ref. 46).

One knob MIG welding equipment leaves a minimum of control for the operator and therefore reduces the operators' training period to the minimum possible. Its main applications have been in the light sheet metal industries, particularly the motor body repair shops for substitution of oxy-acetylene gas welding. The system is not suitable for higher quality work or where a wide variety of applications occur: in this case more control, and hence more complexity is needed.

2.3.7. Programmed MIG Welding (Refs. 48-51)

The development of the single knob MIG welding machines stopped with the relatively light equipment suitable for the welding of sheet mild steel. New developments have broadened the range of applications and brought about the concept of programmed MIG welding. It is well known that when selecting a MIG welding condition the most important parameter is wire feed speed. Normally all other parameters are tuned to this selected value. Programmed welding equipment implies that these other parameters are self-adjusting once the correct programme has been selected. A feed back control or a monitoring and self-adjusting system have been achieved by modern electronics combined with a signal

from a tachogenerator on a wire feed roll. A programmed memory built into the power source can contain all the necessary information for various MIG welding applications. One example is 'MIGMATIC 400' welding equipment produced by AGA. With this unit, it has been claimed that almost all MIG welding applications can be covered by 18 programmes which provide conditions for commonly used wire sizes, gas types and transfer modes for C-Mn steels, stainless steels and aluminium alloys.

An example of the programmed MIG welding process was the use of a plug board technique reported in 1969. It was claimed that costly numerical control and on-line computers can be substituted by low cost pin or plug programme boards. The boards were of 10 x 10 in dimension, gave ten programmes with 30 way selection. Each programme had 30 pin ways, 12 for voltage, 11 for wire feed speed, 5 for inductor selection and 2 for shielding gas. The programmes could be changed either by clip on rocker type switches mounted on standard conventional welding guns or by timer switches, positional transducers or from a record medium such as tape independent from the welding gun. One example of an application was the welding of pipeline butt joints in the fixed horizontal position. Using the MIG (CO_2) process at least four programme changes were used to optimise the weld for different positions on the periphery of the pipe.

The programmed welding concept has gain wide acceptance in recent years with the initial emphasis on the economic benefits from utilising welders of lower technical ability who no longer need extensive machine training. However the application of the concept has proved expensive so that very few programmed MIG welders are now included in manufacturers products. To a great extent the concept has been superceded by synergic MIG welding and its derivatives.

2.3.8. Synergic MIG Welding (Refs. 52 - 57)

The conception of synergic MIG was proposed in 1977 by The Welding Institute. Synergic, as interpreted by Amin (Refs. 52,53) from synerg, meaning working together. The basic principle of synergic MIG is that there should be a combined relationship between the wire feed speed and all the relevant pulse current parameters (pulse repeat

frequency, duration, pulse and background current levels). In order to find out this relationship, the Welding Institute employed an empirical approach with fixed wire feed speeds of 2, 2.4 and 4 m/min and fixed frequencies of 25 and 50 Hz. The criteria used were a balance between the wire feed speed and burn off rate to maintain a constant arc length and control of metal transfer to give 'one drop per pulse'. It should be mentioned here that the so called 'one drop per pulse' has been claimed as a kind of artificial spray (projective) transfer by the authors, even though this is not strictly true. They also reported that the droplet volume increases proportionally with pulse duration at a given pulse amplitude. Given data showed that the droplet volume was $3mm^3$ when pulse duration was 10 m/sec at pulse amplitude of 300A (Ref. 53). It was also claimed that the possible combinations of pulse amplitude and duration can be determined by a given parametric curve for any given droplet volume, in other words, by 'unit pulse'. Having obtained the envelopes of the stable zone which satisfied the criterion mentioned above, the synergic relationship was described as follows: both the background current and either the pulse duration or the pulse repeat frequency vary proportionally with the wire feed speed whereas the excess of pulse level over the background level remains constant.

In practice, a tachogenerator measured the wire feed speed and the output signal was fed to an electronic circuitry which executed the synergic relationship automatically and controlled the transistor power source, resulting in the required pulse parameters for a given feed speed being supplied to the arc. The claims made for the process are substantial (Ref. 53). "It has been found that the synergic relationship is valid over the entire range of wire feed speeds say from 0.5 to more than 10 m/min. This unique feature of synergic pulse MIG welding is shown in Figure 10. Where the mean arc current has been changed from about 25A (0.6 m/min wire feed speed) to about 400A (about 10 m/min wire feed speed) by steadily increasing the wire feed speed, the arc showed a high degree of stability throughout while the metal transfer was maintained in the 'spray' type". In other words a range of 20 times for wire speed and 16 times for current is claimed. In fact, the figure mentioned above (Ref. 53) shows clearly that the wire feed speed and

current ranges are 1.5 to 9.2 m/min and 60A to 370A respectively, a range of 6 times for wire feed speed and 6 times for current. In May, 1981, Salter of the Welding Institute gave a different range of 2 to 7 m/min as the control available from synergic MIG welding (Ref. 57), only 3.5 times for wire feed speed. All results were for 1.2 mm mild steel wire.

Despite some variation in the claims for the process the concept and development of Synergic MIG welding is of considerable importance in the overall progression of MIG welding. The concept has been adopted by a number of equipment manufacturers and appears to be gaining increasing acceptance within industry. One problem has been the high cost of equipment which has restricted use to high quality work. However, in 1981 some lower cost versions were introduced and this development could lead to wider application of the technique.

2.3.9. Application of Computer Techniques in MIG Welding (Refs. 58-61)

The rapid introduction of electronic computer techniques is bound to help greatly in solving the most important tasks facing science and industry in the welding field. When appropriate mathematical models are used, computers can provide the quantitative relationships necessary for making practical judgements regarding the effects of particular parameters of a process on a phenomenon in which we are interested and which is difficult to evaluate by direct measurements. This approach has provided a number of interesting results associated with investigation of the energy particulars of the thermal, diffusional and deformation processes taking place at high temperatures in the weld metal or HAZ. Naturally, successful research of this type depends largely on the corresponding mathematical models. It should be noted that in a number of cases the phenomena studied during welding are so complex that they cannot be related to the recognised differential equations of mathematics, or else the system of equations is so cumbersome that their solution is not within present computer capacity. In these cases it is very effective to use statistical models, in which the connection between the principle parameters or a process is established by the statistical analysis of experimental data.

One practical application was reported by the Welding Institute (Ref. 59). Experiments were carried out to determine the relationship between MIG welding parameters and weld bead dimensions. Based on these relationships a computer programme has been written to calculate the welding parameters required for a desired weld bead size. Results showed that a MIG welding process could be initiated and controlled completely without human intervention.

The main feature was that the application of computer techniques only dealt with the operation facilities but did nothing with the metal transfer processes. As a result weld quality remains the same as the ordinary MIG technique.

Another example of using computers is the Welding Institute's design of a microcomputer based control system for synergic pulsed MIG welding. (Ref. 57). The control system comprises a commercially available microcomputer to perform the control data processing and computation functions, a visual display unit to communicate with the operator and a tape recorder for the bulk storage of data and software control programme. An electronic interface unit was designed and constructed specifically to link the microcomputer to the welding equipment. It is claimed the computed and calibrated output signal from the microcomputer then drives the power source so that a stable arc and consistent metal transfer are maintained at the desired burn-off rate.

2.4. Brief Summary

From the foregoing paragraphs it can be seen that many efforts have been made in order to improve the MIG welding process. These works can be summarised into two groups. The first one was to change the metal melting and transfer processes by means of electrical or mechanical means. Examples are, AC MIG, pulsed MIG and modulated wire feed. The second group involves the simplification and automation of the parameter selection operation and the subsequent equipment adjustment.

In the first group many of the techniques have given certain advantages over the original MIG process but at the same time there are still a

number of difficulties to be resolved. For example, although the pulse technique is attractive it is not easy to set up a working condition. At a given wire feed speed, the pulse amplitude and duration must be adjusted together. In addition the mean current, determined by a combination of the four pulse parameters, must be that giving a burn-off rate equal to the wire feed rate in order to maintain a constant arc length. To accomplish such adjustment is difficult in practice. Furthermore, even minor changes in wire feed which frequently occur with commercial equipment, can lead to degeneration of the established welding condition, causing arc and metal transfer instability, burn-backs or stubbing and these can result in defective welds as well as the frustration of the operator. In fact, the more important factor is the optimum parameter combination of pulsed MIG which still has to be sorted out, which leads to the second group of work on parameter optimisation.

The selection of parameter combinations must be based upon further understanding of the basic electro-mechanical and metallurgical process occurring at the wire tip, that is the metal melting and transfer process. Without a correct understanding of these processes it is impossible to identify and obtain the optimum operating conditions. All of these developments were based on empirical data but insufficient theoretical foundations have been given. This situation leads to some undesirable results and the Synergic MIG process was reported with very different data at different times, a direct result of the limited empirical data and lack of the desirable theoretical base. Similar reasons explain the lack of popularity in industry of pulsed MIG welding. Without sufficient knowledge and understanding of optimum parameter selection the developments of one knob controls, programmed MIG and other techniques become of limited benefit.

In brief, at the present time, the most important thing which has to be done is the fundamental research work on MIG welding technology. Otherwise further improvements of MIG welding will be very difficult to achieve.

Lancaster wrote (Ref. 62) that knowledge of welding physics has been acquired slowly and it is only recently that significant progress has been made in the study of those physical phenomena which are specifically

associated with arc welding such as metal transfer and the physics of welding arcs. The investigation of such problems is producing information and ideas that have particular value in the development of welding processes. This situation leads to the main aims of present work which has been carried out in order to make further understanding of the electro-mechanical, thermal and metallurgical processes at the molten wire tip in MIG welding. Based on these results improved parameter selection and its control can be derived readily.

2.5. Fundamental Research Work on MIG Welding

As mentioned previously, fundamental research is essential for the further development of MIG welding. So far the depth of understanding that has been reached in this field is still far behind the practical application of MIG welding techniques. In recent years the fundamental research work has been accelerated and a lot of excellent papers have been published by scientists in different countries. The work in this field is referred to as 'arc physics', 'arc phenomena', 'metal transfer', 'mass flow', 'heat flow and drop temperature', 'physical properties of a MIG welding arc', etc., but it can be divided mainly into two aspects, the heat balance of the melting process and the molten metal transfer process. The first aspect relates to arc properties, wire resistance, Joule heating, arc heating, heat transfer, wire temperature and droplet temperature, whilst the second aspect includes the drop formation, forces acting on the heated wire tip and liquid metal, molten metal movement, drop detachment and drop velocity.

Most published work has dealt with only one or two items, such as forces, resistance or wire extension but it is very important to link these physical properties together and to the welding parameters and variables of welding processes. It is because the real process is very much complicated that the different variables and phenomena effect each other seriously. So far most published work has only described some individual physical properties mentioned above rather than attempt a systematic explanation. Therefore, some of this work has led to incorrect conclusions. For example, without correct knowledge of the

metal transfer process using 'one drop per pulse' as a criterion of pulse technique is incorrect because 'one drop per pulse' includes globular transfer. At the moment the systematic work which connects; all the heating processes and acting forces together and subsequently derives the relationship between the welding variables still has to be carried out.

This is the main aim of the present work and the following survey deals mainly with the MIG welding of mild steel using argon based gas mixtures.

2.5.1. MIG with Steady Current

2.5.1.1. Heat balance of wire melting process

There are two heating sources in MIG processes, the anode heating by the arc and the Joule heating by the wire resistance. In this section information on the physics of the welding arc is reviewed as a necessary prelude to a subsequent study of previous work on arc heating and Joule heating.

2.5.1.1.1. The welding arc

An arc is essential for arc welding and it has the following functions:

a) heat source,

b) high temperature of the arc leads to chemical reactions between the metal and gases in the arc area,

c) forces produced by arc cause gas flow and metal movement.

Most of the experimental work on the physics of the welding arc has been on inert gas shielded arcs with a non consumable tungsten cathode. It is generally assumed that the processes derived for a tungsten cathode arc can be used to explain those occurring in a consumable electrode arc, except for metal transfer. The electric arc may be defined (Refs. 63-66) as a self-sustained discharge having a low voltage drop and capable of supporting large currents. An arc between two electrodes can be divided into three regions, each with

different physical properties (Figure 6). The cathode fall region is a very thin layer (approx. 10^{-6} cm) characterised by a positive space charge which causes a steep voltage rise and hence a very strong electric field. The anode fall region has similar properties and a negative space charge leads to a steep voltage drop and strong electric field. Between these two regions is the arc column which occupies most of the space between the electrodes. The arc column is characterised by electrical neutrality (absence of a space charge) and quasi-thermal equilibrium. The arc is a non-ohmic resistance to that the voltage-current characteristic has the form shown in Figure 7. (Ref. 114). The fall in voltage with increasing current at low currents (up to 30-60 amps) is not fully understood but several suggestions have been made such as that the increase in temperature of the arc with increase in current leads to higher electrical conductivity and requires lower potential, or that the cross section of the current carrying part of the arc is larger and more electrons are present at high temperature. After a minimum voltage then the current increases with voltage in a nearly linear manner depending on the type of arc (Figure 8, Refs. 7, 67). This represents a situation of a straight dependence between current and potential.

All the arc characteristic curves can be represented by an equation composed of a hyperbola and a straight line. The hyperbola (V=C/I) is required to express the negative characteristic and also the knee of the curve, whilst the straight line (V=A+BI) plays a dominant part in representing the gentle gradient of the positive characteristic, whereas the contribution of the hyperbola is progressively reduced with increase of current. The equation is as follows:

$$V = A + BI + C/I \qquad (1)$$

where V is arc voltage, I is arc current, A is a constant, which might be affected by arc gap, and B and C are constants

that might be affected by the boiling point of the anode or its oxide, or by the cathode material. Some empirical data of A, B and C can be found from papers (Ref. 10). Figure 9 shows the arc voltage of different processes. Most reported work has dealt with argon shielded tungsten electrode and less work has been carried out on arcs with consumable electrodes. A brief general review on the arc phenomenon is helpful to give a better understanding of the background to present work.

2.5.1.1.2. Arc Column

The arc column is composed of neutral particles (atoms and molecules in the excited and non-excited states) and charged electrons and ions. Thus the current is bipolar with electrons travelling towards the anode and positive ions towards the cathode. The number of electrons and positive ions in each volume unit of the column is equal so that the arc column is electrically neutral. A consequence of this is that the electric field is constant, in most cases the field is about 10V/cm . (Refs. 69,7,70).

In the welding arc one or both electrodes are liquid and metal transfer may take place with the consequence that the welding arc is a metal vapour arc. The low ionisation values of metals in comparison to those of gases has a significant influence on arc temperature. When an element with a lower ionisation energy than the metal to be welded is added to the arc, current remaining constant, the arc temperature decreases. The arc temperature is strongly dependent on thermal conductivity. The lower the thermal conductivity at constant arc current and effective ionisation energy the higher the arc temperature.

The stability of the arc column is closely related to its electrical conductivity. Low ionisation energy and high arc temperature is of advantage. The stability of the arc increases by addition of elements such as K, Na, which have low ionisation energy. Stable arcs are observed in gases with relatively low thermal conductivity such as Ar and Kr whereas

arcs are rather unstable in relatively high conductivity gases such as He, H_2, Na, and CO_2. The temperature of an arc is important for metal transfer. Figure 10 shows a scale of temperatures occurring in various types of arc by Finkilnburg and Maecker (Ref. 63). For argon-tungsten arc, an isothermal map has been given in AWS Welding Handbook (Ref. 10). Figure 11; similar maps can be found in many other books. King (Ref. 71) has suggested average temperatures of 6000-7000^{o}K for a metal vapour arc, but in the centre of a 200A Ar/Al arc a temperature of 15000^{o}K may be reached; this will increase to 23000^{o}K at 300A current.

2.5.1.1.3. Cathode Fall Region

The voltage drop at the cathode is of the order 9-20V. There are two kinds of cathodes (Ref. 70), thermionic and non-thermionic cathode.

When a cathode is heated to a sufficiently high temperature of T^{o}K, electrons are emitted with a current density J, given by the Richardson-Dushman equation:

$$J = AT^2 e^{-b/T} \qquad (2)$$

where A equals approximately 60A/cm^2(^{o}K)^2 for most metals

$$b = \frac{\Phi_o e}{K}$$

Φ_o is the work function of the cathode surface, e is the charge on an electron and K is Boltzmann's constant. The current density for thermionic emission thus depends critically upon the cathode surface temperature unless it is of a sufficiently high value it is not possible to reach the current densities which are required for thermionic emission. It is only when cathodes are of refractory materials such as tungsten or carbon, which have boiling points of about 4000^{o}K or higher, that thermionic emission can occur. The current density may be 10^3A/cm^2 on tungsten cathodes.

Non thermionic cathode arcs exist with all consumable electrode arc welding processes. When a refractory material is used as the cathode and the emission of electrons from it occurs thermionically, the condition can be reasonably well defined theoretically, i.e. equation (2) can be applied. However other explanations must be used for non-refractory cathodes. Electrons can be emitted from the cathode surface and accelerated from rest by an electric field, Ec, which is due to a positive-ion space charge at the end of the cathode fall region with cathode fall voltage of Vc, a phenomenon known as field emission. Field emission has generally been used to explain electron supply from non-refractory cathodes and requires the application of a large external electric field. The electric field in this region cannot be measured directly but the minimum current densities can be calculated as more than $10^7 A/cm^2$. (Ref. 69). There is another theory, the 'T-F Theory' for explanation of cold cathode emission suggesting that it is caused by the simultaneous effects of electric field and surface temperature. It seems to be satisfactory for explanation of emission and cathode fall current flow for only certain arcs. (Ref. 69). Ecker proposed that the electric field at the cathode surface varies instead of the average field. This can be named 'individual field components emission' (Ref. 69).

The other proposed possible electron liberations are - electron liberation by Auger capture by positive ion proximity, electron liberation by photons, electron liberation by excited or metastable atoms, electron liberation by lowering of work function due to negative space charge inside the cathode metal where it has been suggested that this may be sufficiently lowered for non-thermionic emission to occur, due to the presence of a negative space change in the metal lattice in the neighbourhood of the cathode spot where the current is very high because of the pinch effect. Electron liberation by charging of oxide layers by positive ions has also been suggested. Thin insulating layers such as oxide patches or

dust on a cathode surface can become charged by incident positive ions and if they are charged to the breakdown field of the dielectric, large emission currents can flow (Malter and Pautow, Ref. 69), this mechanism has been connected with 'cold cathode' arcs (Drnyvesteyn, Ref. 69). The positive ion charge may produce a field of about 10^7V/cm across semi-conducting layers (generally oxide). The use of non-metallic coatings which produce thin surface layers of semi-conducting material at high temperature can make possible electrode negative or AC welding because the transferring drop is not moved sideways or upwards. This may be due partly to these surface layers continually giving good new emission sites near the electrode tip so that the wandering of the cathode spot is avoided or limited.

It is noted that the burn-off rate of steel wires in MIG and other consumable electrode arcs with electrode negative is about twice that of electrode positive arcs. No suitable explanation has been given yet.

Another important feature of cathode is the cleaning action of aluminium welding (Ref. 7, 69, 71). A number of emitting sites which move over the metal at random with a speed of nearly 500 m/sec (Ref. 69) and remove Al_2O_3 from the surface. Moving cathode spots remove oxide from the surface of iron and copper is not important.

2.5.1.1.4. Anode fall region (Refs. 20,65,69,72,73)

The anode has been less investigated than the cathode but three things have to happen at the anode, the temperature must fall from that of the arc column to the anode temperature, positive ions must be produced and the ions must be accelerated. The anode drop is very difficult to measure or estimate. Busz-Peuckert and Findenburg gave a figure of 5 to 10 volts, Sugawara reported as 4.2V for a 10A arc and Hamilton and Guile gave values of 4 to 7V in argon and 2.5 to 10V in air. (Ref. 69).

Anode current density has been estimated at 100A/cm^2 to 10^5 A/cm^2. The temperature of anodes has been estimated between 4000 to 7000^{o}K (Refs. 69,75).

2.5.1.1.5. Arc shape

The shape of the luminous region of an arc depends on many factors. It is determined primarily by the energy balance which governs both the size and shape of the arc, the gas composition and metal vapour in particular having a marked effect (Ref. 75,76). Ludwig (Ref. 77) pointed out that high current welding arcs are influenced by the self-magnetic field produced within the discharge which acts to compress or pinch the conducting plasma. The thermal expansion of the plasma opposes the magnetic compression and the geometric form of the discharge is controlled by the interaction of these opposing forces. An arc in a high thermal conductivity plasma such as helium has a spherical expanded arc shape whilst argon arcs have a contracted cone shape.

Glickstein (Ref. 78) stated that vapours of minor elements entering the shielding gas will change the radial temperature distribution. Current density distribution is directly related to the temperature which is dependent on electrical conductivity so that all of these will effect the arc configeration and weld bead shape as well.

Cooksey and Milner (Ref. 76) proposed that the arc shape is determined by two opposite factors: vapour emitted from the electrode tip and the velocity of plasma jet. Figure 12 shows the effect of these two factors. The plasma jet will increase the heat loss from the arc and constrict it, the degree of constriction being an indication of the velocity of the jet. Vapour emitted from the electrode tip will modify the appearance of the arc and, if it is assumed that the properties of the arc are not appreciably altered, three extreme cases can be distinguished.

a) When gas flow in the arc region is limited to velocities below about 100 cm/sec, the velocity of emission and diffusion of the vapour from the electrode causes it to flow in all directions, comparatively unaffected by the velocity of the gas. The whole of the arc region is filled with vapour. (Figure 12a).

b) When there is a high velocity jet associated with the arc, e.g. 10^4 to 10^5 cm/sec, and a low rate of vapour emission, then the vapour flows along and thus delineates the stream lines. If the stream lines in a welding arc were the same as those determined for the 200A carbon arc in air the arc would appear as in Figure 12b.

c) When the electrode has a high vapour pressure the velocity of emission of vapour is comparable to that of a plasme jet. Vapour will then flow across jet stream lines and it is not possible to determine whether a jet exists from the appearance of the arc. From the above explanation it can be noted that the visual arc shape represents the radial temperature gradient. (Refs. 75,76,79,80). The dissociation process reaches a peak at the temperature at which a core is formed inside the arc. This occurs for diatomic gases such as N_2 and H_2 but for monatomic gases, e.g. Ar, no core can be seen. In other words, the visual arc shape represents the radial temperature gradient.

In an arc with consumable wire the bright core of an arc is generally accepted as metal vapour. For the explanation of the vapour emission from the anode surface various workers have made some estimation about the anode surface temperatures. Cobine and Burger took 3750^{o}C as the anode temperature (Ref.79), Mental and others suggested 4000^{o} to 7000^{o}K(Ref. 75) and Watanabe took 4000^{o}K (Ref. 79). At these temperatures the surface exists in boiling state and the metal vapour ejects into the surrounding space perpendicularly to the surface. It is then accelerated by the electrical field to high speed, approximately 2-3x10^4 cm/sec, or 1x10^3 - 7x10^3 cm/sec for carbon anode (Rollason, Ref. 63).

From the explanations mentioned above a reasonable derivation can be deduced. The visual arc shape in the MIG process is mainly determined by the shape of the boiling surface of the anode spot and the amount of the metal vapour which depends on the heat content of the surface, i.e. the temperature distribution beneath the surface.

2.5.1.1.6. Anode Heating

For electrode positive MIG arcs, the anode heating is one of the two heating sources. The measurement and calculation of the anode heating were the aim of investigators for a long time. Based on the knowledge of the arc mentioned above, it is possible to explain how the anode heating was evaluated.

The heat entering the anode comprises the energy of the current carrying electron stream and heat transfer from the arc column. The electron contribution to the anode heating Ha is given by the thermal energy of the electrons at the high temperature of the column, 3KT/2e. plus that required as a result of acceleration through the anode drop Va and the heat of condensation $I\Phi$. Where Φ is the work function of the anode material and I is the current. Heat entering the anode from the hot gases and plasma of the arc column is much more difficult to quanitfy as it will have components due to conduction, convection and radiation. There was less argument about the calculation of anode heating from the electrons than from the gases in the arc column; the typical equation is as follows: (Refs. 81,82,83)

$$Ha = I (\Phi + Va + 3KT/2e) \qquad (3)$$

The main problem is how to estimate the values of these three terms. There are data generally used by different investigators.

The thermionic work function used to be taken between 3.9 and 4.7 Φ, with an average value around 4.4, (Refs. 78,85,86,87), but lower values of 3.48 have recently been suggested, (Ref.84). It would be expected that most of the work function contributes to the melting. The lower value of Φ can be explained partly by the fact that the work function drops about 10^{-4} V/^{o}K, (Ref.84) which amounts to about 0.3V if the surface is near the boiling point. The work function may also be affected by alloying elements. If the wire contains Mn it will also have a work function of 3.8V (Ref.84). However, some reports still adopted 4.4V (Ref.85), 4.2V (Ref.86), 4.5V (Ref.87) and 4.5V (Ref.78)

The term 3KT/2e is determined by the electron temperature in the column. It will contribute a rather considerable part of the total voltage drop. Assuming, for instance, an arc burning in CO_2, the mean arc temperature will be about 6000^{o}K, which means that 3KT/2e has a value of 0.78 - 0.8V. For an argon arc, having a mean temperature of about 10000^{o}K, the value will be 1.3V approximately, (Ref.85). Ando (Ref.87) adopted 0.78V but more recently, Glickstein has used 1.2V (Ref.78).

The values of anode fall used, cover a wide range; they include 1.8V (Ref.85), 0.2V (Ref.87), 3V (Ref.78), and 1.3V for Va and Φ together (Ref.86). The heat generated by the anode potential drop is not considered to contribute to the melting of the electrode wire (Ref.87).

In summary, the voltages contributing to anode electron heating according to different authors are:

$$Va = 0 \text{ to } 3V.$$
$$\Phi = 3.8 \text{ to } 4.5V.$$
$$3KT/2e = 0.78 \text{ to } 1.2V.$$

The total of these three terms, i.e. $Va + \Phi + \frac{3KT}{2e}$, has been taken as 5.3 tp 6.38V by various workers in the field.

Equation (3) is probably a reasonable first approximation. The anode potential drop is very difficult to measure directly. Va used to be assumed to be constant, but experimental data showed that it is true only at low current, e.g. 20A. At high current, e.g. 200A the anode heat input (potential fall) will be influenced by arc length. There is plenty of work in this field (Ref.57). It might be interpreted that the weld pool supplies metal vapour since the negative ions at the anode from the weld pool can increase the negative space charge and potential drop, and hence increase the dissipation of energy in the anode region.

2.5.1.1.7. Joule Heating

Joule heating is usually considered as negligible in the MIG welding of aluminium. For steel, the effect of Joule heating on electrode melting rate has been investigated systematically over 25 years, starting with Wilson in 1956 (Ref.88). Lesnewich (1958) gave an empirical relationship between the wire melting rate and Joule heating for reverse polarity DC welding (Ref.118). His equation was

$$Mm = (a + bd_w)\, I + C\, \rho\, \frac{lI^2}{d_w^{2.6}} \quad lb/hr \qquad (4)$$

where a,b = constants of electrode composition.

Investigation on Joule heating developed quickly after 1960. Apparently the key point is how to get the correct resistance value of the wire extension, and this can be calculated by potential or by temperature distribution. Most of the previous work has been based on these two principles.

Amson (Ref.89) developed a mathematical method to calculate the voltage along the electrode stickout in terms of three variables; wire feed rate v_w, current I, and stickout ℓ. In order to calculate the voltage, the temperature distribution in the stickout should be known first. A complicated calculation based on a series of presumptions was used allowing a simplified voltage relation to be established:

$$v_w = b_o\, I\, (1 + C_o\, \frac{I^2 l}{v_w})$$

where $C_o = b_2/b_o$ $\quad b_o = \frac{\rho_o}{\pi b^2}$ $\quad b_2 = 0.55 \frac{\alpha}{\pi b^2} b_o^2 \; 1^{\mu c}$

Amson assumed that the specific heat and temperature coefficient of the resistivity are constant which is incorrect and will lead to errors.

Ter Haar (Ref.85) proposed a method by which he calculated the mean droplet temperature in gas-wire arc welding. He derived an equation about the Joule heating:

$$\int_{T_1}^{T_2} \frac{C_p \gamma}{\rho} \, dT = 0.24 \; j^2 t \qquad (5)$$

where T_1 is the starting temperature, T_2 is the temperature of the extension tip as a result of Joule heating, and $t = \frac{l}{v_w}$, l, being the extension and v, the wire feed rate. Using numerical integration, a curve of this value against temperature was obtained. Then $\Sigma C_p \alpha \, \Delta T$ can be obtained. The voltage E_1 for a given stickout of 1 is calculated by

$$E_1 = 4.17 \frac{v_w}{j} \int_{T_1}^{T_2} C_p \gamma \, dT \qquad (6)$$

Then, the Joule heating, H_r, is given by

$$H_r = E_1 . I \qquad (7)$$

His result was 3.4m Ω/cm for 1.6mm dia. stainless steel.

Jelmorini, (Ref.86) employed a probe to measure the voltage U between the contact tube and the wire tip. He used a current range from 100A to 220A for 1.2mm dia. mild steel wire and claimed that the resistance was independent of current. He calculated a value of 7.2m Ω/cm for steel.

Halmøy (Ref.84), calculated the Ohmic heating in the electrode extension by a method of graphical integration. An equation of resistivity in terms of stickout, current and wire feed

rate has derived in form of function of heat content;

$$\int_0^{H_L} \frac{dH}{\rho(H)} = \frac{lj^2}{v_w} = f(H_L) \qquad (8)$$

where H_L is the heat content per unit volume at the end of the extension. Then the curve of $\rho = \rho(H)$ (inversed to $\frac{1}{\rho(H)}$) can be obtained from $H = H(T)$ and $\rho = \rho(T)$. Then $\int \frac{1}{\rho(H)} dH$ with respect to H can be obtained by numerical integration; $f(H_L)$.
Known $f(H_L) = \frac{lj^2}{v_w}$, so for every group of given l, j, v_w, there is a value of Joule heating H_L.
In linear region,

$$H_L = a \frac{lj^2}{v_w} - b \qquad (9)$$

When l is substituted by x (position on wire), the distribution of H along the wire extension also is known. The voltage can be calculated by

$$El = alj - b \frac{v_w}{j} \qquad (10)$$

This is a good work on Joule heating calculation. It is correct from the point of view of the presumed situation, i.e. that there is only a pure Joule heating process. However, in practice, there exists another heat source - the anode heating. Anode heating will change the temperature gradient above the wire tip which will be at high temperature. Therefore the conclusion that the resistance of the stickout is nearly constant is not true and must be corrected.

Waszink summarised the previous work on Joule heating (Ref.90) and pointed out that the resistance of the wire extension is an important quantity in the welding process. Reporting measurements and calculations (Ref.83), he established a mathematic model of temperature distribution in the wire extention

$$\frac{\partial}{\partial z}\{\alpha_s(T)\frac{\partial T}{\partial z}\} + C_p\frac{(T)}{s}\gamma v_w \frac{\partial T}{\partial z} + \frac{I^2 \rho_s(T)}{A^2} = 0 \qquad (11)$$

This led to

$$R = \frac{\alpha l}{A} - \frac{\beta Mm}{I^2} \qquad (12)$$

where $\alpha = 1.35 \times 10^{-6}$ m

$\beta = 0.54 \times 10^{-6}$ j kg^{-i}

$Mm = \gamma v_w A$ wire feed rate.

For 1.2mm dia. mild steel wire: 100<I<250A, 25mm<l<55mm, and 15mΩ<R<35mΩ. It should be mentioned that equation (12) is equivalent to (10).

A main conclusion made by Waszink (Refs.83,90) and Halmøy (Ref.84) was that R nearly unchanged with I. This was interpreted as 'an increase in Joule heating being compensated by an increase in the melting rate. The major part of the power required to raise the temperature of the solid metal to the melting point is supplied by Joule heating. The contribution of the power q, which is transferred into the solid by thermal conduction at the solid-liquid boundary, is much smaller than I^2R'.

These works were limited to a current range of 100 to 250A and did not include the usable current range of 250 to 350A. Another limitation of this work is that the metal transfer mode was not considered so that the results can be taken only as a particular circumstance.

2.5.1.1.8. Brief summary

Previous work on Joule heating shows that the power involved in Joule heating of the wire has been described as a major fraction of the total power supplied to the wire, but the exact value of the wire resistance is very difficult to obtain. The main problem is that the temperature distribution in the extension is difficult to measure. In order to establish the extension temperature distribution, different models have been proposed, but without exception, such models were based on a series of presumptions relating to small current ranges. Therefore the results obtained have not been completely realistic.

Further work is required to look for a new approach to obtain the temperature distribution in the extension from the wire directly rather than by presumption or mathematic models. Also, the Joule heating must be investigated over the whole usable current range and the influence of the metal transfer process on the temperature distribution in the wire extension needs studying to find out the influence of anode heating on the Joule heating process.

2.5.1.1.9. Heat Balance, Wire Melting and Drop Heat Content

Wire melting rate is one of the most important parameters of the MIG process. It is the basic variable which has to be controlled correctly in order to obtain stable MIG welding and it is the criterion of the efficiency of the process. It seemed that the calculation of wire melting rate had been sorted out many years ago (Ref.8) and the equation of wire melting rate has remained unaltered. Is it worth examining again?

As for droplet temperature, this is a new field in welding research; so far little data has been reported but the values are quite scattered. It is known the drop temperature (heat content of droplet) is important because the drop temperature greatly influences the temperature of the weld pool and therefore the size and fluidity. The heat content of the drop also has a decisive influence on weld penetration (Refs.86,90,91).

The investigation of both wire melting rate and heat content of the droplets should be based on the analysis of heat balance occurring on the wire tip and hence a correct understanding of the anode heating and Joule heating processes mentioned above. A brief survey on the previous work in these fields is given below.

In 1958 Lesnewich (Ref.8) suggested that the wire melting rate is composed of anode melding rate Ma

$$Ma = Ca\ I \qquad (13)$$

and the melting rate, Mr, due to resistance heating

$$Mr = Cr\ I^2 \qquad (14)$$

where Ca is dependent upon changes in the specific heat of the electrodes, their chemistry and the electrode diameter, and Cr is dependent upon electrode diameter and the electrode resistivity. Then an empirical equation was developed for mild steel wire reverse-polarity DC process.

$$Mm = Ma + Mr = (0.017 + 0.37A)\ I + \frac{3.69\ 10^{-8}}{A^{1.26}}\ l\ I^2 \text{ lb/hr.} \qquad (15)$$

Erohin and Rykalin investigated the heat balance of the electrode and droplet melting process in arc welding (Ref.6). Their balance equation which explained the relationship between the heat consumed and heat sources,

$$Q_d + Q_6 + Q_7 = Q_2 + Q_3 + Q_4 + Q_5$$

where Q_d is arc heating; Q_6, arc column heating to the drop; Q_7, chemical reactions between the drop metal and gases; Q_2, heat for melting the electrode metal; Q_3, evaporation; Q_4, superheating of liquid metal; Q_5, heat lost from a drop surface. The calculation of every item has been given (Ref.6)

e.g. $Q_d = 0.24\ \eta_d VI$

where $\eta_d = 0.2\text{-}0.5$ etc.

Considering Q_6, Q_7, Q_5 could be neglected, the melting efficiency is determined by Q_2. The heat balance has a simplet form $Q_d = 100\%$. $Q_2 = 50\text{-}60\%$, $Q_3 = 20\%$, $Q_4 = 30\text{-}20\%$. They proposed and important conception: for the same Q_d, the melting efficiency can be increased by the reduction of drop superheating Q_4. Hence by forced detachment of the drop, the melting efficiency could be increased by 15% but no further details were given. A drop temperature of 2200 to 2600^{o}K at 100A to 400A with 3mm and 5mm dia. electrodes was suggested.

Pokhodnya measured the heat contents of droplets in MIG welding by calorimeter. (Refs. 93,94). Mild steel and stainless steel wires, 1.2 and 2 mm diameter and Ar, He and CO_2 shielding gases were used. The maximum mean temperature was 2590^{o}C to 2750^{o}C in CO_2 and 2930^{o}C in Ar+N_2, but the calculation was not given.

Ando (Ref. 87) also measured the heat content of droplets of Al, stainless steel and copper by calorimetric means. He adopted a number of assumptions but failed to establish an accurate heat balance. However, there was one point worth noting: his measurements showed that the heat content drops near the critical point where the mode of the droplet transfer changes from globular to spray form. Even though he did not give accurate values or suitable explanation of this phenomenon it was the first time the transfer mode had been connected with drop temperature. The measured heat content of droplets of steel was 1600°C to 2150°C which seems low compared to other results. (Refs. 93,94).

In 1972, Hear (Ref. 85) gave a 'simplified method' of calculation of heat balance which leads to droplet temperature. This simplified approach was more systematic and clear than any previous calculations. Hear suggested the expression

$$Q_{tot} = Q_e + 0.24E_1I \qquad (16)$$

where Q_{tot} is the total amount of heat available for melting and heating, Q_e, the effective anode heating and E_1I the Joule heating in the stickout. The wire melting rate was considered in the calculations of Joule heating and the heat content of each droplet was calculated by

$$H_{dr} = \frac{Q_{tot}}{M_m} \qquad (17)$$

Using a shielding gas of 80%Ar, 15%CO_2, 5%O_2, 1.6 mm wire with 25 mm stickout and a current of 350A, Tdr was calculated as 2250° - 2810°C depending on voltage.

In 1977 Jelmorini (Ref. 86) gave a more systematic calculation of heat balance and droplet temperature both for MIG and plasma MIG welding. He established the heat balance based on his measurements. Heat H is composed of anode heating and Joule heating:

$$H = H_a + H_r$$

then it is consumed on wire melting and evaporation

$$H = H_w + He \qquad (18)$$

When wire feed rate and droplet temperature are known the H is known. H_r can be calculated simply by I^2R. Now the arc heating of the wire

$$H_a = H - H_r \qquad (19)$$

can be known. It is suggested that H_a = 5.5 J/s for mild steel. It means $V_a + \Phi + 3/2e\ KT = 5.5$. He also suggested that Φ = 4.2V. Therefore only 1.3V is left to account for the other two terms. His results gave T_{dr} as 2400°C and nearly unchanged in the current range 120 - 190A, thus comparing well with Hear (Ref. 79).

A further conclusion (Ref. 86) was:

'Linear relationships are found indicating that the resistance of the wire extension is independent of the current'. In fact, this conclusion only covered currents of 100 - 200 amps which relates to globular transfer. It did not include the most useful range of 250 - 350 amps where the spray transfer mode occurs.

Halmøy (Ref. 84, 1979) investigated the heat balance, including wire melting rate, droplet temperature and effective anode melting potential. He established a relationship between Joule heating, wire melting rate, current and stickout by a simple technique of graphical integration:

$$H_L = a\frac{lj^2}{v_w} - b \qquad (20)$$

H_L is the heat content of the extension end. Combining anode and ohmic heating the traditional wire speed equation (15) was used again

$$v_w = K_1 j + K2\ lj^2 \qquad (21)$$

where K_1 and K_2 are constant. Then he used H_o, heat content per unit volume of droplet

$$H_o = H_a + H_L \qquad (22)$$

using these equations and rearranging gives

$$K_1 = \frac{\Phi}{H_o + b} \qquad K_2 = \frac{a}{H_o + b} \qquad (23)$$

Halmøy claimed that K_1, K_2 and H_o are constants, i.e independent of $\dot{J}$, 1, and v_w. Then the H_o and Φ were obtained by experiment

$$H_o = 11.1 \text{ J/mm}^3 \qquad \Phi = 3.48\text{V}$$

This work indicates that the droplet temperature is only slightly above the melting point and keeps constant. However, the conclusion that many of the parameters such as H_o, K_1 and K_2 are constant lacks either experimental evidence or theoretical explanation and, in fact, is not correct.

Recently, Waszink (Refs. 83,90) calculated the temperature distribution in the wire extension and its resistance from the wire current, I, the wire velocity, v_w, the length of the extension, 1, and the wire diameter, d_w. He reported that an 'analysis of Joule heating, anode heating, and heat flow in the wire leads to expressions for mass flow rate and drop temperature as functions of the welding parameters'. (Ref. 83). He established the relationship between the heat balance process which occurs at the wire tip and the relative welding parameters for processes where the wire formed the positive electrode. Based on previous work (Refs. 84,86,90) he reported that power $I\Phi$ is generated at the surface of the liquid tip by electron absorption ($\Phi = 6.0 \pm 0.5$V). Heat is also supplied to the wire by Joule heating, the resistance of R of the wire extension depending on $I, 1, d_w$. For a given wire material, consequently, the latter four parameters govern the total power, p, supplied to the wire

$$p = I^2R + I\Phi \qquad (24)$$

The ohmic power developed in the solid part of the wire is, in general, not sufficient to raise the temperature of the material from room temperature to the melting point and to melt it. Consequently, there must be a flow of heat from the anode spot to the solid, though the liquid tip. If this heat, thus transferred, is denoted by Q, the melting rate is

then determined by the total power supplied to the solid, i.e. $I^2R + Q$. The drop temperature is determined by the remainder of the power generated at the anode surface, i.e. $I\Phi - Q$, if heat losses by evaporation and Joule heating in the drop are neglected. Consequently, the drop temperature is also a function of I, M_m, and d_w only. R was calculated with the method reported before (Ref. 90) and Q was derived from experimental results which include the measurement of current and wire melting rate.

The main equations for the calculation of R are as follows

$$C_p(T)\gamma\ v_w \frac{\partial T}{\partial Z} + \frac{I^2\rho(T)}{A^2} = 0 \qquad (25)$$

$$\frac{I^2 l}{Mm} = F(T_o) \quad ; \quad I^2R = Mm(T_o)$$

$$T_o = 1042^oK \qquad (26)$$

A curve of H = F(T) can be drawn from the results. From this curve can be derived

$$H = \alpha F - \beta \qquad (27)$$

then

$$R = \frac{\alpha l}{A} - \frac{Mm}{I^2} \qquad (28)$$

$$\dot{Q} = \dot{M}_m \{\Delta H_m + H(T_m) - H(T_o)\} \qquad (29)$$

$\dot{Q}$, heat flow from anode spot to the solid wire.

Figure 13 shows the ratio of Q to the total power supplied to the solid wire. It shows that Q is the major source of heat at low l and low I, while it becomes less important as l and I increase. Waszink mentioned that the dependence of Q on the welding parameters was found to be essentially different for globular and spray transfer, but no details were given.

The work of Waszink on heat balance is the most up to date: he gave a complete concept of the relationship between arc

heating, Joule heating, wire melting rate and drop temperature, and linked them to the welding parameters. His work makes a real contribution to the fundamental research of MIG welding but there are some shortcomings worth noticing.

(a) The influence of the metal transfer mode on heat balance was not considered enough. The metal transfer processes were neglected. No further observations on metal transfer were given, even though Q was found to be dependent on the transfer mode. The analysis of heat balance consequently has not been connected with transfer mode at all.

(b) The calculation of wire resistance was still made by the previous method. As commented previously the temperature was calculated by a mathematical model and the influence of the metal transfer mode was not considered.

2.5.1.1.10. Brief Summary

The relationship between heating sources and heat consumption such as arc heating, Joule heating, wire melting and drop superheating has been established by several workers in recent years. Much progress has been made in linking these parameters but a number of problems remain.

i) The correct temperature distribution in the wire extension: Without correct temperature distribution it will be impossible to obtain the actual resistance of the stickout.

ii) The ratio of the heat energy distribution between the heat consumption of wire melting process and the heat consumed on liquid metal superheating.

iii) A correct understanding of the mechanism of metal transfer.

So far these three problems have not been worked out perfectly. For temperature distribution, no direct method of temperature measurement of the wire itself has been developed. For heat distribution, which should be connected with wire melting

rate, the wire melting rate has been measured only approximately so that details have not been established. Finally, the most important point, all of these phenomena should be based on the real metal transfer mechanism.

It is readily to be understood that the mechanism of metal transfer should be the foundation of all these heat processes which occur at the wire tip, but the metal transfer has not been given enough attention. Some results have been established but investigations have not progressed. In 1962, Erohin and Rykalin noticed that the manner by which the drop stayed at the wire tip could change the drop temperature. Then, in 1969, Ando 'presumed' that the heat content had a minimum value at the critical current at which globular changed to spray transfer. Recently, Waszink observed that the supplementary anode heating to the wire melting Q is influenced by metal transfer mode. All of these individual observations have not been linked together or investigated systematically which is essential for a correct heat balance analysis

2.5.1.2. Metal transfer mechanism

Mass flow,in one form or another, is an essential feature of most welding processes and is particularly important in arc welding using a fusible electrode, where the electrode is at one and the same time a heat source and a source of liquid filler metal. The manner in which the liquid metal transfers from the electrode to the weld pool has been the subject of much research.

The present literature review is limited to the metal transfer process of MIG welding.

2.5.1.2.1. Classification of metal transfer on arc electric welding process

Classification of metal transfer in arc welding has been examined in International Institute of Welding (IIW) documents, resulting

in a final document in 1972 (Ref. 95). The main point is as follows.

Observation by high speed photographic and oscillographic techniques established that there were different types of material transfer which could be classified in either of two ways which, although essentially different, in many respects are associated. These two ways are either to define the transfer according to the principle active agent (such as gravity or short circuit) or according to its physical characteristics and appearance (such as size and frequency). The document gave several reasons to explain why its classification was based on phenomenological categories rather than physical mechanisms (Ref. 95).

(a) The physical mechanisms are not sufficiently known. In spite of a large amount of research work already devoted to metal transfer, only a part of the observed phenomena can be explained in quantitative terms.

(b) Most of the observed types of metal transfer are due to several forces. To decide what force is the dominant requires a knowledge of the process not only on a qualitative but also on a quantitative basis. This knowledge is in part still missing.

(c) A classification based on the phenomenology of the processes is to be preferred because phenomena (size and frequency of droplets, short circuits, etc.) can be observed more easily than forces.

(d) A classification system based on phenomenological observable phenomena are the basis of further work to define the different forces in more detail.

Ref. 95 shows the proposed classification of metal transfer. Globular transfer is characterised by droplets substantially larger than the electrode diameter detaching themselves at low frequencies. In drop transfer, the electrode tip melts until the weight of a droplet exceeds the restraining force

of surface tension. This type of transfer takes place in low current density processes and the dominant force governing detachment is gravity. Spray transfer is characterised by droplets smaller than the electrode diameter detaching themselves at high frequencies. Electro-magnetic forces are the dominant factor in this transfer mode, occurring especially with high current density processes. However, other forces such as mechanical or aerodynamic forces may equally cause spray transfer. The current value above which spray transfer takes place is known as the threshold or critical current. Projected transfer; in projected transfer, droplets are detached before they grow too large and are projected with considerable velocity. The molten tip of the electrode has no tapered shape. Streaming transfer is a special type of projected transfer. A characteristic feature is the tapered electrode tip from which a rapid succession of small droplets detach themselves to give the appearance of virtually a continuous stream of liquid. Rotation transfer is achieved with high current densities and a long length of protruding electric wire or by plasma heating of the electrode. As indicated above, this classification lacks the accurate explanation of the physical mechanisms. However, there are some vague conceptions particularly in terms of mechanisms such as gravity or short circuiting transfer. Many observations have been reported (Refs. 76,96,97) on different kinds of metal and their alloys, indicating spray and globular transfer modes in Ar. Six systems were reported. In Type 1, large drops developed and detached with little influence of arc forces; examples are transfer of most metals in Ar at low currents with electrode positive. With Type 2, the drops were much smaller than Type 1 and occurred in the high current welding of Al and Cu in Ar with electrode positive. The drop in Type 3 was distorted, lifted or repelled from the plate and occurred with electrode negative polarity with the low melting point metals being associated with the formation of a cathode spot. With Type 4,

the end of the electrode was tapered and a fine spray of drops streamed off. Typical examples were the high current transfer of steel and Ni in Ar with electrode positive. Aspects which were not explained by existing theories were the tapered electrode end and the streaming of the molten metal along the taper. In Type 5, the molten metal from the electrode tip streamed off in an upward direction associated with pronounced vapourisation of the electrode tip material. This type of transfer occurred with the high vapour pressure metals, Mn, Zn, Ca, etc. For Type 6, the drop and arc moved sideways and the neck was thrust in the opposite direction.

Lancaster (Ref. 10) and Haberlin (Ref. 98) proposed that for 1.2 mm steel MIG process (Ar based shielding gases) the transfer modes were globular under 190A, spray from 190 - 250A, stream from 250 - 325A and, over 345A, rotation. (Figure 14).

2.5.1.2.2. Model of metal transfer mechanism

In order to investigate the metal transfer processes quantitatively, it is necessary to establish a physical model to show the relationship between the geometric dimensions of the wire tip, anode spot position and liquid metal movement. Based on the model, calculations can be carried out so that the function of the model is to link the physical phenomena and theoretical analysis. Therefore to establish a correct model is of great importance.

One of the early models was proposed by Greene et al (Ref. 110), Figure 16. If the current lines diverge in the drop the Lorentz force which acts at right angles to these current lines has a component aiding drop detachment. If the current lines converge, a component of the Lorentz force opposes detachment. Serdjuk (Ref. 111) proposed models for globular transfer, Figure 17a, and spray transfer, Figure 17b. The taper was assumed as being formed by liquid metal completely, as liquid metal flowed downwards along the liquid conic surface. The

arc root covered the whole conic surface. All of Serjuk's qualitative analysis of the metal transfer mechanism was based on this assumed model. Amson (Ref. 112) proposed a model, Figure 18, with the solid liquid interface in a similar position to Serdjuk's.

Ando (Ref. 87) proposed that the liquid-solid interface was of conic shape and assumed that the conic taper was caused by the heat conductivity of the wire, Figure 19.

Matsunawa (Ref. 70) proposed a 'simplified model of an electrode tip', Figure 20, and assumed that the anode root covered the whole liquid metal which comprised the entire conic tip. He derived a complicated equation of the acting forces and interpreted some phenomena of high pressure Ar arc welding processes.

Hiltunen (Ref. 113) reported on the inner circulation of the droplet in the MIG/MAG welding with an unusual model, Figure 21. Finally, Waszink has recently proposed a new model of globular and spray transfer (Ref. 83). Figures 22 and 23 show his models of globular transfer. A notable difference was a region of solid together with liquid metal existing in the wire just above the drop. Figure 23 shows the solid-liquid interface shape, position and anode surface. Figure 24 shows his new model of spray transfer in which the concept that the liquid metal flows downwards along the conic surface is adopted again.

2.5.1.2.3. Brief Summary

Over some 20 years, many models of metal transfer were proposed. Based on these models, the metal transfer process, the acting forces, the drop movement and the heating processes have been analysed and calculated. Unfortunately, none of these models were based on much experimental evidence. It is surprising that such an important aspect of arc welding has been established mainly on presumption with insufficient

experimental evidence. If the models are inadequate they will become an obstacle to further development of MIG fundamental research. Therefore, it is essential to establish a more reasonable model of metal transfer mechanism based on experimental observation.

2.5.1.2.4. Acting forces during metal transfer process

An IIW report (Ref. 95) proposed the forces governing metal transfer in the arc region as follows:

(a) Gravitational forces;
(b) Electro-magnetic forces (including so called pinch effect and related interactions);
(c) Surface or interface tension;
(d) Mechanical forces (externally induced vibrations, etc.);
(e) Forces due to vaporisation (including forces caused by chemical reactions, formation of gas bubbles, etc.);
(f) Aerodynamic forces.

These forces can be dominant, secondary or absent; for example, gravity gives a positive contribution to detachment in flat position welding but not in the overhead position. Electro-magnetic forces, which play an important role in metal transfer, are more dominant in spray transfer or short circuiting transfer than in large drop transfer and play an important part in bridging transfer.

Lancaster (Ref. 62) also described the forces which cause the transfer of metal from a fusible electrode, the following are the most important:

i) Surface tension;
ii) Gravity;
iii) Electro-magnetic force;
iv) Hydrodynamic forces due to gas flow.

Later (Ref. 10), he emphasized again the surface tension, the Lorentz force, gravity and the drag force stemming from

plasma flow. Watanabe (Ref. 79) counted the following forces as most significant: gravity, electro-magnetic force, surface tension force, repulsive force by oxide vaporisation.

There was less argument about the principle of the calculations of these physical qualities.

Electro-magnetic force (Refs. 56,73,105)

The electro-magnetic force (Lorentz force) is due to the interaction of the electric current with its own magnetic field. In a cylindrical conductor there is a radial compressive force due to the self induced magnetic field which is zero at the surface and increases to maximum in the centre. For a solid conductor with constant current density j across its section the magnetic force per unit area is

$$F_p = \frac{Ij}{100}\left(1-\frac{r^2}{R^2}\right) \text{ dynes cm}^{-2} \qquad (30)$$

where I is current, r, radius at any point, R, radius at the boundary of the conductor. When the conductor is of conic shape, the difference of pinch force at two cross sections will cause an axial component force which equals to

$$F_m = I^2 \log \frac{R_1}{R_2} \times 10^{-2} \text{ dynes} \qquad (31)$$

R_1 and R_2 radii.

Surface tension force F_s (Ref. 29)

$$F_s = 2\pi R\sigma \qquad (32)$$

R, radius of boundary between solid and molten drop,

σ, surface tension force.

where
$$\sigma = 2.1\frac{T_1 - T}{\left(M\frac{1}{\gamma}\right)^{2/3}} \qquad (33)$$

$$T = 3/2\ (T_{boiling})^{\circ K}$$

M, molecular weight,

γ, specific gravity.

Gravity force F_g (Ref. 62)

$$F_g = g\gamma M_{dr} \qquad (34)$$

g, acceleration due to gravity,

γ, density of steel,

M_{dr}, volume of liquid drop.

Drag force by gas flow F_{gf} (Ref. 96)

$$F_{gf} = \frac{1}{2}D(1+(R^2 - d_w^2) / R^2) \qquad (35)$$

$$D = 14.5\ \nu_g^{3/2} R^{3/2} \gamma_g^{1/2} \eta_g^{1/2} \qquad (36)$$

where ν_g, gas velocity. η_g, gas viscosity. γ_g, gas density.
R, radius of drop. r, radius of wire.

Repulsive force of oxide vaporisation F_R (Ref. 99)

$$F_R = m_v V_v \qquad (37)$$

m_v, mass of vaporised oxide,

V_v, velocity of vapour.

Compared with heat balance, the dynamic analysis of metal transfer is insufficient. Systematic investigation, particular linking with welding variables, is still required.

In order to interpret the detachment process of the molten drop from the wire tip by analysis of the behaviour of these forces quantitatively, first of all the value of these forces have to be chosen properly. All the forces are determined by the geometrical shape and dimension of the wire tip and molten metal. Every researcher has given his explanation by his own model of the transfer mechanism.

Serdjuk (Ref. 111) regarded the pinch force, F_{pinch}, and the surface tension force, F_s, as the determining forces for the drop surface between solid and liquid phase of the electrode metal

$$F_p = F_s \qquad (38)$$

He assumed that a 'taper stream' (Figure 17b) occurred on a liquid conic tip. Based on this model some equations were established. Watanabe (Ref. 79) gave an equation to express the forces condition of drop detachment. There are four forces involved

$$F_g + F_m - F_s - F_r = 0 \qquad (39)$$

The main feature of his theory was that the vaporisation of oxides from the surface of the molten electrode tip should be considered as a factor which governs the transfer mode. In globular transfer the repulsive force induced by oxide vaporisation which pushes up the droplet was found to be greater than the gravity force. According to his calculation the repulsive force was about one tenth of the electro-magnetic force and roughly equal to the gravity force.

Matsunawa (Ref. 70) calculated the detachment condition of detachment by electro-magnetic force based on his assumed mechanism (Figure 20). He considered that the forces were function of taper index, α, (Figure 20). The detachment force F_m of molten metal increases with the increase of α and tends to be a constant value. He derived the force acting on the plasma F_p and claimed that F_p is always much larger than F_m. Because the plasma has viscosity, and a part of F_p will act as a metal detachment force by friction. So his conclusion was that the resultant detachment would be accelerated with increase in taper index.

Lancaster (Ref. 10) reported that the theory of instability has been applied to drop detachment in MIG welding and a relative model of a liquid cylinder carrying an axial electric current has been established. It seems there is still a long way to go with this theory.

Needham, Cooksey, Miliner (Ref. 96) postulated that high velocity plasma jets in the arc were responsible for the drop detachment in high current density welding arcs. The proposed mechanism was that the plasma jet exerts a force

on the globule as it forms on the end of the electrode wire, and when this force exceeds the restraining force of surface tension the globule begins to pull away from the electrode, the acceleration increasing as the area of the restraining neck decreases and thus exposing more of the globule to the jet. After the globule has become detached from the electrode it accelerates freely under the action of the jet to a terminal velocity which is determined by the force on the globule and the distance over which this force acts. This work was limited to aluminium. Lancaster disagreed with this theory (Ref. 114). The assumption that gas flowed down the electrode over the drop at the tip and the drag of the gas flow on the drop surface reached a high enough value to overcome the restraining force of surface tension was very unlikely to be correct. The flow would be most likely to occur in the manner indicated in Figure 25b and take the easiest path and flow radially, a direction which would not give rise to any detaching tendency. In other words, the important point to note was that in the present case gas flow would not develop a positive detaching force.

2.5.1.2.5. Brief summary

The metal transfer process is essential for arc welding using a fusible electrode. The manner in which the liquid filler metal transfers from the electrode to the weld pool has been the subject of much research. Work has been carried out in this field, different models were established, calculation and interpretation of metal transfer mechanism based on these models was reported. However, the theories varied and the proposed models were often completely different from each other. Most papers took the electro-magnetic force balanced by the surface tension force as the dominant acting forces of the detachment mechanism. Some noteworthy assumptions and observations were reported, but these ideas have not been connected yet with the physical processes of MIG welding. In other words, the systematic theory which links the mechanism model, acting forces and their calculation together with welding variables has not been established.

The key point is the establishment of a metal transfer model which can represent the real metal transfer mechanism at the wire tip. The observation of the metal transfer process is very difficult because of rapid changes in the complicated electro-magnetic, mechanical and thermal processes that occur in a very small region. Therefore the research approach has to be improved.

2.5.2. MIG Welding with Pulsed Current

2.5.2.1. Pulsed MIG process

So far there are only a few reports dealing with the heat balance and metal transfer analysis under pulsed current conditions, most work is limited to selection of parameter combinations, much of it on aluminium. Relatively few papers consider pulsed MIG welding of mild steel.

Reports (Refs. 7,9,28,106, 109-111) on parameter function, parameter combination and parameter adjustment have used empirical methods to establish the operating envelope of four main parameters and the level and duration of peak current and base current. The criteria for envelopes defined in pulsed MIG mainly contain two aspects. First, the metal transfer idea of 'one drop per pulse' was interpreted as 'artificial spray transfer'. However, none of the work using this concept gave any further information about either the real meaning of the so called 'one drop per pulse' or any experimental results about the metal transfer process under pulsedcurrent conditions. Thus nobody explained the relationship between 'spray transfer' and 'one drop per pulse'. Another criterion was that the wire feed rate had to match the melting rate under condition of 'one drop per pulse'. Once again the relationship between wire melting rate and the other four main parameters was established by empirical methods. Some effort was made to establish an equation for the calculation of wire feed rate by the setting of four pulse parameters (Refs. 29,118,119,120):

an example was 'synergic' MIG welding. The same problem arose, because of lack of basic knowledge of metal transfer and heating balance of pulsed current MIG welding, none of the established equations can represent the real process and the relationship postulated by The Welding Institute for 'synergic' MIG, cannot be reproduced in practice. However, it must be admitted that the assumptions are good enough to have given an improvement in pulsed MIG welding including a successful example of adaptive control with AC (Ref. 121).

Some of the work was concentrated on the method by which the pulse parameters could be obtained by calculation. Needham (Refs. 9, 34) reported that with pulse control the individual droplet transfer was highly reproducible and that the size and velocity of the transferring droplets could be altered independently of the mean current and wire feed speed. The drop size was given directly by the wire feed and pulse frequency whilst the transfer velocity was dependent on the ratio of the pulse to the background or premelting current levels. Afterwards, Partington and Needham (Ref. 122) tried to find out some general relationship between the 'given size of droplets' and the pulse parameters with Al. Their work was also carried out experimentally. The analysis of the data indicated that for a given pulse duration the increase in the square of the current required for detachment was proportional to drop mass. It was suggested that controlled transfer implied the displacement of the liquid mass through a fixed distance and hence the impulse applied by the current pulse was defined by the change of momentum required in the pulse time concerned. On this basis the main distinction between subthreshold and spray transfer is one between a static and dynamic balance of forces and for controlled transfer of a drop of mass, m, the current for a practical range of values is given by

$$I = \sqrt{\frac{m}{K}\left(\frac{2S}{gT_p^2} - 1\right) + C^2} \qquad (40)$$

S, distance. C, threshold value of I. T_p, pulse time.

This hypothesis has not been developed subsequently.

At the same period, Paton et al (Ref. 29) carried out some theoretical analysis on the metal transfer in pulsed processes. He offered an equation for pulsed current calculation by which artificial spray transfer could be achieved. It is worth noting that he linked the metal transfer force analysis for steady current with the MIG process under pulsee current. When the condition

$$F_m \geq F_s(T) \qquad (41)$$

was fulfilled, a neck will be formed and drop detachment occur. The temperature distribution of the wire tip can be calculated as

$$T(X,t) = 660\ e^{-15.8}{}_x\ e^{17.1\ t} \qquad (42)$$

and it is known that

$$F_s = F\ (T) \quad \text{and} \quad F_m = F\ (I)$$

Thus the condition of $F_m \geq F_s$ can be obtained at every I by sufficient t. In other words, the necessary current level and its duration of pulse for controlled metal transfer can be obtained. The most valuable idea of this work is that the metal transfer theory of steady current was introduced into pulse process analysis. However, only the forces of F_m and F_s have been considered and the mechanism of metal transfer and its difference from steady current was not examined. Additionally, there was too little experimental evidence given to support the theory.

Potapevskii et al (Ref. 123) examined aluminium, copper, stainless steel and carbon steel. He proposed a conception of 'pulse energy' which 'governs force magnitude and duration, and the pulse frequency'. He gave a schematic drawing, Figure 26, but no more details about parameter calculations have been given.

Paton (Ref.124) established equations of 'necessary current pulse amplitude' and 'necessary current pulse frequency'. He presumed that the amplitude of the current pulse does not greatly depend on the welding conditions but is governed by the nature of the electrode wire metal, the dimensions of the wire, and the radius of the arc column so that it may remain unchanged during the welding process. The frequency of the current pulse depends substantially on the welding conditions. However, he still used the conception of 'the diameter of the transferred droplets can be prescribed'. This work was used to establish an automatic control system of pulse MIG.

Needham (Ref.125) investigated the effect of pulsed current on the steel/CO_2 welding process. The conclusion was: 'in general for CO_2 shielding there is no advantage over steady current operation'.

Lenivkin (Ref.120) established the envelope of pulse MIG in the given welding method by several equations. He did not pay attention to the basic process of metal transfer other than mathematic calculation.

Heiro and North (Ref.126) measured the droplet temperature during pulsed arc welding in 1976. This was the first time in research of pulsed MIG that an experimental approach similar to that used for steady current MIG was applied. He proposed a concept of 'pulse energy' again.

$$E = I_p V_p T_p \qquad (43)$$

E, pulse energy, I_p, peak current, T_p peak duration.

Then he gave the data of the drop temperature proportional to this pulse energy and inversly proportional to pulse frequency. He did not do much observation on metal transfer. His peak time range was 5 to 100 msec and the drop size seems to have been similar at various conditions. Some of his data correlates poorly with currently accepted values.

Buchinskii (Refs. 127, 118) investigated the parameter selection of steel wire pulsed MIG in argon-base mixtures. He only gave some envelopes of parameters established by empirical methods, e.g. T_p = 2.5 - 5 msec, I_p = 1.8 - 2.8 $I_{critical}$, f = 25 - 100 Hz. It should be pointed out that these figures are reasonable even-though no analysis was given. This will be demonstrated later in the present work.

Araya (Ref.128) investigated pulsed MIG of aluminium using a transistor controlled power source. He used 'one pulse one droplet' as the criterion of controlled MIG and an equation

$$T_p \cdot I_p^k = \text{constant} \qquad (44)$$

was proposed. It was the first paper to propose that the drop detachment can occur during the base current period. The drop shape was also found to be changeable. However, no theoretical interpretation has been given in this report.

In 'Synergic MIG Welding', proposed by the Welding Institute, (Refs.53-55) no theoretical interpretation has been given but 'one drop per pulse' was taken as the criterion of 'artificial spray' transfer. The burn-off characteristic with pulsed current was presumed to be linear, pass through the origin, and be coincident with the burn-off curve of steady current at 8 m/min. One of the conclusions was that the drop volume could be chosen arbitrarily by the 'unit' pulse with any wire feed rate. The given pulse duration range was 4 to 28 msec (Refs. 53-55) but it will be shown later that under such pulse duration it appears impossible to get 'one drop per pulse' transfer.

2.5.2.2. Brief summary

Few papers on pulsed MIG welding deal with fundamental aspects and the heating process and metal transfer phenomenon of pulse processes are far from understood. In fact, this field has still to be explored. So far, parameter selection for pulsed MIG has mainly been established by empirical means. The only proposed criterion of controlled MIG is that of 'one drop per pulse'.

In order to improve pulsed MIG further, it is necessary to get a better understanding of the basic physical process and to establish heat balance and a metal transfer analysis.

2.5.3 Summary and Discussion

The application of MIG welding with consumable electrodes has developed rapidly in recent years. At the same time fundamental research on the MIG processes has been carried out with the purpose of improving the understanding of this welding process. However, improvements in weld deposit quality are desirable. The main shortcomings of the original MIG processes which have to be improved are arc stability, spatter and fume generation, mismatching between the transfer mode and the desired current range, and positional welding characteristics. Some individual innovation has been made but a real breakthrough which can improve all of the above problems effectively has still to be made.

The reason for this unsatisfactory situation can be ascribed to the arrangement of research on MIG welding, since gaps occur between the various aspects under investigation. These gaps arise because of the multidisciplinary nature of arc welding and difficulties in communication between specialists. Thus physicists and engineers working in arc physics, weld pool metallurgy and equipment design fail to take account of advances made in complementary areas.

Arc physicists have often developed detailed theories of arc behaviour and metal transfer characteristics based on minimal (and sometimes outdated) experimental evidence and over-simple assumptions, frequently shrouded in complex mathematics. Two examples will suffice to demonstrate the problem: use of data accumulated with water cooled electrodes and the limitation of metal transfer modes to globular and spray, separated by a clear transition point. The result has been that work to enable operating parameters to be selected without empirical experimentation has been little used and pulsed MIG welding has found little application.

A second gap can be found between metallurgical research into weld deposits and metal transfer investigations despite the importance of the heating process, the metal melting and the chemical reactions that occur during the transfer to the metallurgy of the welds. The exact form of metal

transfer could well be of critical importance to the properties and structure of the resultant weld metal.

Equipment design is a problem, particularly with modern transistorised power sources, since the exact requirements of the welding engineer often fails to be imparted to the power source designer. This has resulted occasionally in sets which fail to perform well or which are too expensive.

Finally, pulsed MIG welding has been investigated as if it bore no relationship to continuous current MIG. This approach has restricted the theoretical understanding of the pulsed MIG process. So far the only proposed criterion of controlled MIG is the 'one drop per pulse' concept and the real metal transfer process has never been mentioned. A simple concept of 'one drop per pulse' is meaningless in that it includes the globular transfer mode which is just the transfer mode to be avoided by the pulse technique. An investigation of metal transfer in pulsed MIG welding related to the transfer observed in continuous current MIG welding is essential if real 'controlled transfer' MIG welding is to be achieved and this investigation has been a major objective of this work. To achieve this objective further studies on continuous current MIG welding using a genuinely constant current MIG power supply has been necessary. The result of the work has been to fill in at least one of the gaps mentioned above and provide a sounder base for further developments in controlled MIG welding.

CHAPTER 3 - EXPERIMENTAL TECHNIQUE, EQUIPMENT, MATERIAL AND ERROR ANALYSIS

CHAPTER 3. EXPERIMENTAL TECHNIQUE, EQUIPMENT, MATERIAL AND ERROR ANALYSIS.

3.1 Research Programme Design

3.1.1 Basic aims of work,

The basic aims of the present work were:

1. To further develop the theory of metal transfer phenomena and heat balance of DC MIG processes;
2. To establish some fundamental research into the pulsed MIG welding process;
3. To establish a conception of controlled MIG based on the knowledge obtained above;
4. To look for some possible applications of these developments, e.g. positional operation, automatic control of MIG, etc.

3.1.2 The principle of approach adopted.

Usually the scientific results depend on the approach adopted and in particular new ideas should be based on a new research approach. Sometimes the traditional conception of a phenomenon has persisted for many years even though it is inadequate or incorrect. A reason for this persistance is that the approach has not been improved. In the present work several principles, given below, were adopted.

1. Every derivation must be based on real processes, observational results or experimental data. Presumption based on imaging is not sufficient.
2. Knowledge of steady current should form the basis of pulsed current investigation.
3. The existing theory of steady current MIG must be checked completely by experimental observation.
4. Metallurgical observations can be correlated with arc physics data.
5. A temperature measurement system should be established to obtain the temperature from the wire extension directly.
6. Theoretical interpretation should be related directly to operational characteristics and welding variables; the possible application prospects should be considered.

3.1.3 Research programme

The research programme developed from the above pronciples is presented in Fig.27.

3.2 Equipment

3.2.1. Power Source (Ref.129)

The AWP M500 transistor regulator provides direct closed loop control of the welding current, in the range 5-500A and at frequencies in the range 1 Hz to 10 kHhz. The main technical characteristics of the AWP M500 are:

1. Input voltage: 380/440 3 Phase, 50 Hz. maximum open circuit voltage 55V DC.
2. Output characteristics Arc voltage DC current-voltage relationship variable between constant current and constant voltage.
3. Current rise time variable between 0.1 - 10 msecs in 0.1 msec steps.
4. Welding current control: current levels in range 0-500A in 1A steps with accuracy of $\pm$ 0.5%.
5. Pulsed current control; pulse peak 0-500A in 1A steps, Peak time 0.001 to 9.999 secs in 0.001 second steps. Background time 0.001 to 9.999 secs in 0.001 second steps.
6. Reproducibility and accuracy. (see Figure 95)
   Current: $\pm$ 1% at full scale setting.
   Timing: $\pm$ 0.5% for each control.

3.2.2 Wire feed unit.

The wire feed unit employed was a BOC TF2.0. It provides a continuously variable wire feed speed from about 0.5m/min to 16m/min. The wire is fed through a flexible conduit from the wire feed unit to the torch, together with the welding current conductor and water cooling pipes.

3.2.3 The test rig.

The test rig (Fig.29) consisted of a transverse table capable of moving in one direction of the horizontal plane with speeds continously variable from 0.06 to 0.27m/min. A portal frame held the welding torch above the table and provided it with horizontal and vertical movement. An adjustable

built-in scale allowed the setting of the nozzle-work distance. The relation between table speed setting and actual table speed was;

$$T_s = 1.41 + 2.56\ N_s \text{ cm/min}$$

where T_s table speed, cm/min

N_s table speed setting

3.2.4 Control of arc length and stick-out.

Arc length and stick-out were controlled by projecting a magnified arc image (magnification of 5) on a calibrated screen. A 135mm focal distance lens was used (Fig.29).

3.2.5 Water cooling system.

Two separate water cooling systems for cooling the torch and power unit were used.

3.2.6 Photographs.

Black and white 35 mm photographs of the arc were taken, using the following settings;

shutter speed 1/60 sec and 1/250 sec,
lens aperture f 11 and f 5.6.
One heavy density filter was used.

3.2.7 High speed cine film.

Using a high speed cine camera Fastex 16mm black and white films of the arc were done using filming speeds of 5000 and 7500 frames per second.

3.2.8 Current and voltage records.

Throughout all the work an Ultraviolet Oscillograph (UVO) recorder was used for recording arc voltage and current.

For instantaneous phenomena observation of the metal transfer processes, a Transient Recorder model 513A was employed. It was used for monitoring the voltage and current by displaying on an oscilloscope. UVO records of current and voltage were also obtained through the transient recorder.

Mean welding current and wire feed speed were monitored and measured, at any time, with the power source meters.

Figure 30 shows a diagram of the instrumentation layout and Figure 28 the instrumentation rig.

3.3. Materials

3.3.1 Wire electrode.

Mild steel wire, BOC Bostrand LW 1 of 1.2mm diameter was used. It was copper coated, with a nominal composition (%):

C	Si	Mn	P	S	Cr	Mo	Ni	Al
0.08	0.93	1.45	0.013	0.019	0.07	0.05	0.06	<0.01

B	Co	Cu	Nb	Sn	Ti	V	W
<0.001	0.01	0.22	<0.01	0.009	0.006	<0.01	<0.02

3.3.2 Base material.

All test welds were made on mild steel plates of 300 x 50 x 15 mm.

3.3.3. Gas supply.

The 'Argoshield 5' (Argon with 5% CO_2) was supplied from a K size cylinder. Gas flow was monitored and regulated by means of tapered tube and float devices. Gas flow rate: 20 l/min.

3.4 Error Analysis

All experimental measurement and theoretical calculation is subject to error and in this section an attempt is made to outline the accuracy sought in the work and possible sources of error.

3.4.1 Measurement errors.

1. Current readout on power source should be correct to 2% after correction according to the measured deviation.
2. Arc length control. The arc length was controlled by monitoring the arc image on the screen. The magnification of the projecting system was 5 times. The possible error of measurement of the image was 1mm approx. Therefore, the possible error on real arc length was

$$\delta\, 1\% = \frac{\Delta 1}{1} = \frac{1}{5} \times 1\text{mm} \times \frac{1}{10} \times 100\% = 2\% \quad \text{(arc length = 10mm)}$$

3. Droplet volume (diameter, mass, etc.) The drop volume was calculated by

$$M_{dr} = \frac{v_w\, \Delta t.A}{N}$$

where Δt considered time lapse

N number of droplets within Δt

If the timer error of the high speed camera is negligible, the error of drop volume δM_{dr} can be considered negligible comparing with whole experimental procedure because the number of droplets was very easy to count.

3.4.2 Droplet velocity V_{dr}.

The mean velocities were calculated by

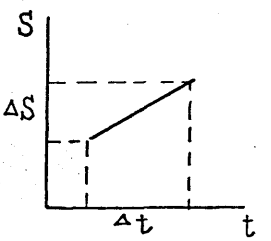

$$V_{dr} = \frac{\Delta S}{\Delta t}$$

where S considered travel distance of droplet
t time lapse.

The measurement of distance was carried out by magnified arc image, therefore the error can be kept to less than 2%. The accuracy of Δt depends on the camera timer. The total error may be estimated as no more than 5%.

The instantaneous velocity error could be larger because the lapse between two frames is 0.143 msec: any change of velocity within this timelapse cannot be discovered. The instantaneous velocity was measured by the trend of several points of drop position. The error of instantaneous velocity might be considered up to 10 - 20%.

3.4.3 Resistance of wire extension.

Resistance of the electrode extension was calculated by

$$R = \int_0^1 \rho(T)dl$$

The main error in resistance was caused by the error of temperature distribution which was determined by four temperatures. The two temperatures between current contact tube and melting front were determined by metallographic: recrystallisation temperature. Assuming the error of these critical temperatures was 10% or 150°C (in fact the error of temperature estimation might be $\pm$ 50°C maximum, i.e. 3%)

From Fig. it can be seen that the error of integration will be less than 10%.

Considering the error of area OACDB to OAB equals

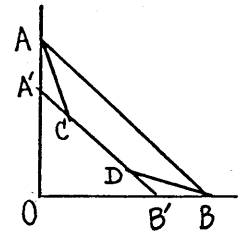

$$\frac{OAB - OACDB}{OAB} \times 100\% =$$

$$\frac{1/2\ (1/2\ (OA \times OBO) - 1/2\ (0.90A \times 0.9\ OB))}{OAB} \quad \% = \frac{0.19/2\ OAB}{OAB} \%= 10\%$$

If the other factors are considered as negligible, the error of R caused by metallurgical measurement can be considered at 10%.

3.4.4. Error of heat content of droplet caused by metallurgical observation.

The heat content of droplets was calculated in terms of mean drop temperature by

$$T_{dr} = T_m + \frac{(Hr + Ha) - Hm}{M}$$

Assuming errors in Tm, M, Hm and Ha are negligible compared to other factors, the main error source is Hr.

It is known

$Hr/Ha < 0.4$ at middle current range (chapter 5)

$Tdr = Tm + \Delta T \quad \Delta T/Tm = 0.4$

error of R can be 0.1R

$Hr = I^2R$

Therefore the error of Tdr

$$\delta Tdr = 0.1 \times 0.4 \times 0.4 = 0.02\ Tdr \text{ (or 2\%)}$$

As an example, if 800°C and 650°C were taken instead of 650°C and 500°C as the two critical temperatures, the calculated mean drop temperature will be 2488°C instead of 2418°C. The error can be calculated as

$$T = \frac{2488-2418}{2488} \times 100\% = 3\%$$

It is unlikely that such large errors would arise in locating the re-crystallisation temperatures.

CHAPTER 4 - EXPERIMENTAL OBSERVATIONS AND RESULTS

CHAPTER 4 . EXPERIMENTAL OBSERVATIONS AND RESULTS

As mentioned in Chapter 3 all the work was carried out with 1.2mm diameter mild steel wire (Bostrand LW 1) and Ar+5%CO_2 shielding gas deposited on mild steel plate. Metal transfer was examined by high speed cine photography at 7000 frames per second and UVO voltage recordings which were then related to temperature distribution in the electrode as determined by metallographic observations. Cinephotography and voltage records of free flight transfer over the current range 50A to 400A established three distinct modes of metal transfer with distinct characteristics. These modes can also be obtained in pulsed current welding which has significant implications for the control of pulsed MIG welding.

4.1 Metal Transfer Under Constant Current

In order to achieve the initial objective of further developing the theory of metal transfer and heat balance in constant current DC MIG welding, the equipment and techniques described in the previous chapter were used to examine metal transfer phenomena over a wide range of current from 50 - 400A at 5A intervals, thus providing a more detailed survey of metal transfer than was currently available. In this survey the mode of metal transfer was determined for each current and related burn-off characteristic and temperature distortion in the electrode extension.

4.1.1 Metal transfer modes.

a) Globular transfer mode (Below 250A).

A lot of work has been carried out on globular transfer and reports have given plenty of information about this kind of metal transfer. Therefore, it was not taken as a major aspect in the present work, but, in order to offer a general picture of the MIG metal transfer process, a brief examination of globular transfer was undertaken.

It is well known that the metal transfer process takes the globular form when the current is below a transition current at which the globular transfer changes into spray transfer. Under the welding condition adopted in present work, this transition current was 250A $\pm$ 5A.

Fig. 31 shows the globular transfer mode: a large spherical liquid metal drop is suspended under the wire tip. The

visible arc, formed largely by incandescent current carrying metal vapour, is diffuse and the arc root covers all the globule surface. It can be seen from Fig. 32 that when the current increased from 91A to 147A, the size of the drop was reduced from 2mm dia. to 1.4mm dia, approximately. The droplet detachment feequency of globular transfer was always below 100 hz. When the current reached the transition level, the detachment frequency jumped to between 300 Hz and to 600 Hz.

The microstructure of the wire tip in globular transfer is shown in Fig.32. Once again this picture shows that the drop size reduced with increase in current. An UVO trace of the arc voltage is shown in Fig. 34. It should be noted that the trace during the formation of one globule is not as smooth as might be expected. The figure indicates the surface boiling caused by superheating of the liquid metal when the liquid globule remains in the arc leading to large voltage fluctuations. The boiling causes a lot of metal vapour which can be seen from Fig. 35; the heat content of liquid metal will be considered in a later section. It should be emphasised that the interface between the solid wire tip and the liquid globule is a plane which is perpendicular to the wire axis. There is no neck and no peripheral fusion has been found above the liquid globule.

b) Drop spray transfer mode (Above 250A, below 270A).

The traditional conception of metal transfer classification is that when current is above the transition point, the globular transfer will change into the spray transfer mode. From experimental observation in the present work it has been found that there are two different kinds of spray (or projected) transfer. Between 250A and 270A $\pm$ 5A a particular metal transfer mode has been detected and this has been designated as 'drop spray' transfer mode.

Drop spray transfer is associated with a particular arc shape shown in Fig.36, having a restricted, nearly cylindrical incandescent envelope. Further frames of high speed cine film are

shown in Fig.37. It is suggested that the formation of the thin columnar arc is because the amount of metal vapour is too small to occupy more volume. It can be seen clearly from the picture that the vapour has been ejected largely from the liquid metal surface.

Another important feature of the drop spray transfer mode is that the droplets always take a perfect spherical shape which is demonstrated clearly in Figs. 37 and 38. All the droplets are the same size. The UVO arc voltage traces, Fig. 39, support the cine photographs in that all the voltage peaks, which represent drop detachment, are of the same shape and dimension. The detachment frequency of the drop spray transfer mode increased with current, Fig.33, from 250 to 300 Hz at the lower transition current of 250A to 600 Hz just below the second transition current of 270A. Above the second transition current the drop spray mode no longer occurs. The droplets formed in drop spray transfer were measured at 0.9 - 0.7 mm in diameter approximately, the variation being inversely related to current.

The drop velocity has been calculated by measuring the relative displacement of the drop versus the time from a fixed datum in successive frames of the high speed cine film. The displacement curve of the drop with time is shown in Fig. 40. The instantaneous velocity of the drop was obtained by differentiation. These calculations, Fig. 40, demonstrate that the droplet velocity remains nearly constant from melting, through detachment and transfer to the weld pool. However, there is a possibility of a very short term acceleration in between two frames of the cine film, but it cannot be identified accurately because of the limited cine film speed of only 7000 frames per second. The observed velocities were of the order of 1.3 - 1.7 M/sec.

The macrostructure of the wire tip of drop spray transfer is shown in Fig. 41. The main feature is the conical tip that has been formed. The melted metal and solid parts of the electrode wire can be easily distinguished by

microstructure; the melted metal has a dendritic crystal structure whilst the unmelted metal still keeps the fibrous structure of the cold drawn wire. From both parts of Fig. 12 it can be seen that fusion only occurred beneath the conical tip and the interface between solid and liquid is nearly a flat plane. There is no evidence of side fusion on the conic surface. In order to provide more evidence which could demonstrate that there was no peripheral fusion on the conic surface, the microstructure of the conical part was observed at higher magnification, Fig. 42. The copper coating deposited on the wire surface remained on the surface of the conical part adjacent to the molten droplet, Fig. 42a. Comparison with unheated electrode wire, Fig. 42b, shows no intrinsic differences and indicates that the copper coating on the wire surface remained unmelted as far as the spheroidal drop.

c) Stream Spray - Above 270A

When the current increased over 270A, the drop transfer mode changed suddenly into another process. This third transfer mode has been signified as 'stream spray' and has the characteristics of spray transfer as designated by previous workers. Firstly, the visible arc formed by incandescent current carrying metal vapour took on a conical shape as shown in Fig. 43. This conical arc envelops a column or string of liquid metal which breaks into a stream of small droplets transferring across the arc. Frames from a high speed cine film given in Fig. 44 clearly demonstrate the difference from drop spray transfer previously presented in Figs. 37 and 38. The quantity of incandescent current carrying metal vapour is much greater than that of drop spray transfer and, moreover, the liquid metal transfers to the pool in an irregular manner. As a result of these factors the visible arc is diffused and takes a conical shape.

The drop shape and size of stream spray transfer is completely different from the drop spray transfer mode.

Fig. 44 shows several types of stream spray transfer. Fig. 44a shows the different size and irregular shape of the detached liquid metal pieces (it is difficult to call it drop) whereas Fig. 44b shows spatter occurring during the transfer process, whilst, at the same time a lot of metal vapour is being produced. The direction of droplet detachment and propulsion can deviate from the axial direction as demonstrated in Fig. 44c and 44e which is another possible reason why the visible arc takes a conical shape. Fig. 44d shows irregular metal transfer with three droplets gathering together. On the whole, for the stream spray mode, metal transfer is irregular and in different shapes and sizes.

The arc voltage traces (Fig. 45) are in good agreement with the transfer process observation shown by the cine films. Fig. 45 shows the typical UVO traces of stream spray transfer. The trace is characterised by a series of different size peaks with irregular time intervals. These irregular peaks represent the irregular detachment of liquid metal pieces in different sizes. As a matter of fact, it is difficult to count the real frequency of drop detachment in stream spray transfer.

The wire tip in stream spray transfer can be seen from Fig. 43. The typical feature is that a liquid string or column extends into the arc column. Its shape and size remains nearly the same throughout the usable current range. The metal string expands a little at the end of the string and then usually detaches at the root of this expanded part.

The displacement and velocity of the drops (or liquid metal pieces) has been observed and calculated in the same way as that in drop spray transfer. The relative displacement of the drop was measured from a fixed datum with time: results are shown in Fig. 46. The instantaneous velocity of the droplet during this period can be calculated

by $\frac{dS}{dt}$. The velocity of the droplets in stream spray transfer process is of the order of 0.7 - 0.9 m/sec and this velocity remains nearly constant during the whole transfer process. Once again it has to be mentioned that the short term acceleration in between two frames is possible but cannot be demonstrated.

4.1.2. Transient Points

It is known from the foregoing paragraphs that there are three metal transfer modes occurring in different current ranges. The transient points between these three transfer processes have been investigated also.

When the current reached the first transition point, the globular transfer changed instantaneously to drop spray transfer. There was no intermediate situation between the two and Fig. 47 shows the UVO trace which was taken just at the transient situation. This first transient point at which the globular changes to drop spray or vice versa is shown in Fig. 47a: it can be seen that the two transfer modes occurred alternatively by accidental interferences such as current fluctuation, unstable wire feed rate, etc. No matter what the interference was, the change occurred suddenly and the two transfer modes always maintained their characteristic features. For example, the globular transfer always kept a detachment frequency at 90 HZ whereas the drop spray transfer frequency was 500 HZ. It should be mentioned once again that there is no intermediate transfer mode between globular transfer and drop spray transfer and no intermediate transfer frequency between 90 HZ to 500 HZ at this transient point.

The second transient point occurs at about 270A at which the transformation from drop spray to stream spray occurs. Once again the transformation occurs without any intermediate process. It can be seen from Fig. 47b that the transformation occurred suddenly by accidental interferences. The maximum frequency of drop spray transfer remained in the range 600 HZ to 800 HZ but when the stream spray occurred, the metal transfer became irregular and the frequency could no longer be counted readily.

4.1.3. The Burn-Off Characteristics of Different Transfer Modes

The burn-off rate versus welding current curve, Fig. 48, has been established using current increments of 5A. The current range adopted was 100A to 400A which covered most of the usable current range in practical use. It was found that there were two distinct discontinuities at 245-255A and 265-275A. These two currents are coincident exactly with the two transition currents mentioned above. This observation is in contradiction with the traditional concept of the burn-off characteristics of mild steel which does not recognise marked discontinuities. The electrode melting rate increased markedly on the transition from globular to drop spray transfer at 240 - 250A and fell at 260 - 270A on transition to stream spray transfer. The details of the burn-off rate at these transient regions with different electrode extensions are shown in Fig. 49. It can be seen that the melting rate of the drop spray transfer mode deviated from the original burn-off rate curve by above 0.5 m/min, i.e. it was nearly 10% larger. In other words, the melting efficiency of the drop spray transfer mode is nearly 10% higher than the globular and stream spray transfer modes.

4.1.4. The Temperature Distribution in the Wire Extension Part

In order to calculate the resistance of wire extension, the temperature distribution in the wire extension has been observed.

Several investigations have been carried out on the temperature distribution in the wire extension (Ref. 84, 86) but the problem remains, how to distinguish the variation in the temperature distributions between two processes with very small variations in arc parameters. It is important that the errors in the measurement of temperature, resistivity, etc., should be less than the difference between the parameters caused by different metal transfer modes. Therefore the conventional temperature measurement approach such as pyrometer, calorimetric measurement and thermocouple are not suitable since these methods will find it difficult to distinguish the temperature variation between two wires which are operating under welding currents that differ by only 5 - 10A. The ideal approach would be to measure the temperature directly in the metal itself and for this purpose a metallographic approach to temperature measurement was adopted. (Ref. 130).

Certain fixed temperatures can be established in the cold drawn mild steel electrode: the temperature at the contact tube is 70°C (Ref. 86) the fusion boundary establishes a temperature of 1537°C and two further temperatures can be allocated to recrystallisation in the cold worked wire (500°C has been taken as the temperature associated with the start of recrystallisation and 650°C as the completion based on Ref.). From metallographic examination of electrodes the four temperatures can be determined and a temperature distribution proposed for various conditions. The observation results and the postulated temperature distribution of different current ranges are shown in Fig. 50.

It is known that the resistivity of mild steel increases with temperature, Fig. 51 (Ref. 90). Thus the resistance of the wire extension can be calculated by the following equation

$$R = \int_0^1 \rho\ (T)\ \frac{dl}{A} \qquad (45)$$

Fig. 52 shows the calculated values of the variation of extension resistance with current (metal transfer modes).

4.1.5. Metal Transfer Process Observation by High Speed Film

Drop Formation and Growth

i) Drop Spray Transfer

The metal transfer process of drop spray has been investigated further by using high speed film.

For welding conditions of 250A and a wire feed rate of 7.0 m/min, Fig. 53 is the high speed cine film of the metal transfer process. It shows a typical process of drop formation, growth and detachment for drop spray transfer. Frame 1 to frame 2 shows the detachment process of a previous droplet. As soon as this drop has been detached, the wire tip was melted by anode heating continuously and a new drop started to form (frame 3). The

volume of this drop got larger whilst the arc root covered the whole spherical surface. The shape of the droplets was perfect spherical and the visible arc which was composed by metal vapour just surrounded the liquid drops and formed a thin column-like arc. It shows that the heat content of the liquid metal is relatively low.

ii) Stream Spray Transfer

Fig. 54 shows the metal transfer process of stream spray. In order to examine the process from the beginning, frame 12 was taken as the first stage of the process when a drop detached from the string by ebullition. Then the remaining liquid bar started to be elongated butno spherical drop was formed (frames 13 - 18). The parameters for Fig. 54 were: 290A, 1.2 dia. wire.

Drop Detachment

Traditional conception of drop detachment is that the forces imposed on the drop are the main factors causing its detachment. But in the present work it has been found that the momentum of the drop was mainly gained before detachment, so that there was no substantial force contributed to drop during or after detachment. Fig. 55 shows the drop detachment process of drop spray transfer and stream spray; the time lapse between frames 1.8 msec in each case.

i) Drop Spray

From Fig. 55a it can be seen that just before the detachment action, the neck was very thin but the arc root only enveloped the drop surface. Therefore the current density at the neck was very high. The current density in the neck shown in Fig 55a was about 70×10^4 A/mm^2. This current would heat the neck drastically. The picture shows that when the neck was vaporised, instead of liquid metal at the neck root, there is a bulk cloud of metal vapour filling up the space between the wire tip and the detached drop which contributed to the current

conduction instead of the former liquid metal neck. The velocity of the drop remained almost unchanged during this process (Fig. 40).

ii) Stream Spray

Even though the metal transfer process of stream spray is completely different from the drop spray process, the mechanisms are the same. Fig. 37b shows the drop detachment action of stream spray as it has been explained in a foregoing paragraph; there was a string-like liquid metal hanging under the wire tip inside the arc column. After a certain time ebullition occurred at the hottest part. High speed film showed that the position where the ebullition occurred could vary, but most of the ebullition and detachment occurred at the root of the expanded end. Fig. 37b shows clearly when the ebullition occurred, at which stage a bulk cloud of metal vapour was ejected from the string. The vapour cloud can even be seen outside the arc column. The velocity measurement once again showed there was no substantial change in the drop momentum during this period.

iii) Detachment Time Lapse

The time lapse necessary for ebullition of the liquid neck can be calculated as follows: for drop spray, using dimensions of Fig. 37a, the ebullition dimensions of the neck were taken as 0.35 mm in diameter and 0.3 mm in length. The mass should be

$$m = \gamma . 1. \frac{\pi D^2}{4} \qquad (46)$$

giving

$$m = 7.8 \times 0.03 \times \frac{\pi}{4} (0.035)^2 = 0.00023 \text{ gm}$$

The resistance R equals

$$R = \rho \frac{1}{A} \qquad (47)$$

ρ, resistivity, 1.4×10^{-3} mΩ at 2400^{o}C (Fig. 22)

so that

$$R = 1.4 \times 10^{-3} \times \frac{0.3}{0.96} = 4.4 \times 10^{-3} \Omega$$

For 1 gm liquid metal heated to boiling point, the heat required is

$$H = \Delta T C_{pl}$$

known

$$\Delta T = T_b - T_{dr} = 700^{o}C$$

$$C_{pl} = 0.8 \ J/^{o}C$$

so we have

$$H = 560 \ J/gm.$$

If

$$I^2Rt = H$$ The neck will be heated to vapour

substituted and rearranged:

$$t = \frac{H}{I^2R} = 0.43 \text{ ms.}$$

Known the lapse between two frames of cine film is 0.14 ms.

So the number of frames between the formation of the neck and its vaporisation equals to

$$N_{frame} = \frac{0.43}{0.18} \doteq 3$$

The order is in agreement with experimental observation (Figure 66).

4.2. Metal Transfer Under Pulse Current

The power source was programmed to give square wave current pulses as drawn schematically in Figure 56. Current increase and decrease was virtually instantaneous but variations did occur in both base and peak currents during the times that these were operating, as shown in later figures. Droplet development and detachment were investigated at three stages; the first stage was during the imposition of the pulsed current and thus covered base current, current increase and the initial period of peak current; the second stage covered the period that peak current was applied and the third stage covered the reduction of current from peak to base level and the time at base current.

4.2.1. Stage 1: Increase in current from base to peak level

Metal transfer was examined initially when current was increased from a 50A base to 380A peak and maintained for 8 ms. The current pulse and arc shapes at various times are shown in Figure 57 whilst the metallographic structure of the wire tip at four selected times is shown in Figure 58.

At low current, Figure 57, the arc and wire tip were barely visible indicating low temperatures and, presumably, small amounts of metal vapour in the arc. With current increase the brightness and diameter of the arc increased over a period of some 1.5 ms at a current of 375A. For this period and up to 6 ms further, the arc was predominantly cylindrical in shape but then took on a more traditional 'bell' shape.

At the start of the current pulse, Figure 58a, the electrode tip was hemispherical and molten, with no sign of necking, this would appear to be an early stage of low current gravity or globular transfer. The current pulse was sufficient to initiate necking at the fusion boundary as shown in Figures 58b and 58c. This necking process lasted about 2 ms before drop detachment which left the wire tip with a diameter of 0.7 mm at the solid liquid interface, Figure 58d. Reference to Figure 57 (frame 19) shows that a thin cylindrical link of molten

metal joined the wire and the drop prior to detachment with the arc root enveloping the drop. The physical picture of transfer given by Figures 57 and 58 are thus self-consistent. The fusion boundary at the wire tip was a plane perpendicular to the wire axis, Figure 58, and in contradiction to Ando (Ref. 81), there was no evidence to indicate that the speed of melting was different between the wire centre and surfaces. The heating and necking process is thus identical to that of constant current drop spray transfer, see Figure 41.

Droplet detachment occurred, Figure 57 (frame 21), some 0.3 - 0.4 ms after the arc root enveloped the molten droplet (the time interval between successive frames was 0.18 ms). On detachment, ebullition clearly occurred at the neck root, Figure 57 (frame 22), with metal vapour spreading out from the incandescent arc column. The ebullition is comparable to that occurring with drop spray transfer at constant current but was slightly more obvious, presumably due to the higher current. Ebullition lasted less than 0.2 ms after which droplet detachment was complete, Figure 57 (frame 23).

The drop velocity, Figure 59, was determined by measuring drop displacement with time from frames of the high speed cine film as described in the previous sections. It would appear that the molten drop began to gain speed at the start of the necking process, Figure 57 (frame 19), and detachment gave a small amount of acceleration before droplet speed reduced to a constant 1.5 ms^{-1}.

4.2.2. Stage 2: Peak current levels

If the high pulsed current was maintained after detachment of the first droplet further transfer occurred, Figure 60a. However the droplet formation was quite different; in fact stream spray transfer developed with all the phenomena associated with that mode of metal transfer at continuous current, see Figure 44.

After detachment of the first drop, Figure 57 (frame 24) and Figure 60 (frame 24), the arc root remained above a narrow neck of molten wire

with a small spherical droplet on the end. This droplet barely varied with time, Figure 61 (frames 24-27), up to 0.2 ms, but the molten neck, or string, projected further into the arc. The overheating of the liquid string and droplet resulted in the typical conical arc shape for stream spray transfer, Figure 60 (frame 42). After approximately 3 ms, from the beginning of the formation of the second drop, ebullition occurred in the liquid metal string and also released excess metal vapour into the arc and its surroundings, Figure 60 (frame 42). Immediately stream spray transfer occurred, Figure 60 (frame 43), and this form of transfer continued as long as peak current was maintained.

Displacement of the end of molten string with time was measured, Figure 61, and used to calculate droplet velocity. This velocity was constant at 1.1 ms^{-1} before detachment, increased to 1.5 ms^{-1} on detachment and then fell to 1.2 ms^{-1} during transfer to the base-plate. Errors if measurement are such that these variations, either on detachment of in comparison with drop spray transfer, have little significance.

4.2.3. Stage 3: Reduction of current from peak to base level

No reports have been found regarding the situation in pulsed MIG welding when current reduction from the pulse level to the base level occurs before completion of the process of droplet formation and detachment. In fact, it is necessary to examine two cases; first the reduction of current before drop spray transfer can occur and secondly current reduction during stream spray transfer.

For the case of current reduction during drop spray transfer, the situation is shown by high speed cine film frames in Figure 62. In this case the pulse was terminated after 2 ms and before the necking process was completed or transfer occurred. The cine film frames are complicated by the presence of a droplet (drop spray transfer) from a previous pulse; this has been ignored in this presentation. As demonstrated in Figure 57, necking started after approximately 1.5 ms from the imposition of a current pulse and detachment after 4 ms. Surprisingly, Figure 62, indicates that the necking initiated at the peak current level of 380A is continued and resulted in droplet

detachment after completion of the pulse and subsequent current reduction to 100A. The diameter of the neck was virtually the same as that measured in Figure 57 (frame 19). Droplet detachment occurred about 1.2 ms after current reduction to 100A, Figure 62 (frame 5). The neck appeared to develop during the first three frames when resistance heating was inadequate to vaporise the neck. However when the neck thinned sufficiently it was heated to incandescence, Figure 62 (frame 4), and vaporised to give droplet transfer. Droplet displacement both before and after detachment is shown in Figure 63, which indicates a droplet velocity of 1.5 m/s.

When the current pulse was extended to allow the first (drop spray) droplet to be transferred at high current the second and subsequent droplet transfers would be in the stream spray mode (Figure 60). In Figure 64 a situation is shown in which the pulse time is extended to 8 ms, this enabled drop spray transfer to occur after 3-4 ms and a stream spray transfer arc subsequently developed with a characteristic liquid string extending into the arc column. On reduction of the current from 380A to 50A the conical arc shape was retained although the brightness of the arc was reduced (Figure 64) and stream spray transfer continued for at least 2 ms, possibly longer. Molten droplet displacement is shown in Figure 65.

A survey of the change in wire tip shape is presented in Figure 66, in which the tip shape is related to the time and current situation.

4.3 Metal Transfer Control.

Based on the experimental results, a method was developed by which the drop spray transfer mode can be reproduced at any working current range rather than the limited 250 to 270A range in which it was first observed. This new MIG process has been designated 'Controlled drop spray MIG welding'. The experimental results are reported below.

The current range used for experiments was 60A to 300A and the relative wire feed rate range was 1.3 m/min to 9 m/min approximately. It should be mentioned that this range was limited by the adjustment characteristics of the power source employed in that the minimum increment of T_p and T_b were 1 msec. Figure 67 shows the UVO traces and relative welding current with the wire feed rate used during the trials. From the UVO traces it can be confirmed that all the metal transfer processes of these welding procedures belong to the typical drop spray transfer mode under pulse conditions. These traces show that even though the current level was reduced before drop detachment, the metal transfer still continued and, moreover, stream spray transfer was prevented completely.

Figure 68 shows a typical metal transfer process of controlled drop spray MIG in terms of a cine film together with UVO trace. From these pictures it can be seen that the particular column arc shape is that of a drop spray arc and the droplet appearance is of perfect spherical shape. Droplet detachment can be seen in Figure 68 and is typical of the drop spray transfer process, even though the mean current is beyond the critical value of drop spray. Figure 69 shows the fume formation rate and spatter of different transfer modes within a low current range using continuous or pulsed current. It can be seen clearly that compared with globular or conventional pulse welding the controlled drop spray MIG process has much less fume and spatter. Figure 70 is another group of arc photographs within a higher current range of 260A to 300A. From these photos it can be seen once again that the controlled drop spray MIG has much less fume formation rate and spatter than the constant current MIG and the ordinary pulse MIG

with stream spray transfer. This figure also demonstrates that even if the mean current increased to a very high value, pulsed MIG can maintain low fume and spatter characteristics provided that drop spray transfer is maintained.

The transfer mode can be distinguished also by the arc shape indicated on the photographs. Drop spray transfer maintains a cylindrical arc as opposed to the conical arc of stream spray transfer or diffuse arc of globular transfer.

Bead on plate trials showed that the positional welding characteristics were also satisfactory. Positional welding ususally needs lower temperatures in the weld pool to avoid flooding, high drop speeds for better penetration and avoid gravitational effects. It is knows (Ref.91) that the penetration is proportional to the drop speed. Drop spray transfer MIG has a higher drop speed and lower heat content and it is believed consequently that drop spray MIG is more suitable for positional work than the other MIG processes.

Figure 71 shows the bead-on-plate deposits which were done by controlled drop spray MIG in the horizontal position with different currents from 41A to 143A. Welding speeds were limited to 200 mm/min by the welding table. It should be noted that Figure 71c was done on thin plate of 1 mm in the horizontal position. Figure 72 shows the overhead positional weld bead done by controlled drop spray MIG at different currents from 67A to 138A. The travel speed once again was limited by the table to 200 mm/min.

Figures 70 and 71 show that controlled drop spray MIG welding has satisfactory positional capability at different currents. It also can be seen from these pictures that there is not spatter, undercut or lack of fusion in the current range employed or the different positions adopted.

CHAPTER 5 - THEORETICAL CONSIDERATION

CHAPTER 5. THEORETICAL CONSIDERATION

5.1 Heat Balance at the Electrode Tip.

The basic principle of MIG process is that the consumable electrode heated by electrical energy melts at the tip in the form of droplets which then transfer down to the weld pool. The heat balance on the electrode tip should be investigated from both the heat input and heat consumption aspects.

5.1.1. Heat Input.

The energy contributed to the electrode heating comes from two different sources: Joule heating and arc heating, generated by the passage of electric current through the electrode wire and the electric arc respectively.

a) Joule heating.

Joule heating is generated when welding current passes through the electrode extension between the contact tube and the arc root. The energy generated by Joule heating can be calculated by

$$H_r = I^2R \qquad (48)$$

b) Arc heating.

The energy gained from the arc at the anode is supplied by electron absorption. The energy given up by the electrons is made up of three components, energy gained by acceleration through the anode fall region, IVa, thermionic energy released when the electrons are captured by the anode, $I\Phi$, and the thermal energy of the hot electrons, $\frac{3}{2}\frac{kT}{e}I$. The anode heating can be expressed as

$$H_a = IV_a + I\Phi_o + \frac{3}{2}kT\frac{I}{e} \qquad (49)$$

where T: temperature of electrons

The work function used to be taken as 4.4V (Ref.85) but the anode fall potential in metal vapour is short on data although perhaps it can be estimated as about IV. This aspect has not been investigated further in present work.

The heat input to the anode, H_a, can be simply expressed as

$$H_a = K\ I$$

where K is a constant equal to the sum of Va, Φ and $\frac{3kT}{2e}$.

A rough estimate has been made for K of 6.3V and this value has been used in the present work. So the anode heating at a given current equals

$$H_a = 6.3\ I$$

The other energy sources of heat passing to the anode from the arc are heat conduction and radiation from the hot gas, energy from chemical reactions, Joule heating, neutral and excited atoms striking the anode and surface recombination of dissociated gas. In the present work all of these heating factors are neglected.

5.1.2. Heat Consumption

The available heat energy generated may be consumed in following ways; heat used on wire melting, heat consumed on super-heating of liquid metal, heat lost on vaporisation, other heat losses due to conduction, radiation, water cooling in the torch and the cooling effect of the shielding gas. However, the dominant heat consumption is due to wire melting and liquid metal super-heating. In the present work all the others are considered as negligible.

a) Heat consumed on wire melting

The heat energy consumed on wire melting can be determined by the following equation:

$$H_w = H_m \cdot M_m$$

$$H_m = \int_{T_o}^{T_m} C_p\,(T)\,dT + H_l \qquad (50)$$

$$M_m = W_m \frac{100}{60} \frac{\pi d_w^2}{4} \gamma \qquad (51)$$

$$= 1.3 d_w^2 \gamma\ W_m \text{ gm/sec}$$

so the expression for H_w becomes:

$$H_w = 1.3\gamma\, W_m d_w^2 \left(\int_{T_o}^{T_m} C_p\,(T)\,dT + H_l\right) \qquad (52)$$

b) Heat consumed on super-heating of liquid metal

After melting, the liquid metal remains in the arc column and therefore it will be heated to higher temperatures than the melting point. The excessive heat content ΔH is equal to:

$$\Delta H = M_m . C_{pl} . (T_{dr} - T_m) \qquad (53)$$

c) Heat consumed on vaporisation

The temperature of anode spot has been reported as more than $4000^{o}K$. (Refs. 69,75). The surface of the liquid metal will be vaporised when the temperature is above the boiling point. Part of heat energy will be consumed on metal vaporisation and the excess will be consumed on super-heating of the liquid metal in deeper layers below the boiling surface. This part of the energy has been calculated in the last section already and here only the heat consumed on vaporisation, H_e, is considered as:

$$H_e = H_{lv} . M_e \qquad (54)$$

d) Other heat consumed

Heat could also be consumed in the following different ways: radiation from the hot spots on the anode surface, energy lost by dissocistion of molecular gases at the heated anode surface, heat conducted away through the anode structure, heat conducted or convected away to the surrounding gas, energy lost due to ion emission (if any), the cooling function of the water cooling torch and cold shielding gas flow. In the present work all of these heat losses are neglected.

5.2 Forces acting on the wire tip and liquid metal.

There are six possible forces acting on the wire tip and molten metal during the metal transfer process in a gas shielded arc:

1. Electromagnetic force, F_m;
2. Surface tension force, F_s;
3. Gravity force, F_g;
4. Reaction force due to vapourisation of materials;
5. Flowing gas drag force;
6. Explosive force.

According to the present observations, the dominant forces are the electromagnetic force and the surface tension force. Compared to these two forces, the other forces are much less important. Therefore, most attention has been given to the electromagnetic force and the surface tension force.

5.2.1 Electromagnetic force.

This force is one of the most important forces of the metal transfer process. This force results in constriction of metal, detachment of droplets and induces high velocity gas flow. Experimental observations showed that changes in electromagnetic force were critical in determining the metal transfer mode.

The Lorentz force, acting on a cylindrical conductor, is proportional to the square of the current density;

$$F_p = \frac{\mu_o I^2}{4\pi^2 R^2} \times 10^2 \quad \text{dynes/cm}^2$$

R; diameter of conductor

Thus, for conical cylindrical conductors, there is a force on the vertical direction:

$$F_m = I^2 \log \frac{R'}{D} \times 10^2 \text{ dynes}$$

For the present work, R' and D can be obtained from cine film stills and micrography: therefore F_m at given current can be calculated.

5.2.2 Surface tension force

The surface tension force F_s is given by:

$$F_s = \pi D \sigma(T)$$

The expression $\sigma(T)$ is:

$$\sigma(T) = 2.1 \frac{(T_c - T)}{(M \frac{1}{\gamma})^{2/3}}$$

where $T_c = \frac{3}{2} T_{boiling}$

and M is Molecular weight.

The calculated $\sigma(T)$ has been drawn in Figure 74.

5.2.3 Gravity force

This force is given by:

$$F_g = m\ g \text{ Dynes}$$

5.2.4 Reaction force due to vapourisation

The order of this force can be estimated from the work of Heile (Ref.106) Watanabe (Ref.79) and Rykalin (Ref.130). Watanabe gave a calculation of the repulsive force due to vapourisation as:

$$F_r = \sum_{n=1}^{3} \Delta M_{yn}\ v \cdot \frac{\sum_{n=1}^{1} V_{yh}}{\frac{\pi R_a^2}{4}}$$

where $\sum_{n=1}^{3} \left(\Delta M_{yn} \right)_v$ is the quantity of vapourised materials.

V_{yn}; volume of vapourised materials

R_a ; the diameter of liquid metal.

Under conditions of 800A and a 4mm diameter electrode, Watanabe (Ref.79) stated that the material vapourised at 30 to 40 mg/sec. Heile (Ref.106) measured the fume formation rate directly and he obtained 3.3 to 6.7 mg/sec at 150A to 350A. The repulsive force given by Watanabe (Ref.79) with the above conditions and 30V to 34V is 64 to 128 dynes. According to data of Heile, the fume generation of a 1.2 diameter mild steel wire is ten times less than that of Watanabe; therefore it is possible to presume

(Ref.106) that the repulsive force of present condition is of the order of 6 to 12 dynes.

5.2.5 Other forces

For gas drag force, there was no evidence found in present work to be used to support the hypothesis of previous workers (Ref.96).

The explosion, or ebullition, of the drop neck is an important factor for detachment process, but this force has no substantial influence on drop velocity. The ebullition at the neck will be discussed later.

CHAPTER 6 - DISCUSSION

CHAPTER 6. DISCUSSION

6.1 Metal transfer mode and its classification

It is well known that the metal transfer modes of MIG welding have been classified into globular, spray and rotation transfer: IIW has developed this classification of metal transfer (Ref.95) which is generally accepted. In this classification, spray transfer and streaming transfer have been proposed. The spray transfer is described as that occurring when droplets are smaller than the electrode diameter and detach at high frequency, above a specific critical current. Streaming transfer has been described as a projected transfer detaching from a tapered wire tip, but no details of its features and the conditions of its formation have been given. Lancaster, (Ref.10) summarised the work carried out by many people in this field, covering different welding processes, gases and materials. He gave the transfer model of 1.2mm diameter wire as follows: when the current is below 190A the drops are spherical, whereas above 190A a conical point forms at the wire tip and the drops detach from the tip of the cone. Another transition occurs at about 250A and above this current the conical tip suddenly transforms into a long cylinder of liquid metal and a stream of fine drops is projected. At higher currents the streaming transfer transforms into rotating transfer. However, no details of the detachment mechanism were given. From the work mentioned above it can be seen that for MIG welding with steel wire the transfer modes between globular transfer and rotating transfer are somewhat uncertain although this range is the most useful for practical use. In the present work it has been found that the current at which the globular transfer mode transformed to spray was about 240A for 250A for 1.2mm steel wire with an Ar5. CO_2 gas shield. The regular drop spray transfer covered only a narrow range of 20A. The most important

implication of the new transfer mode is that the transfer modes have a significant influence on MIG welding applications. It was found that all the main features such as heat balance at the wire tip during the melting process, the metal transfer mechanism, the heat content of the droplets, the drop velocity and the fume generation were controlled by the mode of metal transfer. Therefore the discovery of this new metal transfer mode could change some basic ideas about MIG processes. It also has significant industrial importance. The influence of the metal transfer mode on the welding variables will be discussed in detail later in this chapter.

6.2 Heat balance of the wire melting process

6.2.1 Heat balance of the wire tip and drop heat content.

The heat balance of the metal transfer process is very important for further understanding of the MIG welding process. The thermal processes in the wire tip determine the wire melting rate and hence productivity in the practical situation. The heat content of the drop is also important in terms of the main influencing factor on the weld pool temperature which is connected with weld quality and properties. Therefore the purpose of the heat balance investigation was to further understanding of the relationship between the transfer mode, the wire melting rate and the temperature of the melting tip, including the molten drop itself. From results obtained in the present work, it has been confirmed that the heat balance of the different metal transfer modes is the decisive factor which determines most of the operational features of the MIG welding process.

Based on the analysis in the previous section, the heat balance of the wire melting process can be established as follows:

$$\text{Heat}_{\text{input}} = \text{Heat}_{\text{consumed}}$$

or

$$H_r + H_a = H_w + H_e + \Delta H \qquad (55)$$

Using this equation, the heat content of the droplets at a given current can be calculated. Then, the influence of the metal transfer mode on heat balance can be obtained. The heat content of a drop that has just been melted is given by:

$$H_{dm} = m \int_{T_o}^{T_m} C_{pm}(T)dT + H_1 \qquad (56)$$

If superheating is taken into account the mean drop temperature T_{dr} is given by:

$$T_{dr} = T_m + \Delta T \qquad (57)$$

Now

$$\Delta T = \frac{\Delta H}{C_{pl}{}^m} \qquad (58)$$

For first approximation, the mean specific heat C_{pl} is used, $0.8 J/g/^oC$, so we have the equation as follows:

$$T_{dr} = T_m + \frac{\Delta H}{C_{pl}{}^m} \qquad (59)$$

By this equation, the mean drop temperature at any given current can be obtained.

Substituted and rearranged, we have:

$$T_{dr} = T_m + \frac{1}{C_{pl}{}^m}(H_r + H_a - H_w - H_e) \qquad (60)$$

or

$$T_{dr} = T_m + \frac{1}{C_{pl}{}^m}\left\{\frac{4I^2}{\pi d^2}\int_o^1 \rho(T)dl + IV_a + I\phi_o + \frac{3}{2}KT\frac{I}{e} - \left[C_{pm}(T_m - T_o) + H_1\right] \times 1.3\, d^2 \gamma W_m - H_{lv} M_e\right\} \qquad (61)$$

Using this equation the mean drop temperature has been calculated in small current increments in order to reveal the effect of the different metal transfer modes on the heat balance of the melting process. Figure 76 shows the calculated results of mean drop temperature with current and hence transfer mode. These calculations are thus in general agreement with the experimental observations that the mode of metal transfer significantly influences the heat balance of the electrode melting process. Figure 77 shows the comparison with the data of others.

From Figure 76, it can be seen that the drop temperature is approximately 2750^{o}C to 2800^{o}C during the globular transfer mode. Drop spray transfer gives the drop temperature of 2400^{o}C - 2500^{o}C. When stream spray transfer occurs, the drop temperature increases immediately to 2700^{o}C - 2800^{o}C again. This temperature reduction is coincident with the critical current and the change of the wire melting rate. Apparently when the metal transfer mode transforms from one mode to another, the heat balance at the wire tip changes as well. In drop spray transfer, part of the heat which was consumed on super-heating of the globular transfer droplets is not required and is used to melt the wire. So the drop temperature reduced and the wire melting rate increased. This redistribution of the heat is caused by the change of metal transfer mechanism. The duration within which the drops stay in the arc before detachment is different which causes different super-heating results. The longer the duration, the more energy will be consumed on heating the metal to higher temperature: as a result the drop will be more super-heated. The more the super-heating, the more vapour will be generated from the electrode material. This suggestion also explains why the drop spray transfer mode takes a thin column-like arc whilst the stream spray transfer mode has a conic triangle arc shape since the generation of excess vapour increases the size of the current carrying envelope in globular and stream spray arcs.

6.2.2 The wire melting rate

The wire melting efficiency is determined by the heat distribution between wire melting and the super-heating of the liquid metal. If α represents the ratio between the heat consumed on the wire melting and the total

anode heating energy, we have

$$\alpha = \frac{H_a - \Delta H}{H_a} \qquad (62)$$

Clearly α is the melting efficiency of the wire under given welding conditions. The value of α for different welding currents (or different transfer modes) has been calculated and the results are shown in Figure 78. It can be seen that the drop spray transfer mode has the highest melting efficiency. The reasonable derivation from this theory is that the burn-off characteristics of the wire should be determined by the metal transfer mode. The burn-off rate of the wire under the metal transfer mode which has the higher melting efficiency α should be larger than that of the transfer mode which has lower α. This analysis has been demonstrated clearly by the experimental observations (Figures 48 and 49).

According to the traditional calculation of the burn-off characteristics of MIG welding there are two heating sources; Joule heating and anode heating. An equation was given early in 1958 (Ref.8) and was used up to recent years, which included two separate terms.

$$W_m = aI + b\, l\, I^2 \qquad (63)$$

and a and b are considered as constants.

The discontinuities in the burn-off curve of mild steel obtained in present work demonstrate that this equation is correct only for one transfer mode. It cannot be used for interpretation of the change caused by different transfer modes. Now, based on the knowledge of how metal transfer mode affects the heat balance in the melting process, an improvement of this equation has been carried out.

It has been demonstrated that both the resistance of the electrode wire extension and the heat used for electrode melting changes with the mode of metal transfer. These two factors have to be considered in the calculation of the wire melting rate. Using α, we have

$$W_m A \gamma H_m = H_r + \alpha H_a \qquad (64)$$

Substituted and rearranged, we have

$$W_m = \frac{K\alpha}{A\gamma H_m} I + \frac{R}{A\gamma H_m} II^2 \text{ cm/sec} \qquad (65)$$

Let $\frac{K}{A\gamma H_m} = a$ $\frac{R}{A\gamma H_m} = b$ (66)

It is known: $K = 6.3$ $\gamma = 7.8$ gm/cm^3 $H_m = 1308$ Joules

Then we have

$$a = 0.055\alpha \qquad b = 8.67R \times 10^{-6}$$

Both α and R are dependent on metal transfer mode. Therefore a and b are dependent on metal transfer mode. Using data of α and R in Figures 52 and 78, the calculated results are in good agreement with the experimental data of burn-off characteristics.

6.3 Metal Transfer Mechanism

The investigation of the metal transfer mechanism includes the following aspects; the drop formation process, the shape of the molten tip and growing droplet, the interface between solid tip and liquid drop, the forces acting, the movement of the liquid drop and the detachment process of the droplets.

6.3.1 Model of metal transfer mechanism

The model of the metal transfer mechanism is of great importance in quantitative investigation of the metal transfer process because the model has to take into account all of the major forces contributing to transfer. Thus, a model should be able to represent the realistic metal transfer process. It has been mentioned previously that many models have been proposed to explain metal transfer in the MIG process, but most of them were only loosely based on experimental observation.

In the present work, in order to investigate the metal transfer process further, models have been established based on the examination of the high speed cine films, UVO records and metallographic structure of the wire extension.

a) Globular transfer mode.

A model for globular transfer mode is given in Figure 79; the shape of the wire tip and drop has been known for many years, but in the present work emphasis has been placed on examination of the interface between the solid part of wire and the liquid drop. From Figure 41 it can be seen clearly that this interface is a flat plane which is contrary to some of the previous conclusions, Figure 23, (Ref.83). A second point from the observation is that the arc root covered the whole spherical surface of the globule and not just the lower surface which has been implied by many earlier workers.

b) Drop spray transfer

This transfer mode has not been observed or reported previously and so has not formed part of the spray transfer models previously developed, Figures 17-24. In the present work drop spray transfer has been observed directly in high speed cine films (Figure 53) and by metallography, and indirectly in UVO recordings. Based on these observations and the dimensions measured from photographs, a proposed model of drop spray transfer process has been drawn in Figure 80. This model is characterised by a conic neck formed at the wire tip above the solid - liquid interface. It is important that the neck is located at the solid part and there is no side fusion on its surface. The liquid drop is suspended under the conic tip. The interface between the solid and liquid is perpendicular to the axis of the wire. From the cine film (Figure 80) it can be seen that the arc root covers the liquid drop surface only. There is no visible arc root on the conic surface. These relative positions of the solid part, liquid drop, arc root and interface between solid and liquid metal are important for explanation of the metal transfer process.

This special model of metal transfer mechanism is only correct for the drop spray transfer process between 250A to 270A for 1.2mm diameter wire in Ar-5% CO_2.

c) Stream spray transfer.

The metal transfer mechanism of stream spray is very different from that of drop spray. This model has been drawn in Figure 81. It is characterised by a string-like liquid metal bar suspended under the melting plane which is connected to the conic tip. Once again there is still no melting on the conic surface above the fusion plane. The visible arc root is below the fusion line and envelops the whole string. The wire tip shape and its geometrical dimensions were based on observation of photographs and micrographs, Figures 80 and 81 are examples of molten wire shapes evolved by metallographic examination and cine films. Some of the previous work has described the stream spray as a kind of spray transfer at very high current (Refs. 4, 10). The so called rotating transfer occurs at high current and features a long, bent, rotating string (Figure 82) but it seems unlikely to be found in the useful current range. In present observations most of the liquid strings are less than 2-3mm long without visible bent and rotating motion.

6.3.2 Procedure of drop formation and detachment

Based on the proposed models of metal transfer mechanisms and forces mentioned above, the metal transfer phenomena of different models can now be interpreted quantitatively. Firstly, the drop formation process which determines the transfer mode will be discussed.

a) Formation of conic tip.

The formation of conic tip is the dominant factor of transformation from globular to drop spray transfer mode. Globular transfer is characterised by a liquid drop suspended under the solid wire tip. As mentioned previously, the interface is a plane perpendicular to the wire axis. The solid part of tip is a cylindrical column (wire). When welding current increases to critical point, e.g. 250A, the necking process occurs, and drop spray transfer results. As mentioned in the literature

survey (2.1.2.), so far, all the interpretations on the conic tip, no matter kind of model is presumed, were based on side melting processes. However, the experimental observations in present work show that the previous theory of side wall melting is incorrect.

All the experimental observations showed that the conic tip of the MIG wire was being formed in the solid state: the neck was being formed by plastic deformation. The evidence for this assertion is given below.

1. Microstructures: it is well known that the cast structure is characterised by dendritic crystal structure but from Figure 41 and Figure 58 the fusion line between solid and liquid metal is clearly visible as a plane perpendicular to the axis of the wire; no evidence of melting has been found on the conic surface.
2. Surface condition: usually there is a copper coating layer on the wire surface (Figures 42 and 83) and it was found that this copper coating remained on the conic surface of the electrode wire tip (Figures 42 and 83); this observation strongly denies that the conic tip was formed by molten metal flow along the conic surface (2.1.2) as the copper would melt and flow before the steel.
3. Position of arc root: most of the previous models presumed that the arc root enveloped the whole conic surface (Figure 38), but this was not supported by experimental observation; on the contrary the high speed film showed that the arc root only covered the liquid drop surface under its neck and no arc was found above the neck (Figure 38). Thus, all the evidence supported the view that the conic tip was not formed by melting.

Based on the analysis above, it is proposed that the only possible way to form a conic tip from a cylindrical metal is

plastic deformation. It is known that the pinch force F_p equals

$$F_p = \frac{\mu_o I^2}{4\pi^2 R^2} \left(1 - \frac{R^2}{r^2}\right) \qquad (67)$$

From this equation F_p is proportional to current square. When the diameter of drop of globular transfer is larger than the wire diameter, the divergence of the current reduces the pinch force. On the other hand, the temperature distribution is such that the tip has highest temperature. Therefore the highest temperature and highest pinch force are both located at the root of the drop just at the end of the solid part adjacent to the liquid drop. The steel strength adjecent to the liquid boundary is near zero and it is reasonable to presume that there is no sudden change of strength when metal is heated to melting point. For 0.08% steel the partially melted region of (δ + liquid) has a width of about 50^0C, Figure 75. Therefore, when the current increases above critical value of 240 to 250A, the pinch force exceeds the strength of the two-phase metal and causes plastic contraction. The very beginning of this contracting process can be seen from Figure 84, in which the slightly necked part is above the fusion line.

As soon as the contraction starts, the necking process will continue as a unidirection reaction process because the pinch force is proportional to the square of current but is inversely proportional to the diameter of the conductor. When the necking starts, the pinch force will increase rapidly with the reduction of the conductor's cross section area. The necking process is accelerated until it reaches a new stable state. As a result, the conic tip is formed suddenly above critical current with a fusion plane of 0.6 - 0.7mm diameter. At the same time, the formed conic surface has an angle of 35^o to 45^o from the wire axis. This observation can also be used as evidence for the formation process of conic tip.

b) Mechanism of transformation from one mode to another

The mechanism of metal transfer mode transformation can be established by calculation of the forces acting on the wire tip using the experimental observations and measurements.

The forces can be calculated by the size of the drop, neck diameter and effective current conductor dimensions. From Figure 53 it is known that drop frequency is 688 Hz, drop diameter is 0.72mm and the time lapse per frame is 1.82 msec. Then the changing magnitude of the forces can be calculated successively frame by frame. The electromagnetic force and surface tension force are considered as dominant forces whilst the gravity and vaporisation forces have been neglected because of their relatively smaller values comparing with the other forces. The calculated data are shown in Table 5.

The calculated results have been plotted as curves of forces against time in Figure 85; from this figure the relative magnitude of the two main forces can be seen. At the beginning, before the fourth frame, the surface tension force of the molten tip was larger than the electromagnetic force but after 1.8 ms the electromagnetic force started to exceed the surface tension force. This variation occurs because the difference between the drop and neck cross sectional areas increase as the drop grows and the neck gets thinner. As a result the surface tension force, Fs, is reduced and the electromagnetic force, Fm, increased. It should be emphasised that the period during which the surface tension force exceeds the electromagnetic force is very important for the formation of the drop spray transfer mode. This will be explained in a later section on stream spray but it can be mentioned here that the surface extension force exceeds the electromagnetic force at the beginning of the drop formation. As the wire tip is melted, the molten metal can only stay at the tip but cannot move downwards. Therefore a spherical drop starts to grow. As the drop grows larger the difference between the two forces reduces leading to drop detachment and transfer.

When the welding current is increased to the second critical point of 270A at which the drop spray mode changes to stream spray transfer, the balance of the forces will change their cumulative effect and another substantial transformation in the metal transfer mechanism will occur.

The forces of 270A can be calcualted by the method described below. It is known that the neck diameter at 250A is 0.5mm and the neck diameter at 290A is 0.3mm (Figure 54). Therefore we can assume that the neck diameter for 270A is 0.4mm. At the same time, the liquid metal temperature increases above boiling point, so the surface tension coefficient should be 900 dynes/cm^2 (Figure 74). The effective conductor R' is taken at 0.9mm diameter so that we can calculate the forces by

$$F_s = \pi D\sigma(T) = \pi \times 0.04 \times 900 = 113 \text{ dynes}$$

$$F_m = I^2 \log \frac{R'}{D} \times 10^{-2} = 253 \text{ dynes.}$$

If we compare the data of Table 5 and Figure 53, it can be seen that the main difference between the processes of 270A and 250A is that the electromagnetic force was higher than the surface tension force at all times at 270A.

It has been explained before that at the initial stage of a drop formation process the melted metal at the tip will be drawn back towards the fusion line and form a spherical drop if the surface tension is the largest force. However, the situation is different when current exceeds 270A as is shown by the calculation. As soon as the tip is melted, the electromagnetic force which squeezes the liquid metal downwards is much larger than the surface tension force which tends to draw the molten drop upwards. As a result the spherical drop can no longer be formed and then the liquid metal moves downwards and forms a liquid metal string which is shown in Figure 54. When a spring-like drop has been formed instead of a spherical drop, the stream spray transfer process occurs. This is the essential theoretical interpretation of the transformation of drop spray to stream spray. It is believed that this proposed theory explains the experimental observations and measurements for both the present and previous work.

6.3.3 Dynamic Analysis of the Forces Acting on the Tip

The forces and their resultants were calculated using the model of metal transfer mechanism proposed above. The drop movement was known by the measurements based on experimental observation. The following equation must be satisfied:

$$F \Delta t = \Delta mv$$

where F is the resultant of acting forces, Δt the duration of force action, m the mass of the drop and Δv the change of drop velocity.

a) Drop spray.

For the drop spray transfer process shown in Figure 53 the diameter of the drop is 0.72mm and the mass of the drop equals to 0.0015gm. The original velocity of the drop due to the wire feed speed is known to be 7.0m/min or 0.116m/sec and the diameter of the neck before detachment was measured as 0.5mm. Consequently the velocity of the bar tip, v_{bar}, is given by

$$v_{bar} = v_{wire} \frac{d_w}{d_b} \qquad (68)$$

d_w: 1.2mm, d_b diameter of neck 0.5mm

So we have $v_{bar} = 0.116 \frac{1.2^2}{0.5^2} = 0.67$m/sec.

Let m', v_{dr}' represent the mass and velocity of droplet at t_1

m'', v_{dr}'' represent the mass and velocity of droplet at t_2

then we have $\Delta mv = m''(v_{dr}''-v_{bar}) - m'(v_{dr}'-v_{bar})$

known $v_{dr}' = v_{bar}$

therefore $\Delta mv = m''(v_{dr}''-v_{bar})$

where m'' = 0.0015gm, v_{dr}'' = 1.7 x 100 cm/sec, v_{bar} = 0.67 x 100 cm/sec

Substituting Δmv = 0.155 gm-cm/sec.

The work done can be calculated by

$$Ft = \int_{t_1}^{t_2} F_m(t) - F_s(t) \quad dt \qquad (69)$$

Using the data of Figure 53 and considering the time of the third frame as zero, t_1 was taken as 0.15ms, where the surface tension force just equals to the electromagnetic force. Time t_2 was taken as 1.18ms, where the detachment was completed. Then the value of Ft was obtained by numerical integration. The result is 0.158 dynes-sec.

Comparing with the calculation of Δmv, the results are in good agreement with each other. This result demonstrated that the proposed model and the dynamic analysis of metal transfer mechanism is likely to be correct.

b) Stream spray

From the proposed model of stream spray transfer it is known that no spherical drop has been formed but only a liquid string hanging under the wire tip. Therefore the electromagnetic force and the surface tension force did not play the same role which has been described for drop spray transfer simply because of the geometrical dimension of wire tip and drop have changed completely. According to the metal transfer mechanism proposed, it is known there was no substantial force imposed on the drop during the whole process. Therefore the only source from which the drop momentum is gained should be the original wire feed movement of the wire tip. Under the conditions of Figure 54, the drop measured velocity is 0.7 to 0.8m/sec. The calculated velocity of the liquid bar end equals to

$$v_{bar} = v_{wire} \frac{d_w^2}{d_b^2}$$

v_{wire} is 7.46m/min, or 0.124m/sec, d_w is 1.2mm and d_b is diameter of the liquid string measured from cine film 0.5mm.

So we have $v_{bar} = 0.124 \frac{1.2^2}{0.5^2} = 0.71$m/sec.

This value exactly equals to the measured drop velocity from the cine film of stream spray, Figure 54. It demonstrates very well that the analysis of drop detachment mechanism in stream spray transfer is correct.

This point is also emphasised by Waszink (Ref. 83) although his terminology is somewhat different. Waszink's conclusions and expressions are identical with those given above. It is interesting that two workers have identified a major new force simultaneously.

6.4 Metal Transfer Mode Under Pulse Current Condition

The experimental observations, although limited present a very interesting picture of metal transfer in pulsed current MIG welding. Two modes of metal transfer were found; the drop spray mode for the first droplet formed and detached during a current cycle (from the start of one pulse to the start of another) and the stream spray mode for the second and subsequent droplets. Thus for the most quiescent and efficient metal transfer in pulse welding the aim should be drop spray mode. These phenomena can be interpreted by same theory proposed in the study of constant current (Ref.133). At the beginning of high level current imposed on a low level current, the temperature of wire tip is still low because of the thermal delay effect. The surface tension force of melted metal exceeds the electromagnetic force for a short time. As a consequence the liquid metal is drawn back and forms a spherical drop. However, if the high current is maintained, the temperature of the wire tip increases rapidly and the transfer condition is changed to that of stream spray under steady current since compared to the electromagnetic force, the surface tension force is too low to keep the molten metal in spherical shape. Then the liquid metal will be squeezed by the pinch force and a string is formed. These mechanisms have been explained quantitatively in the section. However, what was completely unexpected, once droplet formation has been initiated during the peak current cycle it progresses to completion and transfer even if the current is reduced to the base level of 100A or 50A, Figures 62 and 64. This situation occurred with both the first drop spray mode droplet transfer and subsequent stream spray mode droplet transfer and subsequent stream spray mode droplets. Such a situation has not previously been reported and has significant implications for the design of pulsed MIG welding equipment. The shape of the wire tip in relation to time and current is important in identifying drop formation and metal transfer

mode and observations are presented in Figures 58 and 66. For the first droplet (drop spray mode), the change in wire tip shape is shown in Figure 58, with melting, necking and detachment of a droplet. However, these changes in tip shape, droplet development and detachment are not necessarily synchronous with current, as indicated in Figures 57, 60, 62 and 64. The reason is believed to be due to the fact that heat flow in the wire tip will require a specific time to occur after the heat has been generated. However, the pinch force necessary to cause necking will depend directly on current level and be synchronous with it. Adopting this physical picture, the frames of the cine films presented in Figures 57, 60, 62 and 64 can be interpreted as demonstrating that the necking process requires 'high' current for 1-2ms before it becomes evident. However, necking and detachment can occur for 2ms or slightly longer after reduction of the arc current to a low level of 50A or 100A, due to a time lag effect arising out of the heat flow. Thus droplet detachment will occur even in the absence of the pinch effect provided that melting and necking has already started during the high current pulse.

Whilst Figure 66 shows the tip contour, Figure 83 gives details of the conical surface of the electrode tip. The surface coating of copper indicated by the arrows, remains virtually intact during the necking process, indicating that the copper has not melted and that necking has taken place in the solid although highly plastic part of the electrode. This conclusion is also supported by the microstructure of the wire which is typical of steel heated to a high temperature but not melted. These results are consistent with those found under constant current conditions. The total time for droplet detachment, t_d, requires four distinct stages: heating, necking, droplet growth and droplet detachment. The significance of a major variable such as current can be different for each stage which can lead to apparently contradictory conclusions. Thus t_d is inversly proportional to the peak current level recorded at the initiation of necking, as demonstrated in Figure 86, but t_d remains independent of current level at the point of detachment. Thus the choice of peak current will determine the rate of droplet detachment but the frequency of pulsing is relatively unimportant.

The initiation or triggering of droplet detachment occurs at the heating and necking stages when the Lorentz (pinch) force exceeds the resistance to plastic deformation of the heated electrode wire. Since both heating and the Lorentz force are current dependent, the higher the current the less the time for necking to start. The effect of a current pulse in initiating necking is demonstrated in Figure 87 which has been derived from the cine film shown in Figure 66. The time lag effect can be seen clearly.

The necking and detachment process is unidirectional and once started must proceed to droplet transfer. From Figures 66 and 87 the heating time can be measured as approximately 1.5ms and is followed by very rapid necking which occurs within a single frame of the cine film (less than 0.2ms) to give a conic tip with a diameter of 0.7/0.8mm, a figure which is also supported by measurements from the cine film frames shown in Figure 53. The final detachment is by overheating and ebullition of the thin neck separating the droplet from the wire. However, once the narrow neck has been formed even a low current (50A or 100A in the present work) is sufficient to cause drop detachment, as shown in Figure 64 (frame 4). A similar mechanism also has been found in the fundamental research of flash butt welding (Ref.134) where each liquid metal contact (bridge) was burnt off by Joule heating ebullition as well. The necessary energy for the ebullition of contacts has been reduced drastically by controlling the necking process from directional process to unidirectional process. Therefore it is not surprising that the ebullition of the drop neck in pulsed MIG can occur at low current after the peak. These two processes are self-consistent with each other.

It is interesting to consider the movement of the molten droplet under pulsed current conditions and to attempt to explain the observed facts by dynamic balance. Drop development and detachment will be influenced by

a) movement of liquid metal between the wire tip and the drop;
b) the electromagnetic and surface tension forces;
c) the detachment effect of ebullition.

In the case of stream spray transfer, droplet velocity can be determined from Figures 61 and 65, covering detachment at peak and base current (380A and 50A). It is surprising that the velocities in both cases were in same order round 1.3m/sec. This fact can be interpreted by dynamic balance occurring at the wire tip; from high speed film it can be seen that, compared to drop-spray which has a different cross section at the drop root, there was no significant downwards electromagnetic force imposed on the string-like bar. The wire tip was being squeezed to thin bar immediately after melting. It is known that under same mass flow, the liquid speed is inversely proportional to the cross section and as a result, the end of the liquid bar is being accelerated to a greater speed than the solid wire speed. The string end velocity can be calculated from the original melting rate by

$$W_1 S_1 = W_2 S_2 \qquad (70)$$

where W_1 is wire melting rate, S_1 is cross section of wire, W_2 is the velocity of liquid string end and S_2 the cross section of string. The calculated results are shown in Table 3. These results demonstrate that the dynamic analysis is consistent with observation.

With drop spray transfer the situation is more complicated. The electromagnetic force is important in this transfer mode. Three factors should be taken into account in the detachment process: the electromagnetic force, the surface tension force and the liquid string movement. The relationship between acting forces and the droplet movement can be expressed as follows:

$$F\Delta t = \int_{t_1}^{t_2} Fm(t)-Fs(t) \; dt = \Delta mv_{dr}$$

where $\Delta mv_{dr} = m''(v_{dr}''-v_{bar})-m'(v_{dr}'-v_{bar})$

known $v_{dr}' = v_{bar}$.

So we have $\Delta mv_{dr} = m''(v_{dr}''-v_{bar})$.

The m'', v_{dr}'', v_{bar} can be obtained by measurement (Figure 57) and are 0.0071gm, 1.8ms^{-1}, 0.58ms^{-1} respectively. Then the Δmv_{dr} can be calculated as 0.87g.cm/sec. $F\Delta t$ can be calculated as 0.97 dynes sec.

Therefore results prove that the dynamic analysis and established relationship between these acting forces are in good agreement with experimental observation.

6.5 Controlled MIG

Based on obtained results described above, it is possible to discuss genuine improvement of MIG process. It is important to understand, firstly, the main purpose and the relative criteria for improvement of MIG processes. Secondly, we must establish the basic principle of the methods of improving the MIG process.

Since the MIG welding processes were introduced much work has been reported on the improvement of MIG techniques. One of the most important developments was the pulse current technique. It was claimed that a synthetic spray transfer could be obtained at currents below those at which spray transfer occurs naturally. However, the aim (or the criteria) of these works were limited to getting 'one drop per pulse of current'. So far, few works have dealt with the improvement on the essential process of MIG other than the number of droplets. In fact, there is much more potential in welding process control which can be used to improve the MIG welding process in may aspects other than producing a process of 'one drop per pulse'. Most of the features of the MIG process such as spatter, fume generation, penetration and positional characteristics are determined by metal transfer mode, so that it is reasonable to presume that the MIG process can be improved effectively by metal transfer mode control. The metal transfer mode control is possible only after the essential knowledge of the metal transfer mechanisms of constant and pulsed current have been obtained.

In following sections, the shortcomings of MIG are discussed in order to define the problems that need to be solved. Subsequently the principles and application of mode control are discussed and assessed.

6.5.1 Features of MIG Welding and its Shortcomings

All the main features of MIG welding are determined by the metal transfer mode. The main operational characteristics of MIG and the relationship between these characteristics and metal transfer mode are discussed below.

a) Spatter.

Spatter in MIG welding is one of the most troublesome problems in practical operation (Refs. 135, 136, 137, 138). Spatter wastes metal, damages work surface, reduces weld quality, reduces productivity and may injure operators. Spatter is mainly caused by metal ebullition at high temperature. Figure 87 shows the tip of globular transfer wire: the pits from which metal has been ejected were caused by ebullition of the surface metal. Quigley reported a similar phenomenon (Ref.139). The drop in globular transfer mode has a higher temperature caused by superheating when the liquid metal has stayed for a long time in the arc column. Figure 89 shows the spatter mechamism of stream spray transfer. It is known the detachment mechanism of stream spray is ebullition occurring at the neck of the liquid string (Figure 90). If the ebullition occurs at the tip it will result in a bubble (Figure 89): when the bubble explodes, the small metal pieces are ejected and form spatter particles. It was observed that this sort of spatter happened at a frequency of 3 to $5H_z$. The ebullition was caused by superheating of the liquid string which stayed for a relatively long duration in the arc column. From these phenomena it can be assumed that spatter is unavoidable for globular transfer and stream spray transfer. Figure 37 shows the drop spray metal transfer mode; it can be seen there is no ebullition because of the lower heat content of the liquid drop compared to the other modes. The drop heat content of different metal transfer modes are shown in Figure 76.

b) Fume formation rate.

Welding fume is composed of metal vapour which is generated by ebullition. It causes pollution and may damage health. Early in 1975, Heile (Ref.106) found that the fume formation rate changed with current (Figure 73). The present work has shown that the change of fume formation rate proposed by Heile is exactly in agreement with the different transfer modes (Figure 73) and demonstrates that the drop spray transfer mode, which has lowest drop heat content, generates minimum fume.

c) Positional characteristics.

It is known that ordinary 'spray' transfer cannot be used for positional welding because of flooding of the high temperature pool. Globular transfer cannot be used for positional welding because of low drop speed and momentum such that transfer does not occur. Dip transfer allows positional welding but low heat content can cause lack of fusion. The drop speed of drop spray is higher than the others: the measured velocity of the drop in drop spray transfer process is 1.2 to 1.7m/sec whilst the velocity of the drop in stream spray is 0.7 to 0.9m/sec. It is believed that the drop spray has better positional ability than the others if the current can be controlled, giving adequate droplet momentum and higher heat content than in dip transfer.

d) Deposit rate.

It is known from Figure 48 that the drop spray has the highest wire melting efficiency which occurs because the drop endures less superheating than the globular transfer and stream spray transfer modes. As a consequence more heat can be utilised by the wire melting process. This effect results in discontinuities of the burn-off characteristics of constant current MIG process, Figures 48 and 49, and the melting rate of drop spray is nearly 10% higher than that of other transfer modes.

From above it can be seen that all the important features of the MIG process are tightly linked with metal transfer modes. Compared to the globular and stream spray modes, the drop spray has several advantages. The welding process with drop spray transfer is spatter free, has minimum fume generation rate, good positional characteristics, high deposit rate and good weld appearance because of regular drop transfer. However, drop spray transfer is unavailable because it only can exist under extremely strict conditions in a very narrow current range of 20 amps. It is impossible in practical use to do all the welding work within such a limited range which is why the ordinary MIG welding process is always accompanied by large amounts of spatter and fume.

6.5.2 Metal Transfer Mode Control and 'Controlled Drop Spray MIG'

From the foregoing paragraphs, the ideal MIG process should be a welding process which keeps all the features of the drop spray transfer mode but which can be performed through the working current range. The approach by which drop spray can be reproduced beyond its original 20 amps range has been clearly indicated by the pulsed current experimental work which offers a way of controlling metal transfer mode, giving a process which may be termed 'controlled drop spray MIG welding'.

Metal transfer by regular small spherical globules only occurs at 250 to 270 amps under constant current with a 1.2 diameter mild steel wire. Metal transfer mode control must recreate the physical conditions for drop spray at currents beyond the critical current range of 250 to 270A using the experimental results obtained in pulse welding.

a) Sufficient pinch force for formation of necking at wire tip.

Drop spray is started at the moment when the necking process occurs and results in a conic tip. The current value is 250A for 1.2mm mild steel wire shielded by Ar-5%CO_2 gas and if the current is lower than 250A the neck will never be formed. Figure 90 shows wire tips in globular transfer at 91A and 147A in which, even though the drop stayed at the tip for more than 20ms, no neck developed. The reason is that the strength of the metal adjacent to the fusion line is always the same value but the pinch force is proportional to the square of the current; only when the pinch force exceeds the metal strength will the necking start (Figure 92). It was reported that 'one drop per pulse' could be obtained when the peak current was lower than 250A (Refs. 52, 54, 92, 98) but in fact it was only an intermittant globular transfer, not 'spray' transfer as was claimed.

b) Proper tip temperature.

In order to keep the molten drop in a spherical shape

at the molten tip and avoid the liquid string of stream spray, the temperature of the molten wire tip must be controlled. From the foregoing paragraphs the spherical globule will be formed at the conic tip if the surface tension force exceeds the pinch force immediately after the conic tip has been formed. Since the surface tension force is inversely proportional to the temperature, if the melted metal at the conic tip is heated further, the reduced surface tension force will be no longer enough to form a globule under the acting pressure of pinch force and a liquid string is formed instead of the spherical globule. As a consequence, stream spray occurs. Under pulse condition, the high level current is imposed after a low level current whilst the tip temperature is low. Therefore, no matter how high the current level is, the first drop should be detached in drop spray mode. After the first drop has been detached, the tip is heated to a higher temperature and successive metal transfer will be of stream spray mode. All of these mentioned phenomena have been confirmed by observation.

In order to maintain drop spray transfer only, the pulse current must be reduced to a low level in time. Let t_d represent drop detachment time when we have

$$t_d = t_1 + t_2 + t_3 \qquad (71)$$

where t_1 is heating time for preparing necking process; it depends on current and usually lasts 1 to 1.5ms; t_2 is necking and drop growth time; t_3 is detachment time, during this time part of the neck is heated to boiling point and leads to drop detachment; it normally lasts less than 0.2ms. Detachment time, t_d, is inversely proportional to peak current (Figure 93) but is independent of the current duration. It has been confirmed that the necking process is an unidirectional process: after its start it will go on to the end inspite of current changes, even if the current reduced to low level.

It is known that the liquid string will be formed after the detachment of the first drop. If the current level is kept unchanged after the detachment of the first drop the occurrence of stream spray transfer will be unavoidable. Thus the correct duration, t_p, peak pulsed current can be expressed as

$$t_1 < t_p < t_1 + t_2 \qquad (72)$$

If $t_p < t_1$, the necking process is not triggered so that no drop can be formed. If $t_p > t_1 + t_2$, a string will be formed and stream spray will occur after the first drop. After the reduction of the current, drop detachment is still possible because the necking process is unidirectional as mentioned before.

c) Combination of parameters to give drop spray transfer.

The drop spray transfer mode is the only metal transfer process which can deliver regular spherical liquid drops from the wire tip to the pool. The volume of the drop is determined by the ratio between surface tension force and electromagnetic force. It is known that all of these forces are determined by current and temperature. Because the conditions of drop spray are fixed, therefore, the drop size is fixed. For constant current the measured drop diameter is 0.7 to 0.9mm. For pulsed current at a mean current of 260A, the measured drop diameter range is 0.9 to 1.1mm. The drop is larger than that of constant current because the necking process of pulsed current starts at an obtuse tip whilst in constant current the necking process starts at a conic tip. From the explanation above it is comprehensible that the detachment frequency versus current should be fixed when the drop spray is being reproduced at any current beyond the critical current range of 250-270A.

Let f represent the drop detachment frequency. We have

$$f \doteq \frac{M_m}{m} \qquad (73)$$

The calculated results are shown in Figure 94. Curve 1 is taken as a mean value by measurement. The shaded area shows the possible frequency range versus wire feed rate obtained by experiment. It can be seen that they are in good agreement.

For a given frequency T_b will be fixed (T_p was known before). Then the base current can be chosen according to required melting rate. In other words, for the drop spray transfer mode all the four parameters are fixed within a small tolerance. This theory and present observations do not support the opinion that the volume of drop and its relative parameters can be selected at will. The theory has been applied with success in some brief positional welding experiments (Figures 70-72) but, obviously, considerably more tests are needed.

CHAPTER 7 - CONCLUSIONS

CHAPTER 7. CONCLUSIONS

1. In MIG welding with 1.2mm diameter steel wire and Ar-5%CO_2 gas shielding, three modes of metal transfer have been identified, termed globular, drop spray and stream spray transfer. The drop spray mode has not previously been identified and occurs over a narrow current range between the previously identified globular and spray transfer.

2. The heat content and mean temperature of transferring droplets depends on the transfer mode with drop spray transfer signficiantly lower than the others.

3. A model for droplet formation and detachment has been proposed for both forms of spray transfer based on metallographic examination of electrode wires and high speed cinephotography.

4. The dominant forces acting on the electrode tip are surface tension and electromagnetic. Droplet momentum is gained before detachment in both drop spray and stream spray transfer.

5. Drop spray transfer is characterised by regular droplets with low spatter and fume formation, it is projected and can be used in all welding positions.

6. Discontinuities occur in burn-off rate, with drop spray transfer giving a higher efficiency than other transfer modes.

7. Droplet detachment occurs by metal vaporisation at the neck of the droplet, other forces are not significant.

8. The high melting efficiency, low spatter and low fume formation of drop spray transfer would be of considerable industrial significance if it could be extended over a wider current range.

9. Metal transfer under pulsed current conditions occurs in the drop spray and/or stream spray modes provided that the peak current is above that at which globular transfer occurs.

10. The first droplet transferred in pulsed current welding is in the drop spray mode but subsequent droplets transferred during the same current pulse, or within 4ms of completion of the current pulse, will be in the stream spray mode.

11. The time for the formation and detachment of a droplet is inversely proportional to the magnitude of the peak current but independent of the duration of peak current, provided sufficient heat is generated to melt the wire tip.

12. Once droplet development has initiated the droplet will detach after a specific time, characteristic of the wire diameter and peak current, whatever the current level at the time of detachment; the first drop in a pulsed current cycle will be in the drop spray mode subsequent drops in the stream spray mode.

13. Necking occurs by plastic deformation of the heated wire due to the Lorentz force and melting occurs below the neck.

14. Droplet detachment is caused by ebullition of the Joule heated molten metal separating the necked wire and the drop.

15. Droplet velocity is determined largely by the speed at which molten metal is squeezed into the drop but additional momentum may be provided in drop spray transfer by electromagnetic forces arising from the variation in current carrying cross sectional area at the wire tip.

16. Improvement of MIG processes can be achieved by means of metal transfer mode control which must be based on the following principles:

a) Establishing the conditions of transformation from globular to drop spray transfer by offering sufficient electromagnetic force and keeping a low tip temperature for sufficient surface tension force;

b) Preventing the transformation from drop spray to stream spray by cooling down the tip temperature in time;

c) Matching the pulse frequency to the drop detachment frequency according to the fixed drop size with current;

d) Combining all the parameters to adjust the wire melting rate to fulfil the required wire feed rate.

17. Based on the proposed principles, a new MIG process termed 'Controlled Drop Spray MIG' has been developed. The main feature of this new MIG is that metal transfer is kept in drop spray transfer mode. This new MIG process is spatter free, has minimum fume formation rate and good weld appearance. Positional welding trials showed that the proposed method is satisfactory both on horizontal welding and overhead welding.

FIGURES

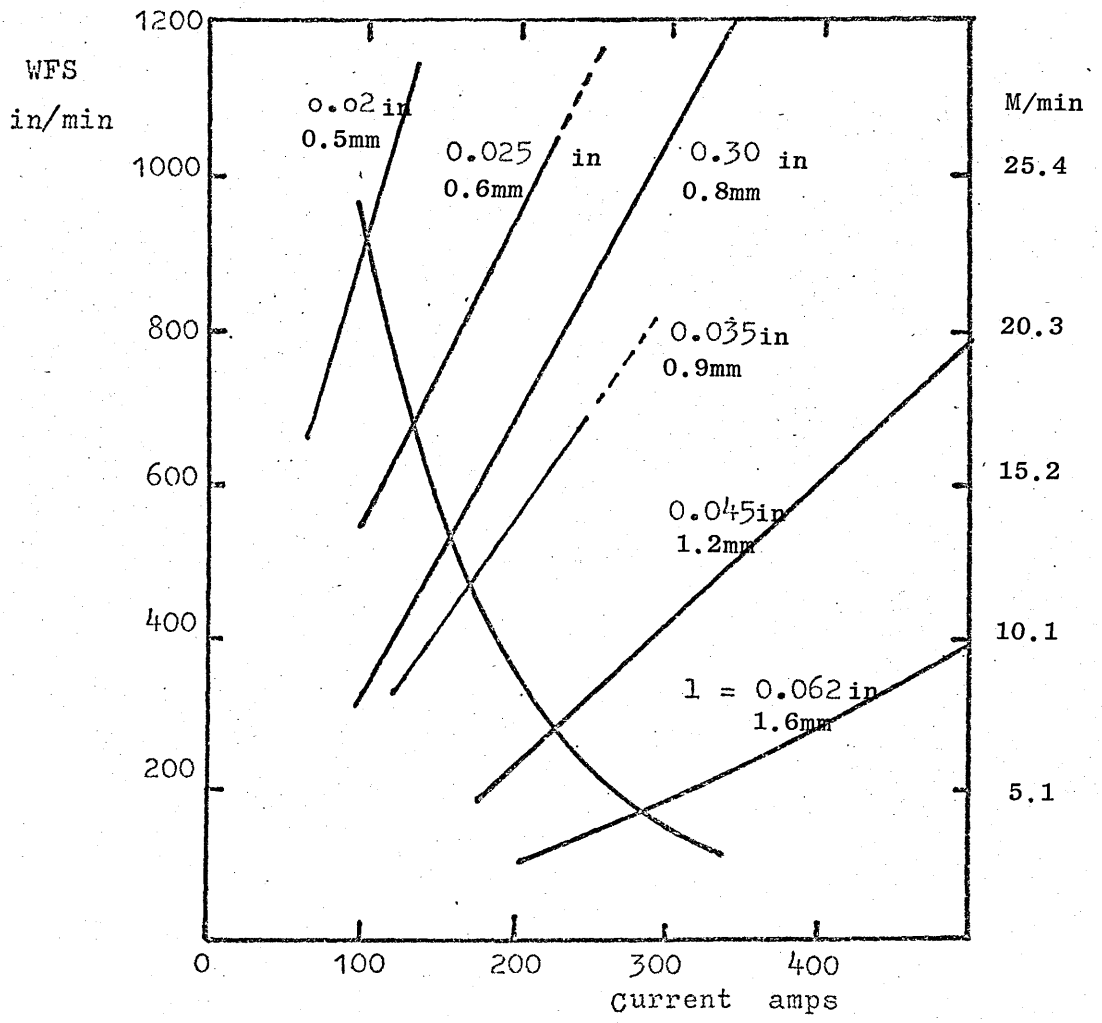

Figure 1. Burn-off curves for steel gas metal-arc electrodes. WFS; wire feed speed. 1; wire extension, in.

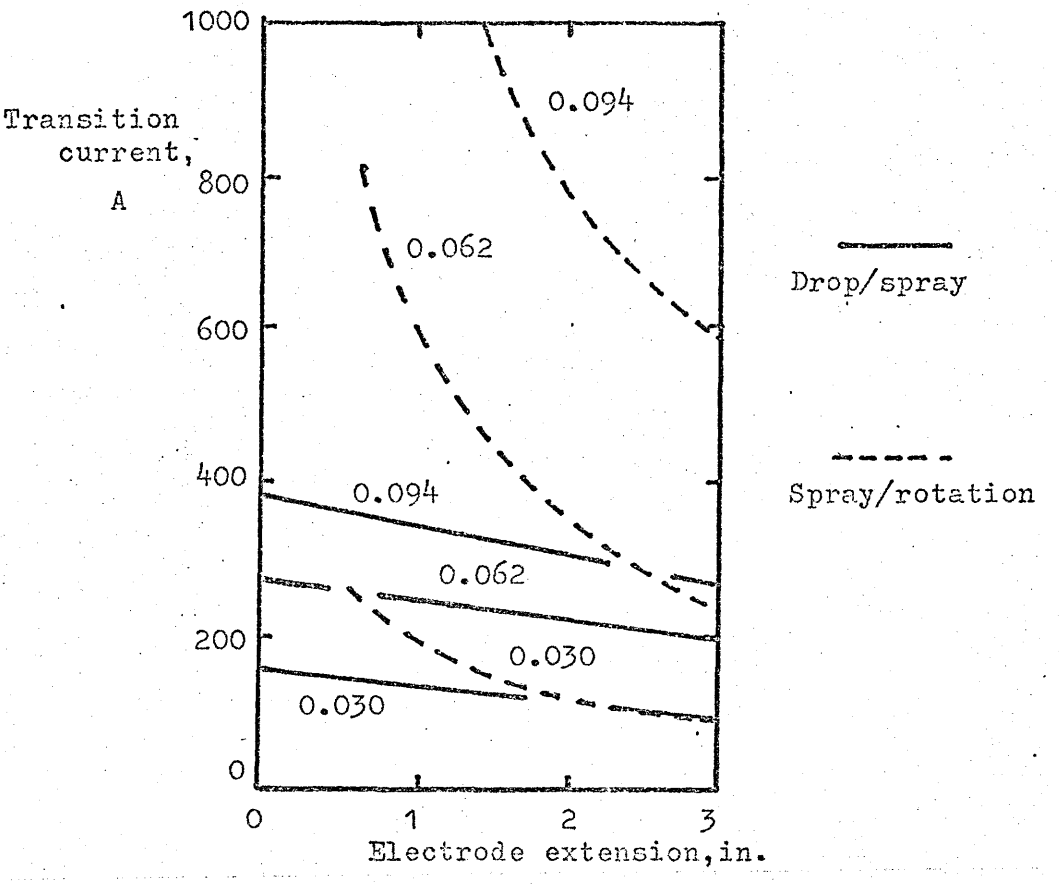

Figure 2. Effect of electrode extension and diameter on transition current.

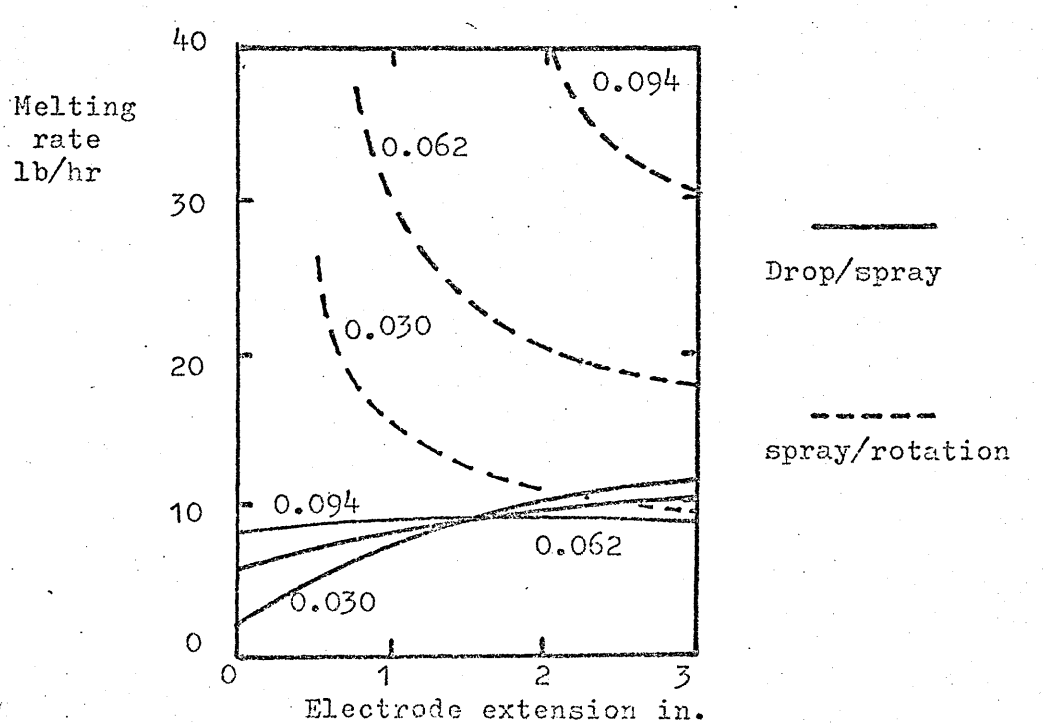

Figure 3. Effect of electrode diameter and extension on melting rate and transition current.

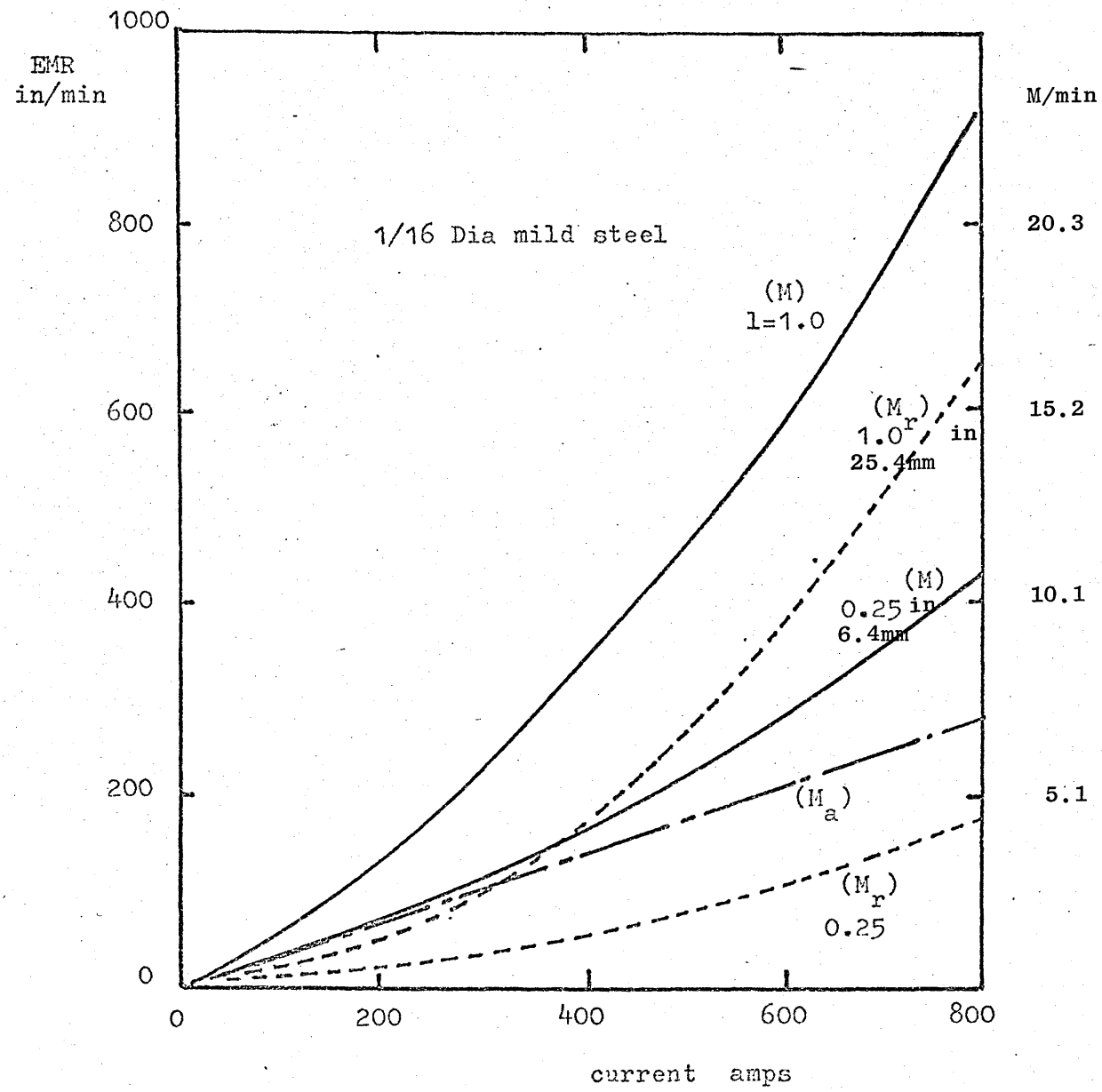

Figure 4. The variation of electrode melting rate with current.(106)
l; extension.
M; real melting rate.
M_a; melting rate by anode heating.
M_r; melting rate by resistance heating.

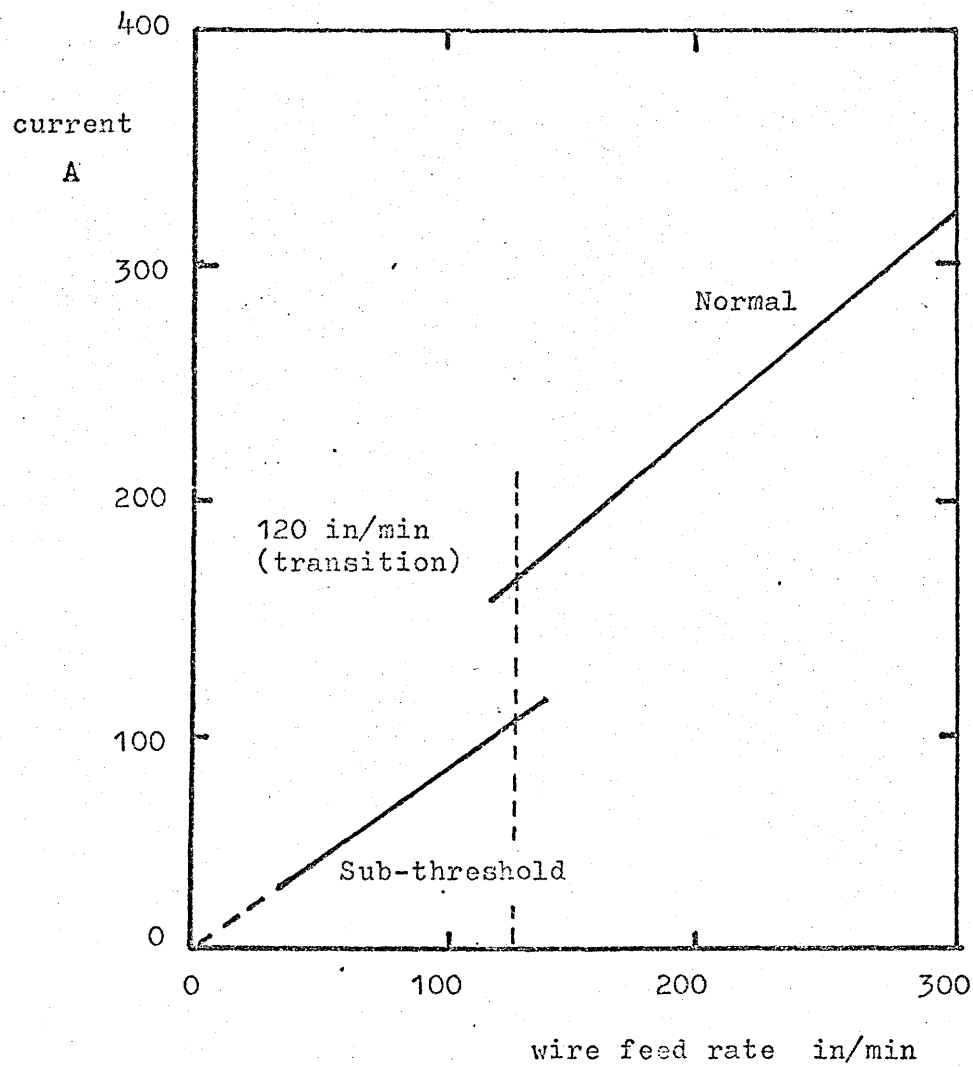

Figure 5. Burn-off characteristics, 1/16 in. dia. aluminium, argon gas shield, 22V arc.

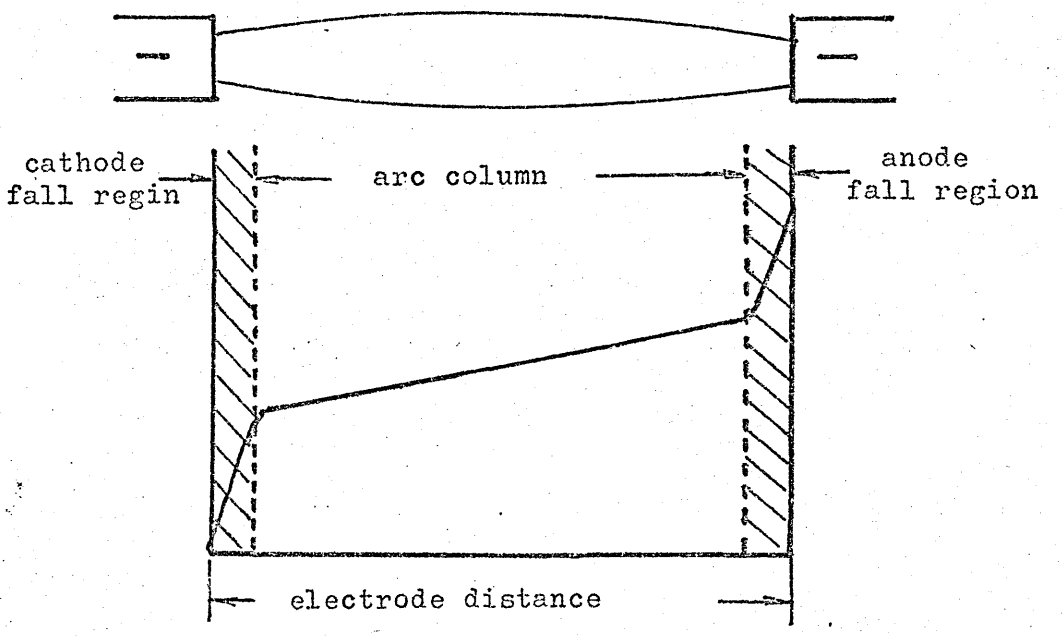

Figure 6. Schematic representation of the three different regions of the electric arc.

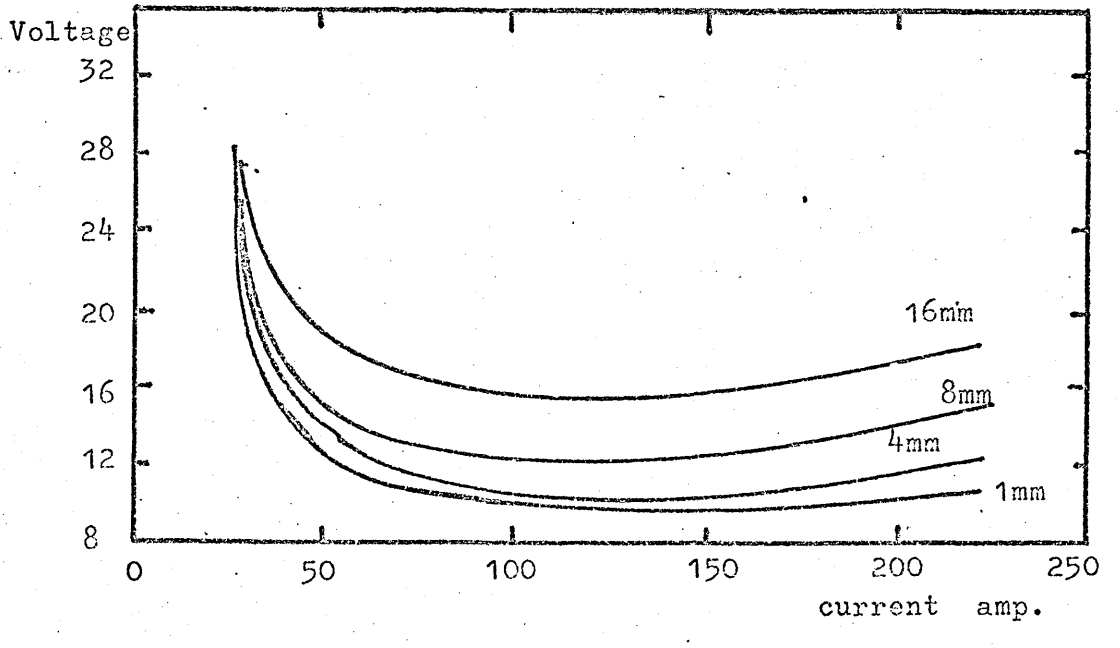

Figure 7. Arc characteristics with different arc length.

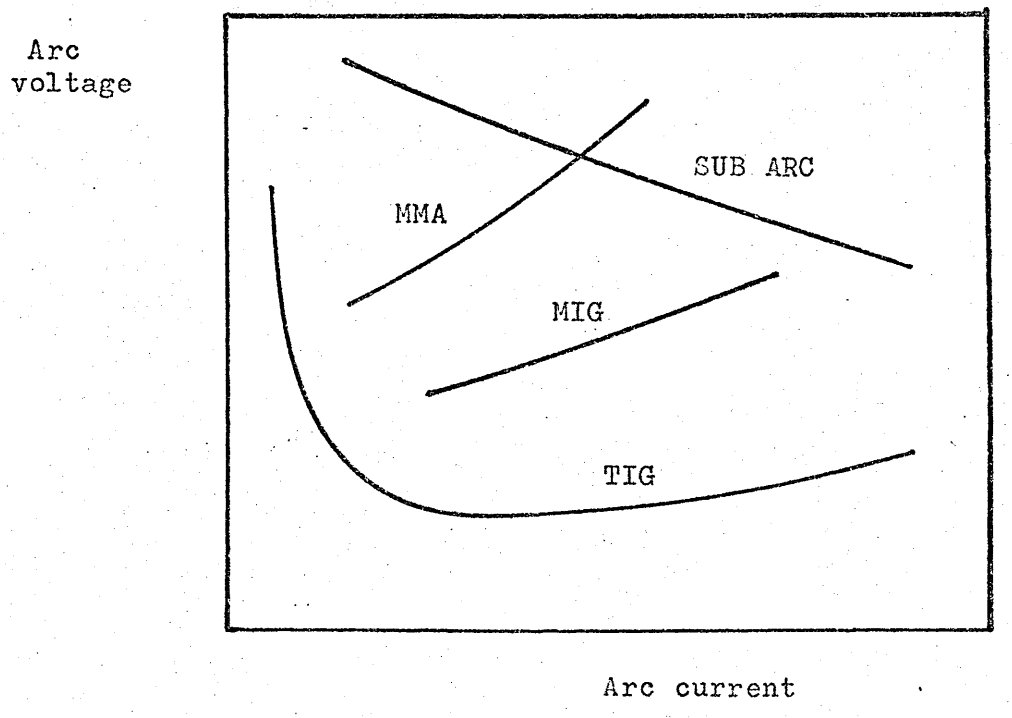

Figure 8. Typical arc characteristics of different processes.

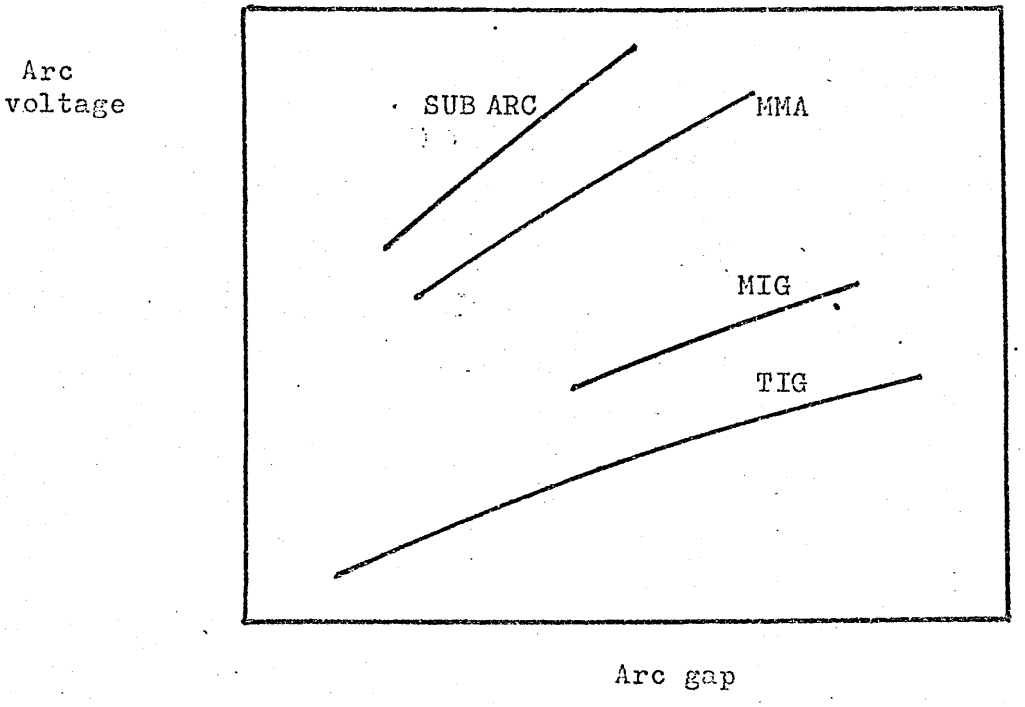

Figure 9. Relationship between voltage and arc gap.

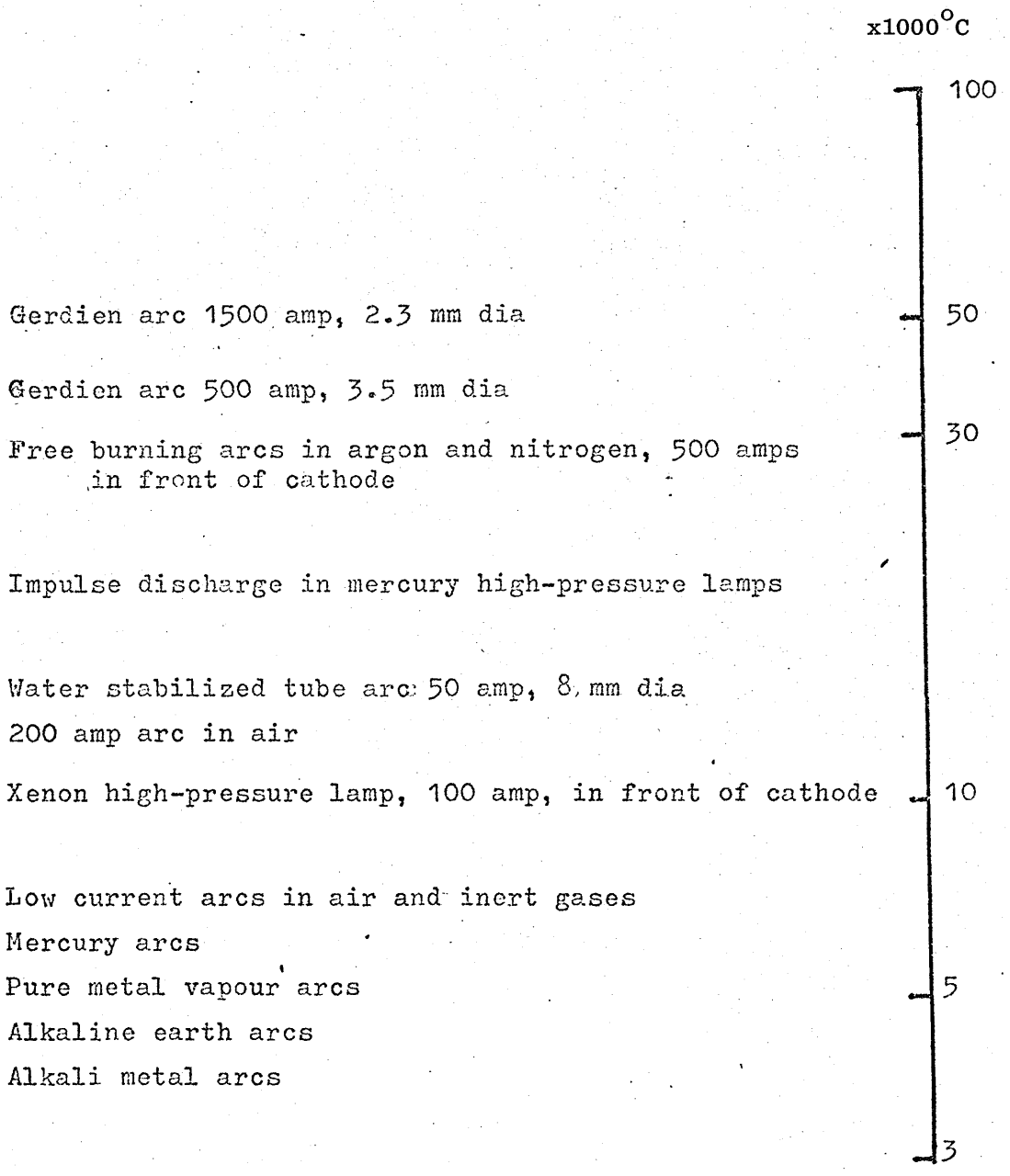

Figure 10. Scale of temperatures occurring in various types of arc (63)

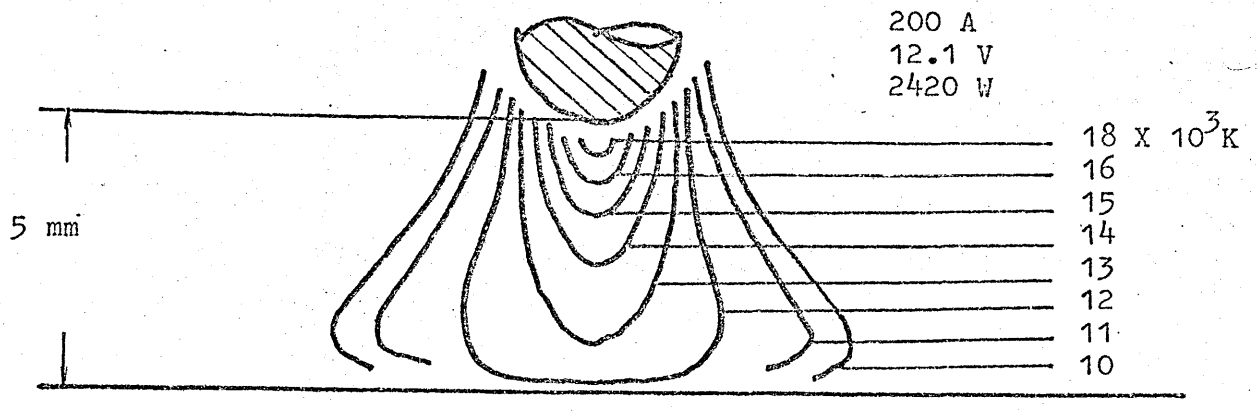

Figure 11. Isothermal map of an argon-tungsten arc. (65)

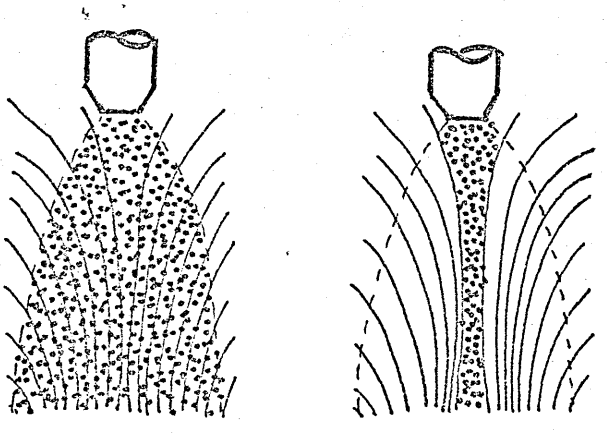

Figure 12. Flow lines and 4000°K isotherm for a 200A carbon arc.

a. When the gas flow is below 10^2cm/sec, the luminous region of the arc is completely filled with vapour.
b. When there is a high velocity jet, e.g. 10^4-10^5cm/sec, and a low rate of vapour emission the vapour flows along the stream lines. (73).

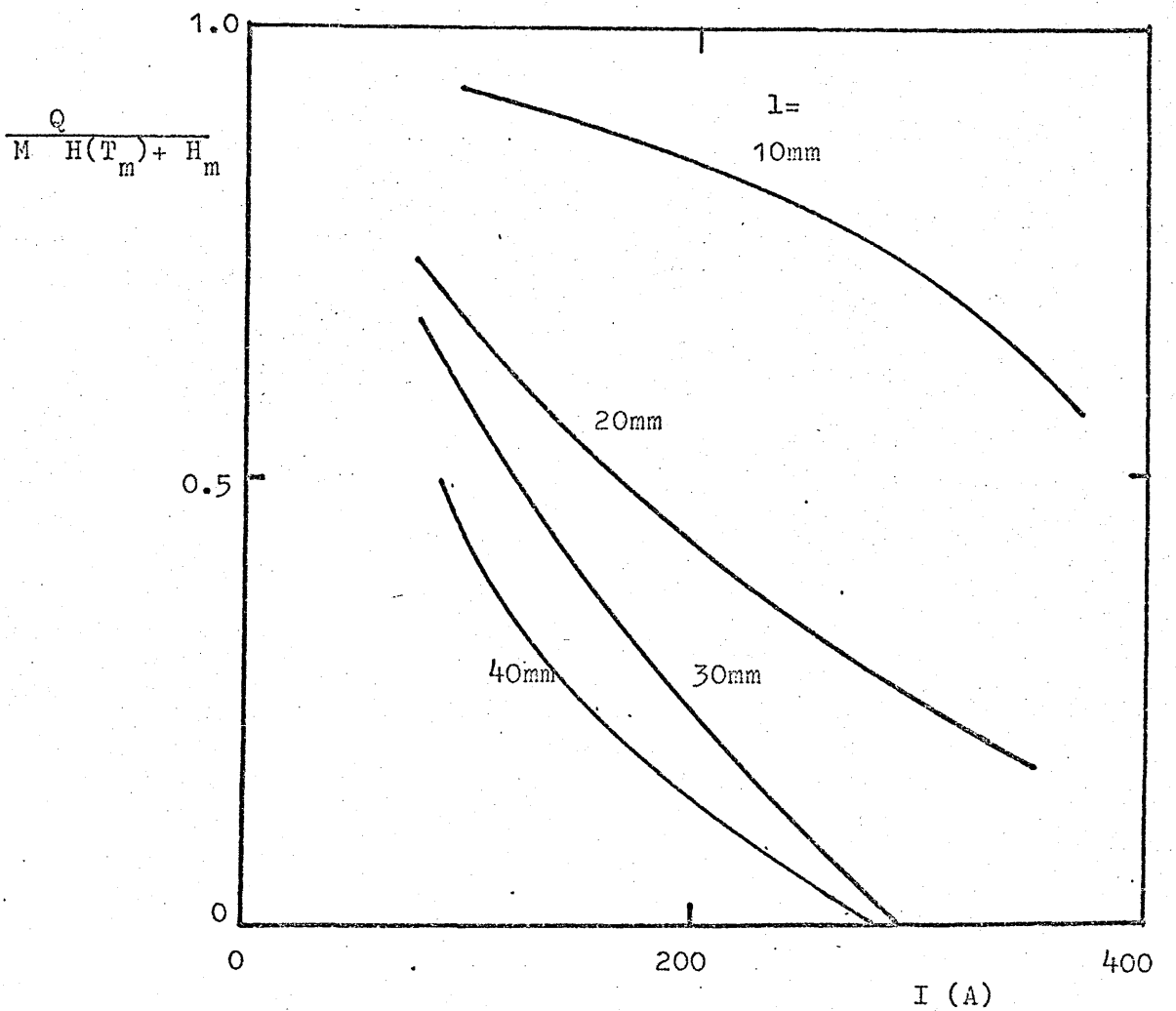

Figure 13. The ratio of Q, the heat flow from the anode spot to the solid through the liquid, to the total power supplied to the solid wire. (83).
l; extension.

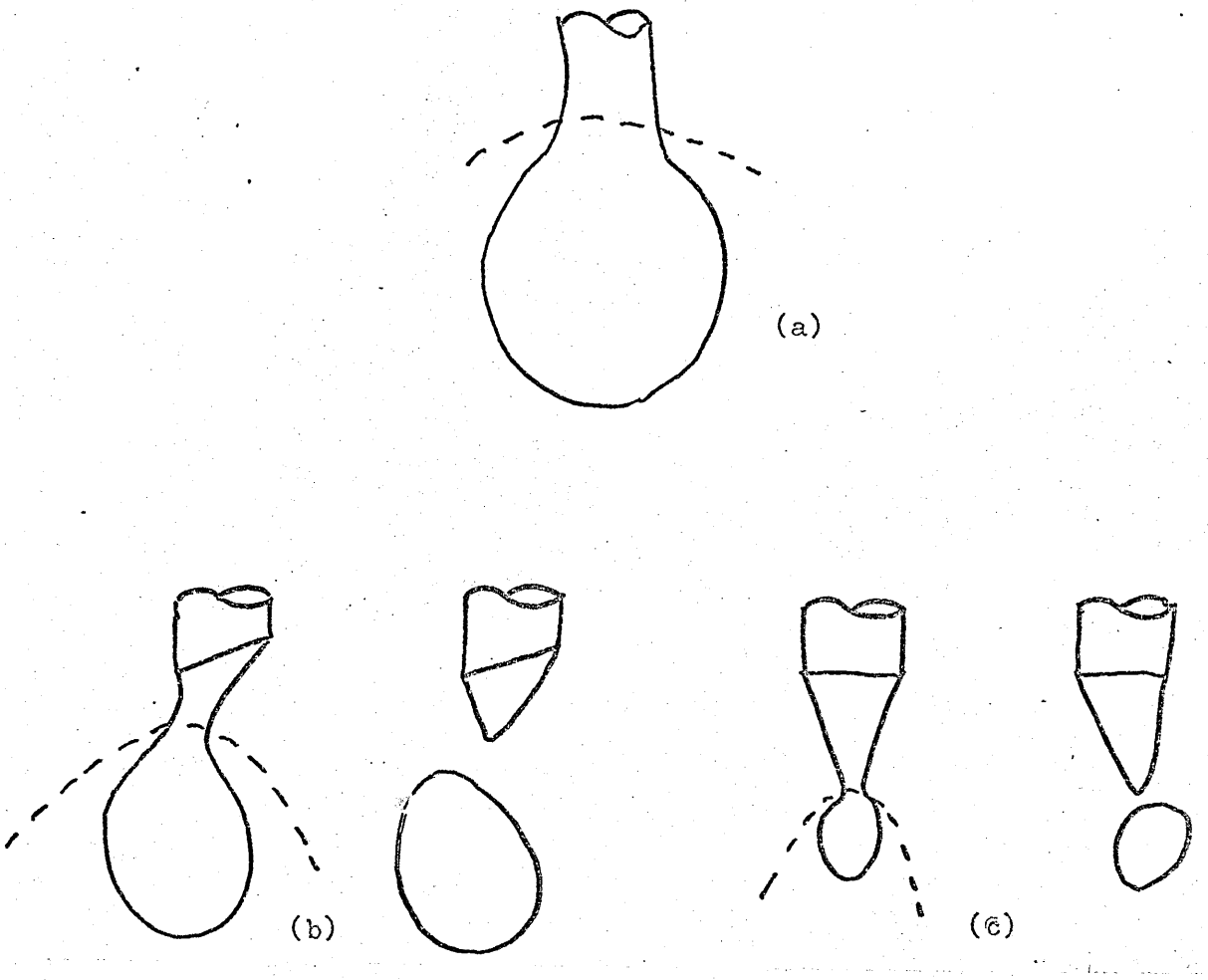

Figure 14. Metal transfer from 1.2mm mild steel electrode wire tip in argon;
(a) 140A. (b) 190A. (c) 220A. (104).

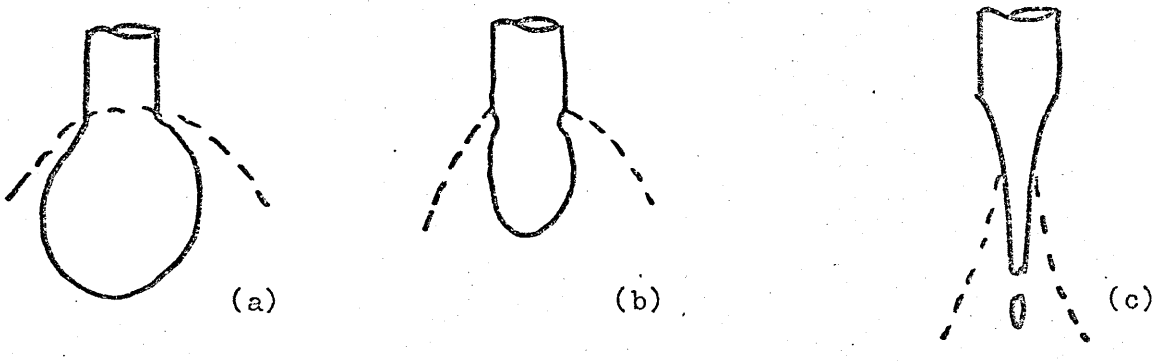

Figure 15. Metal transfer from 1.2mm mild steel electrode wire tip in argon;
(a) 180A, (b) 200A, (c) 260A. (99).

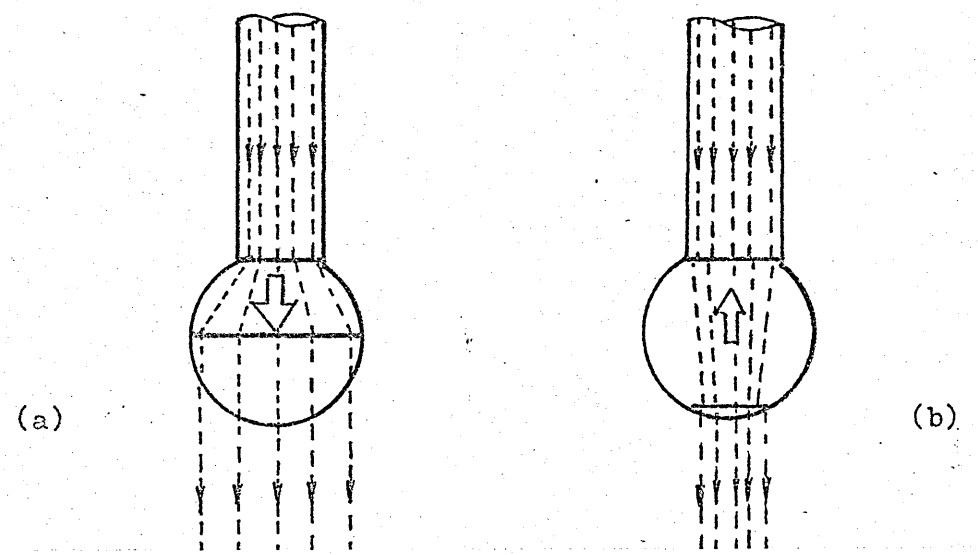

Figure 16. Effective area on drop detachment force, (a) if the current lines diverge in the drop the component aids drop detachment, (b) if the current lines converge, a component of the Lorentz force opposes detachment.

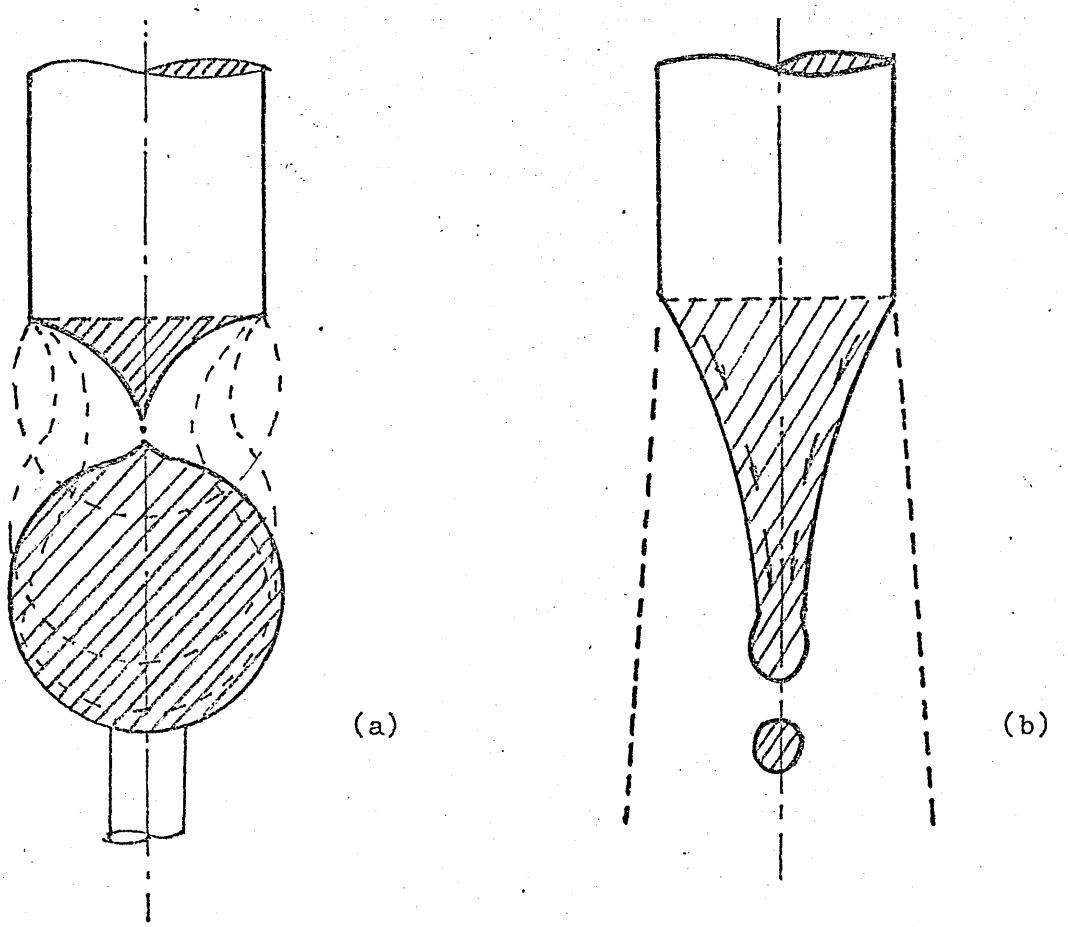

Figure 17. Model of metal transfer mechanism (111).
(a) Globular transfer.
(b) Spray transfer; the molten metal on the electrode face moves along the tapering tip, and only at the end of the electrode does drop formation and detachment occur.

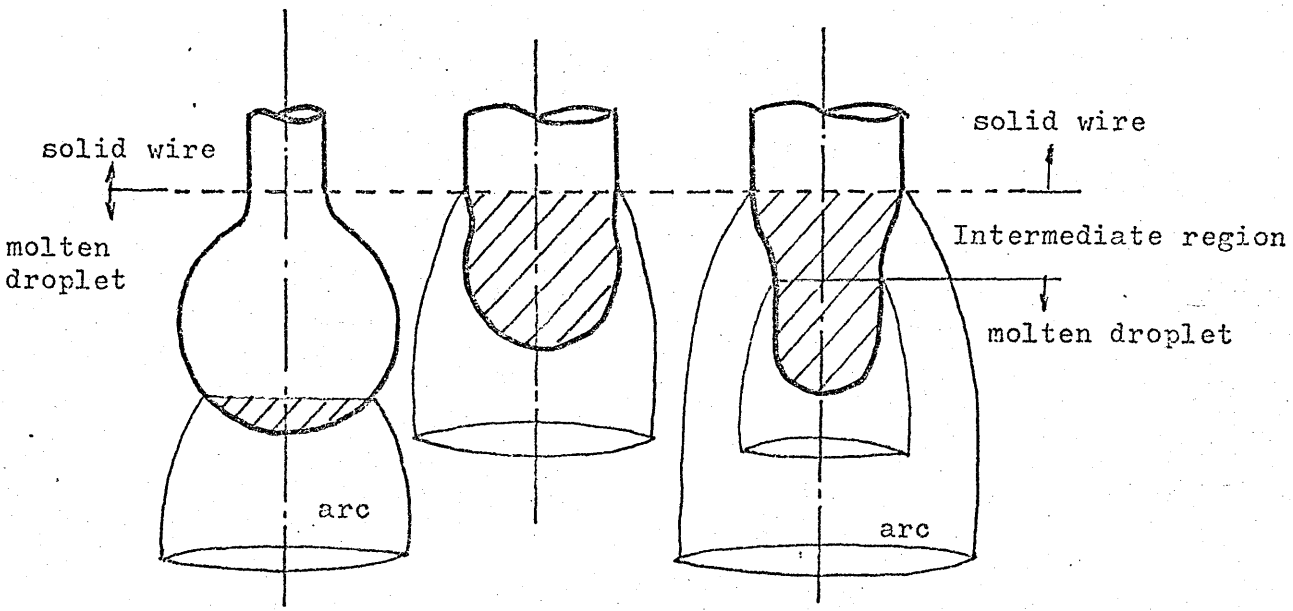

Figure 18. Approximate molten tip shapes for electrodes in consumable arc welding (89)

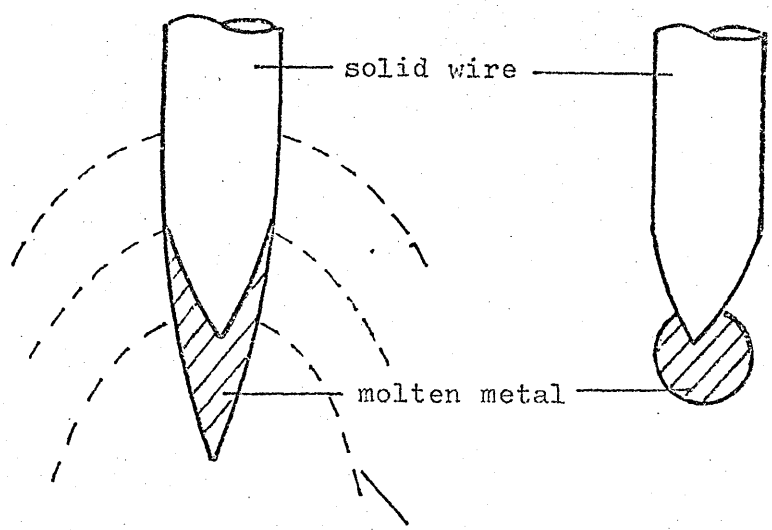

Figure 19. The typical shape of electrode tips of steel wires in MIG welding. The pencil-point-like tip in steel wire is considered to be related to the low heat conductivity (87)

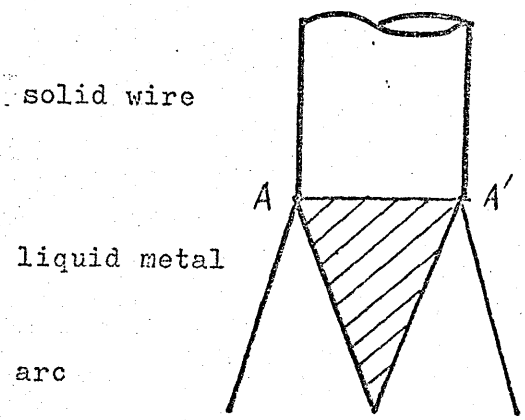

Figure 20. A simplified model of a tapering electrode tip of streaming transfer MIG.
A - A'; interface between liquid and solid metal (70)

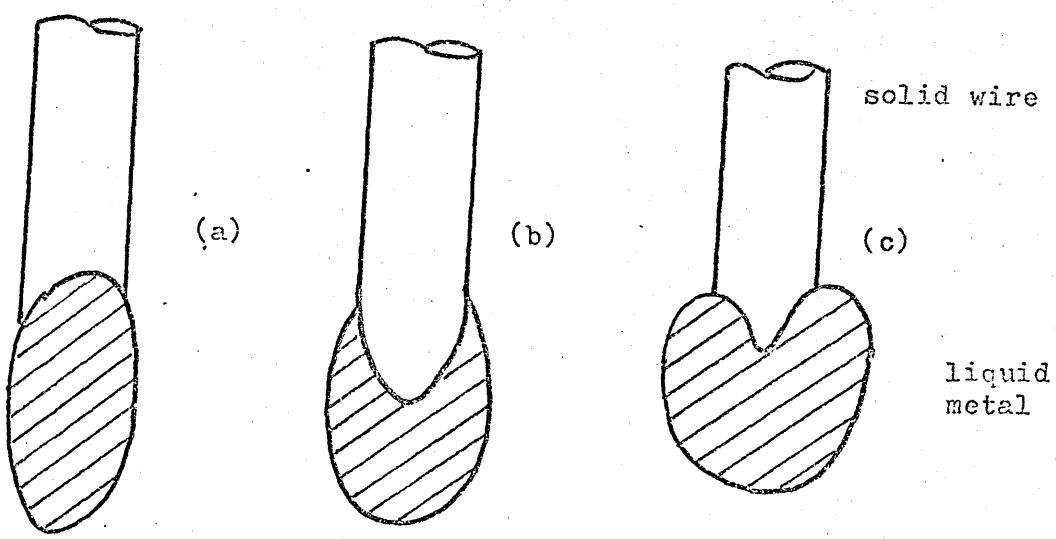

Figure 21. Model of metal transfer mechanism by Vesa Hiltunen (113)
(a) The solid liquid interface is upwards curved
(b) The solid liquid interface is downwards curved
(c) The downwards curve with necking process

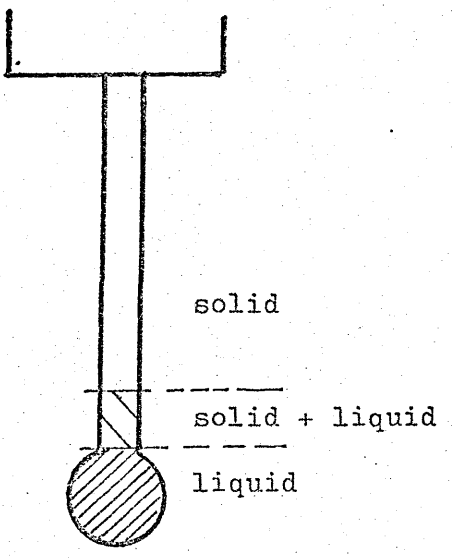

Figure 22. The region of solid and liquid. Partially melted region of electrode extension (83)

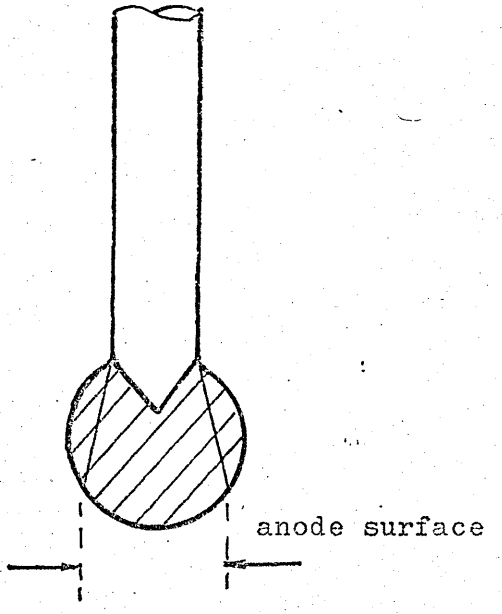

Figure 23. Model of globular transfer mechanism (83)

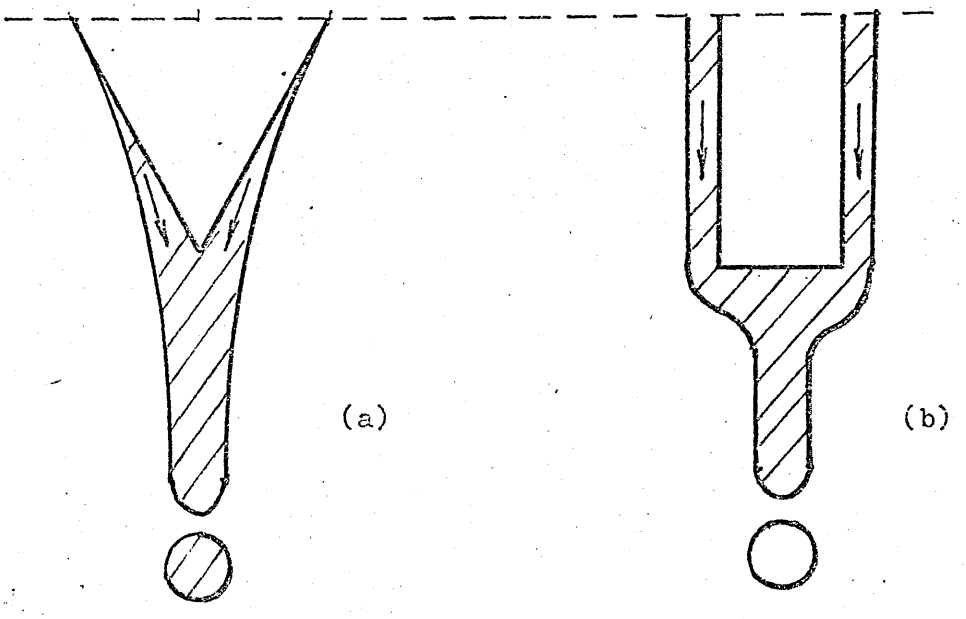

Figure 24. Model of spray transfer mechanism (83)
(a) The real tip; a continuous flow of liquid metal goes downwards along the conical tip of the wire
(b) The model of spray transfer, the conical tip is replaced by a cylinder having the same length

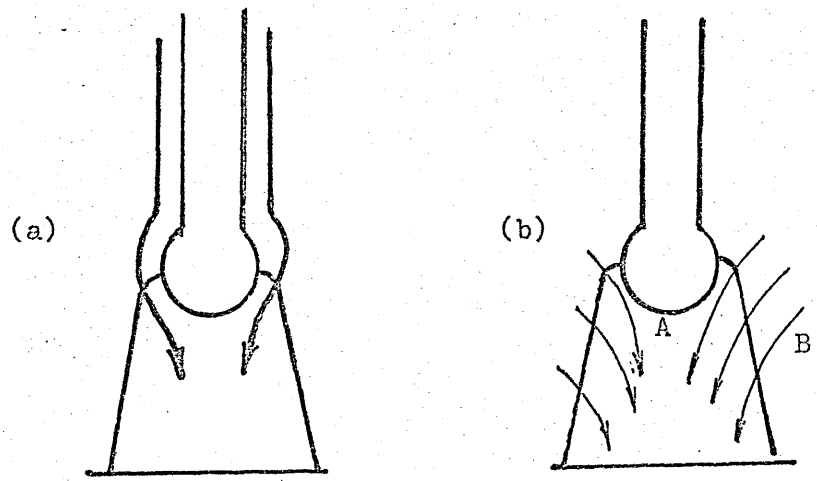

Figure 25. Discussion about drop detachment mechanism
(a) Gas flow theory of drop detachment, supposed direction of flow (96)
(b) Actual gas flow and estimated velocity and pressure conditions outside arc column (114)

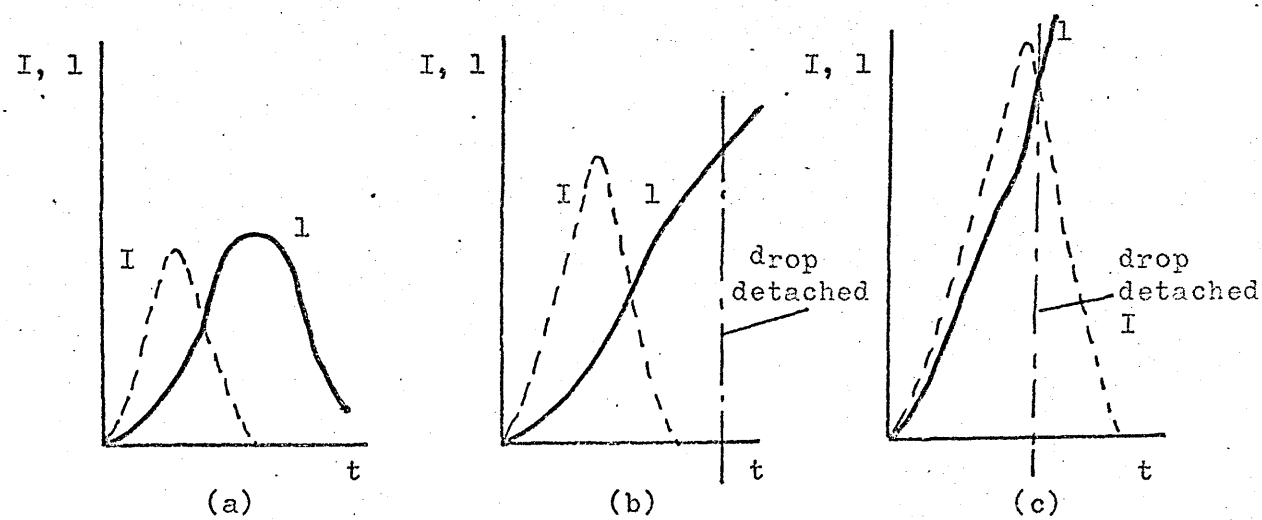

Figure 26. Characteristic curves for droplet movement (1) with pulsed current (123)
(a) The energy of one pulse is not sufficient to expel a drop from the electrode
(b) The energy of pulse is sufficient to expel a drop from the electrode
(c) The energy of the pulse is excessively great. Several droplets may form during a single pulse.

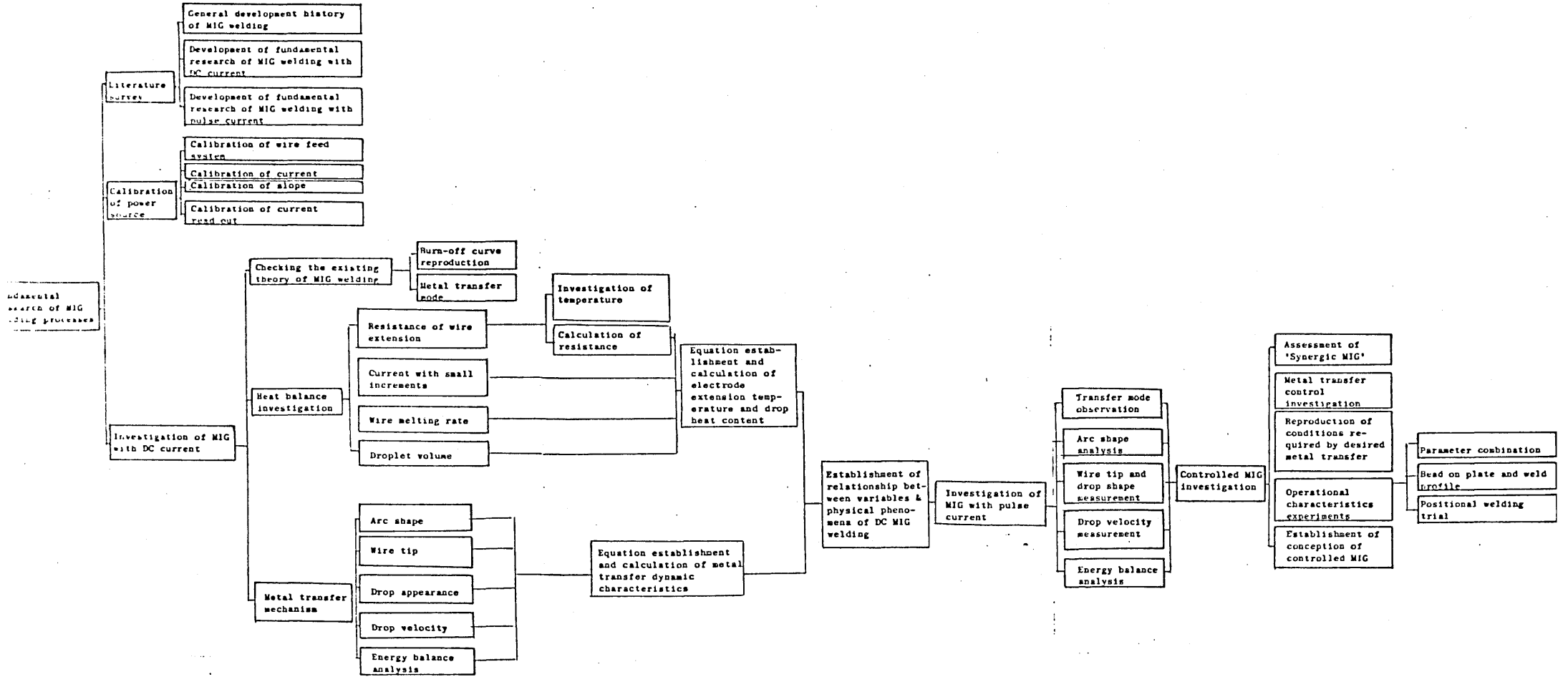

Figure 27. Research Programme

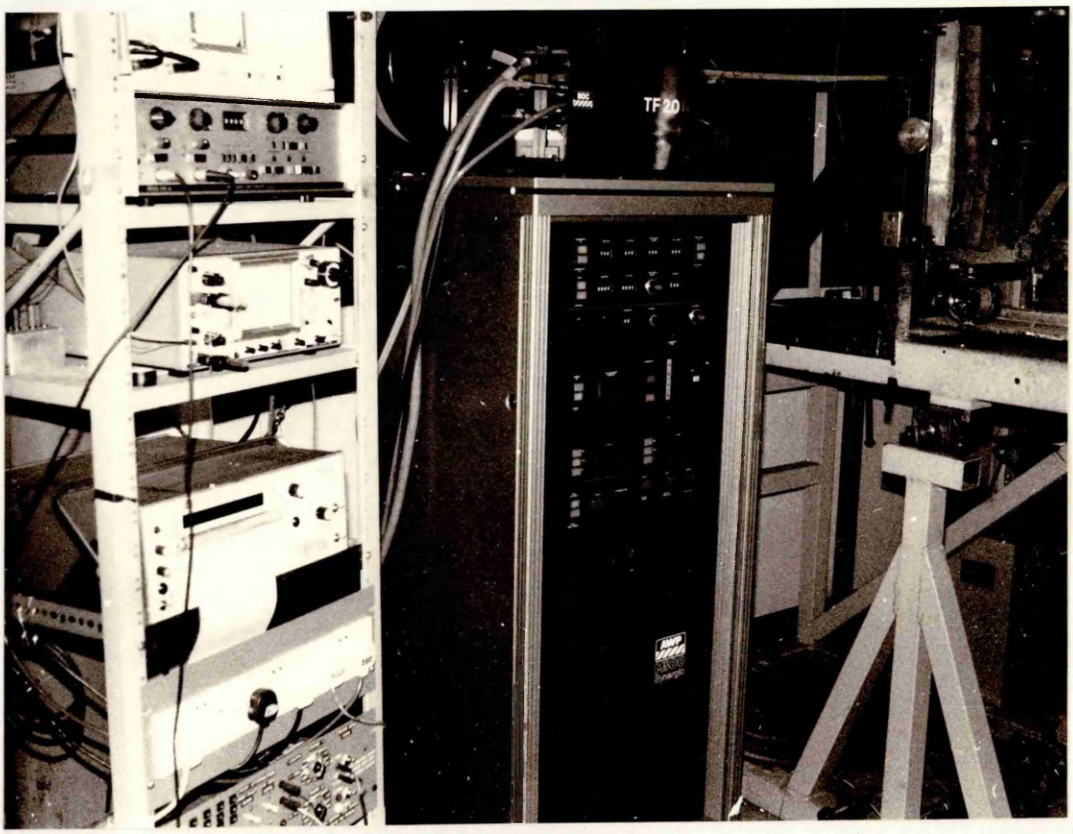

Figure 28. Transistor power source AWP M500

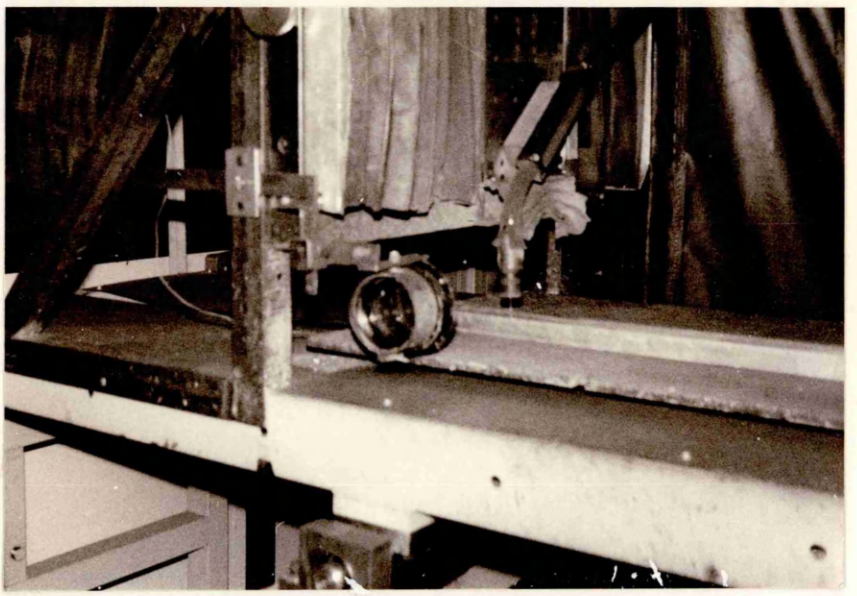

Figure 29. The test rig and the lens

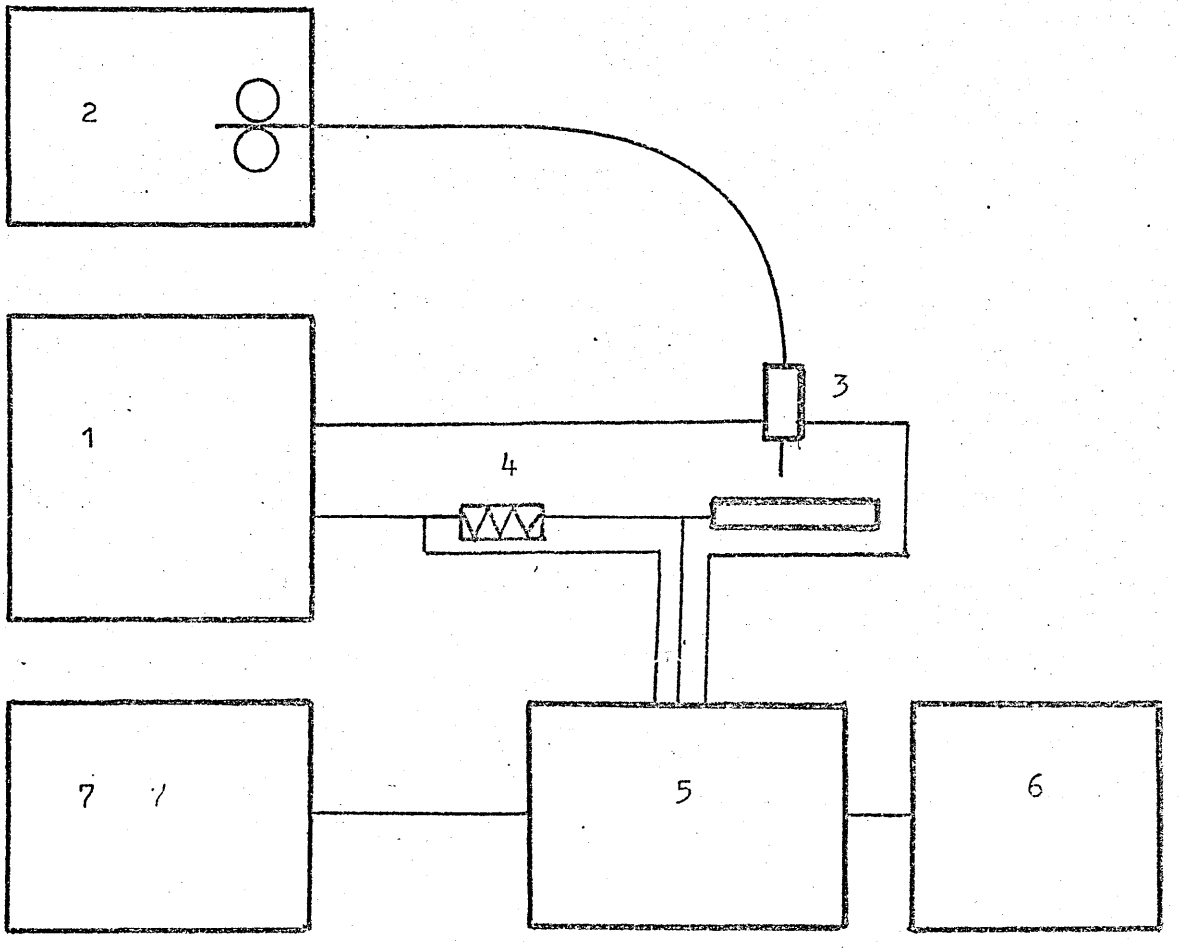

Figure 30. The layout of instrumentation rig, connection diagram

1. power source
2. wire feed unit
3. torch
4. shunt
5. transient recorder
6. oscilloscope
7. ultra violet oscillograph

Figure 31. Globular transfer in MIG welding. 1.2mm dia. mild steel wire, Ar + 5% CO_2, 200A.

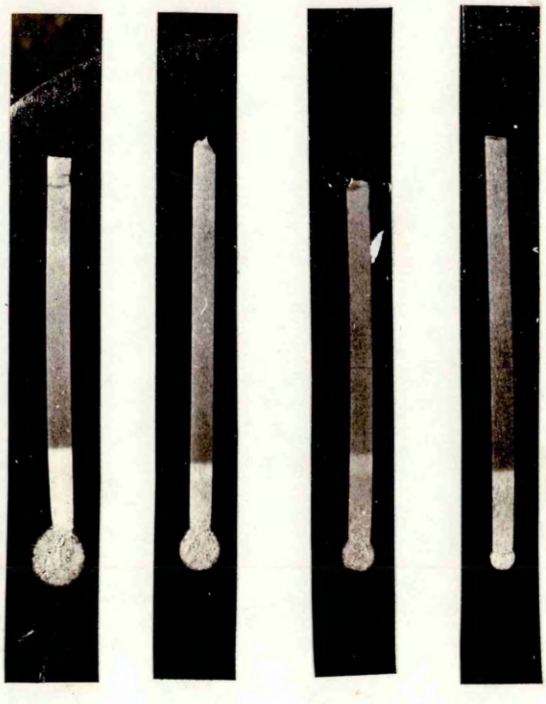

Figure 32. The wire tips of globular transfer. 1.2mm dia. wire, Ar + 5% CO_2.
(a) 91A, Drop frequency f = 13Hz. (b) 147A, f = 14Hz.
(c) 199A, f = 50Hz. (d) 233A, f = 85Hz.

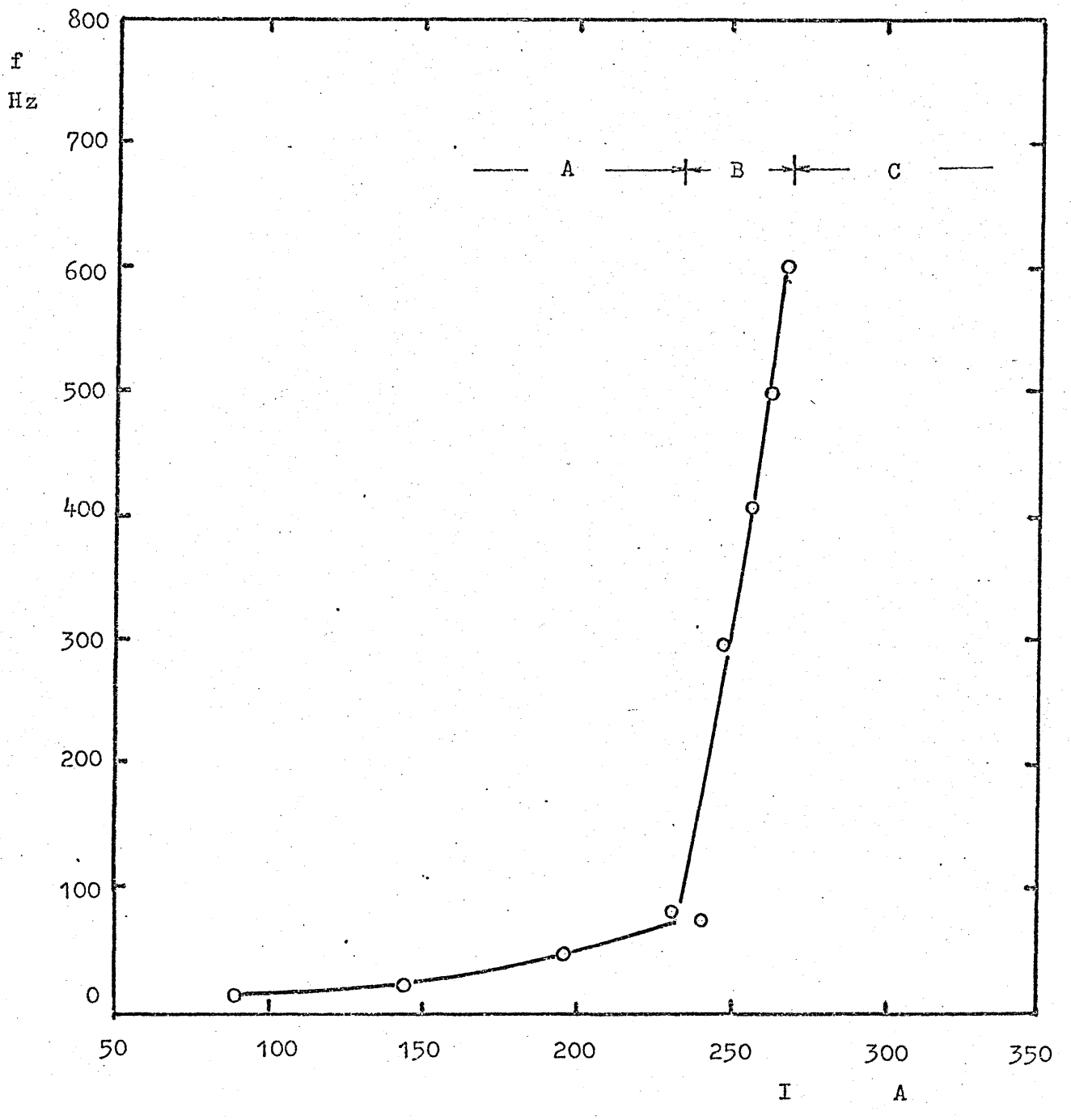

Figure 33. Detachment frequency, f of MIG welding, 1.2mm mild steel wire, Ar + 5% CO_2.
A region, globular transfer mode,
B region, drop spray transfer mode,
C region, stream spray transfer mode.
Note: drop frequency of stream transfer mode cannot be determined.

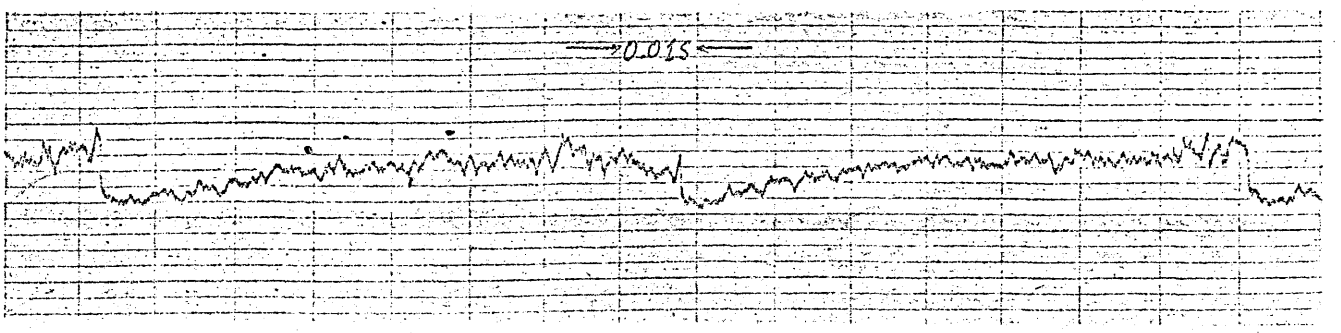

(a)

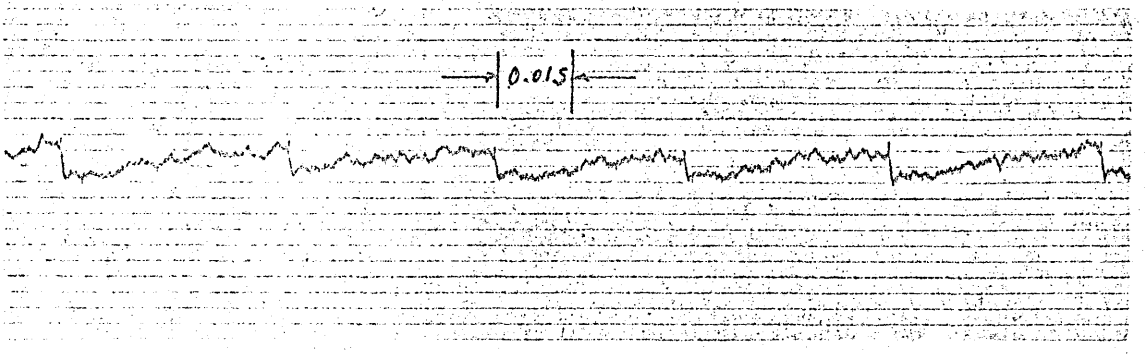

(b)

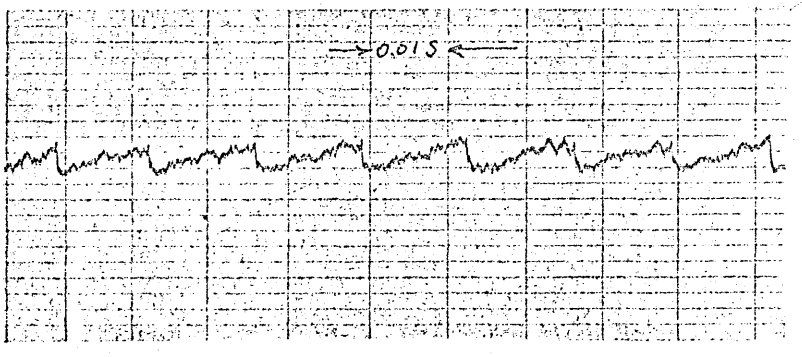

(c)

Figure 34. UVO traces of arc voltages, globular transfer mode.
(a) I = 90A, f = 12Hz
(b) I = 190A, f = 40Hz
(c) I = 235A, f = 77Hz
1.2mm mild steel wire, Ar + 5% CO_2.

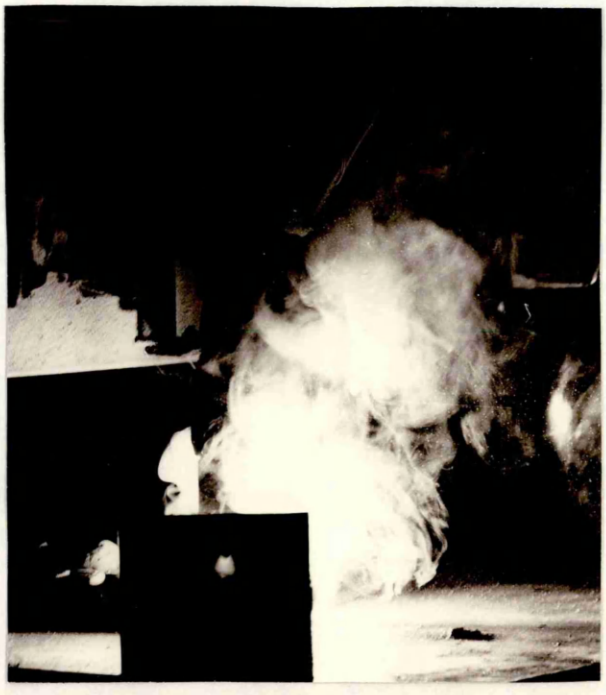

Figure 35. The fume generated from the boiling surface of liquid drop suspended under wire tip, 1.2mm wire, Ar + 5% CO_2.

Figure 36. Arc shape in drop spray transfer, 1.2mm dia mild steel wire, Ar + 5% CO_2.

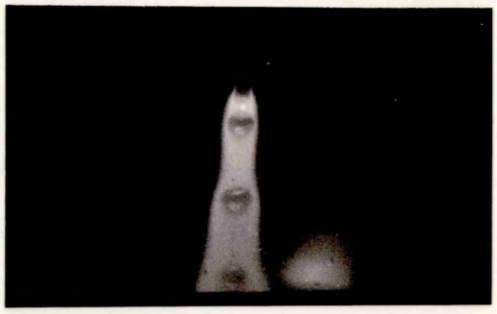

Figure 37. Drop formation and transfer, drop spray transfer mode. Arc shape is formed by metal vapour of drop surface.

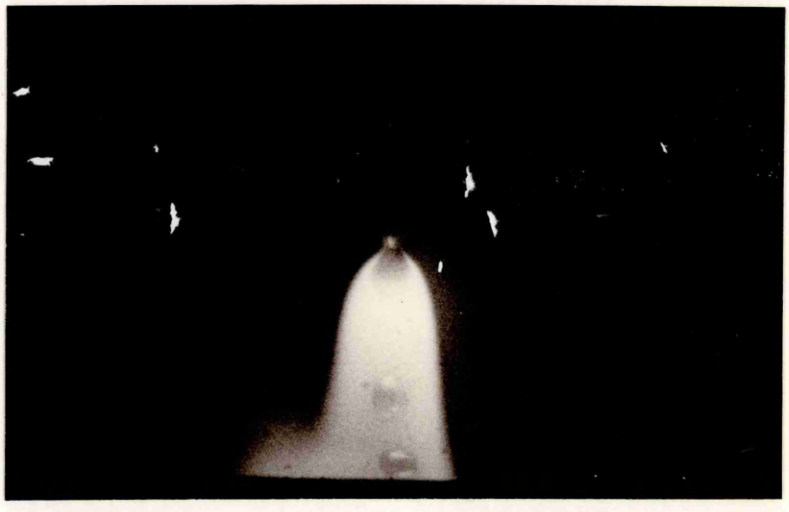

Figure 38. Drop transfer mode: the arc root covers the drop surface just beneath the neck but not the conic tip surface.

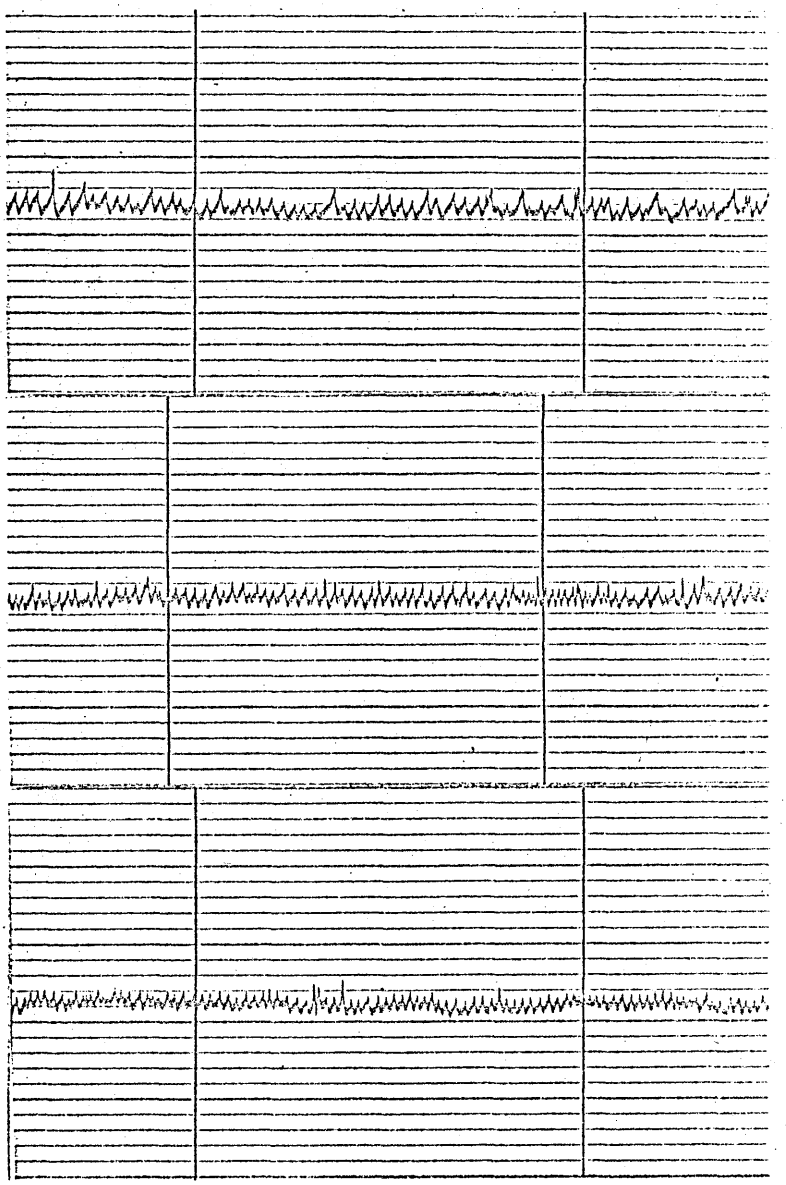

Figure 39. UVO traces of arc voltage, drop spray transfer mode.
(a) 250A, f = 290Hz
(b) 260A, f = 410Hz
(c) 270A, f = 600Hz
1.2mm wire, Ar + 5% CO_2.

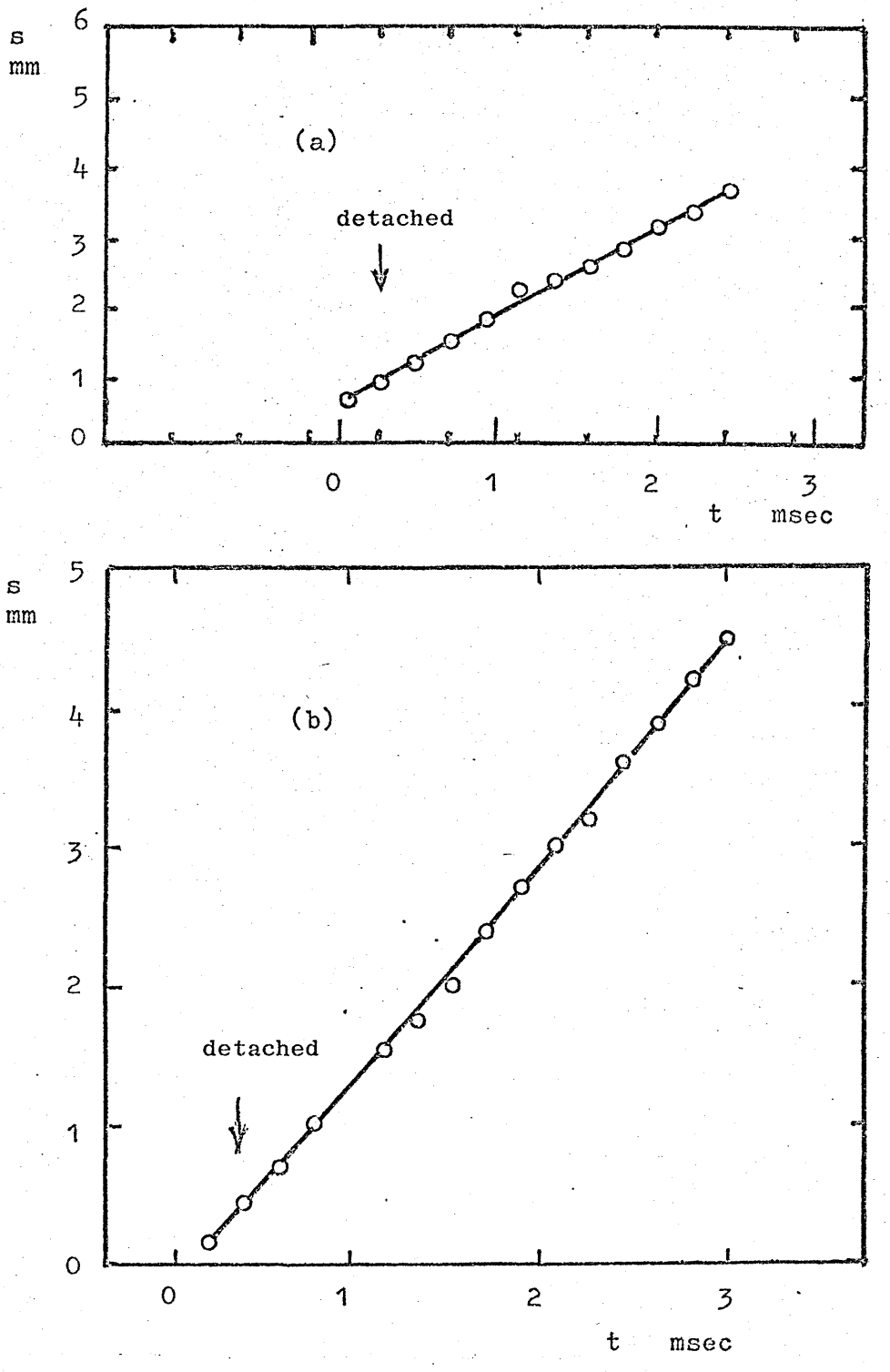

Figure 40. Drop displacement with time. 1.2mm wire, Ar + 5% CO_2.
(a) 250A, f = 281HZ, ds/dt = 1.25m/sec.
(b) 261A, f = 688Hz, ds/dt = 1.50m/sec.

(a)

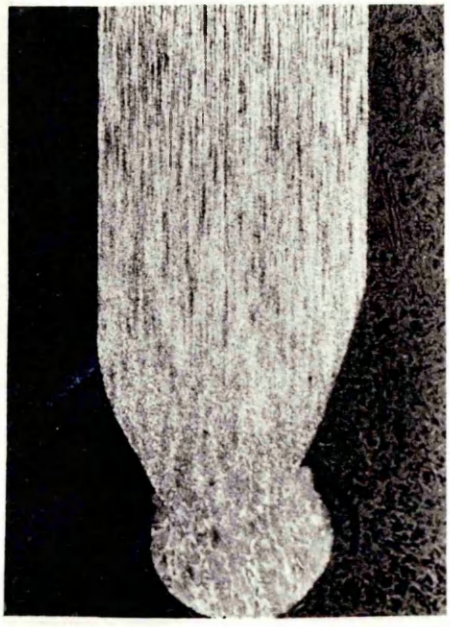

(b)

Figure 41. Microstructure of a drop spray transfer wire tip.
(b) X30
(c) X100

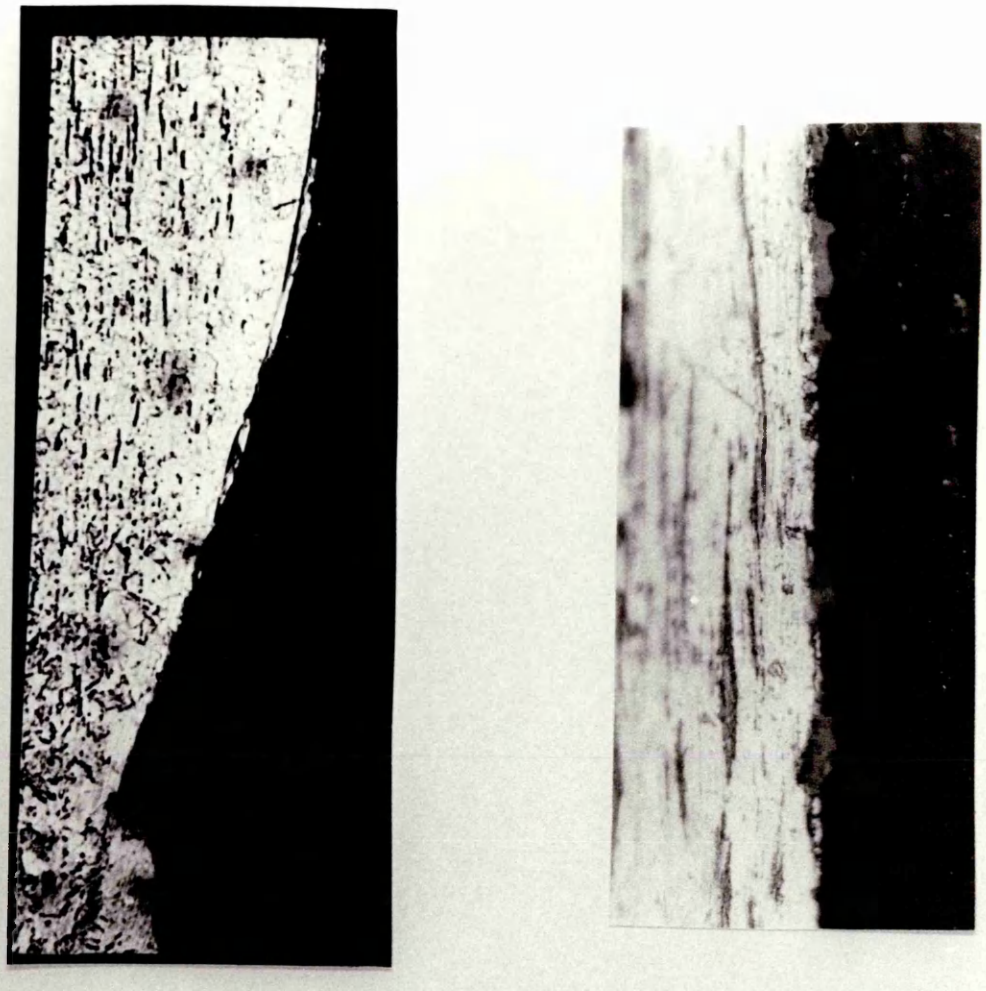

(a) (b)

Figure 42. Copper coating on wire electrodes.
(a) The copper coating remaining on the surface of wire conical tip.
(b) The copper coating on the surface of original electrode wire.
Note: the copper is of a bright yellow colour.

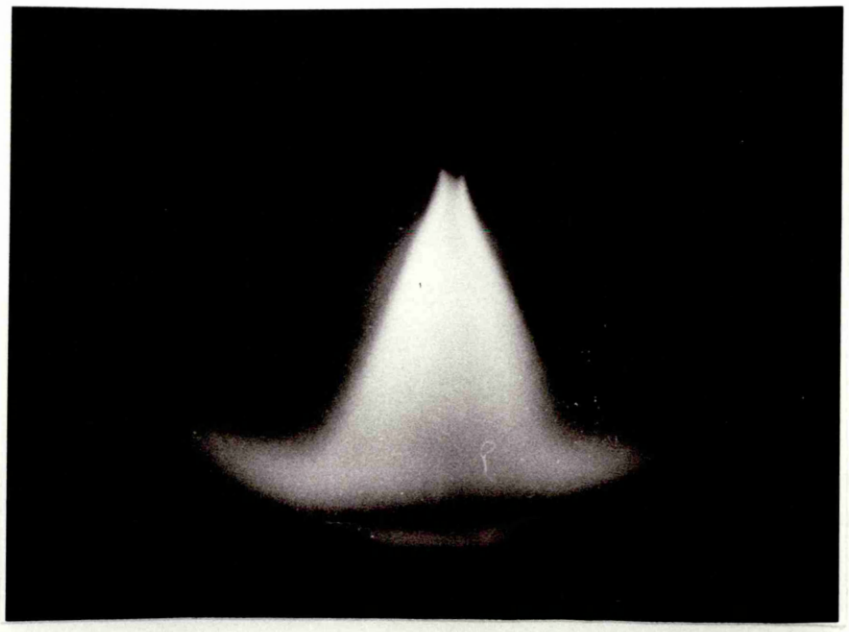

Figure 43. Arc shape of stream spray transfer mode, 1.2mm mild steel wire, Ar + 5% CO_2.

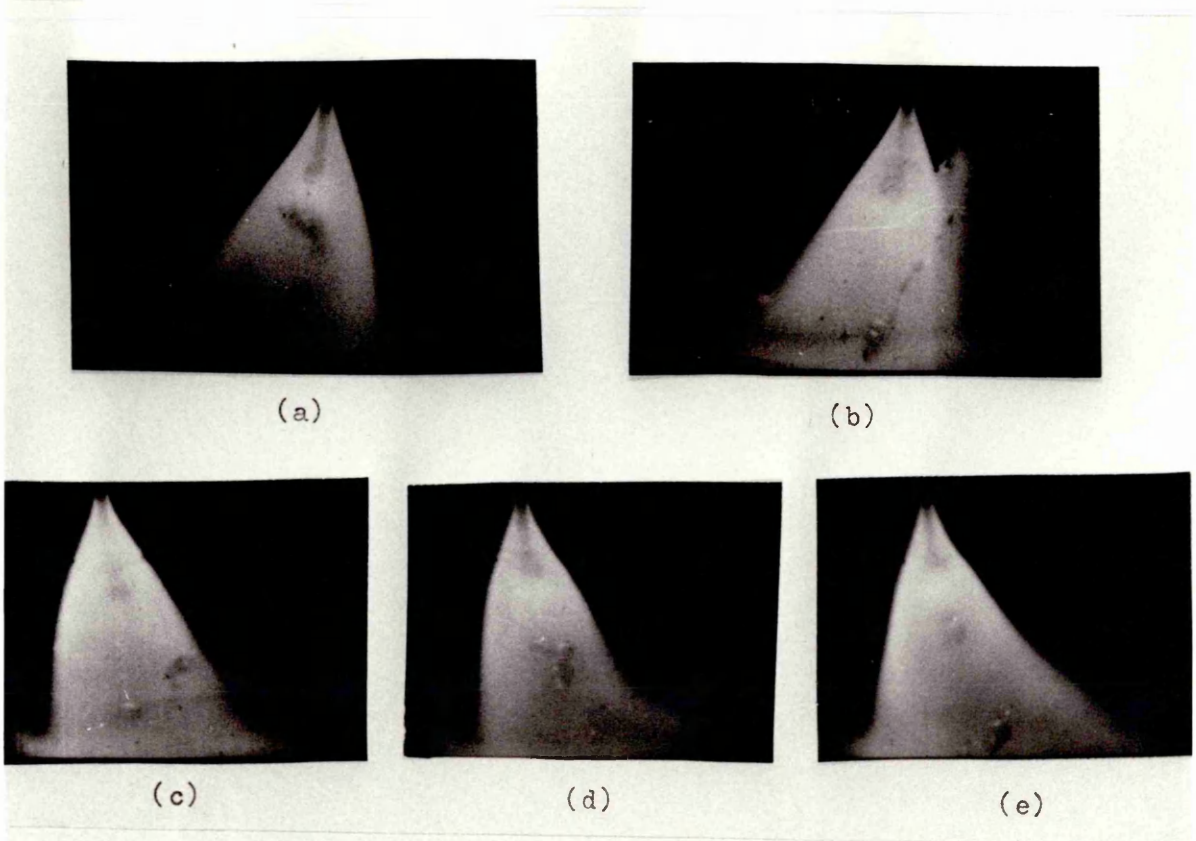

Figure 44. Features of stream spray transfer mode.
(a) Irregular drop size.
(b) Spatter and fume of metal vapour
(c) (d) (e) Irregular and scattered metal transfer.

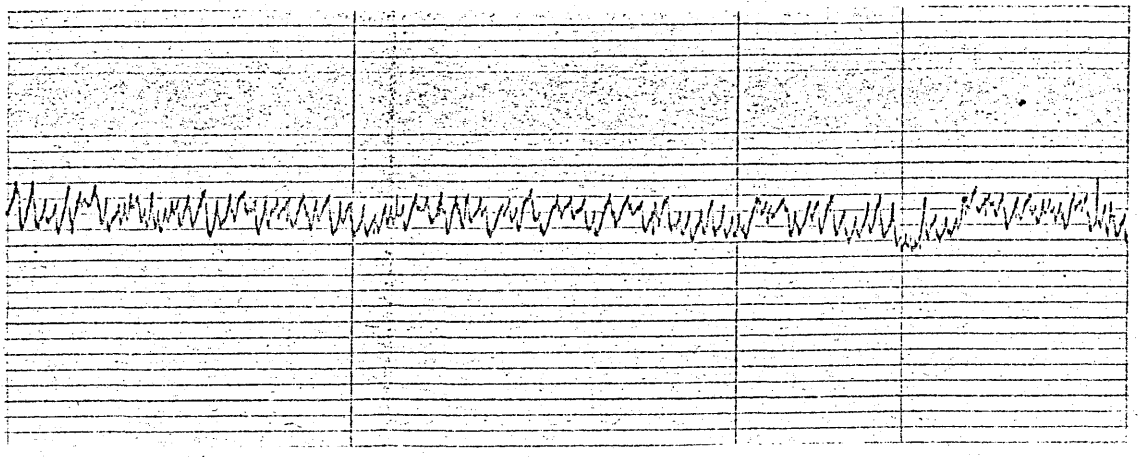

(a)

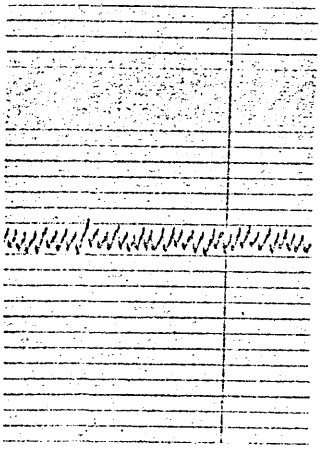

(b)

Figure 45. UVO trace of arc voltage, stream spray transfer mode of 290A, compared with drop spray transfer mode of 260A. (a) 290A (b) 260A.

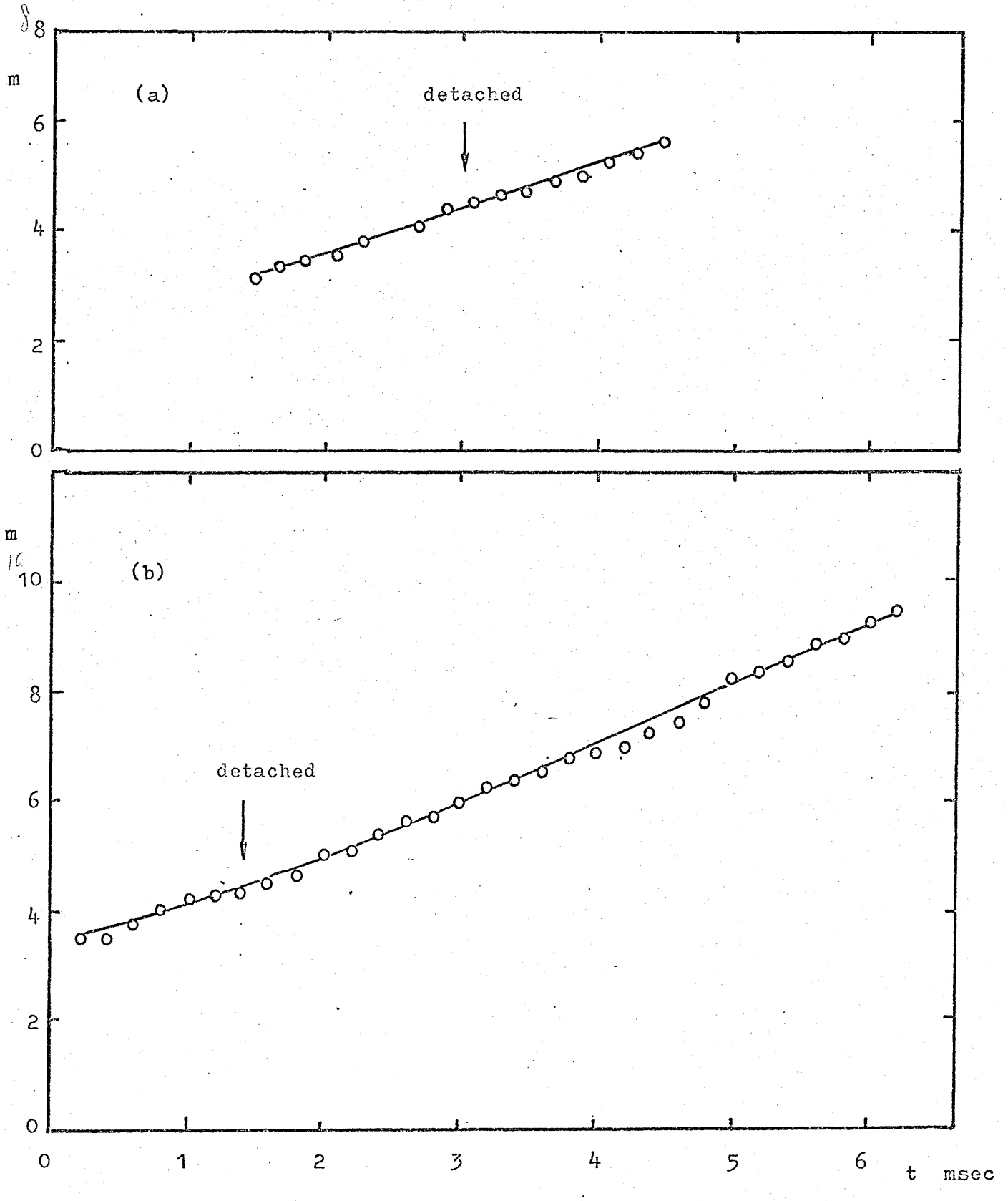

Figure 46. Droplet displacement in stream spray transfer mode.
(a) Mean drop velocity; 0.9m/sec.
(b) Mean drop velocity; 0.7 to 0.8m/sec.

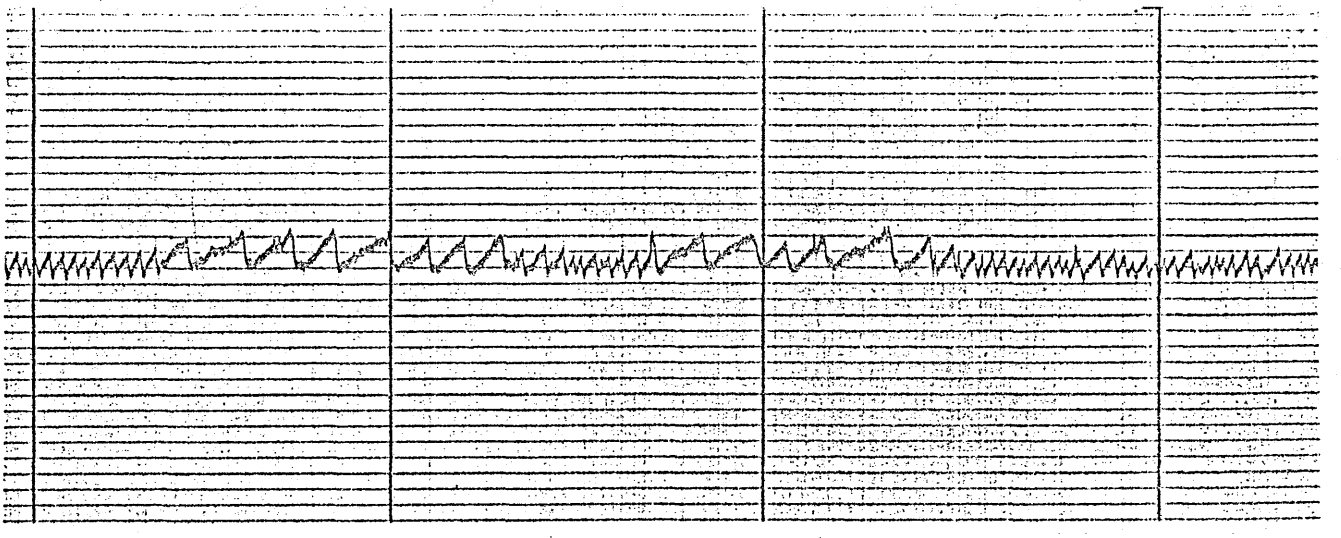

(a)

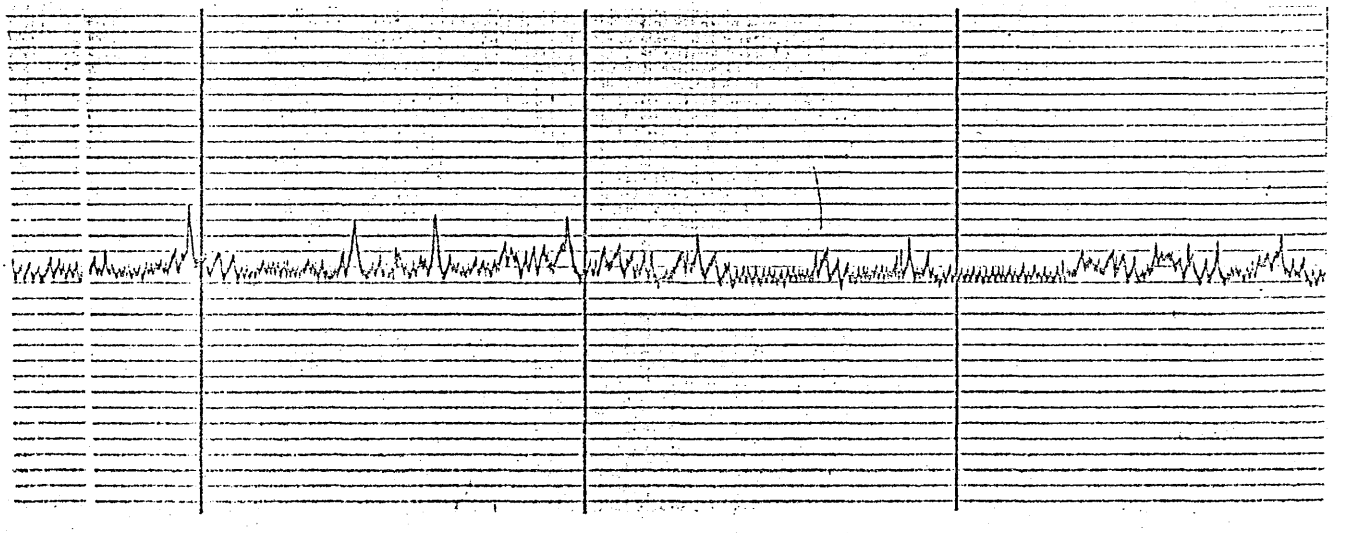

(b)

Figure 47. UVO traces of transition points.
(a) First transition point at which globular transfer mode changed to drop spray transfer mode.
(b) Second transition point at which drop spray transfer mode changed to stream spray transfer mode.

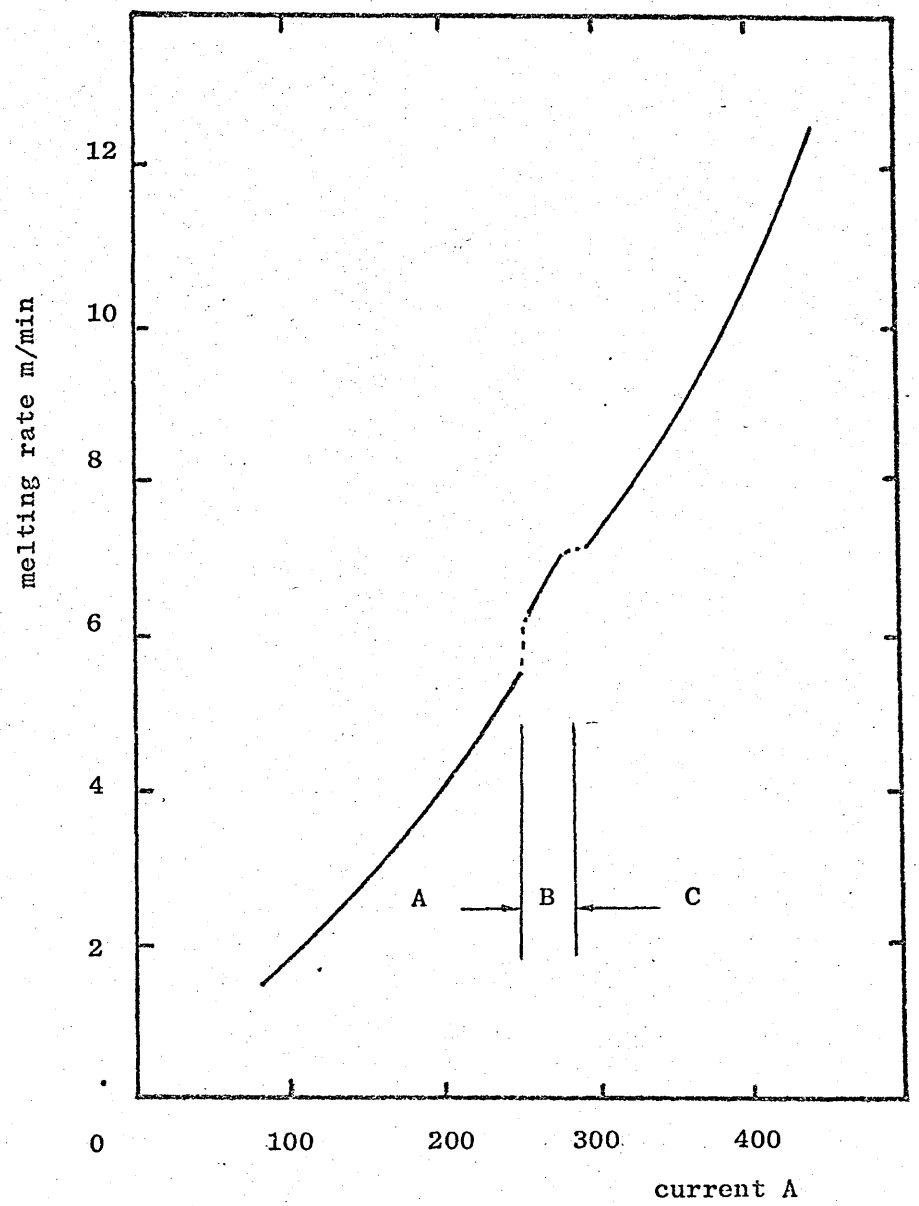

Figure 48. Relationship between the wire melting rate and welding current. 1.2mm dia. mild steel wire, Ar + 5% CO_2. Region A. Globular, Region B. Drop spray. Region C. Stream spray.

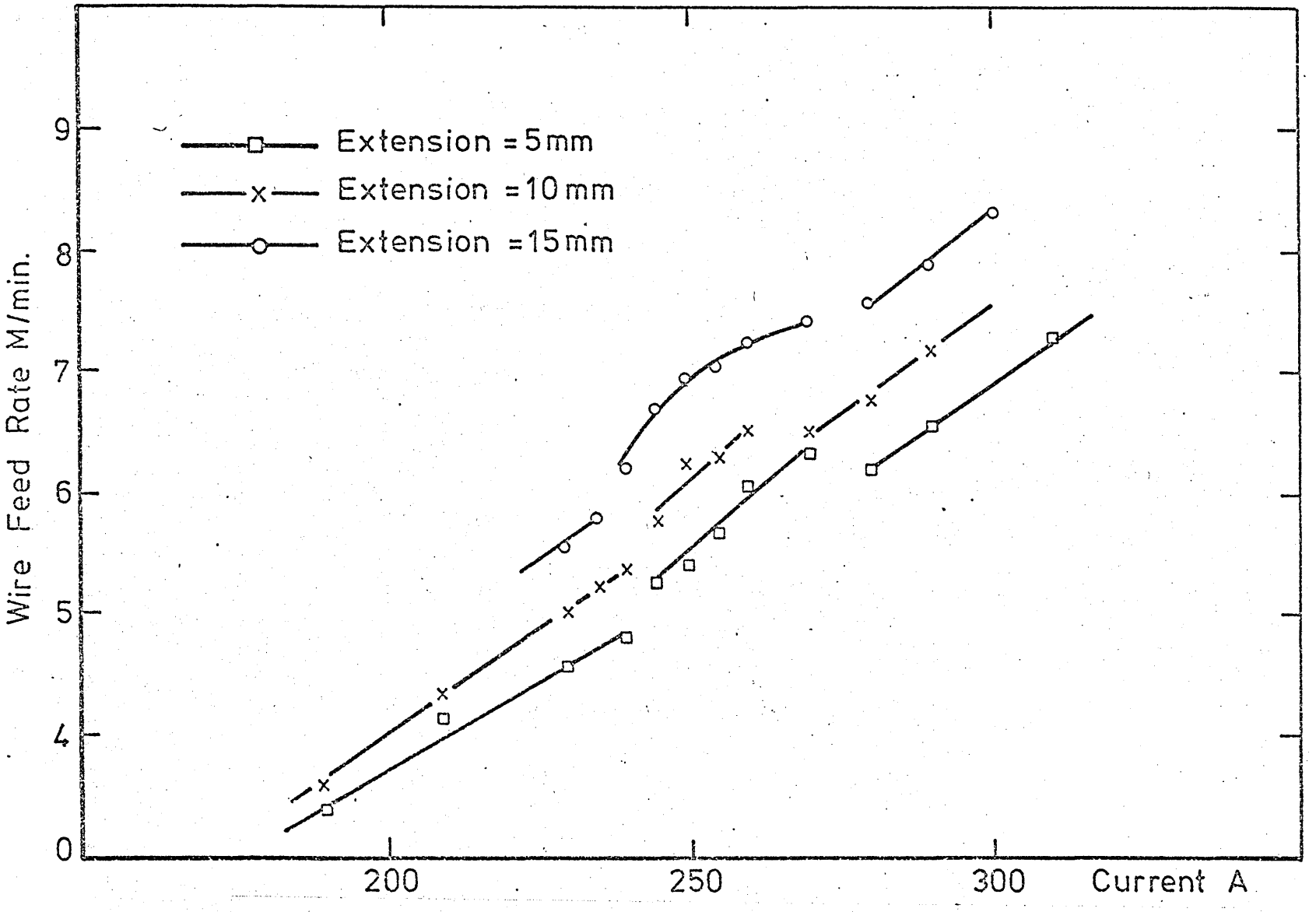

Figure 49. Variation of wire melting rate with current. Data is given in Table 6

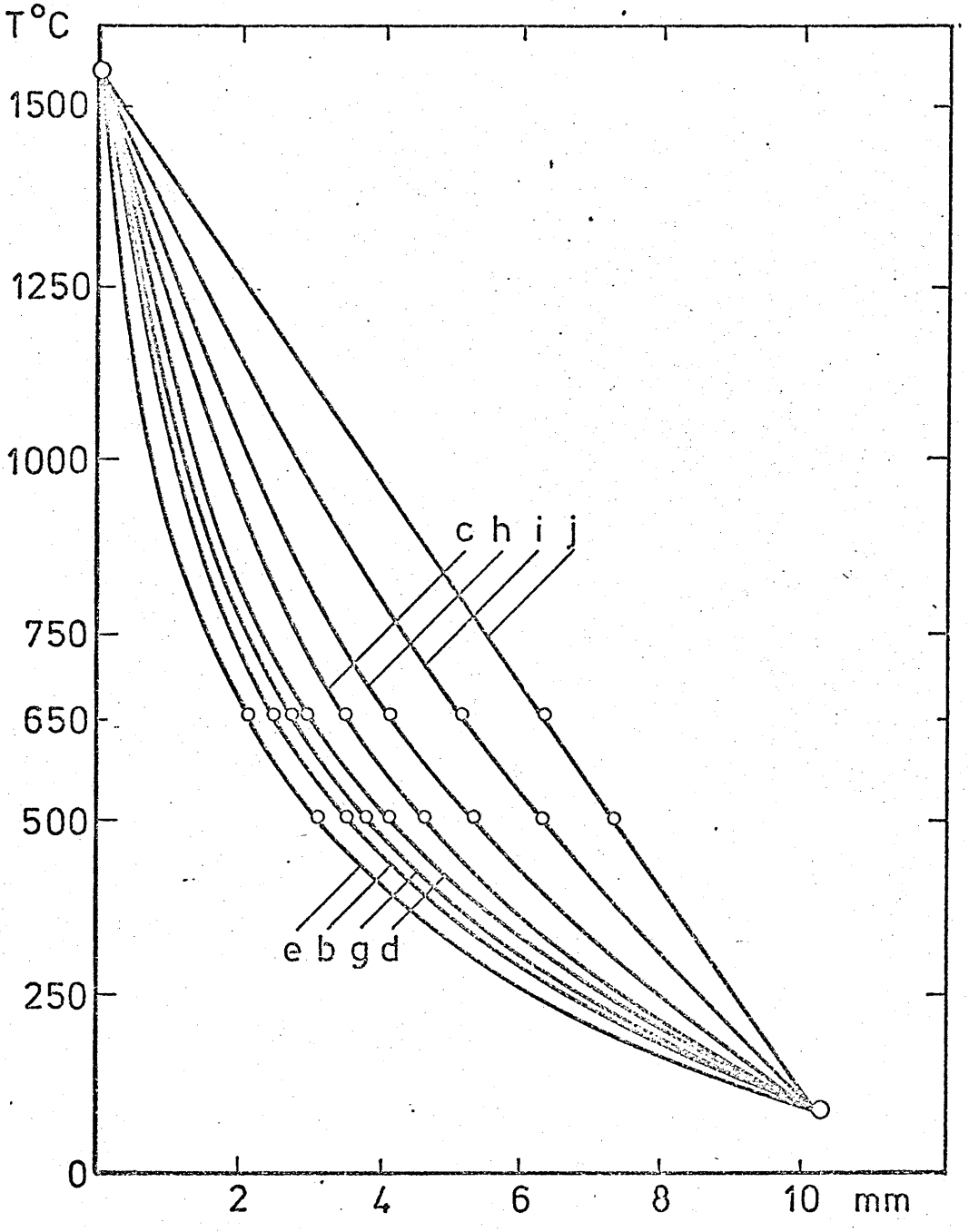

Figure 50. Temperature distribution along electrode extension, 1.2mm wire, 10mm electrode extension, Ar + 5% CO_2.
Value of I for each wire is given as:
e. 242A, b. 147A, d. 233A, c. 199A, h. 357A,
i. 378A, j. 405A.

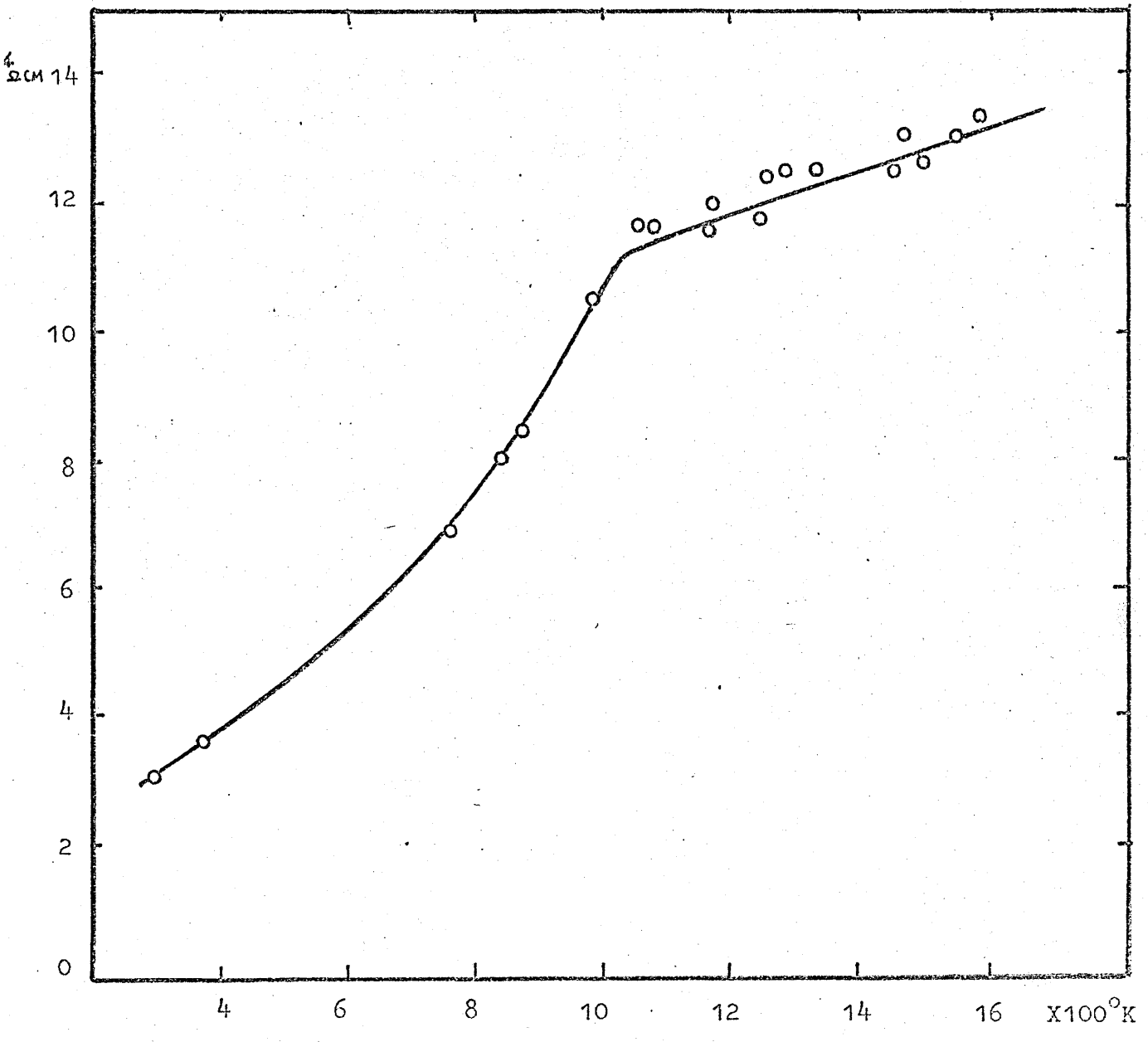

Figure 51. Resistivity of mild steel wire. (90)

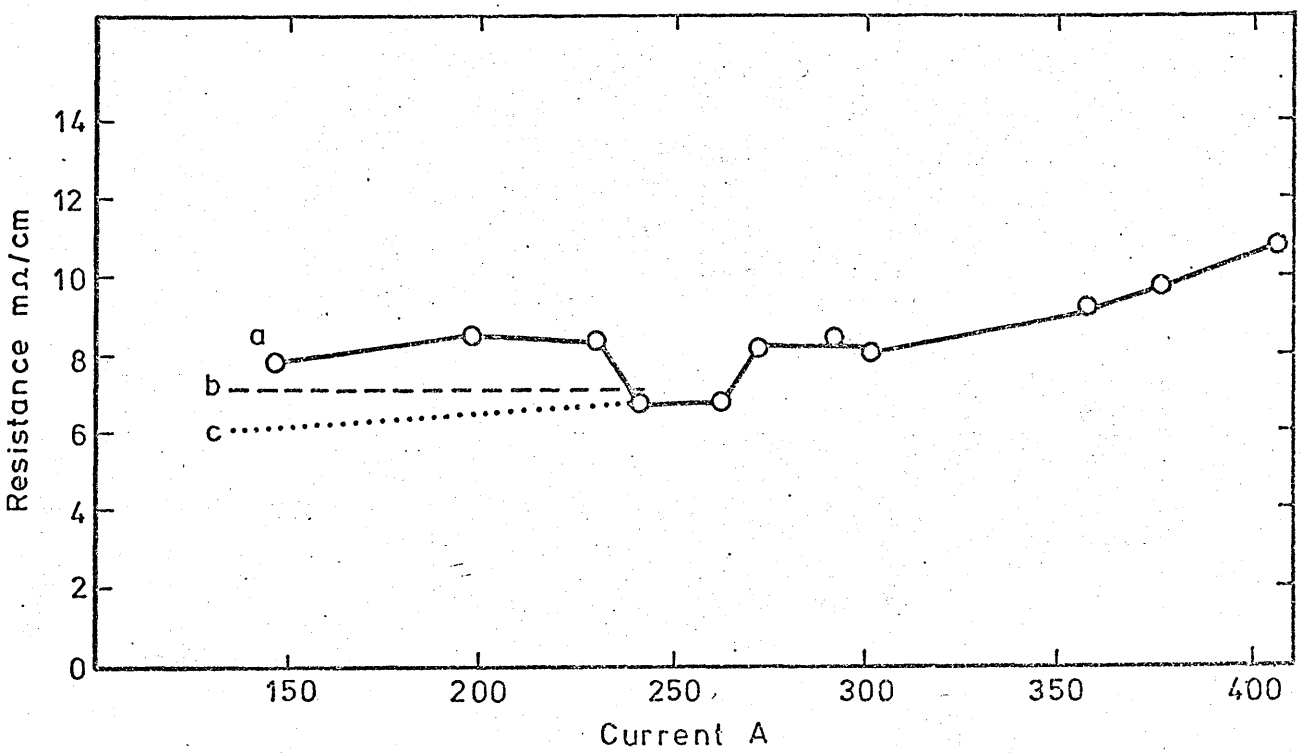

Figure 52. Variation of electrical resistance of electrode extension with welding current, 1.2mm dia wire.
(a) present work
(b) 86
(c) 90

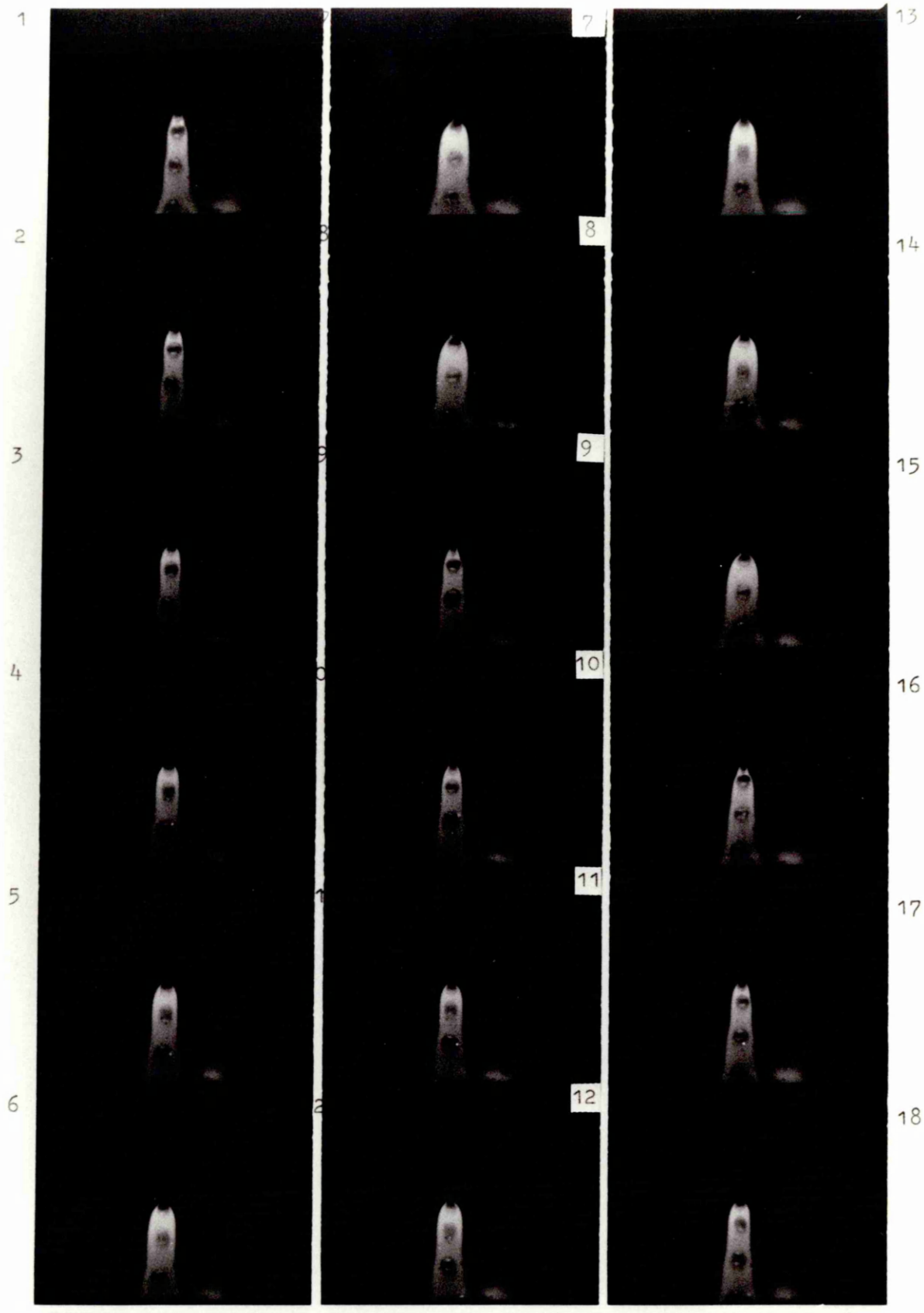

Figure 53. Drop formation, growth and detachment processes of drop spray transfer mode, 1.2mm mild steel wire, Ar + 5% CO_2, 261A, 7000 frames per second.

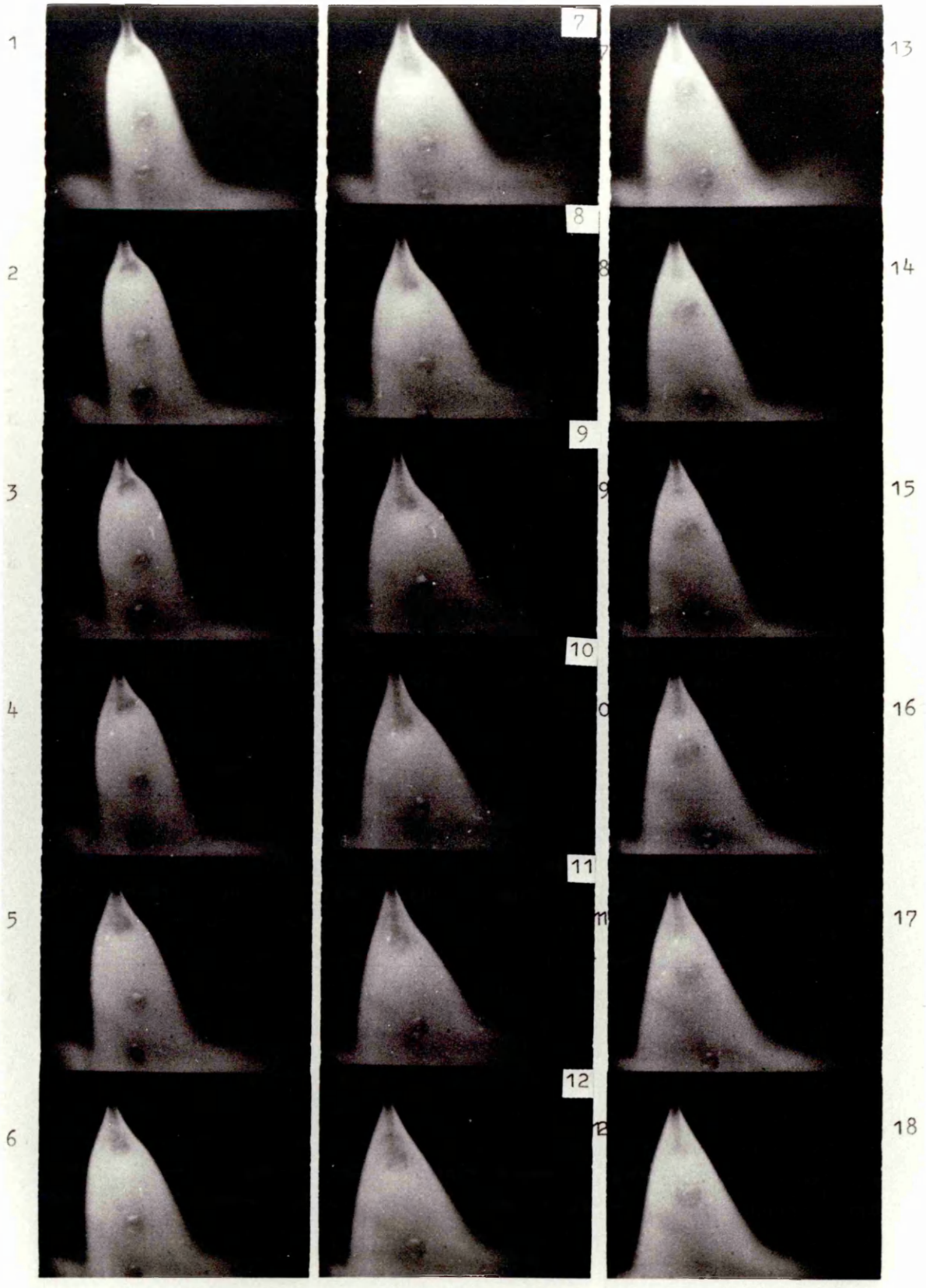

Figure 54. Metal transfer process of stream spray mode, 1.2mm mild steel wire, Ar + 5% CO_2, 290A, 7000 frames per second.

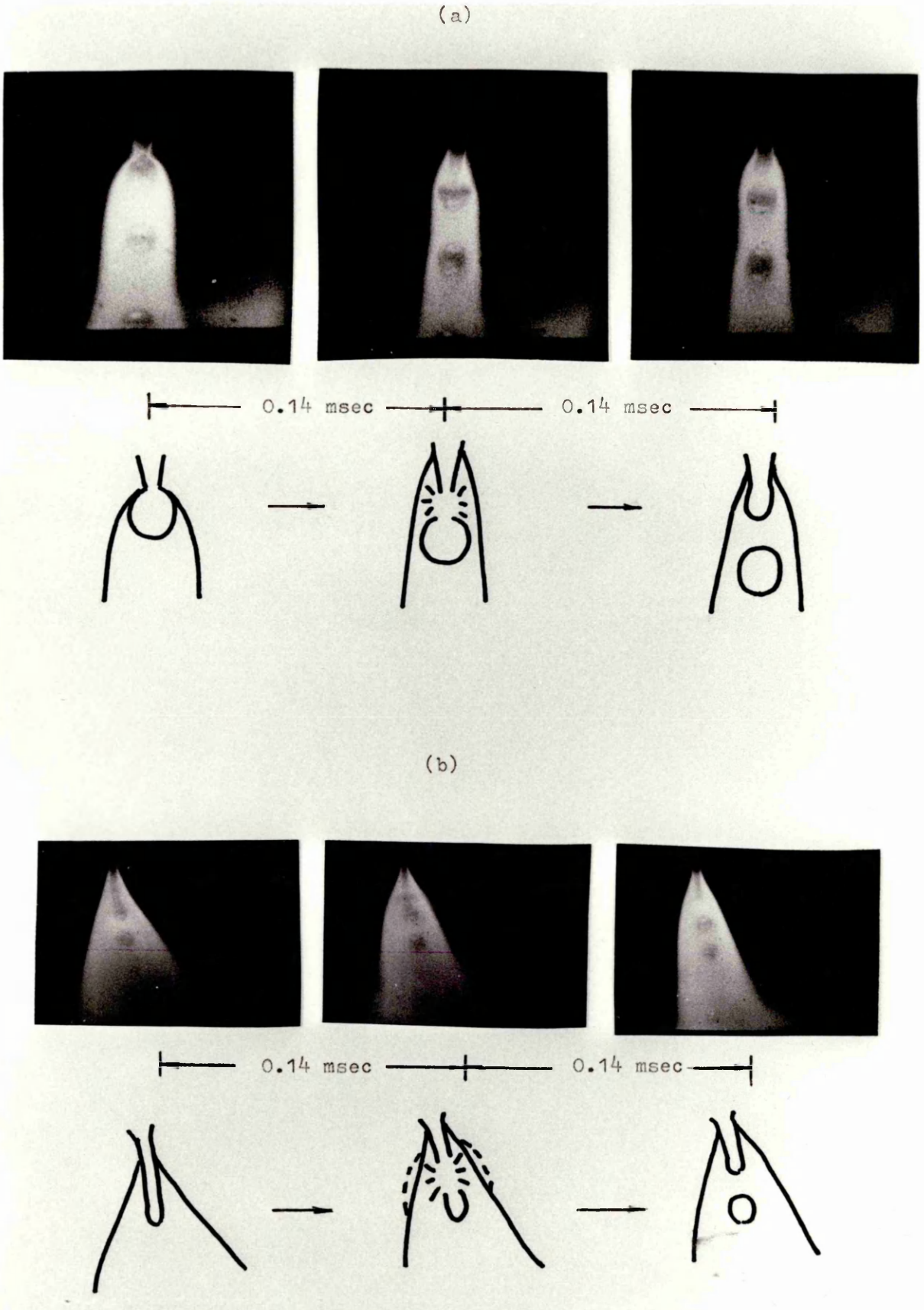

Figure 55. Schematic diagram of drop detachment mechanisms.
(a) Drop spray transfer mode.
(b) Stream spray transfer mode.

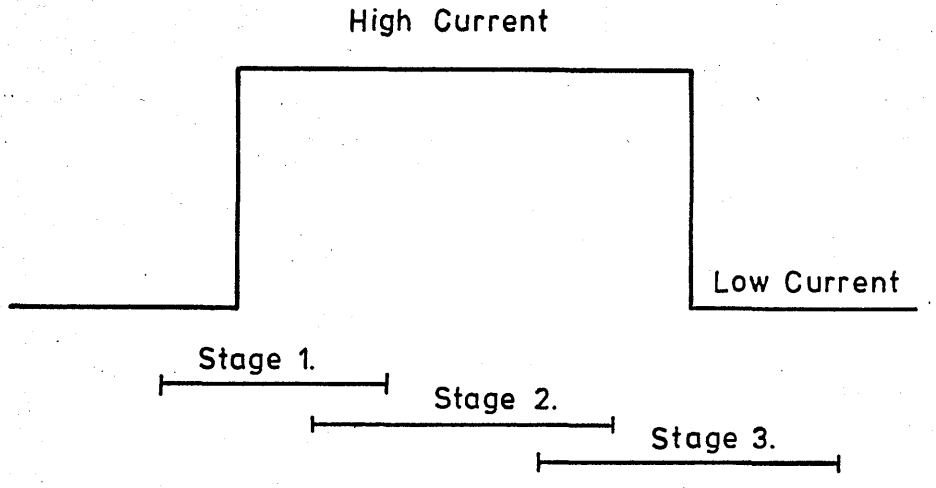

Figure 56. Schematic representation of current pulse indicating stages examined for drop development and detachment.
(a) Metal transfer during imposition of current pulse.
(b) Metal transfer during peak current.
(c) Metal transfer during current reduction to base level.

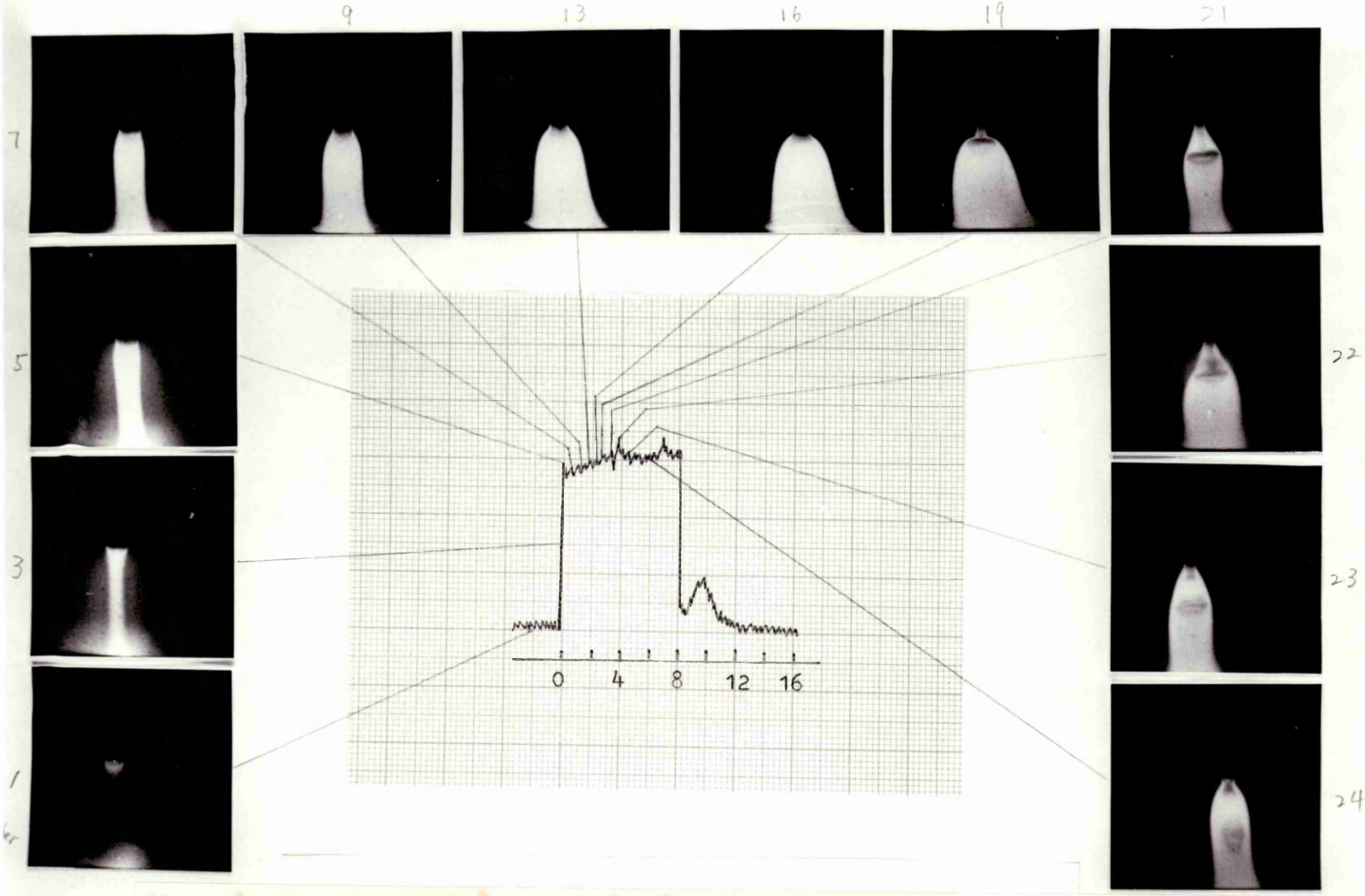

Figure 57. Metal transfer process during which a high current is being imposed, 1.2mm dia. wire, 50A, 380A.

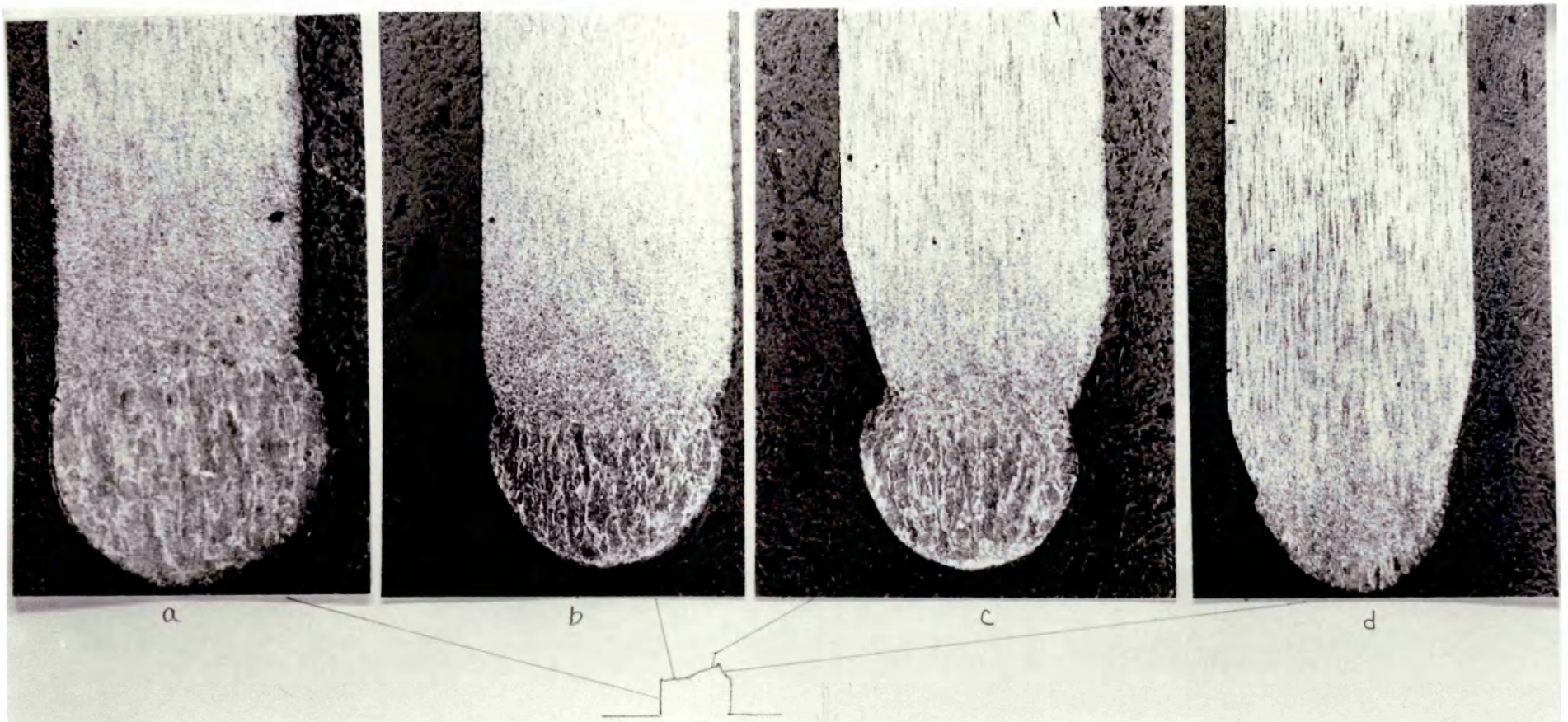

Figure 58. Macrostructure of molten tip.
(a) Current just increased.
(b) Start of necking process.
(c) Before detachment.
(d) Just before detachment.
1.2mm mild steel wire.

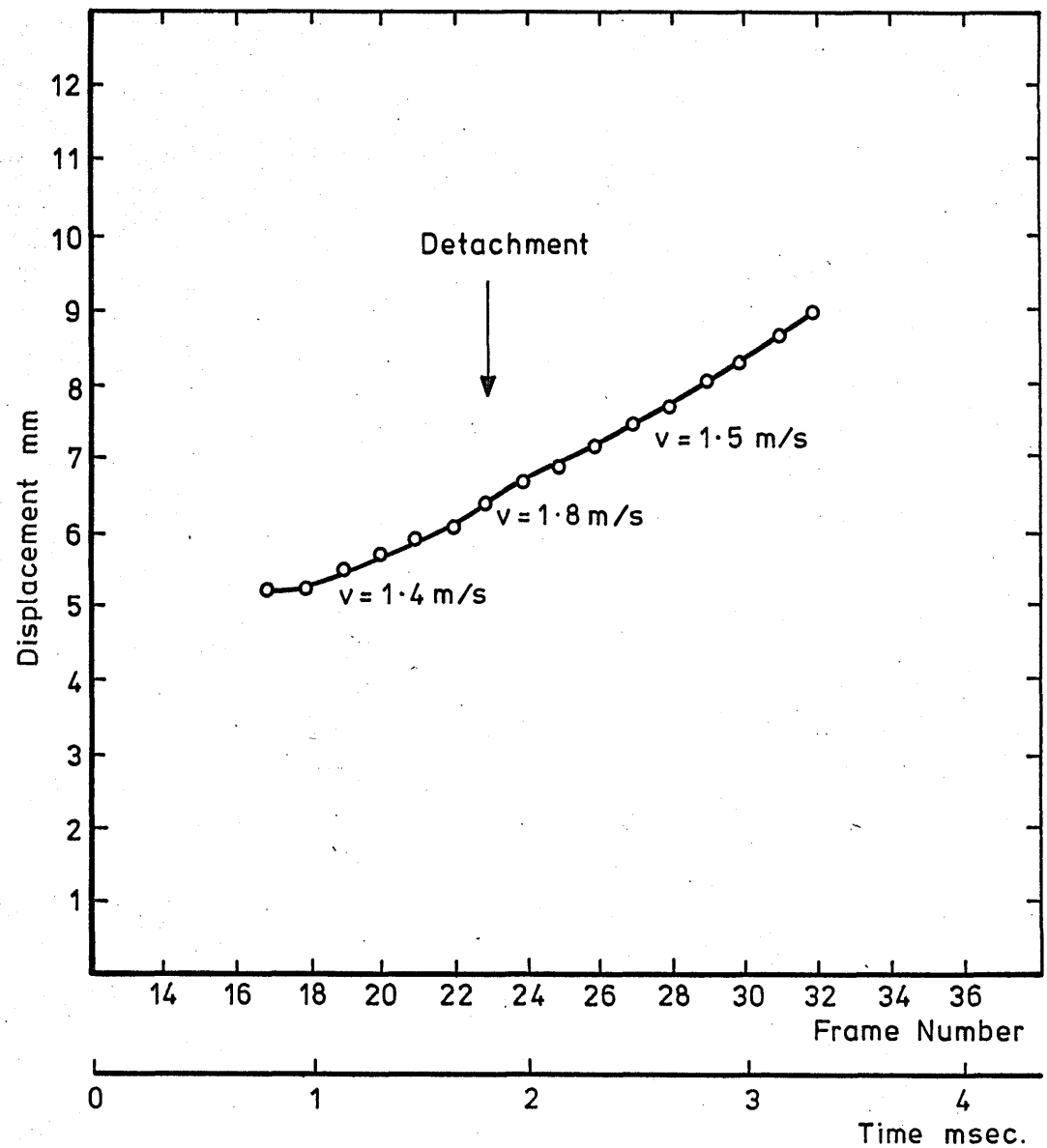

Figure 59. Drop displacement with time and instant velocity during application of current pulse (Reference Figure 57).

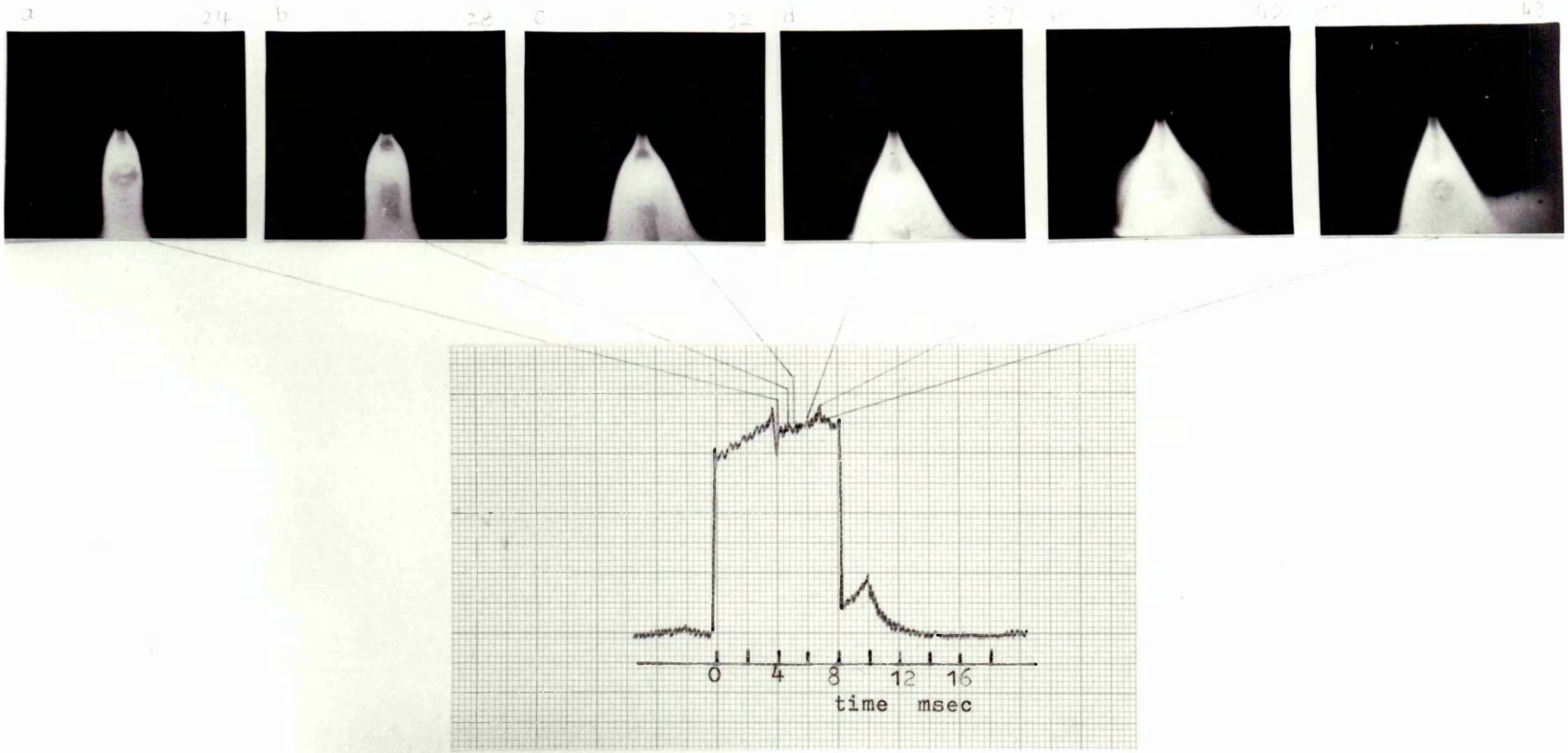

Figure 60. Metal transfer during the current pulse.
(a) 4ms after the high current has been imposed.
(b) 4.8ms after. (c) 5ms after. (d) 5.9ms after.
(e) 7ms after. (f) 7.2ms after.

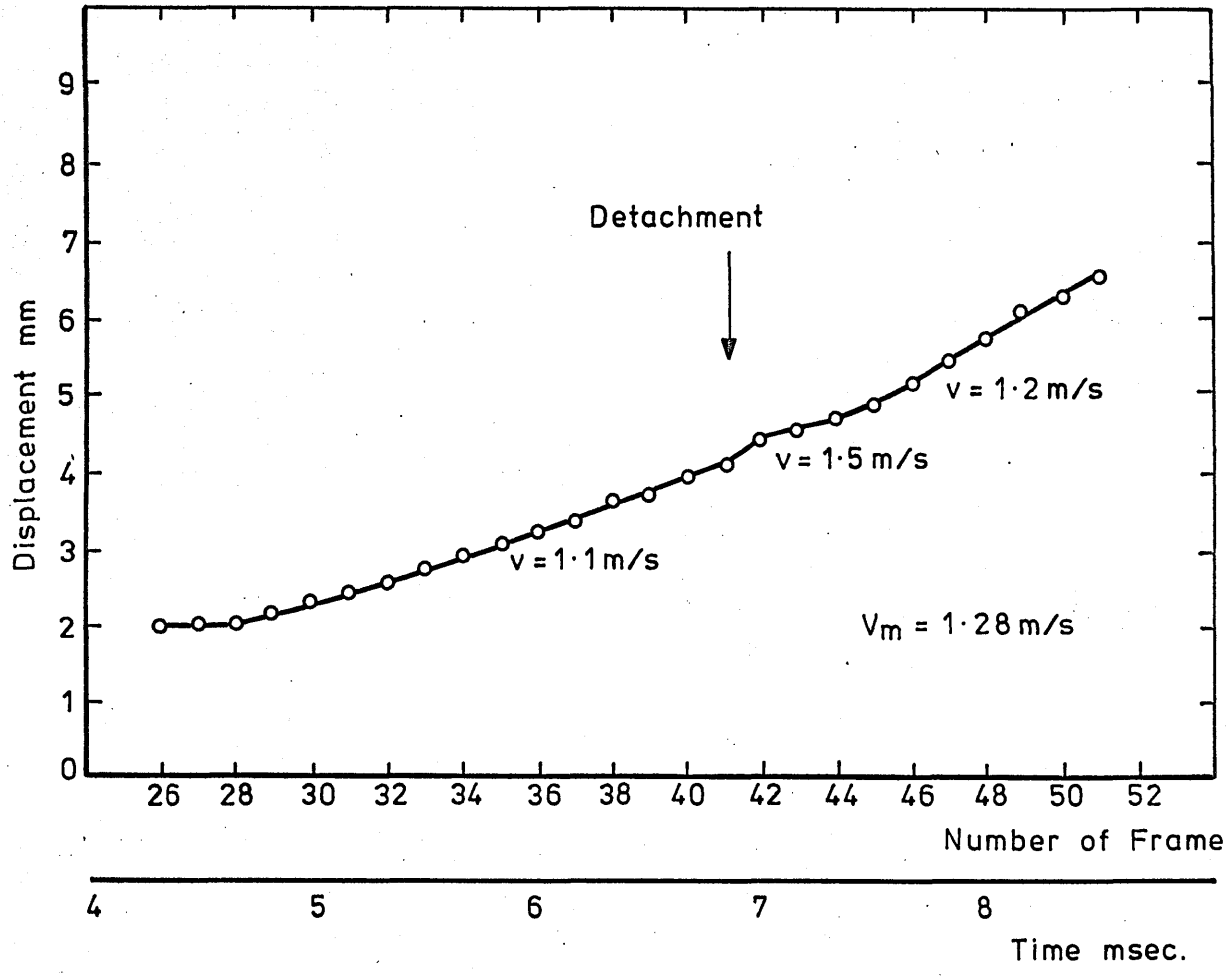

Figure 61. Drop displacement and instant velocity with time during the current pulse. (Reference Figure 60).

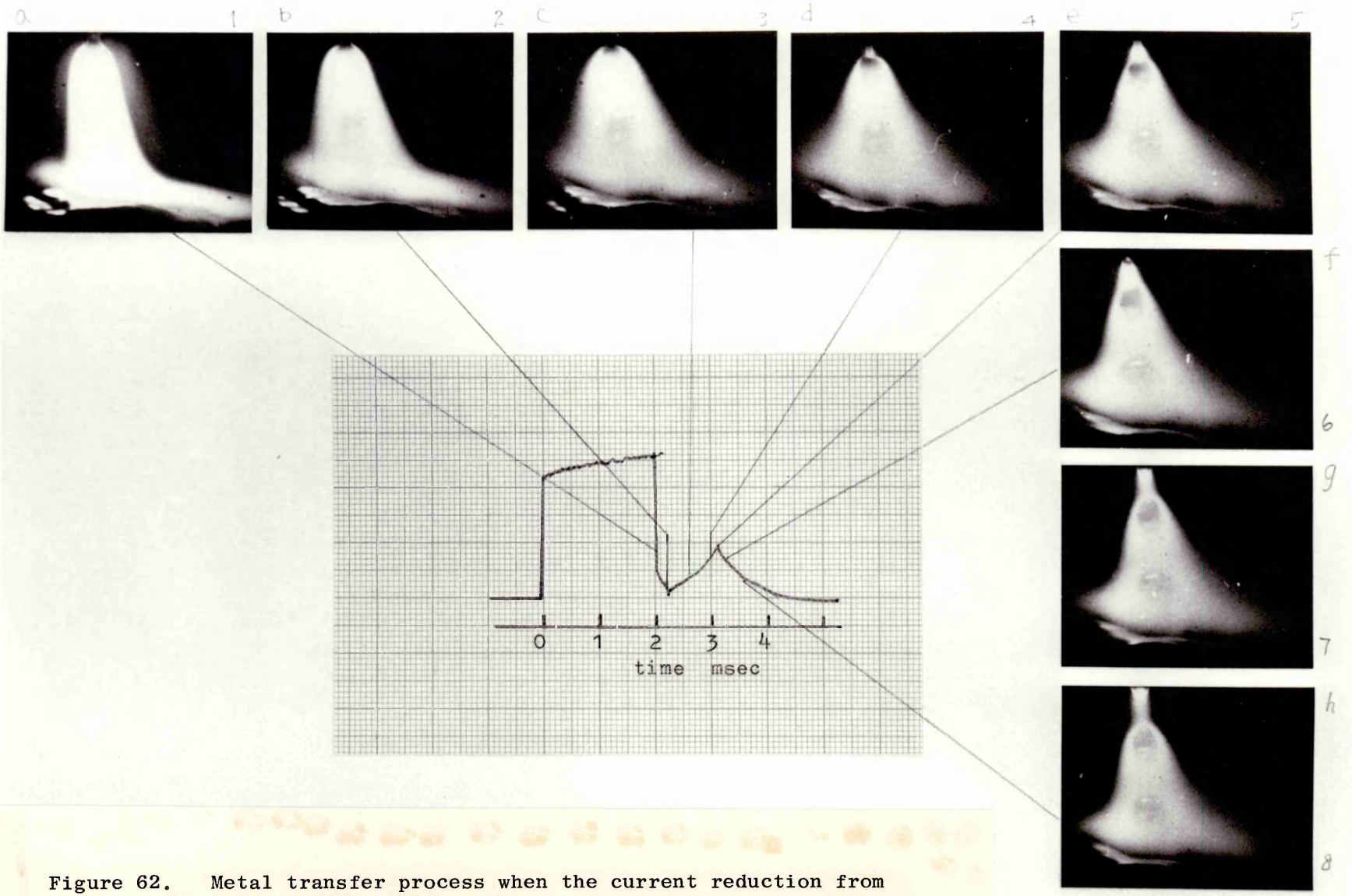

Figure 62. Metal transfer process when the current reduction from peak (380A) to base (100A) occurred during drop formation in drop spray transfer, 1.2mm mild steel wire.

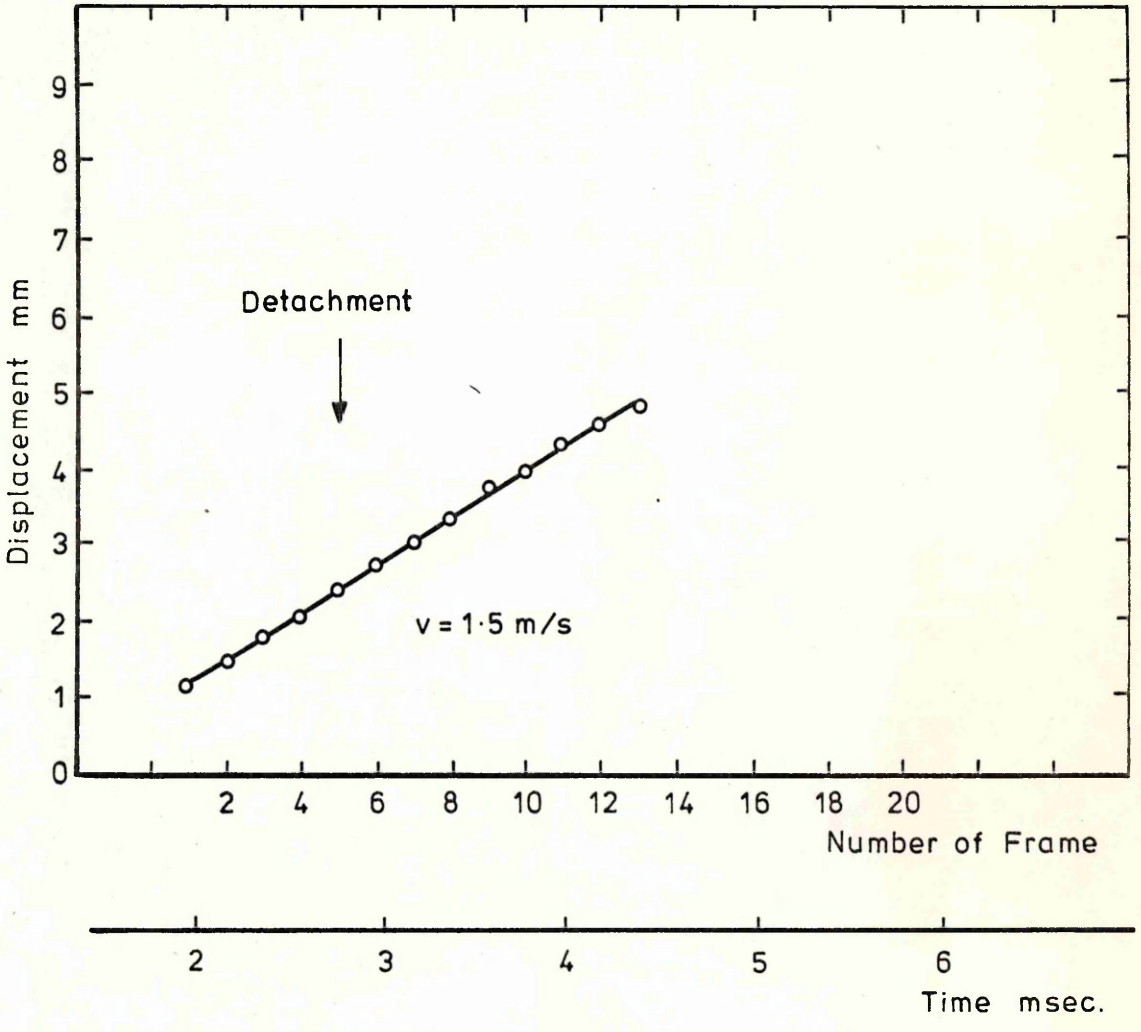

Figure 63. Drop displacement and instant velocity with time in drop spray transfer during current reduction. (Reference Figure 62).

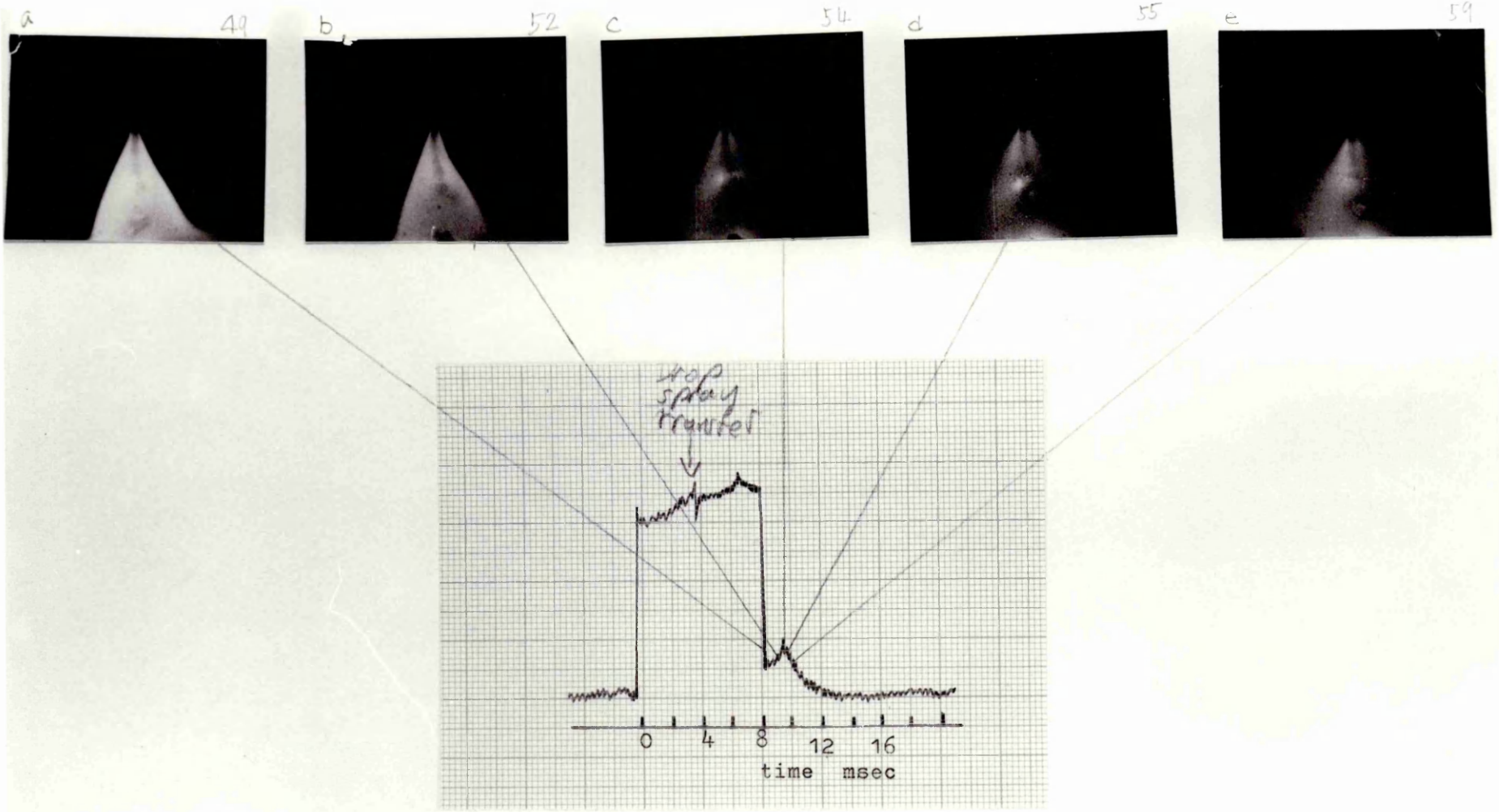

Figure 64. Metal transfer process when the current reduction from peak (380A) to base (50A) before drop detachment in stream spray transfer, 1.2mm mild steel wire.

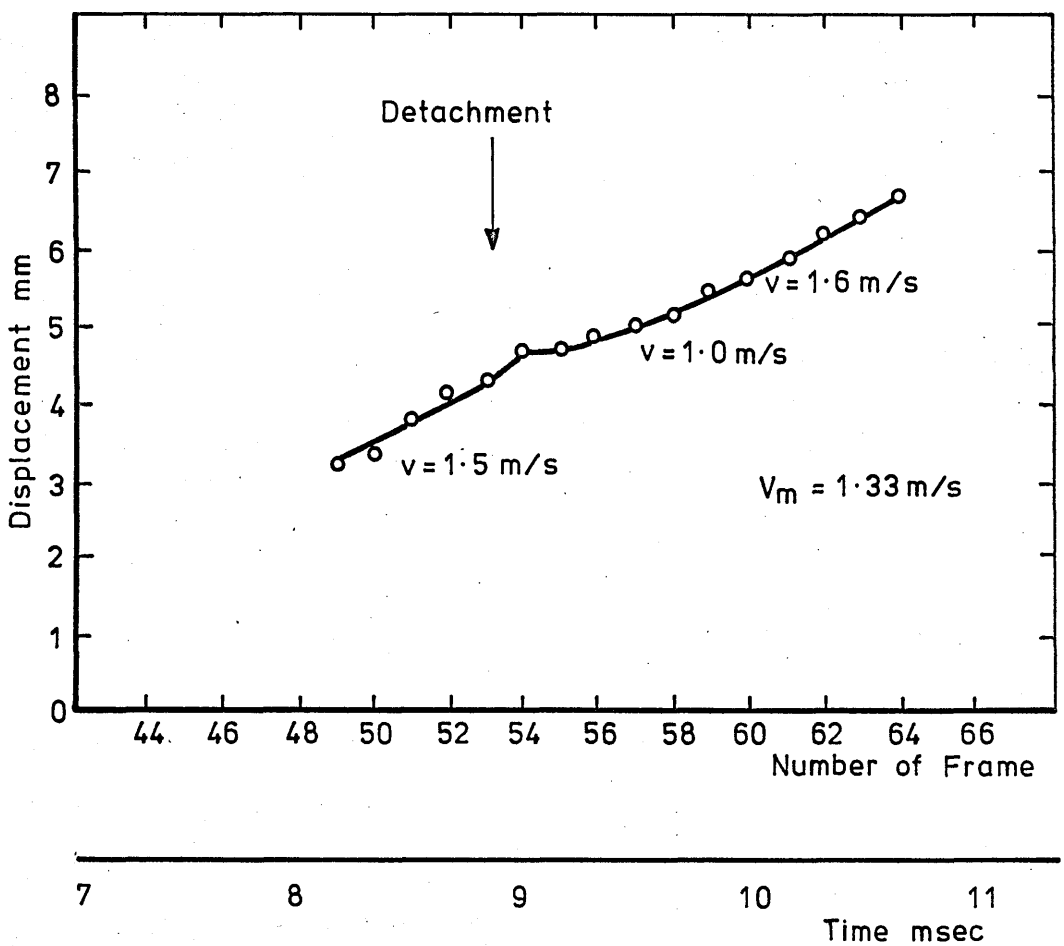

Figure 65. Drop displacement and instant velocity with time in stream spray transfer during current reduction. (Reference Figure 64).

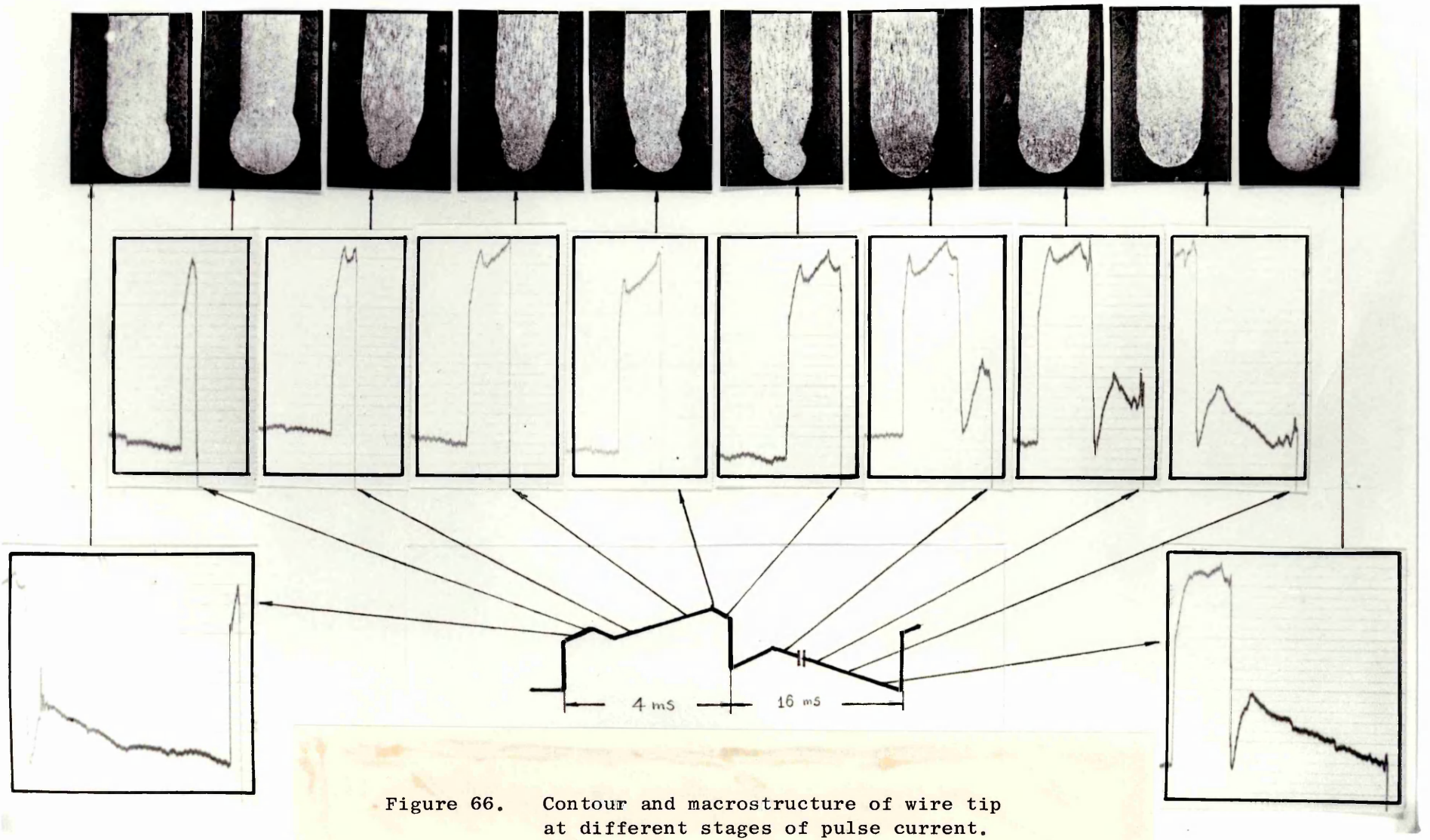

Figure 66. Contour and macrostructure of wire tip at different stages of pulse current. (UVO traces show the moments when the current was switched off), I_p=375A, I_b=50A. 1.2mm wire, Ar + 5% CO_2.

Mean Current	Wire Feed Rate	Droplet Frequency	
58A	1.3m/min	$f_{dr}=25H_z$	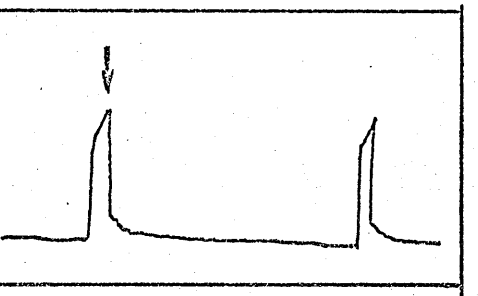
103A	2.8m/min	$f_{dr}=71H_z$	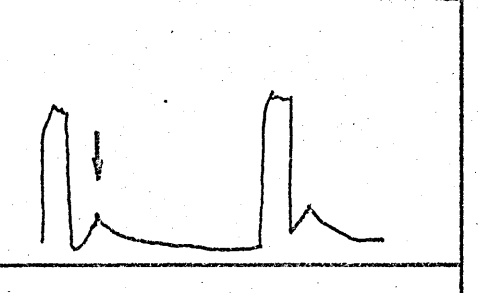
169A	4.7m/min	$f_{dr}=166H_z$	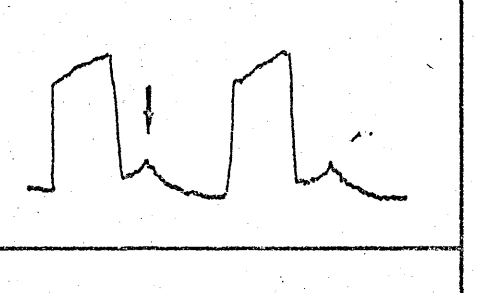
183A	5.0m/min	$f_{dr}=200H_z$	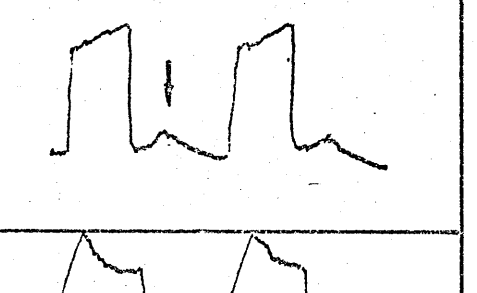
248A	7.6m/min	$f_{dr}=250H_z$	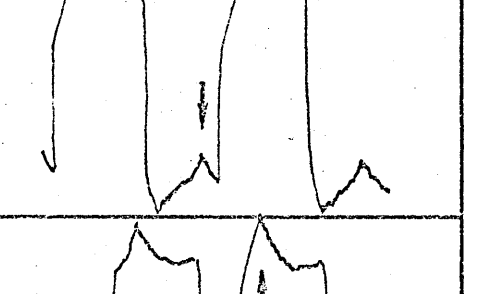
267	8.5m/min	$f_{dr}=333H_z$	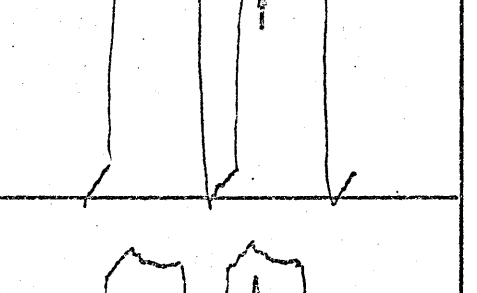
302A	8.8m/min	$f_{dr}=333H_z$	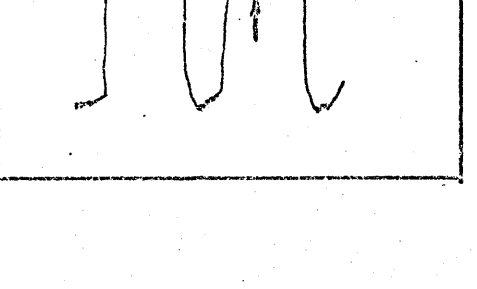

Figure 67. UVO traces of controlled drop spray MIG welding. 1.2mm mild steel wire, Ar + 5% CO_2.

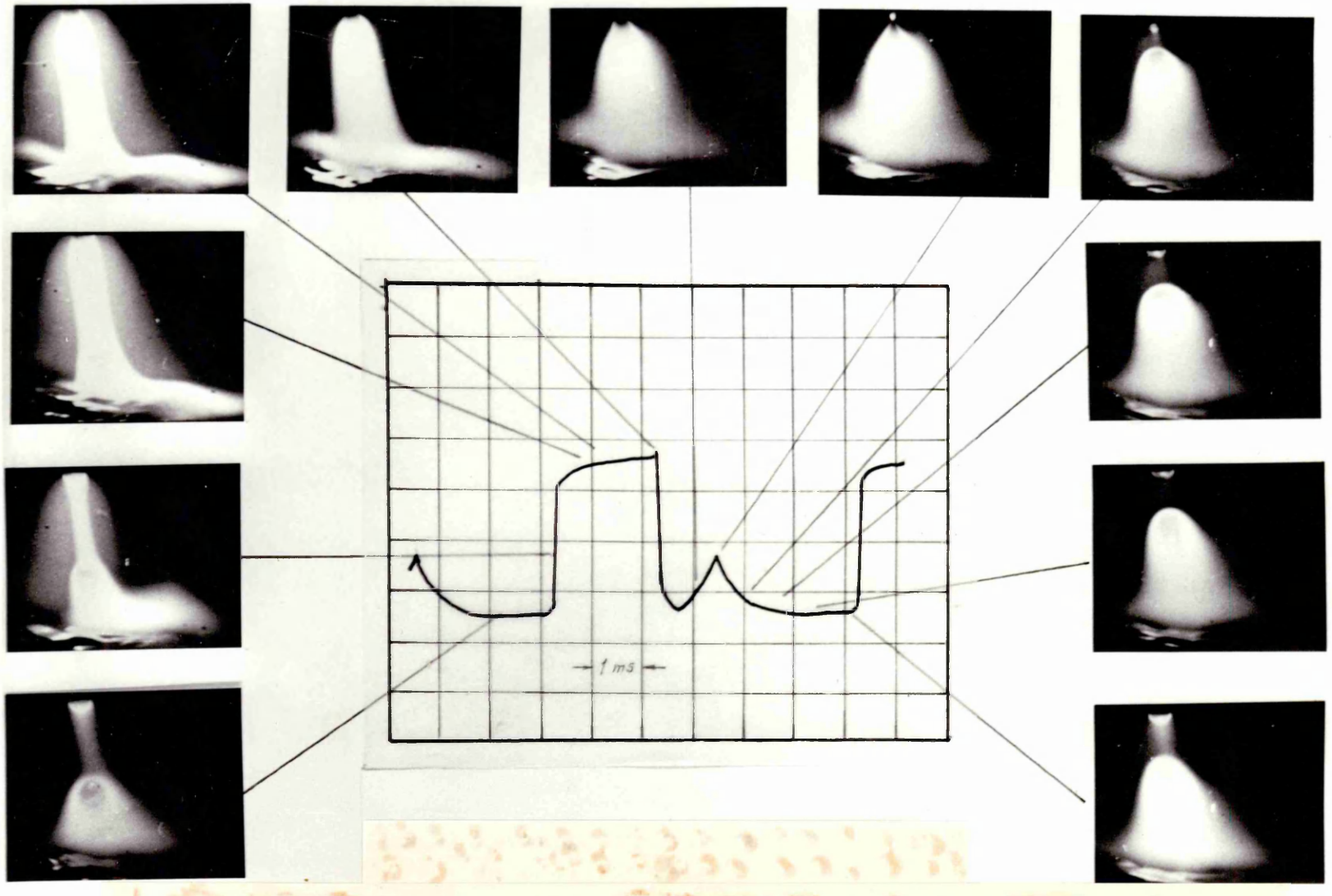

Figure 68. Controlled drop spray transfer process, mean current 302A, wire feed rate 6.1,/min, 1.2mm mild steel wire. Ar + 5% CO_2.

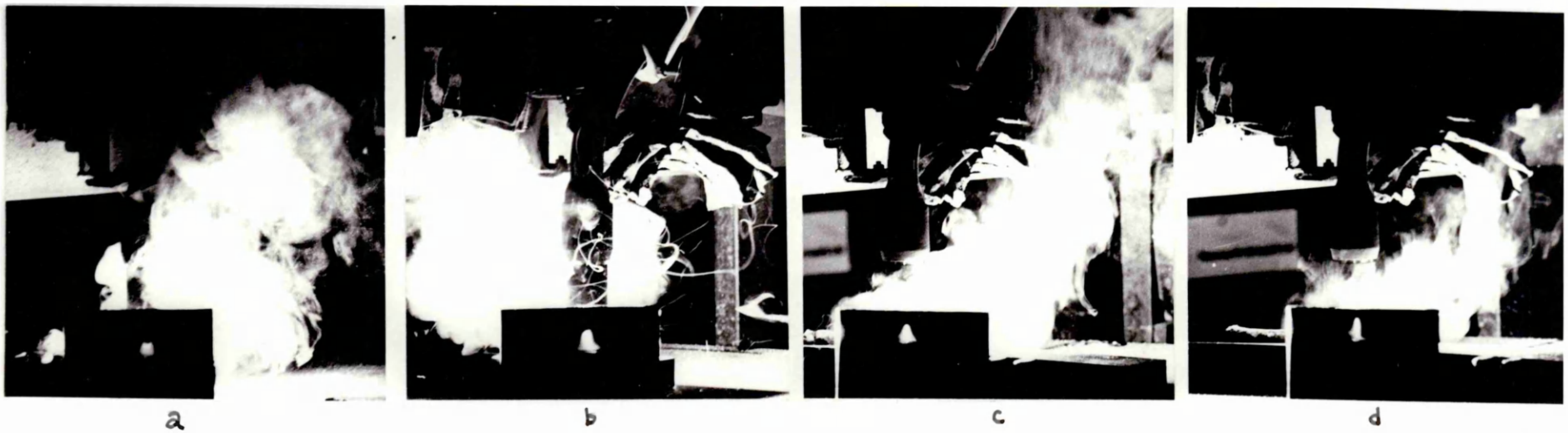

Figure 69. Comparison of fume formation rate of different MIG processes.
(a) Globular transfer 110A, constant current.
(b) Globular transfer 170A, constant current.
(c) Ordinary pulse welding with mean current of 169A.
(d) Controlled drop spray welding, welding current 169A.
1.2mm mild steel wire, Ar + 5% CO_2.

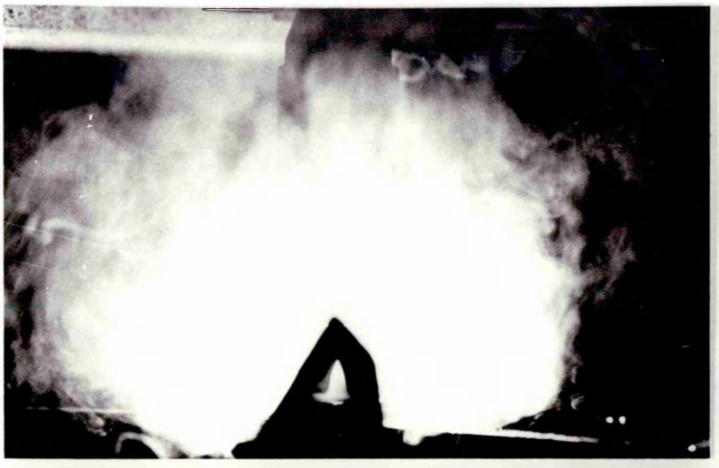

e

f

g

h

Figure 70.

Fume formation comparison of different MIG processes.

(e) Stream spray, constant current, 273A.

(f) Ordinary pulse welding with mean current of 264A.

(g) Controlled drop spray MIG with mean current of 264A.

(h) Controlled drop spray MIG with mean current of 296A.

a

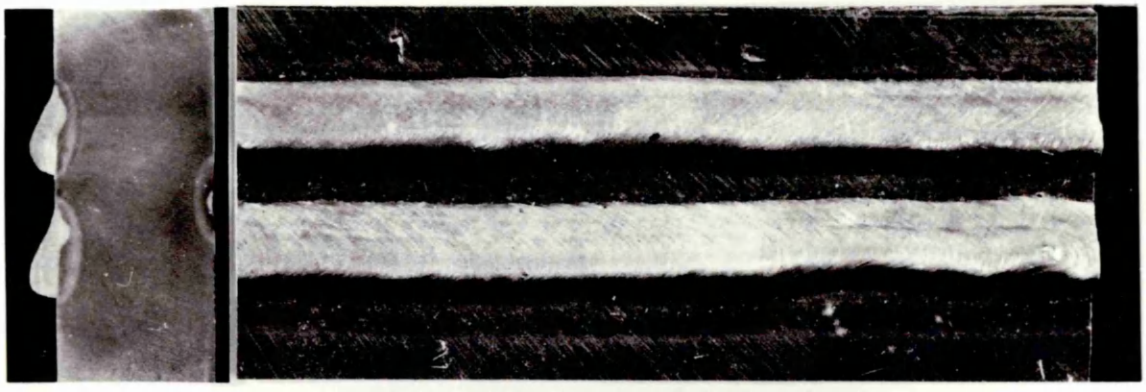

b

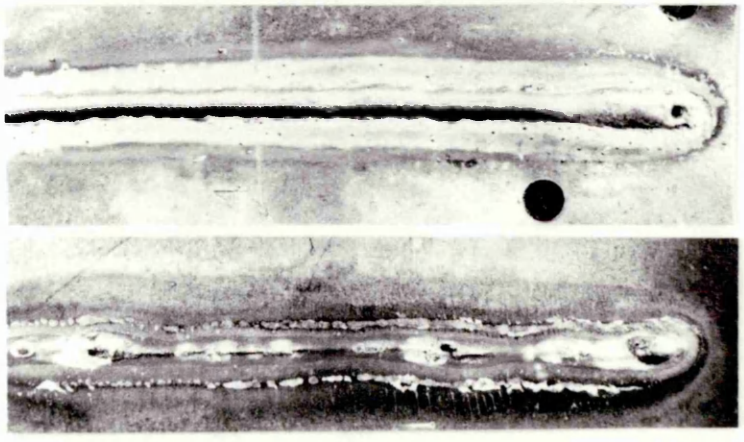

c

Figure 71. Bead on plate deposit in horizontal-vertical position welding, controlled drop spray MIG. 1.2mm mild steel wire, welding speed 200mm/min. Ar + 5% CO_2.
(a) Welding current 143A, wire feed rate 4.0m/min.
(b) Welding current 116A, wire feed rate 2.5m/min.
(c) Welding current 41A, wire feed rate 0.9m/min, 1mm thick steel.

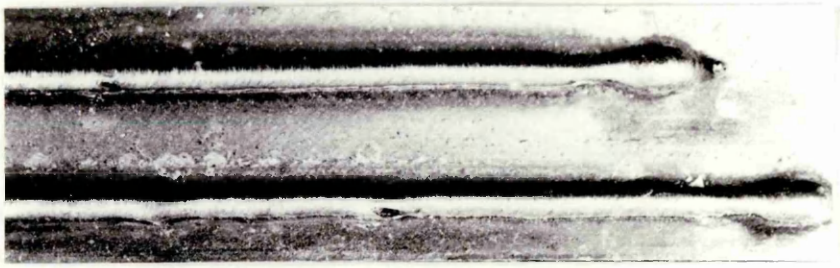

a

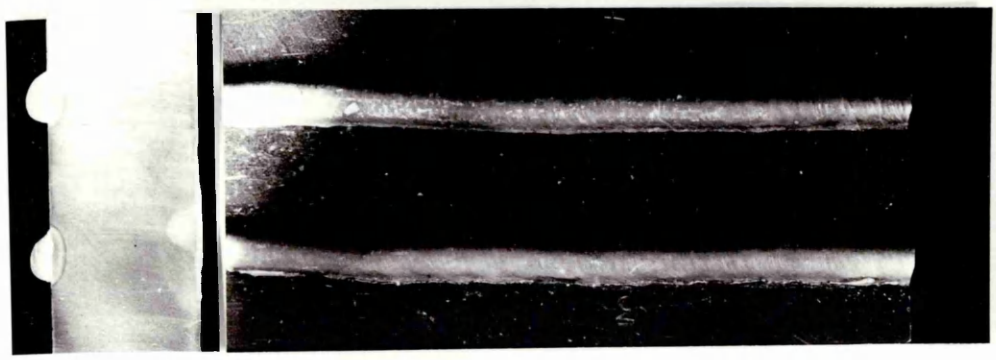

b

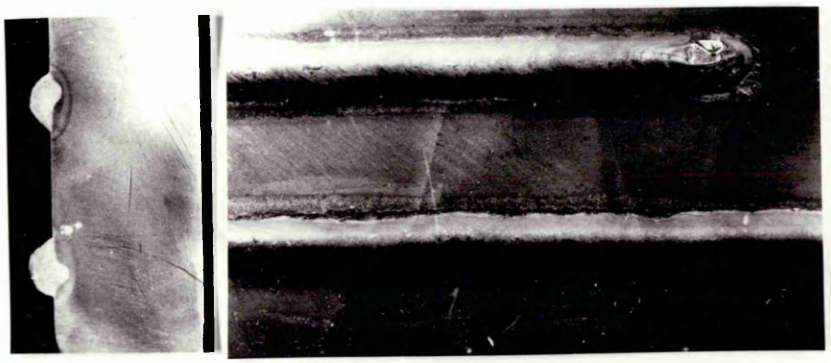

c

Figure 72. Bead on plate deposit in overhead position welding, controlled drop spray MIG, wire diameter 1.2mm mild steel, welding speed 200mm/min. Ar + 5% CO_2.
(a) Welding current 67A, wire feed rate 1.6m/min.
(b) Welding current 106A, wire feed rate 2.6m/min.
(c) Welding current 138A, wire feed rate 3.8m/min.

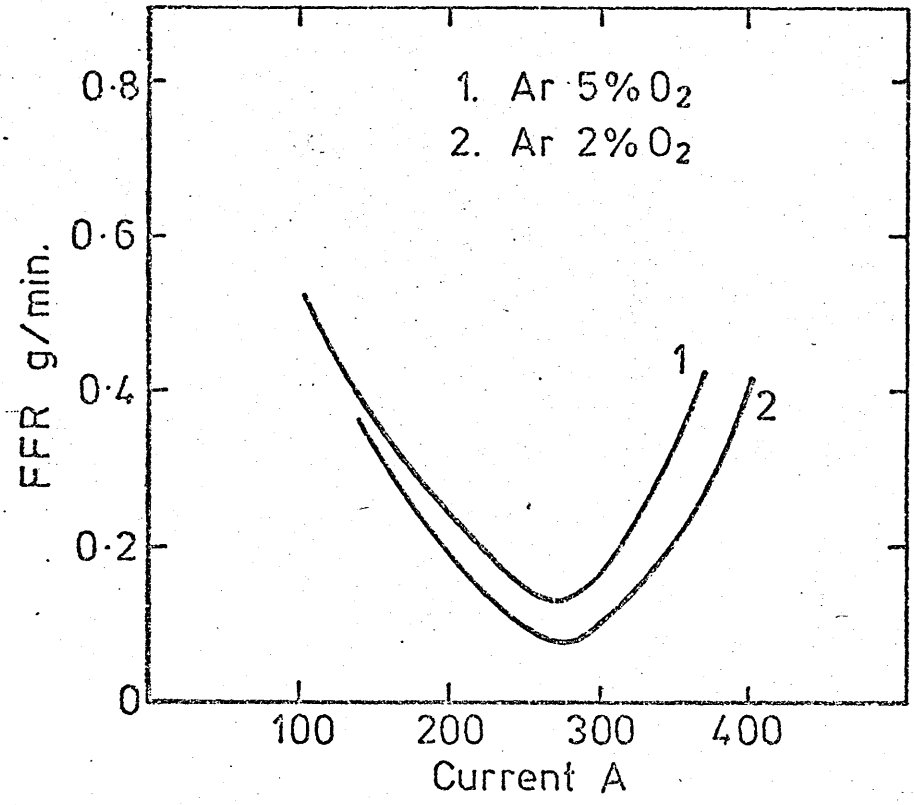

Figure 73. Fume formation rate (FFR) versus welding current, 1.2mm mild steel electrode. (106)

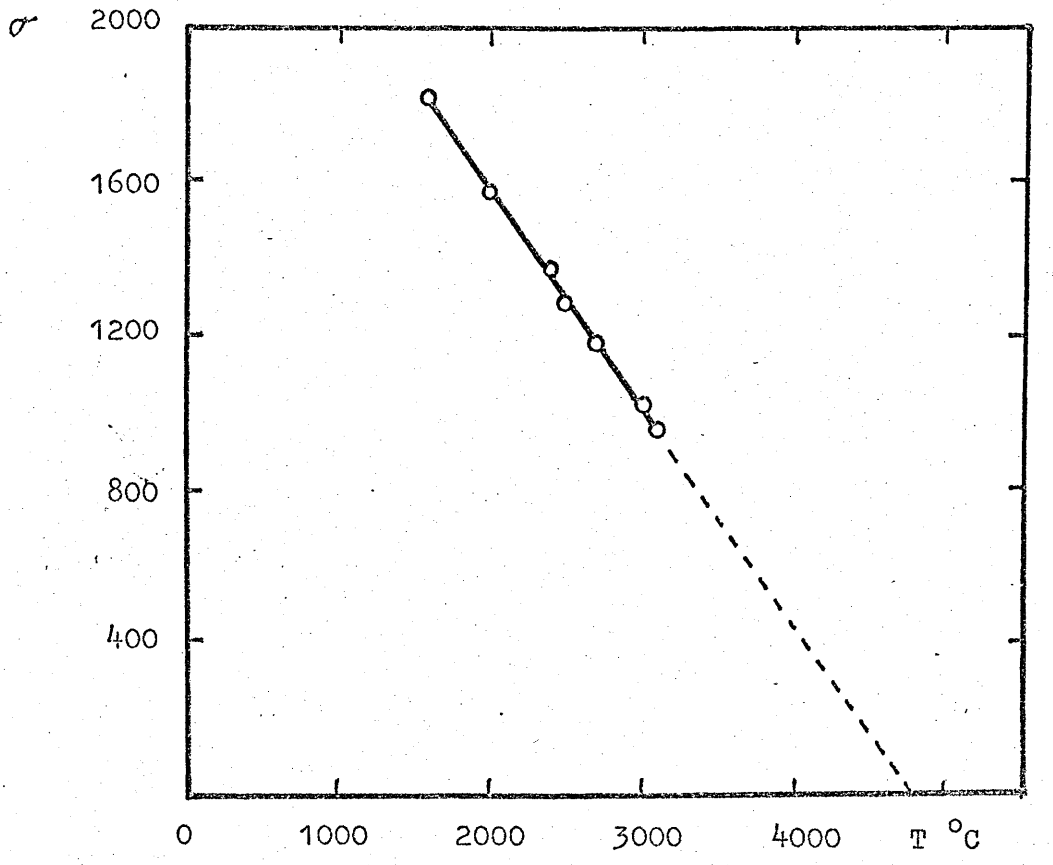

Figure 74. Surface tension, σ of molten metal as function of temperature, T. (29)

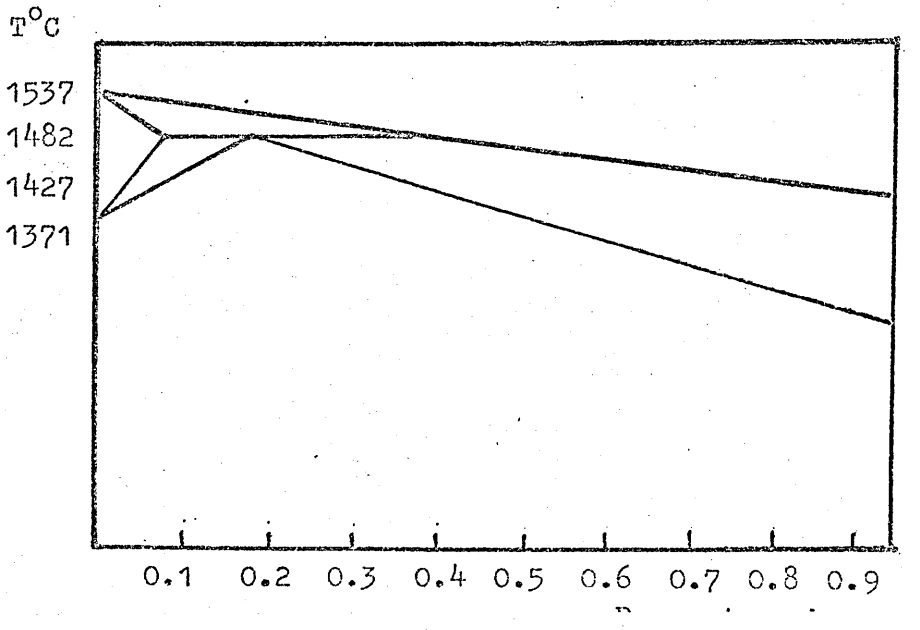

Figure 75. Equilibrium diagrams for Fe-C.

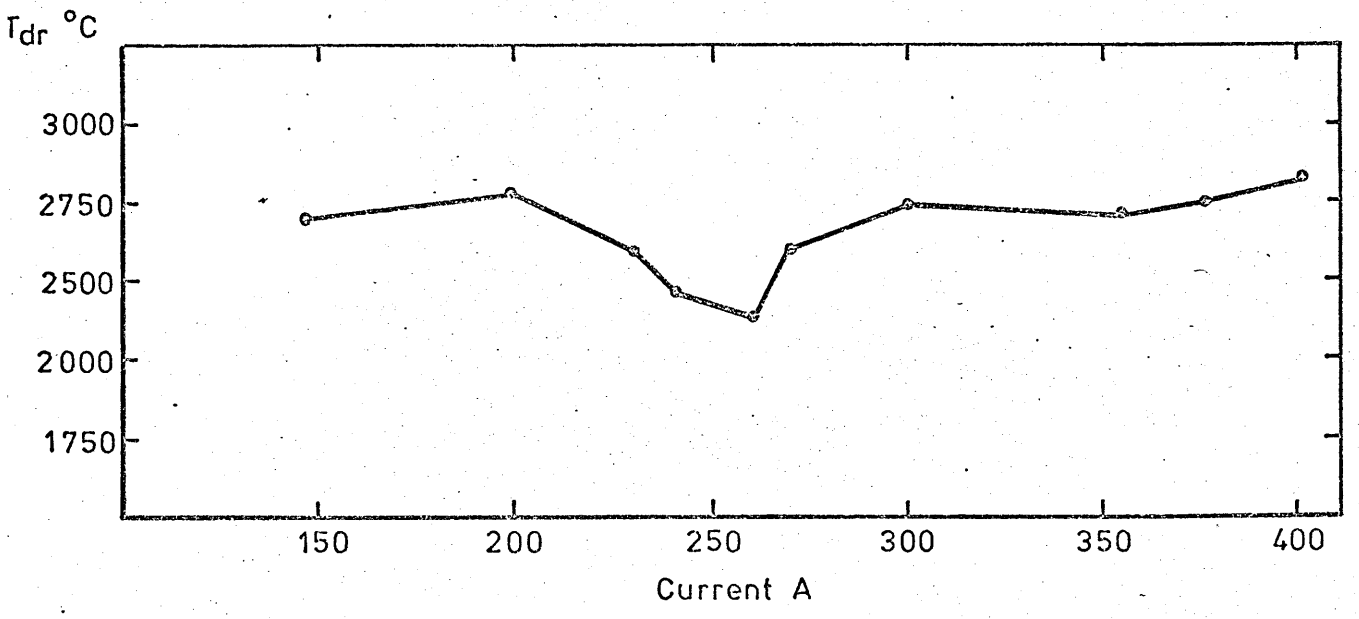

Figure 76. Calculated mean drop temperature as a function of welding current.

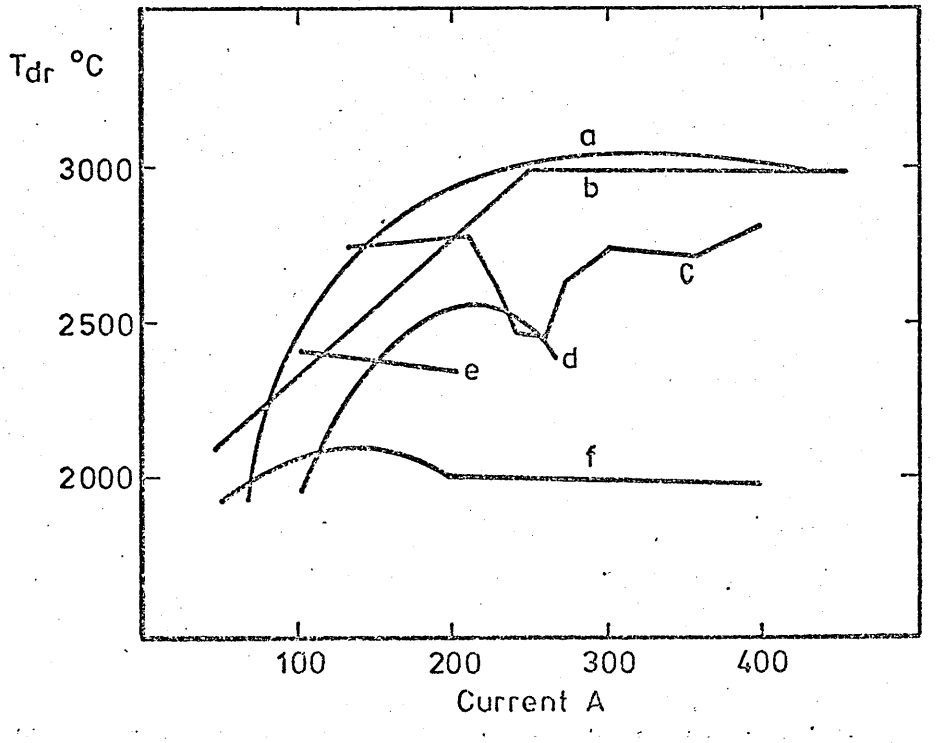

Figure 77. Comparison of calculated drop temperatures reported by various investigators.
(a) 2.0mm wire, Ar + 16% N_2. (87) (b) 1.2mm wire, Ar (93)
(c) 1.2mm wire, Ar + 5% CO_2, present work. (d) 1.2mm wire CO_2 (88)
(e) 1.2mm wire, Ar + 25% CO_2 (80) (f) 1.6mm wire, Ar (81).

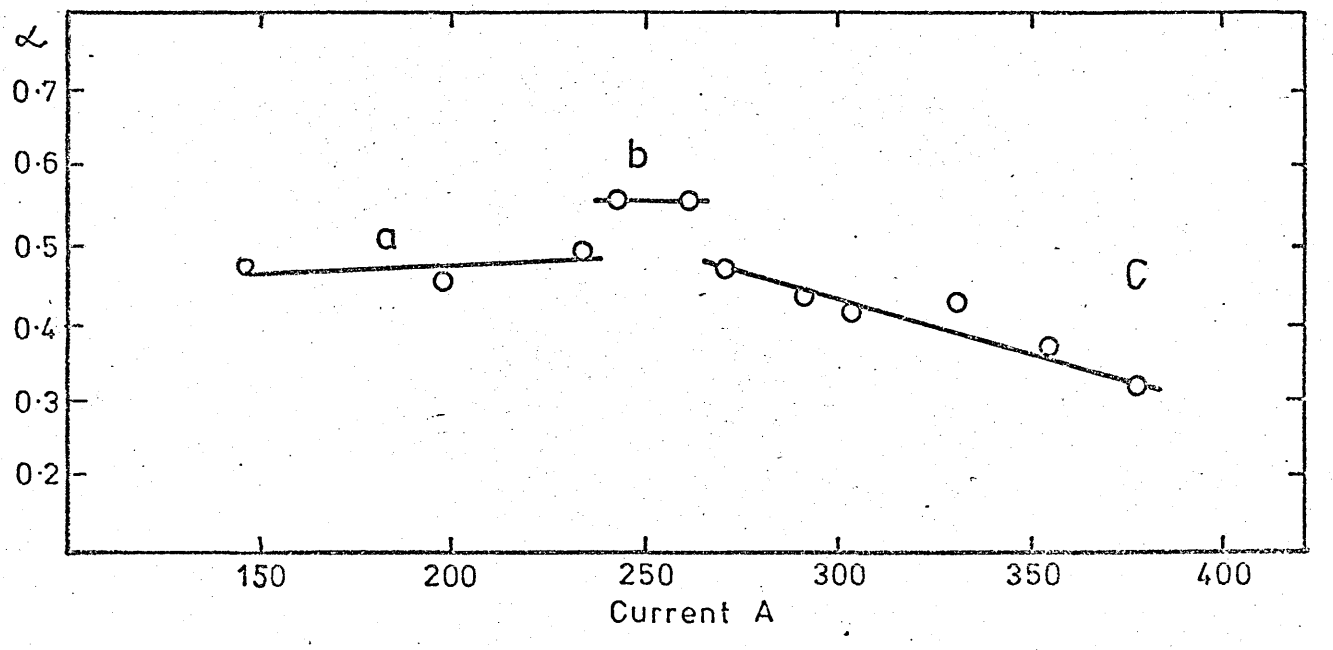

Figure 78. Variation of wire melting efficiency, α, with welding current,
(a) globular transfer,
(b) drop spray transfer,
(c) stream spray transfer.

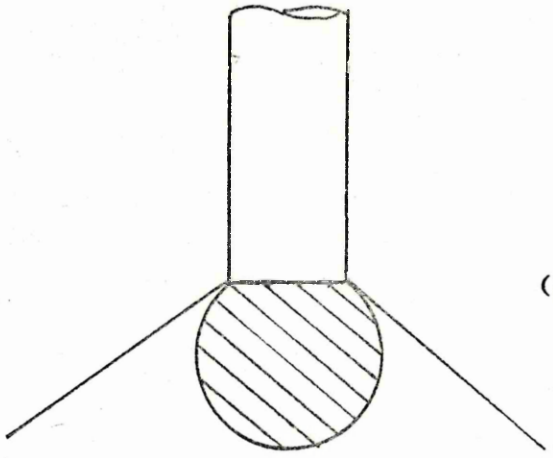

(a)

(b)

Figure 79. Model of globular transfer mechanism
(a) the model
(b) the real phenomenon

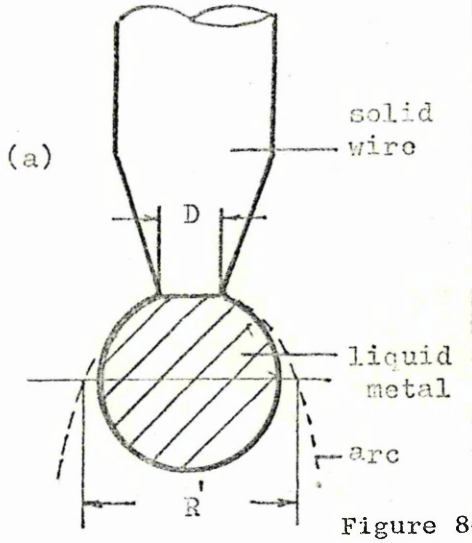

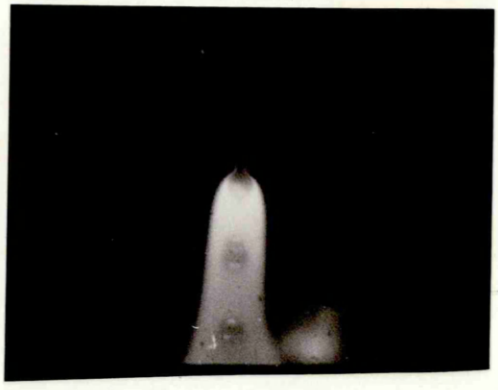

Figure 80. Model of drop spray transfer mechanism,
(a) the model,
(b) the real phenomenon.

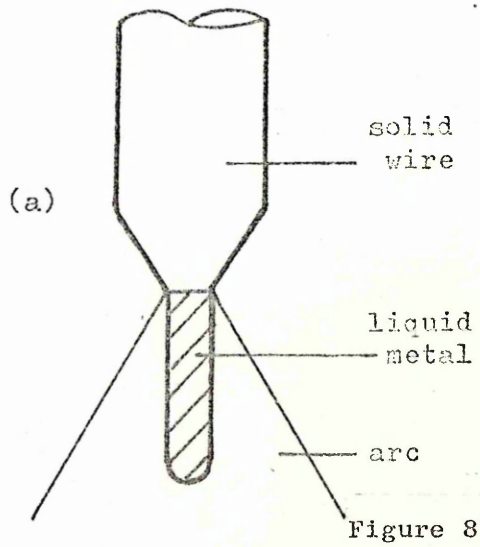

Figure 81. Model of stream spray transfer mechanism
(a) the model,
(b) the real phenomenon.

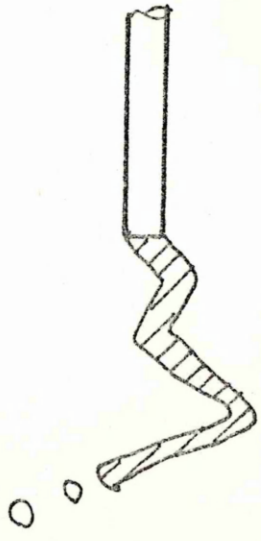

Figure 82. Rotating transfer mode (10)

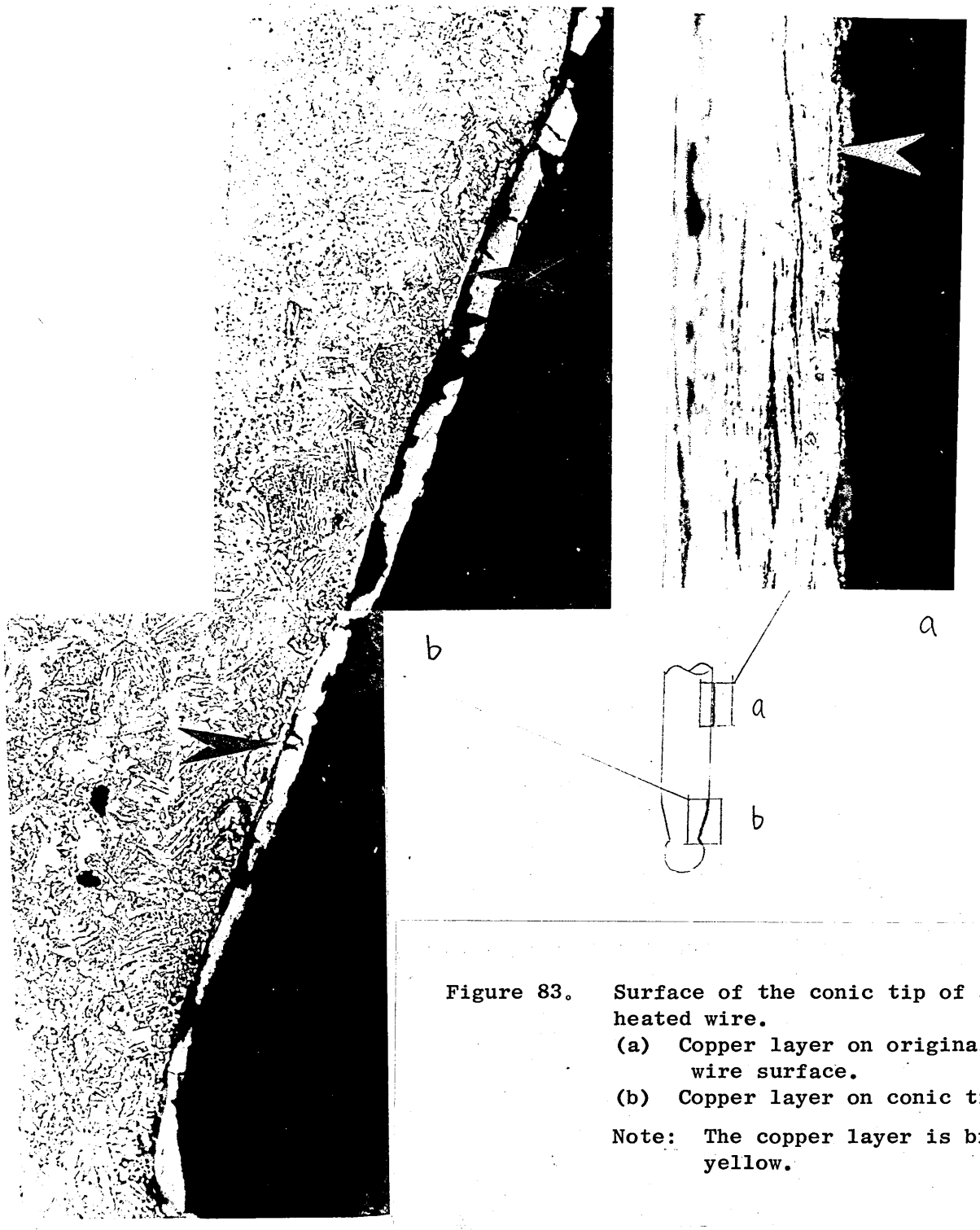

Figure 83. Surface of the conic tip of a heated wire.
(a) Copper layer on original wire surface.
(b) Copper layer on conic tip.

Note: The copper layer is bright yellow.

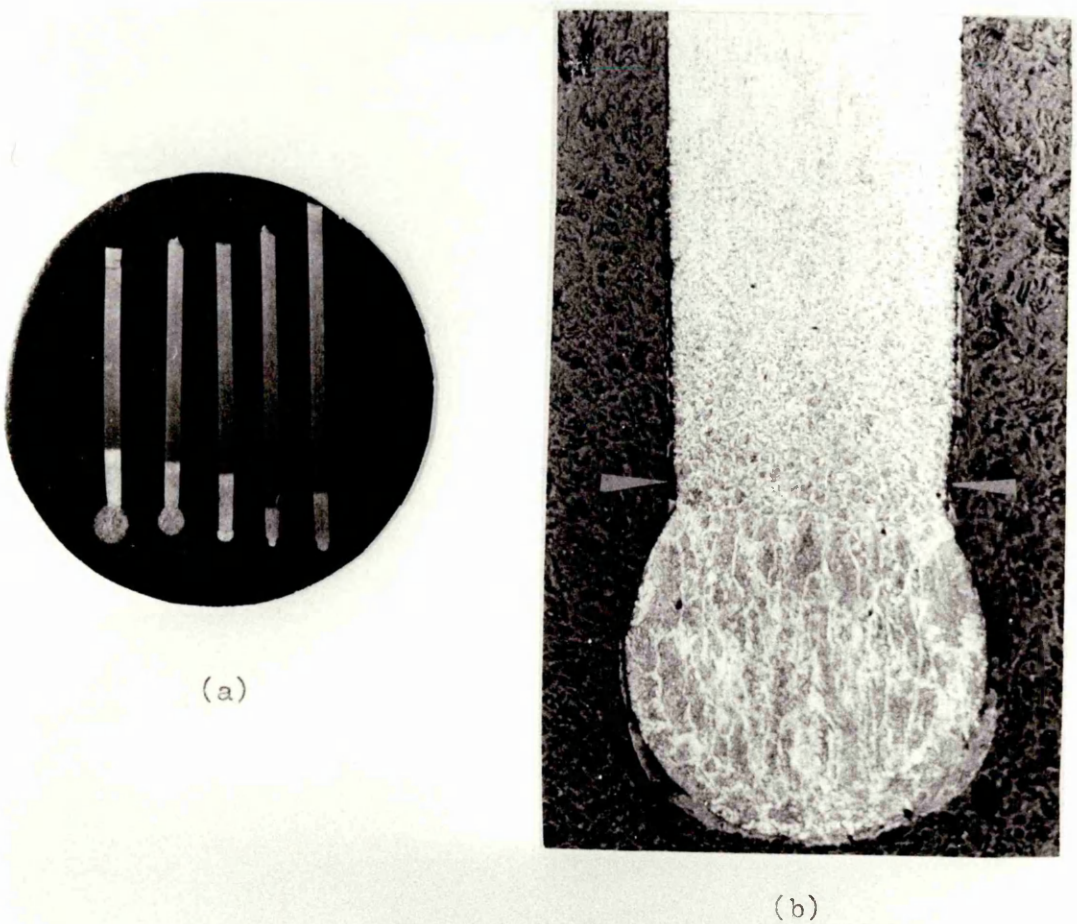

Figure 84. The initial stage of the necking process.
(a) Different stages from globular to spray transfer mode,
(b) The solid wire just above the interface between the solid and the liquid started necking.

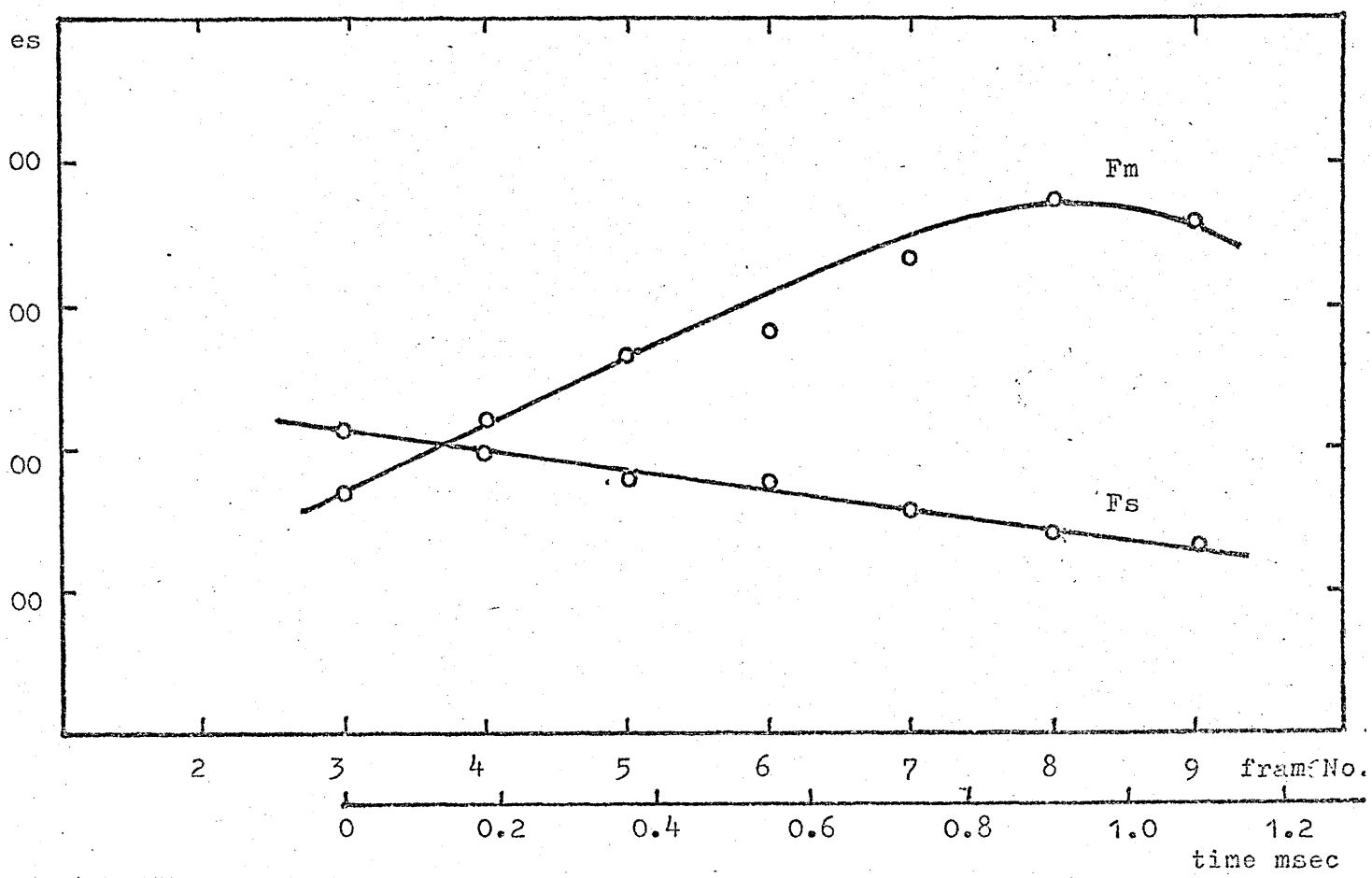

Figure 85. The major forces influencing metal transfer as a function of time (using data from Figure 53).

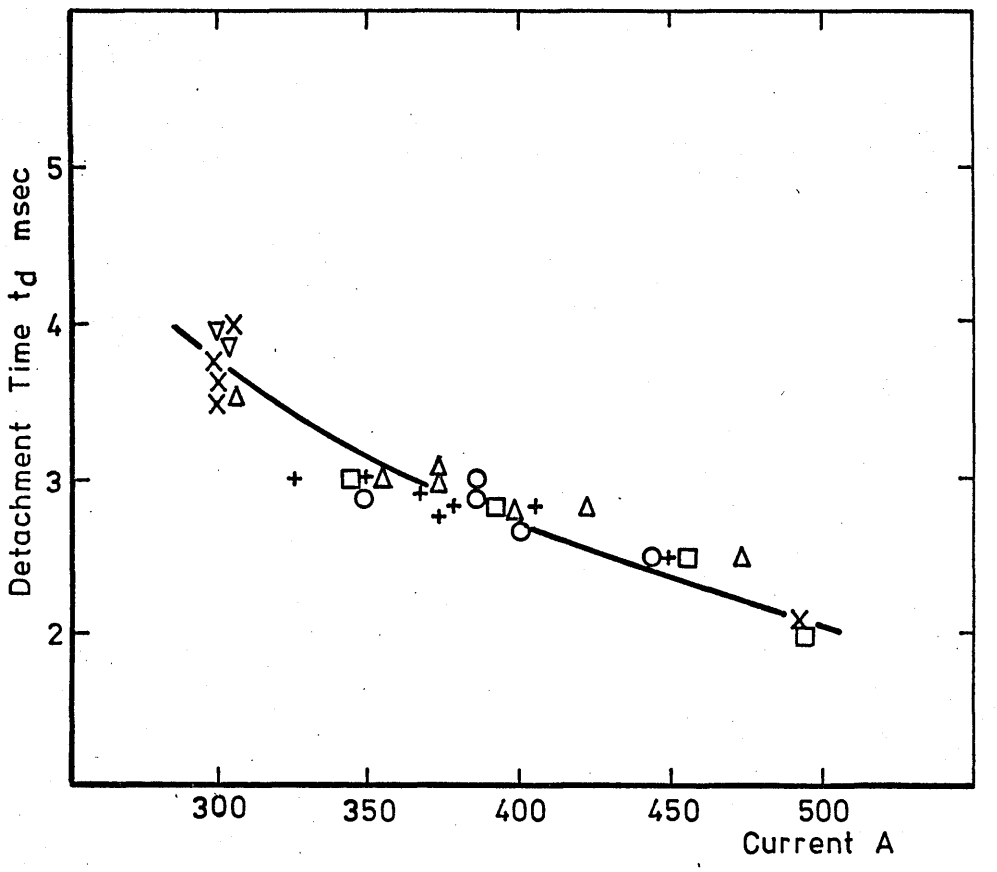

Figure 86. Relationship between the detachment time, t_d, and the trigger current of the necking process.

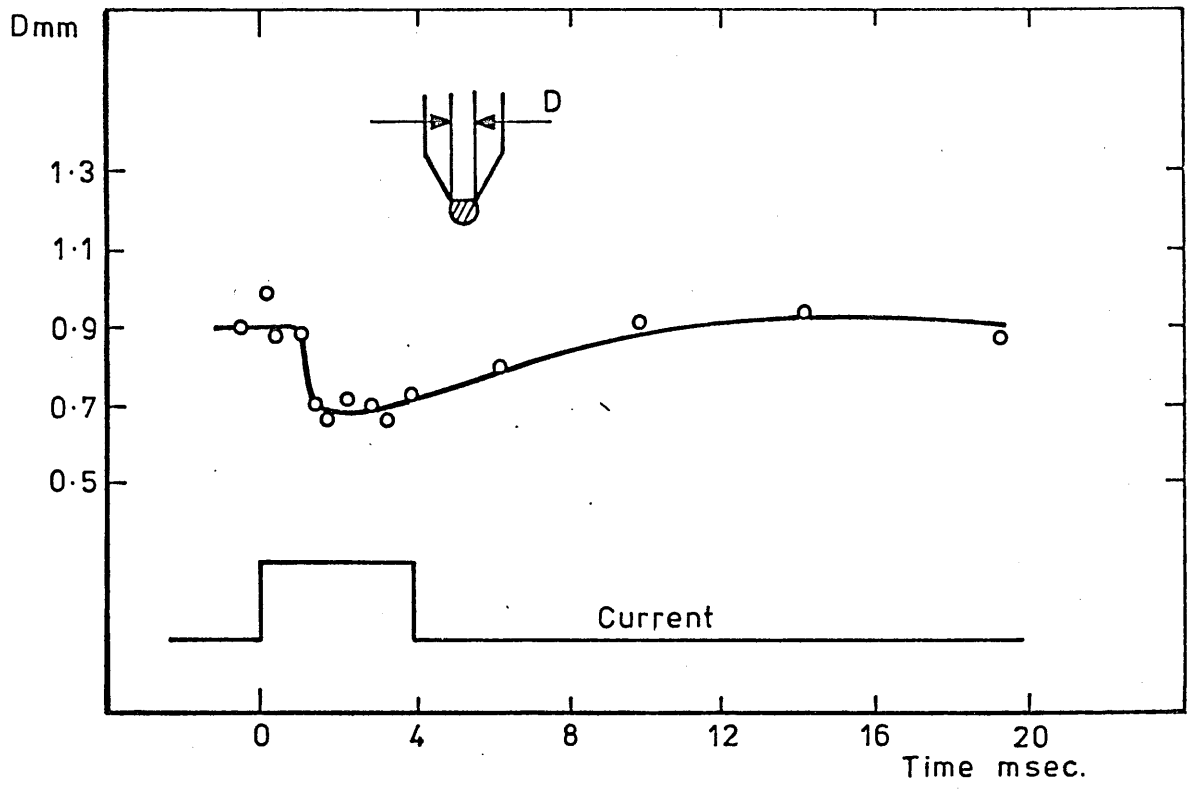

Figure 87. Diameter of interface between solid and liquid parts of the conic tip with time, in same condition as Figure 66.

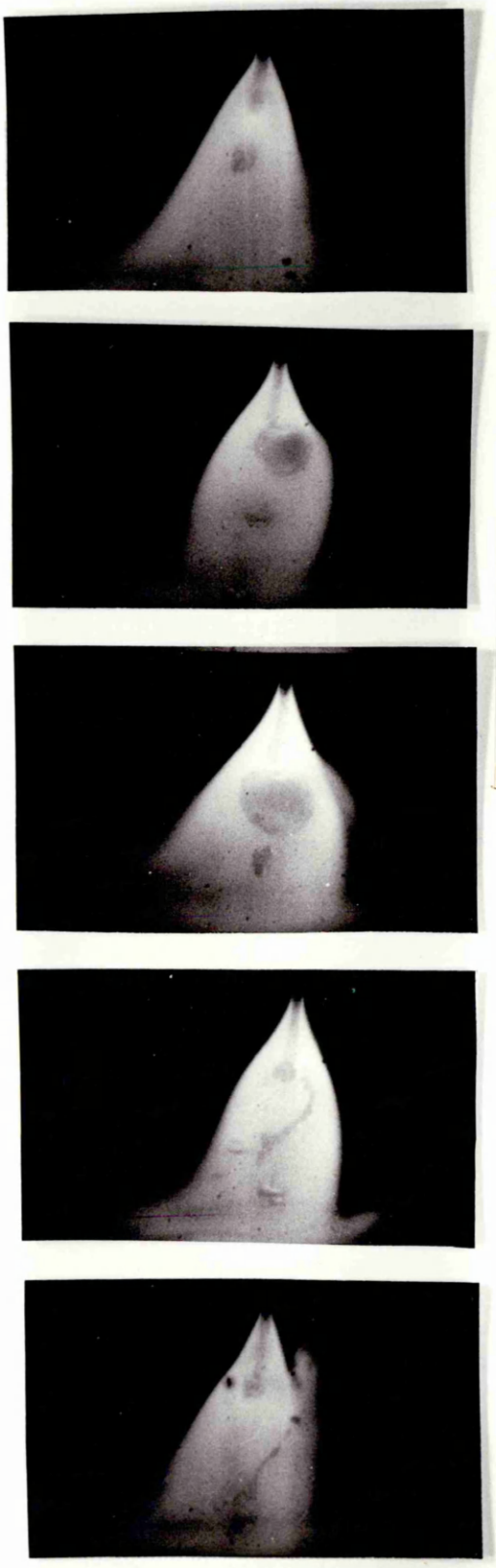

Figure 89. Spatter mechanism of stream spray transfer. Time lapse between frames is 0.43ms, 290A, 1.2mm dia. wire.

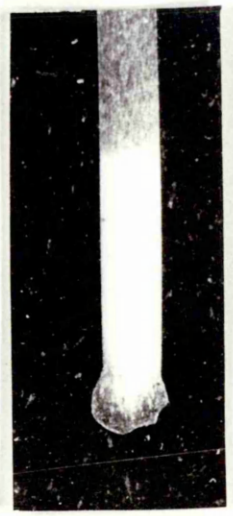

Figure 88. Spatter mechanism of globular transfer.

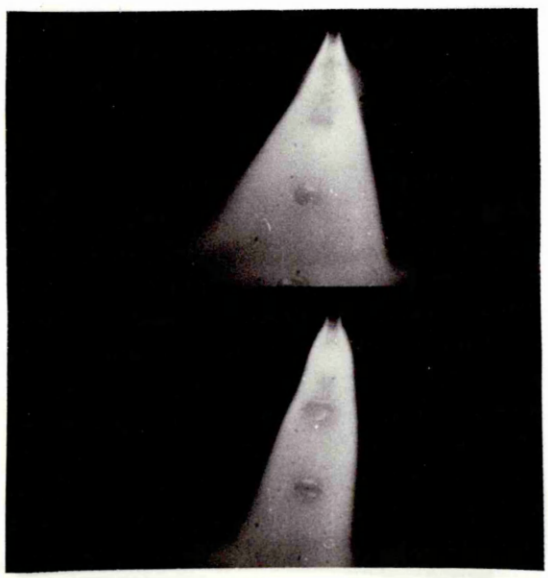

Figure 90. Detachment mechanism of stream spray transfer.

Figure 91. Globular transfer, 1.2mm dia. wire, 91A and 147A.

Figure 92. Drop spray transfer with 1.2mm dia. wire. 253A.

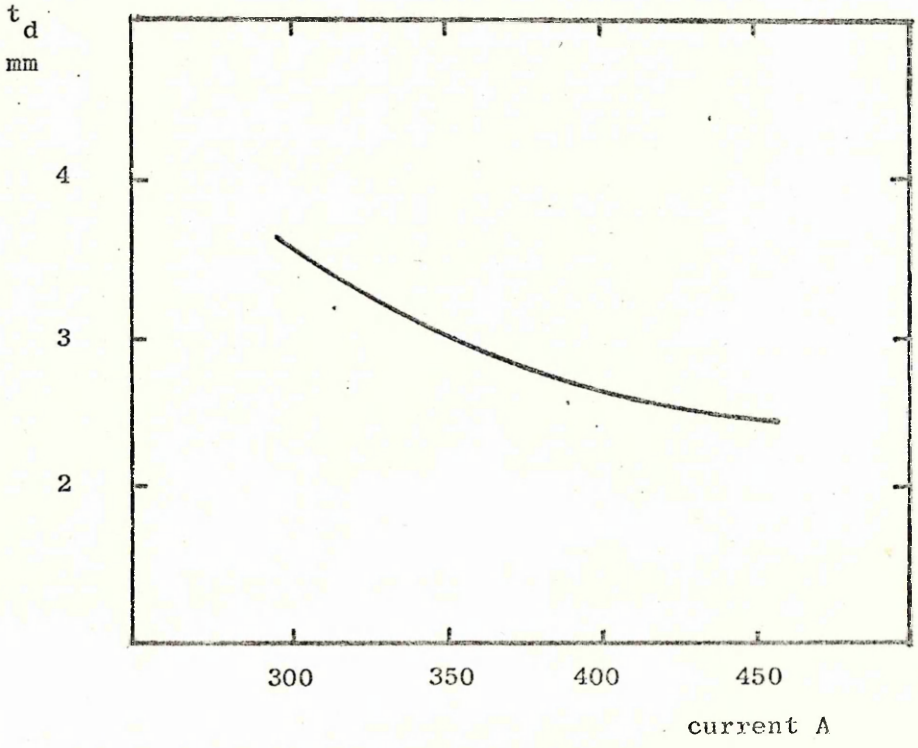

Figure 93. Relationship between detachment time and current.

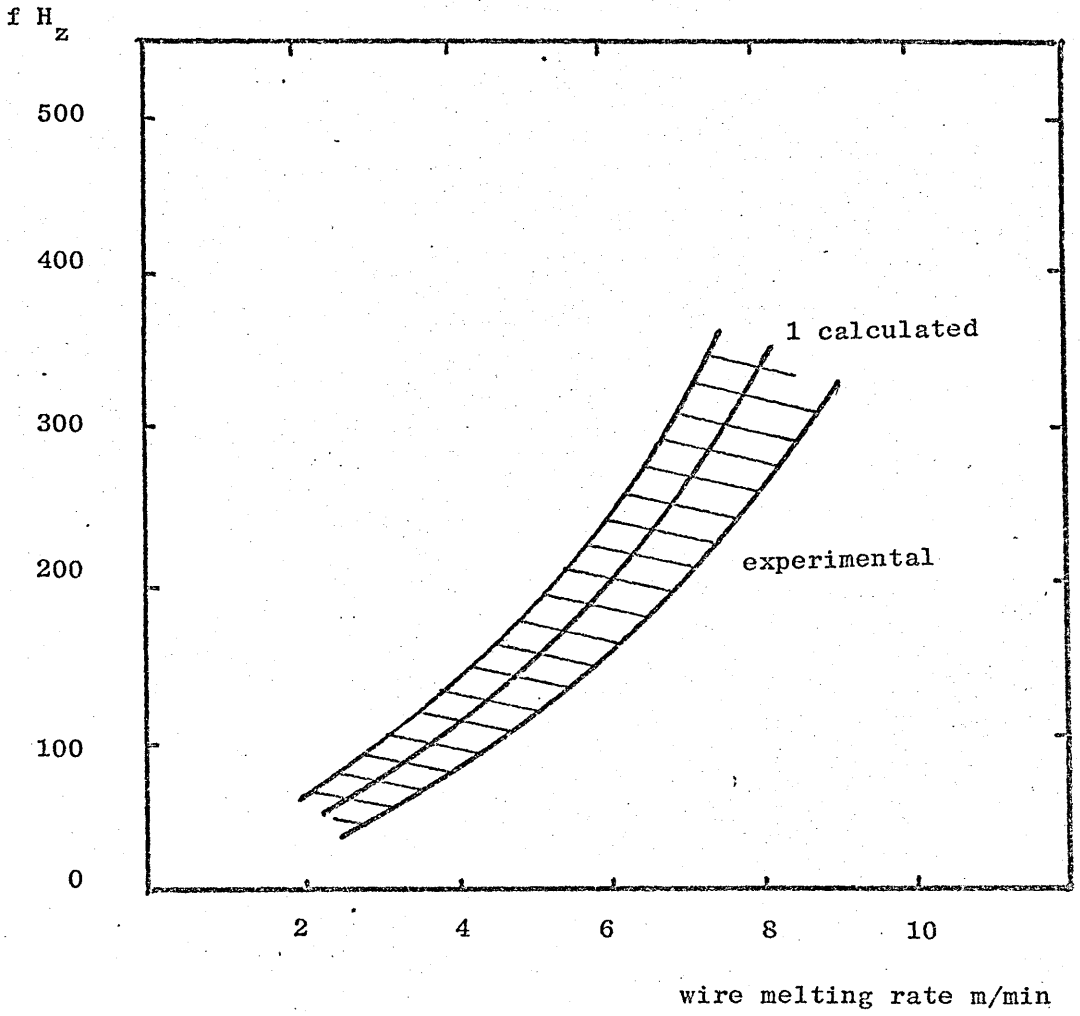

Figure 94. Variation of drop frequency with wire melting rate, 1.2mm dia. wire, Ar + 5% CO_2

Figure 95. Calibration of Power Source

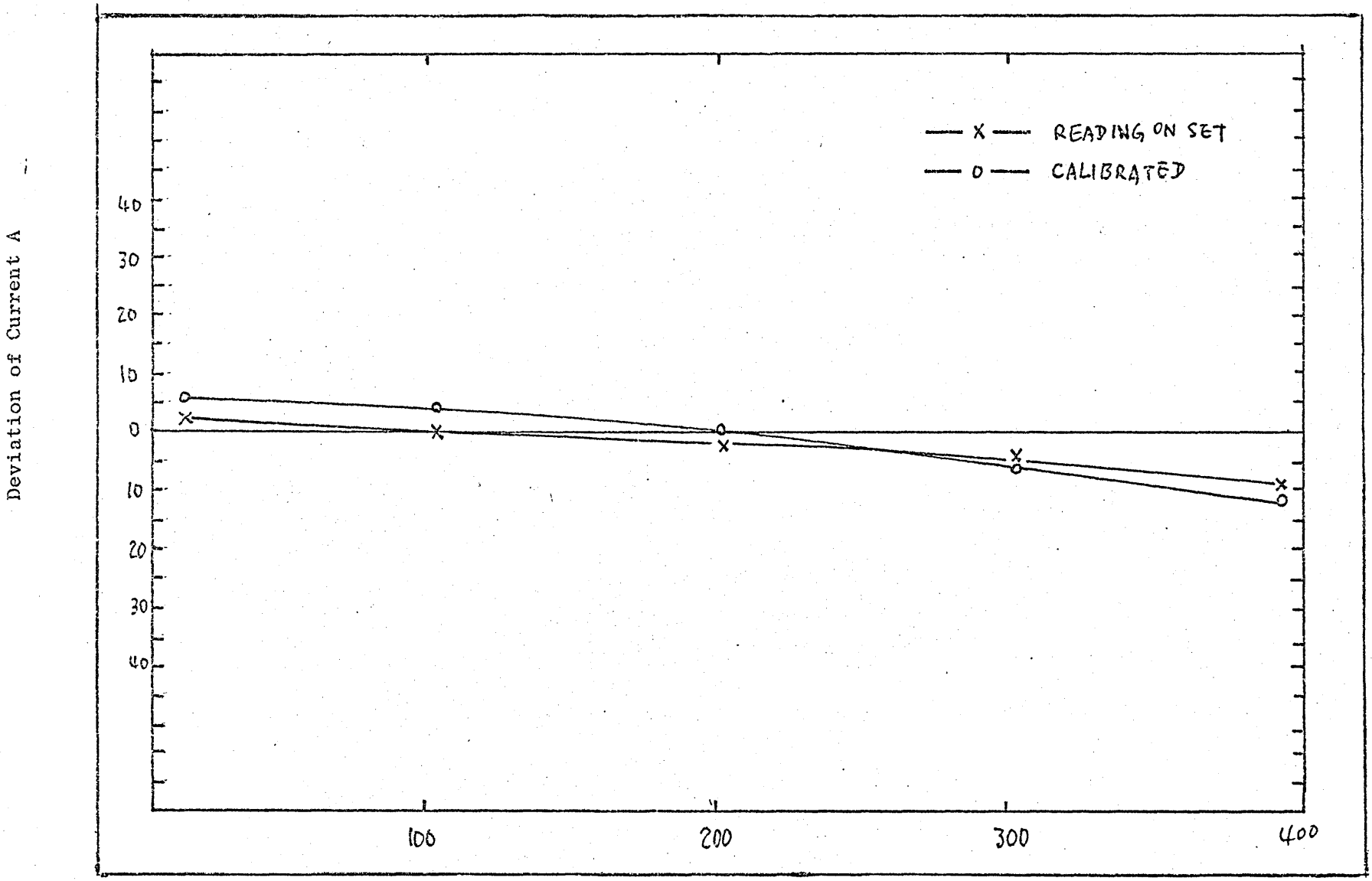

TABLE 1. SHIELDING GASES FOR METAL INERT GAS WELDING (Apps).

Material	Shielding Gas	Comments
Aluminium and alloys.	Argon	Most commonly used, gives a smooth spray arc condition and efficient cleaning action.
	Argon + He	He addition, usually up to 10% to increase heat input on thicker sections.
Copper and copper alloys.	Argon	Good spray arc condition:- requirement for preheat on thicker sections, viz. 6.5mm and above.
	Argon + He	50/50 or 30/70 Ar/He an attractive mixture for reducing level of preheat.
	Nitrogen	Good heat input characteristics:- problem of spatter and fumes.
	Argon + N_2	80% Ar + 20% N_2 mixture:- heating effects superior to argon, problem of spatter.
Titanium, Zirconium and alloys.	Argon	Suitable for spray arc in flat position welding.
	Argon + He	Ar + 25% He improves heat input - suitable for spray arc in flat position, pulsed and short circuiting arc in all positions.
Stainless steels.	Argon + O_2	1-5% O_2 addition usually employed for good spray or pulsed arc condition.
	Argon + O_2 + CO_2	2% O_2 + 5% CO_2 addition, improve short circuit and pulsed arc welding:- consideration on critical applications for possible carbon pick-up.
	Carbon dioxide	May be used where severe corrosion conditions are not likely to be encountered.
Mild and low alloy steels.	Argon + O_2	1-5% O_2 addition for good spray arc where weld composition is critical.
	Carbon dioxide	Suitable for short-circuit, globular and spray type arcs. Limited on certain alloy steel where weld composition is important.
	Argon + O_2 + CO_2	2% O_2 + 5% CO_2 additions used to facilitate spray and pulsed MIG welding. 2% O_2 + 20% CO_2 for smooth spray arc and short-circuit arc welding of thin sheet.
Nickel based alloys.	Argon	Principal gas employed for spray, pulse and short-circuiting arc conditions.
	Argon + He	Use of 15-20% He addition improves heat input and fusion characteristics.

TABLE 2. SHIELDING GASES FOR METAL INERT GAS WELDING (PATON).

Gas	Type of process	d_{el}, mm	Metals welded	Metal thickness, mm	Welding position
Ar	Natural short-circuiting and continuous arc burning	1-4	Non-ferrous metals, high-alloy steels	3-10	Flat
	Stream	0 8-1.6	The same	3-5	All positions
			The same	6-30	Vertical, horizontal, overhead
		1 6-5	The same	5-40	Flat
	Pulsed arc	0.8-2	The same	1.5-5	All positions
			The same	5-40	Vertical, horizontal, overhead
He	Stream	2.5-5	The same	6-40	Flat
		0.8-1	The same	4-6	All positions
			The same	6-40	Vertical, horizontal, overhead
	Pulsed arc	1.2-4.0	The same	10-40	Flat
		0.8-1.2	The same	2-5	All positions
		1-1.6	The same	6-40	Vertical, horizontal, overhead
		2-4	The same	6-40	Flat
	Pulsed arc with enforced short-circuiting	0.8-1.2	The same	2-5	All positions
	As above		The same	6-40	Vertical, horizontal, overhead
Ar + He	Stream	1.6-4	Alloys of aluminium and titanium	8-40	Flat
	Pulsed arc with enforced short-circuiting	0.8-1.2	Copper and its alloys, austenitic steels	3-5	All positions
			The same	6-30	Vertical, horizontal, overhead
	With natural short-circuiting or with continuous arc burning	1.2-3	The same	4-30	Flat
Ar + N_2 (up to 30%)	As above	0.8-3	The same	3-30	Flat
CO_2	Pulsed arc with enforced short-circuiting	0.6-1.4	Carbon, structural and certain high-alloy steels	0.6-5	All positions
CO_2 + O_2	As above		The same	0.6-5	All positions
Ar + CO_2 (>25%)	As above		The same	0.6-5	All positions
Ar + O_2 + + CO_2 (>25%)	As above		The same	6-50	Vertical and overhead
Ar + O_2 + + CO_2 (>25%)	With natural short-circuiting or with continuous arc burning	1.6-5	The same	6-50	Flat
Ar + O_2 (1-5%)	Stream	0.7-1.2	Carbon, structural and high-alloy steels	1-4	All positions
Ar + CO_2 (up to 18%)	Stream		The same		All positions
Ar + CO_2 + O_2 (80, 15, 5%)	Stream		The same		All positions
The same	Stream		The same	5-50	Vertical, overhead
The same	Stream	1.6-5	Technical purity aluminium and aluminium bronze*	5-50	Flat
The same	Pulsed arc	0.7-1.6	Carbon, structural and high-alloy steels	1-5	All positions
The same	Pulsed arc	1.2-1.6	The same	6-50	Vertical, overhead
The same	Pulsed arc	2-5	The same	3-50	Flat

*Mixture of Ar + O_2.

Table 3 Calculation of the drop velocity and the liquid string velocity

I_m A	I_{det} A	W_m m/sec	d_b mm	v_{bar} m/sec	v_m m/sec
290	290	0.123	0.4	1.11	0.90
167	380	0.080	0.3	1.28	1.26
167	50	0.080	0.3	1.28	1.33

I_{det} current at which the drop detached

Table 4 Influence of mean current and the wire feed rate on the detachment time

I_m amps	W_m m/sec	I amps	T_p ms	t_d ms
89	2.2	375	2	3.0
121	3.3	375	2	3.1
167	4.9	375	2	3.0
193	6.1	375	2	3.2
121	3.2	375	4	3.5

t_d detachment time

Table 5 . Calculation of forces, Refer to Figure 53.

Fram No.	1	A 2	3	4	5	6	7	8	B 9
D mm		0.56	0.56	0.50	0.46	0.46	0.40	0.36	0.33
R'		0.89	0.99	1.06	1.12	1.20	1.25	1.29	1.12
Fs		215.0	215.0	191.6	176.3	176.3	153.3	137.9	126.4
Fm		135.0	166.0	220.6	261.2	281.5	334.5	374.7	358.8

A; last drop detached. B; Drop detached.

Table 6. Data of Figure 49

Extension mm / WFR M/min / Current A	5	10	15
190	1.6	2.0	-
210	4.1	4.3	-
230	4.5	5.0	5.6
235	-	5.1	5.8
240	4.8	5.3	6.2
245	5.2	5.8	6.7
250	5.3	6.3	6.9
255	5.7	6.3	7.0
260	6.1	6.5	7.2
265	-	-	-
270	6.3	6.5	7.3
280	6.1	6.7	7.6
290	6.6	7.2	7.8
300	-	-	8.3
310	7.2	-	-

REFERENCES

REFERENCES

.1. Apps, R.L. — Handouts of welding processes, Cranfield Institute of Technology, 1981, Nos.170, 128 and 128a.

2. Milner, D.R., Apps, R.L. — Introduction to Welding and Brazing, Pergamon, 1968, pp.1-8, 64-75.

3, Anon. — The Procedure Handbook of Arc Welding, The Lincoln Electric Company, 12th Edition, 1973, 1.1, pp.1-10.

4. Anon. — AWS Welding Handbook, 7th Edition, Vol.1, pp.53, 61-69.

5. Norrish, J. — Introduction to the MIG Processes. BOC Gases Division.

6. Smith, A.A. — Characteristics of the Short-Circuiting CO_2-Shielded Arc, Symposium Physics of the Welding Arc, The Welding Institute, London, 1962, pp.75-91.

7. Paton, B.E., Potpevskii, A.G. — Gas Shielded Steady and Pulsed-Arc Welding Processes (Review), Avt. Svarka, 1973, 9, pp.1-10.

8. Lesnewich, A — Control of Melting Rate and Metal Transfer in Gas Shielded Metal-Arc Welding, Welding Journal, Vol.37, No.8, August 1958, pp.343-s-353-s, 418-s-425-s.

9. Needham, J.C. — Control of Transfer in Aluminium Consumable Electrode Welding, Symposium Physics of the Welding Arc, The Welding Institute, London, 1962, pp.114-122.

10. Lancaster, J.F. — Metal Transfer in Fusion Welding, Conference on Arc Physics and Weld Pool Behaviour, The Welding Institute, London, 1979, pp.135-146.

11. Watkins, P.V.C. — The Transistor Controlled DC Welding Power Source, Welding Institute Research Report, October 1975.

12. Rienks, F. — Development and Evaluation of a Modulated Power Control for Fusion Welding, Welding Journal, Vol.50, No.5, May 1971, pp.222-s-230-s.

13. Needham, J.C. — Transistor Power Supplies for High Performance Arc Welding, Welding Institute Research Bulletin, Vol.18, No.3, March 1977.

14. Anon. AWS Welding Handbook, 6th Edition, Vol.2, pp.23.29-23.32.

15. Millington, D. Self-Shielding Arc Welding, Welding Institute Research Report, July 1972.

16. Shaw, J. Metal Transfer Characteristics and Metal Properties of Flux Cored Welding Wires, Thesis, Cranfield Institute of Technology, 1973, pp.12-17.

17. Morigake, O. Some Improvements in Self-Shielded Flux Cored Electrodes for Arc Welding, Welding Journal, Vol.55, No.8, August 1976, pp.325-s-327-s.

18. Stular, P. Metal Transfer with Cored Electrodes in Various Shielding Atmospheres, Symposium Physics of the Welding Arc, The Welding Institute, London, 1962, pp.98-102.

19. Ladislavlanyi. The Development of Arc Welding Processes, Welding News 1-2, 1979.

20. Nestor, O.H. Heat Intensity and Current Density Distributio at the Anode of High Current Inert Gas Arcs, Symposium Physics of the Welding Arc, The Welding Institute, London, 1962, pp.50-61.

21. Parks, J.M. Arc Welding Steel Tube Electrode, British Patent Specification, 1,396,596, 4th June 1975.

22. Kobe Steel Ltd. Arc Welding Electrodes for Steel, British Patent Specification, 1,190,994, 6th March 197(

23. Lincoln Electric Company, U.S. Patent Specification 2,909,648.

24. Konshtein, E.I., Lozovskaya, G.S., Martynenko, B.F., Lebedev, B.F. Flux Cored Electrode, British Patent Specification, 1,346,750, 15th February 1974.

25. Buckingham, C.H., Elliott, R. Welding Electrodes and Fluxes, British Patent Specification, 1,379,243, 2nd January 1975.

26. Blake, P.D. Welding Electrodes, British Patent Specification, 1,353,610, 22nd May 1974.

27. Lucas, W. Alternating Current MIG Welding, Advances in Welding Processes, 4th International Conference, Harrogate, May 1978, pp.117-126

28. Lucas, W., Needham, J.C. — Why not AC MIG Welding? Welding Institute Research Bulletin, Vol.16, No.3, March 1975.

29. Paton, B.E. — Controlling Metal Transfer in Arc Welding with a Consumable Electrode, Avt. Svarka, Vol.18, No.5, 1965, pp1-7.

30. Rider, G., Alberry, P. — Pulsed Wire Feed CO_2 MIG Welding Facilities Repair Work, Welding and Metal Fabrication, Vol.46. No.4, May 1978, pp.253-262.

31. Kiyohara, M. et al. — Welding of GMA - on the Stabilisation of GMA, Welding Journal, Vol.56, No.3, March 1977, pp.21-28.

32. Boughton, P. — Two Years of Pulsed Arc Welding, Welding and Metal Fabrication, Vol.35, No.10, October 1967, pp.410-420.

33. Rogerson, J.H. — Practical Application of Pulse MIG Welding to Aluminium, Pulsed MIG Welding, A National Seminar, The Welding Institute, 1974.

34. Needham, J.C. — Pulse Controlled Consumable Electrode Welding Arcs (Review), British Welding Journal, Vol.12, No.4, April 1965, pp.191-197.

35. Needham, J.C., Carter, A.W., — Material Transfer Characteristics with Pulse Current, British Welding Journal, Vol.12, No.5, May 1965, pp.229-241.

36. Krantz, B.M. — The Effects of Pulsed Gas Metal-Arc Welding Parameters on Weld Cooling Rates, Welding Journal, Vol.50, No.21, November 1971, pp.474-s-479-s.

37. Koledinkov, A.S. — The Semi-Automatic Pulsed Argon MIG Welding of VNS-2 Steel, Avt. Svarka, Vol.29, No.9, 1976, pp.41-43.

38. Needham, J.C. — Pulsed Current for Gas Shielded Arc Welding, IEEE Translation on Industry and General Applications, 5-6, 1966, pp.225-233.

39. Boughton, P. — The Use of Pulsed Current to Control Metal Transfer in Welding, British Welding Journal, Vol.12, No.5, April 1965, pp.159-166.

40. Partingron, E.C. — Controlled Transfer in the Open Arc MIG Process-Effect of Pulse Duration and Amplitude, Welding Institute Research Report, August 1966.

41. Heath, D.J. — MIG Pulse Welding with Nickel Alloy Wires, Welding and Metal Fabrication, Vol.44, No.8, October 1976, pp.549-553.

42. Paton, B.E., Zaruba, I.I. — Peculiarities of Arc Discharge when Welding with a Short-Circuiting Arc Gap, Symposium Physics of the Welding Arc, The Welding Institute, London, 1962. pp.102-107

43. Zaruba, I.I. — Special Features of Methods Being Used for Limiting the Short-Circuit Current during CO_2 Welding, Avt. Svarka, Vol.31, No.1, 1978, pp.16-19.

44. Keyser, E. De — Control of Arc Current is Way to Short Arc MIG Welding Quality, Philips Welding Reporter, 3, 1978. pp.5-9

45. Pan, J.L., Zhang, R.H. — A new Method of Controlling the Welding Arc, Schweissen und Schneiden Translation, 10/1981. pp.E180-E181

46. Norrish, J. — Developments in the MIG Welding of Steel Sheet and Strip, Sheet Metal Industries, 3. 1972.

47. Stewart, J.P. — The Welder's Handbook, Reston, Virginia, U.S.A. 1981.

48. Paton, B.E. et al — Controlling the Arc Welding Process by Programming the Electrode Wire Feed Rate, Avt. Svarka, Vol.30, No.1, 1977, pp.1-5.

49. Brown, K.W. — Programmed MIG Welding, British Welding Journal, Vol.1, No.6, June, 1969, pp. 286-293.

50. Morris, J. — How Electronically Controlled MIG Can Cut Costs, Welding and Metal Fabrication, Vol.46, No.10, December 1978, pp.687-689.

51. Lucas, W. — Microprocessor Control in TIG Welding, The Welding Institute Research Bulletin, Vol.20, No.11, November 1979.

52. Amin, M. Watkins, P.V.C. — Synergic Pulse MIG Welding, Welding Institute Research Report, August 1977.

53. Amin, M. — Synergic Pulse MIG Welding, Metal Construction, Vol.13, No.6, June, 1981.

54. Needham, J.C. — Synergic Pulse MIG Welding, The Welding Institute Research Bulletin, Vol.18, No.9, 1977.

55. Amin, M. — Prediction of Square Wave Pulse Current Parameters for Control of Metal Transfer, Welding Institute Research Report, December 1978.

56. Needham, J.C. — Synergic Pulse MIG Welding, The Welding Institute Research Bulletin, Vol.18, No.9, 1977.

57. Salter, G.R. — Arc Welding Researches. The Welding Institute Research Bulletin, Vol.22, No.5, May 1981.

58. Doherty, J. — Arc Welding Procedure Selection - a Mathematical Approach, The Welding Institute Research Bulletin, Vol.21, No.4, April 1980.

59. Doherty, J. — Computerised Control of MIG Welding. The Welding Institute Research Bulletin, Vol.21, No.7, July 1980.

60. Salter, G.R. — Procedure Selection for Arc Welding, Welding Institute Bulletin, Vol.20, No.11, November 1979.

61. Paton, B.E. — Prospects for Using Electronic Computer Technique in Welding Production, Avt. Svarka, Vol.30, No.11, 1977, pp.1-3.

62. Lancaster, J.F. — The Metallurgy of Welding, Brazing and Soldering, London, 1974.

63. Rollason, E.C. — The Electric Arc in Welding, Joining of Metals Conference, October 1959. pp.71-88

64. Denouden, G. — Physical Properties of the Arc Column, IIW Doc.212-184-70.

65. Quigley, M.B.C. Richards, P.H. — Physical Properties of a MIG Welding Arc, Marchwood Engineering Laboratories, July 1972. R/M/N650

66. Quigley, M.B.C. — Physics of the Welding Arc, Welding and Metal Fabrication, Vol.45, No.10, December 1977, pp.619-626.

67. Amson, J.C. Salter, G.R. — An Analysis of the Gas-Shielded Consumable Metal Arc, Symposium, Physics of the Welding Arc, The Welding Institute, London, 1962.

68. Goldman, K. — Electric Arcs in Argon, Symposium, Physics of the Welding Arc, The Welding Institute, London, 1962. pp.17-22

69. Guile, A.E.
Lancaster, J.F.
Arc Cathode and Anode Phenomena, Annual Assembly of the IIW, 1970.

70. Matsumawa, A.
Arc Characteristics in High Pressure Argon Atmosphere. Conference on Arc Physics and Weld Pool Behaviour, The Welding Institute, London, 1979. pp.123-133

71. King, L.A.
Howes, J.A.
Material Transfer in the Welding Arc, Symposium, Physics of the Welding Arc, The Welding Institute, London, 1962. pp.180-8

72. Lochte-Hoetgreven, W.
The Electric Arc between Carbon and Iron Electrodes, Symposium, Physics of the Welding Arc, The Welding Institute, London, 1962. pp.1-13

73. Lucas, W.
Solid Wire AC MIG Welding, Welding Research International, Vol.8, No.2, 1978.

74. Nestor, O.H.
Heat Intensity and Current Density Distribution at the Anode of High Current, Inert Gas Arcs. Symposium, Physics of the Welding Arc, The Welding Institute, 1962. pp.50-66

75. Mantal, W.
On the Physics of Welding Arcs. Symposium, Physics of the Welding Arc, The Welding Institute, 1962. pp.213-222

76. Cooksey, C.J.
Milner, D.R.
Metal Transfer in Gas Shielded Arc Welding. Symposium, Physics of the Welding Arc, The Welding Institute, 1962.

77. Ludwig, H.C.
Plasma-Energy Transfer in Gas Shielded Welding Arcs. Welding Journal, Vol.38, No.7, July, 1959, pp.2865-3005.

78. Glickstein, S.S.
Arc Modelling for Welding Analysis. Conference on Arc Physics and Weld Pool Behaviour, The Welding Institute, London, 1979. pp.1-16

79. Watanabe, I. et al
The Arc Phenemenon in Large Current MIG Arc Welding. Conference on Arc Physics and Weld Pool Behaviour, The Welding Institute, London, 1979. pp.177-192

80. Needham, J.C.
Carter, A.W.
Arc and Transfer Characteristics of the Steel CO_2 Welding Processes, BWRA Report, October 1967.

81. Wilkinson, J.B.
Milner, D.R.
Heat Transfer from Arcs, British Welding Journal, Vol.7, No.2, February 1960, pp.115-128.

82. Apps, R.L.
Milner, D.R.
Heat Flow in Argon Arc Welding. British Welding Journal, Vol.2, No.10, October 1955.

83. Waszink, J.H.
Van den Heuvel, J.P.M.
Heat Generation and Heat Flow in the Filler Wire Metal in GMA Welding, Welding Journal, Vol.61, No.8, August 1982, pp.269-s-282-s.

84. Halmoy, E.
Wire Melting Rate, Droplet Temperature and Effective Anode Melting Potential. Conference on Arc Physics and Weld Pool Behaviour, The Welding Institute, London, 1979. pp.49-57

85. Terhear, K.
A Simplified Method for Calculation of the Mean Droplet Temperature in Gas Wire Arc Welding, Philips Welding Laboratory, 1972. pp.14-17

86. Jelmorini, G. et al
Droplet Temperature Measurements in Arc Welding, IIW Doc.212-411-77, 1977.

87. Ando, K. et al
Mechanism of Formation of Pencil-Point Like Wire Tip in MIG Arc Welding. IIW Doc.212-156-68.

88. Wilson, J.L.
Clavssen, G.E.
Jackson, C.E.
The Effect of I^2R Heating on Electrode Melting Rate, Welding Journal, Vol.35, No.1, January 1956, pp.1-s-8-s.

89. Amson, J.C.
Electrode Voltage in the Consumable-Electrode Arc System, J.Phys.D.Appl. Phys, Vol.5, 1972. pp.89-96

90. Waszink, J.H. et al
Measurements and Calculations of the Resistance of the Wire Extension in Arc Welding. Conference on Arc Physics and Weld Pool Behaviour, The Welding Institute, London, 1979. pp.227-239

91. Esser, W.G.
Walter, R.
Some Aspects of the Penetration Mechanisms in Metal-Inert-Gas (MIG) Welding. Conference on Arc Physics and Weld Pool Behaviour, The Welding Institute, London, 1979. pp.289-300

92. Esser, W.G.
Heat Transfer and Penetration Mechanism with GMA and Plasma-GMA Welding, Welding Journal, Vol.60, No.2, 1981, pp.37-s-42-s.

93. Pokhodnya, I.K.
Suptel, A.M.
The Heat Content of Droplets of Electrode Metal in CO_2 Welding. Avt. Svarka, Vol.23, No.10, 1970, pp.5-8.

94. Pokhodnya, I.K.
Suptel, A.M.
The Heat Contents of the Droplets of Electrode Metal in Gas Shielded Arc Welding, Avt. Svarka, Vol.20, No.2, 1967, pp.16-27.

95. Anon
Classification of Metal Transfer on Arc Electric Welding Processes, Doc.IIS/IIW 535-77.Welding in the World, Vol.15,No.5/6,197

96. Needham, J.C.
Cooksey, C.J.
Milner, D.R.
Metal Transfer in Inert Gas Shielded Arc Welding. British Welding Journal, Vol.7, No.2, 1965, pp.101-114.

97. Lancaster, J.F.
Influence of Heat Flow on Metal Transfer in the Metal Inert Gas Welding of Aluminium. Symposium, Physics of the Welding Arc, The Welding Institute, London, 1962. pp.170-187

98. Haberlin, M.M.
Programme Controlled MIG Welding of Austenitic Steels, Developments in Mechanised Automatic and Robotic Welding, London, November 1980.

99. Pintard, J.
Contribution a l'etude du Transfer de Metal dans le Soudage MIG, Communication presentee a la Societe des Ingenieurs Soudeurs, 17th December 1964. pp.278-287

100. Defize, L.F.
Metal Transfer in Gas Shielded Welding Arcs, Symposium, Physics of the Welding Arc, The Welding Institute, London, 1962.

101. Erokin, A.A.
The Force Exerted by the Arc on the Metal being Melted, Avt. Svarka, Vol.32, No.7, 1979, pp.17-23.

102. Serdjuk, G.B.
Magnetic Forces in Arc Welding Metal Transfer. Symposium, The Physics of the Welding Arc, The Welding Institute, London, 1962. pp.175-188

103. Flintham, E.
Manual, Semi-Automatic and Automatic Arc Welding, BOC Ltd. 1966.

104. Rimskii, S.T.
Svetsinskii, V.G.
Smityan, O.D.
Transfer of Electrode Metal during Welding using Shielding Gases with Oxygen Added, Avt. Svarka, Vol.32, No.10, 1979, pp.19-22.

105. Quigley, M.B.C. — Laser Aids Observation of MIG Metal Transfer. Laboratory notes, Marchwood Engineering Laboratories

106. Heile, R.E. — Particulate Fume Generation in Arc Welding Processes, Welding Journal, Vol.54, No.7, 1975, pp.201-s-210-s.

107. Hiltunen, V. Pietikainen, J. — Investigations and Observations on Material Transfer in Metal Inert Gas (MIG) Welding. Conference on Arc Physics and Weld Pool Behaviour, The Welding Institute, London, 1979. pp.147-162

108. Kiyohara, M. et al — Melting Characteristics of a Wire Electrode in the MIG Welding of Aluminium. Conference on Arc Physics and Weld Pool Behaviour, The Welding Institute, London, 1979.

109. Amin, A. et al — Electrode Tip Behaviour in Spray Transfer Mild Steel MIG Welding, Welding Institute Report, July 1972, pp.59-72

110. Greene, W.J. — Analysis of Transfer in Gas Shielded Welding Arcs. Translation AIEE, 79(2), July 1960, pp.194-202.

111. Serdjuk, G.B. — Magnetic Forces in Arc Welding Metal Transfer, Symposium, The Physics of the Welding Arc, London, 1962.

112. Amson, J.C. — Lorentz Force in the Molten Tip of an Arc Electrode, Brit.J.Appl.Phys, Vol.16, 1965. pp.1169-1179

113. Hiltunen, V. — Some Influences of the Inner Circulation of the Pendant Droplet on its Detaching in the MIG/MAG Welding. IIW Doc.212-509-81.

114. Lancaster, J.F. — Discussion on Metal Transfer. Symposium, The Physics of the Welding Arc, London 1962. Discussion Session 4, pp.158-160.

115. Buchinskii, V.N. — Features of the Pulsed Arc Welding of Steels using a Mixture of Argon and CO_2. Avt. Svarka, Vol.31, No.3, 1978, pp.29-31.

116. Partington, E.C. — Controlled Transfer in the Open Arc MIG Process Effect of Pulse Data Duration and Amplitude, Welding Institute Research Report, 1966.

117. Rider, G. — Pulsed Wire Feed CO_2 MIG Welding Facilities Repair Work. Welding and Metal and Fabrication, Vol.46, No.4, May 1978, pp.253-262.

118.	Buchinskii, V.N. Potapevskii, A.G.	Selecting the Parameters of the Welding Conditions for Pulsed Arc Welding with a Consumable Steel Electrode. Avt. Svarka, Vol.30, No.6, 1977.
119.	Krantz, B.M. Coppolecchia, V.D.	The Effect of Pulsed Gas Metal Arc Welding Parameters on Weld Cooling Rates, Welding Journal, Vol.50, No.11, November 1971, pp.474-s-479-s.
120.	Lenivkin, V.A. et al	The Determination of Controlled Metal Transfer on Pulsed Arc Welding with a Consumable Electrode, Svar. Proiz, Vol.23, No.12, 1976, pp.10-14.
121.	Reynolds, J.	Adaptive Spray - A New Process for Thin Gauge Aluminium, Welding Journal, July 1980.
122.	Parting, E.C. Needham, J.C.	Controlled Transfer Characteristics of the Inert Gas Metal Process, Effect on Duration and Current Amplitude of Current Pulse, BWRA Report , P/16/66.
123.	Potapevskii, A.G. et al	Transfer of Electrode Metal in Argon Shielded Pulsed Arc Welding. Avt. Svarka, Vol.18, No.6, June 1965, pp.16-19.
124.	Paton, B.E.	Automatic Control of Pulsed Arc Welding with a Consumable Electrode. Avt. Svarka, Vol.60, No.1, 1967, pp.4-9.
125.	Needham, J.C.	Arc and Transfer Characteristics of the Steel/CO_2 Welding Process. British Welding Journal, Vol.14, No.10, October 1967, pp.533-549.
126.	Heiro, H.	The Influence of Welding Parameters on Droplet Temperature during Pulsed Arc Welding, Welding and Metal Fabrication, Vol.44, No.7, September 1976, pp.482-485.
127.	Buchinskii, V.N.	Features of the Pulsed Arc Welding of Steel using a Mixture of Argon and CO_2. Avt. Svarka, Vol.31, No.3, 1978, pp.29-31.
128.	Araya, T. Endo, Y. Imamiya, H. Ando, B. Sezima, I.	Transistor Controlled Pulsed MIG Welding of Aluminium Alloys, IIW-XII-c-7-81.
129.	BOC-AWP	Precision Synergic MIG Welding, AWP 8101.

130. Nicholson, S.
Apps, R.L.
Heat Build Up and Weld Nugget Formation in Mild Steel Spot Welds, Conference on Advances in Welding Processes, The Welding Institute, Harrogate, 1970.

131. Rykalin, N.N.
Kulagin, E.D.
Nikolaev, A.V.
Vaporised Electrode Metal and Energy Balance in Welding Arc. Symposium, Physics of the Welding Arc, The Welding Institute, London, 1962. pp.46-61

132. Ishizaki, K.
The Behaviour of a Pendant Liquid Drop and the Phenomenon of Metal Transfer. Symposium, Physics of the Welding Arc, The Welding Institute, London, 1962.pp.210-235

133. Ma, Jilong
MIG Transfer Discover of Importance to Industry, Welding and Metal Fabrication, Vol.50, No.7, September 1982, pp.307-316.

134. Ma, Jilong
Control System Improves Flash Welding Efficiency, Welding and Metal Fabrication, Vol.48, No.10.pp.661-666

135. Zaruba, I.I.
Electrical Explosions as the Cause of Metal Spatter, Avt. Svarka, Vol.23, No.3, 1970, pp.14-18.

136. Lavrishchev, V.V.
The Mechanism of Metal Spattering in CO_2 Welding with a Long Arc, Avt. Svarka, Vol.31, No.6, 1978, pp.33-35.

137. Kyurgerov, N.G.
Reducing Metal Spatter and Stabilising the Process of Welding with a Short Arc, Avt. Svarka, Vol.25, No.6, 1972, pp.36-7.

138. Akulov, A.I.
Spitsyn, V.V.
Rate of Formation and Transfer of a Drop of Electrode Metal in CO_2 Welding, Svar. Proiz, Vol.15, No.12, 1968, pp.7-11.